IntechOpen

Aeronautics

New Advances

Edited by Zain Anwar Ali and Dragan Cvetković

Aeronautics - New Advances

Edited by Zain Anwar Ali and Dragan Cvetković

Published in London, United Kingdom

Aeronautics - New Advances
http://dx.doi.org/10.5772/intechopen.100748
Edited by Zain Anwar Ali and Dragan Cvetković

Contributors
Hicham Megnafi, Walid Yassine Medjati, Uche Emmanuel, Alphanos Mahachi, Trymore Aloni, Lucious Mashevedze, Ilie Nicolin, Bogdan Adrian Nicolin, Cătălin Nae, Guruprasad Ramachandran, Kamaleshaiah Mathavara, Peter Kvasnica, Clélia Mendonça de Moraes, Jenica-Ileana Corcau, Liviu Dinca, Ciprian-Marius Larco, Parul Priya, Sushma S. Kamlu, Zain Anwar Ali, Muhammad Mubashir Iqbal, Rehan Khan, Muhammad Shafiq

First published in London, United Kingdom, 2022 by IntechOpen
IntechOpen is the global imprint of INTECHOPEN LIMITED, registered in England and Wales, registration number: 11086078, 5 Princes Gate Court, London, SW7 2QJ, United Kingdom

British Library Cataloguing-in-Publication Data
A catalogue record for this book is available from the British Library

Additional hard and PDF copies can be obtained from orders@intechopen.com

Aeronautics - New Advances
Edited by Zain Anwar Ali and Dragan Cvetković
p. cm.
Print ISBN 978-1-80355-300-9
Online ISBN 978-1-80355-301-6
eBook (PDF) ISBN 978-1-80355-302-3

Meet the editors

Engr. Dr. Zain Anwar obtained a Ph.D. in Control Theory and Control Engineering from Nanjing University of Aeronautics and Astronautics (NUAA), China. In 2017, he was selected as a highly talented foreign expert by the Ministry of China, Beijing. In 2018–2019, he received research funding from the Higher Education Commission (HEC), Pakistan, and began collaborating with several universities in China, including NUAA, Donghua University, Shanghai University, and Southeast University, with grants provided by the National Nature Science Foundation of China (NSFC). Dr. Ali is an associate professor and editor at Sir Syed University of Engineering and Technology, Pakistan.

Dragan Cvetković obtained a Ph.D. in Aeronautics from the Faculty of Mechanical Engineering, University of Belgrade, Serbia, in 1997. To date, he has published sixty-five books, scripts, and practicums about computers and computer programs, aviation weapons, and flight mechanics. He is currently a full professor and the vice-rector of teaching at Singidunum University, Serbia.

Contents

Preface

Aeronautics involves the research, development, and manufacture of machines capable of air flight as well as methods for controlling airplanes and rockets inside the atmosphere. The development of kites in China in the fifth century marks the beginning of flying. The first versions of a rational airplane were envisioned by the renowned artist Leonardo da Vinci in his paintings from the fifteenth century. Tito Livio Burattini created a miniature airplane in 1647 that included four sets of glider wings. The Wright brothers were American inventors and aviation pioneers who made one of the earliest powered, sustained, and controlled airplane flights in 1903. Two years later, they built and flew the first fully functional airplane, surpassing their record.

Technologies like augmented reality, artificial intelligence (AI), and automation are just a few examples of how modern aviation and space travel has improved. In-flight instruction for pilots is being provided by virtual instructors, autonomous wingmen are surveying the skies ahead, and AI algorithms are assisting with more effective aircraft routing. The demand for engineers and scientists is anticipated to increase by 6% by 2031. The Middle East and South America will see the fastest growth rates in the aerospace industry going forward, with compound annual growth rates (CAGRs) of 10.5% and 10.1%, respectively. The markets in Africa and Eastern Europe are anticipated to see CAGR increases of 8.9% and 8.1%, respectively.

This book presents state-of-the-art research and developments in the field of aeronautics. It includes ten chapters divided into six sections. Chapters discuss topics such as the applications of drones, recent challenges in aeronautics, control approaches for the civil and military domains, modeling and simulation, and modern aviation applications.

Zain Anwar Ali
Associate professor,
Electronic Engineering Department,
Sir Syed University of Engineering and Technology,
Karachi, Pakistan

Dragan Cvetković
Singidunum University,
Belgrade, Republic of Serbia

Section 1

Introduction

Chapter 1

Unmanned Aerial Vehicle for Agriculture Surveillance

Alphanos Mahachi, Trymore Aloni and Lucious Mashevedze

Abstract

The design of a fixed-wing Vertical Take-Off and Landing (VTOL) Unmanned Aerial Vehicle (UAV) for agriculture pest monitoring is the subject of this thesis. It is primarily concerned with the sugarcane pest problem in the KZN region. After seeing the impact of sugarcane on this region and South Africa as a whole, this design was created. The wing, fuselage, empennage, and tilt-rotor mechanism of the UAV are all designed to meet the mission requirements. The aerodynamics, performance, and stability of the UAV are next examined. The highest sustained turning performance was determined using the SEP chart. The UAV has a cargo capacity of 2 kg, a range of 96.7 m, a stall speed of 13.7 m/s, and a flight time of 1.48 hours. Because the UAV is a fixed-wing VTOL system, it can reach more geographically demanding regions and maneuver in windy conditions. The design was followed by the development of an IR thermography camera with 12 Megapixels and a 45 HFOV for the detection of pests. Following that, the tilt rotor mechanism was meticulously designed.

Keywords: agriculture pest surveillance, unmanned aerial vehicle, UAV design, UAV analysis, VTOL, multi-rotor

1. Introduction

1.1 Problem definition

It's tough to tell whether pests and diseases are affecting plants like sugarcane. In this study, the region of KwaZulu Natal (KZN) in South Africa was investigated. KZN is well recognized for its favorable geographical circumstances for sugarcane production, which include high annual rainfall, wetlands, low height, mild temperatures, and the presence of alluvial clay soil. Sugarcane production benefits not only KZN community but also South Africa as a whole; for example, 19.9 million tonnes of sugarcane produced in South Africa come from KZN, resulting in the bulk of sugar mills being based in this province [1]. **Figure 1** shows that 12 of South Africa's 14 sugar mills are located in KZN. Through the production of jobs and the sale of products, society benefits both socially and economically. For example, some people can work in mills for the processing step, while others work on farms. The sugar cane sector in KZN is expected to employ 79,000 people directly and 350,000 indirectly, accounting for about 2% of the South African population and a major portion of the entire

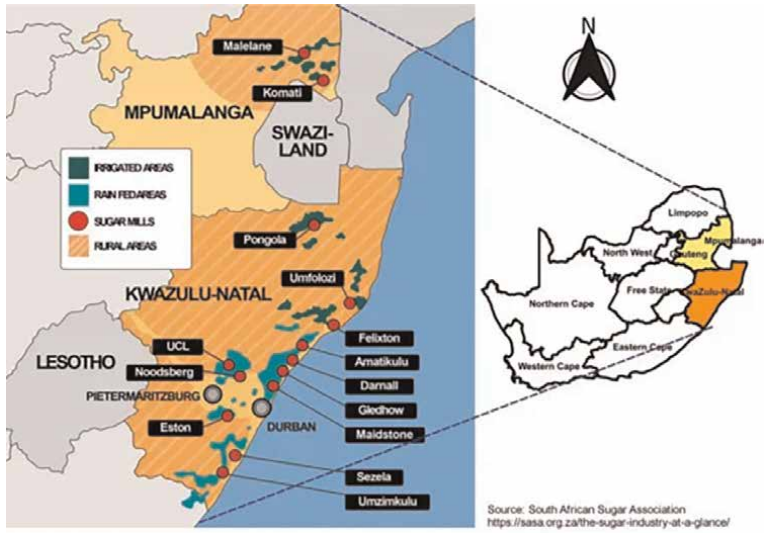

Figure 1.
Sugarcane plantations regions in the Mpumalanga and KwaZulu-Natal provinces [2].

agricultural labour. Sugarcane cultivation contributes over R8 billion to the South African economy, according to the South African Sugar Association (SASA) [2].

Given its agricultural and industrial investments, foreign exchange revenues, high employment, and connections with major suppliers, support industries, and customers, the South African sugar sector contributes significantly to the national economy. It's a diversified industry that combines sugar-cane farming with industrial factory production of raw and refined sugar, syrups and specialized sugars, as well as a variety of by-products.

Pests, on the other hand, have emerged as the most pressing worry when it comes to increasing sugarcane yields in KZN. This is due to the fact that not only does this location have the pest's host plant, but the conditions are also conducive to the pests' rapid reproduction, resulting in a wide variety of pest species. Stem borers, such as Eldana saccharina, the most common sugarcane pest in KZN, are one of these pest species types. According to the South African Sugarcane Research Institute (SASRI), there are four main pest categories that affect sugarcane production: leaf-eaters, leaf suckers, stem borers, and soil pests, but the Eldana is the industry's most serious pest, causing a total loss of over R1 billion per season if left unchecked [3]. Furthermore, with these losses in yield quality and quantity, action must be taken to reduce pest attacks in KZN (and the rest of the world), which can only be done by introducing precision farming, which is a farm management approach that uses information technology to ensure that crops and soil receive exactly what they need for optimum health and productivity [4]. When it comes to pest control, information technology can be used to monitor pests, spray pests, or do both to ensure that crops are healthy and generate a good yield. Monitoring pests before taking action has several advantages: it allows the farmer to implement timely interventions that ensure optimal yields at the end of the season, it reduces the amount of pesticide used because only the affected area can be sprayed before the pests spread throughout the farm, resulting in less wastage of resources and a reduction in the losses that can be incurred by the farmer due to the purchase of excess pesticides. The majority of pest monitoring in the investigated region is done by workers as they go about their everyday

operations, and the difficulty with this method is that by the time an infestation is discovered, a lot of harm has already been done. Another issue is that it is labour-intensive and time-consuming.

1.2 Current solutions to the problem

The application of pesticides without understanding of the pest they are dealing with is a prevalent approach used by farmers in KZN to tackle pest problems. They frequently use a calendar to schedule the spaying practices, which entails researching the pests' life cycles and spraying pesticides when they are most destructive to the plants. This strategy has a number of drawbacks, including the farmer's potential to over- or under-apply pesticides due to a lack of understanding about the pest population in the affected area. Overuse of pesticides can result in losses if too much money is spent on pesticide purchases. Another issue is that the farmer may apply the pesticide too early or too late, because the calendar and analyzing the pest's life cycle cannot always be depended on because there are other aspects to consider, such as meteorological circumstances. Furthermore, if pesticides are applied too late, the affected area may lose most or all of its crops, as in the case of an armyworm infestation.

Furthermore, the problem is being treated by employing human labour to monitor the farm, which is roaming around the farm looking for infested plant areas. This procedure is time-consuming to the point that employees may arrive late at the afflicted area, causing many crops to be harmed. When Eldana borers attack 5-month-old sugarcane plants, it is difficult for workers to notice the frass since the farms are dense at this point, which means utilizing human labour for pest scouting will take longer and may be unsafe because sugarcane can harbor harmful animals such as snakes.

However, by employing more methodical ways, not only is the problem of sudden insect invasion minimized, but it is also possible to detect pests early. As a result, a gadget to monitor the pest and keep the farm informed is required before the infestation spreads throughout the entire farm. To investigate the entire farm, this equipment must be able to go from one spot to another, either by ground or by air. The device must also be able to take photographs in order to visualize and identify pests even inside stems, to store detection data and the GPS location of the infested area, and to be serviceable, which refers to the ease and speed with which corrective and preventive maintenance can be performed on the system.

2. Literature survey

2.1 Pest detection methods

These are the techniques for distinguishing the pest from the crops and collecting data. This can be accomplished by taking photos, listening for pest sounds, and inspecting the crops for pests. The sub-sections that follow will go through some of the present pest detection methods.

2.1.1 Acoustic sensor

The noise level of the pest is monitored by an acoustic device sensor, which alerts the farmer of the precise location where the infestation is occurring whenever the

noise level above the threshold [5]. The acoustic sensors node is connected to the base station, and each sensor will send the noise levels to the base station whenever the noise level exceeds a predetermined threshold. The red palm weevil has been detected using this technology in palm tree plantations [6]. The sensors, coupled with communication modules including a transceiver, are affixed to a tree during the detecting phase and latched to the network of neighboring access points. The optical fiber acoustic sensor is the most commonly utilized acoustic sensor in the detection of red palm weevil.

2.1.2 Imaging sensors

To identify pests, these image sensors employ optics and electronics. The hyperspectral camera, multispectral camera, RGB cameras, and thermal camera are among the imaging techniques used for surveillance, particularly in precision agriculture and military applications, as well as aerial mapping. The hyperspectral remote sensor is concerned with extracting information from objects or scenes on the Earth's surface using light collected by airborne or spaceborne sensors. It has a larger bandpass, which can approach 2000 at times. It's utilized in precision agriculture to discern apart plant species with identical spectral fingerprints, determine plant biochemical composition, and calculate chemical characteristics. Food safety, pharmaceutical process monitoring and quality control, biomedical, industrial, biometric, and forensic applications are all examples of lab-scale applications [7]. **Table 1** lists some of the existing hyperspectral cameras as well as their specifications. The thermal camera is another imaging sensor that may be used to create a heat zone image using infrared radiation with a wavelength of 1400 nm. It is used in agriculture to monitor water stress and irrigation uniformity in crops, as well as to calculate vegetation indices. Food preparation, safety and fire inspections, plastic molding, asphalt, maritime and screen printing, measuring ink and dryer temperature, and diesel and fleet maintenance are some of the sectors that employ them. The Noyafa NF-521 Thermal Imaging Camera, for example, has a temperature range of −10 to 400°C, a basic accuracy of 2%, and an adjustable emissivity of 0.1 to 0.99, with a measurement resolution of 0.1°C. The FLIR Scout TK Compact thermal monocular camera, which is mostly used in wildlife when locating wild creatures and has a temperature range of −40 to 60 degrees Celsius and can catch things up to 90 meters away, is the second option. The multispectral cameras are the next in line, with five bandpass interference filters: red, green, near-infrared, blue, and red edge [8]. It is currently used in agriculture to monitor crop diseases and pests, evaluate the status of the vegetation, and measure nutrient deficit.

Parameter	Hydice	Aviris	Hyperion	EnMAP	Prisma	Chris
Altitude(km)	1.6	20	705	653	614	556
Spatial resolution(m)	0.75	20	30	30	5–30	36
Spectral resolution(nm)	7–14	10	10	6.5–10	10	1.3–12
Coverage (μm)	0.4–2.5	0.4–2.5	0.4–2.5	0.4–2.5	0.4–2.5	0.4–1.0
Number of bands	210	220	220	228	238	63

Table 1.
Parameters of hyperspectral sensors.

3. Design consideration

3.1 Environmental consideration

The climate is primarily subtropical in most of the KZN sugarcane production districts, with typical annual temperatures ranging from 21°C along the coast to 16°C inland [9]. In the summer, however, because to the high humidity, these temperatures can approach 30°C. The yearly rainfall gradient varies as the distance from the shore increases, although it is consistently high, ranging from 25 mm to 1059 mm each year. The Indian Ocean anticyclones, which control the airflow spreading through the region from the Indian Ocean, have an impact on the climate. Because of the abundance of undulating terrains in the region, the climate varies by location, making it suitable for sugarcane production, which dominates the region [10] Dystric regosols and rhodic acrisols are the most frequent soil types in the KZN region of concern, with rhodic soils covering the majority of the area. Sugarcane farming in KZN is further aided by the rhodic soils, which give essential nutrients. As a result, the majority of sugarcane fields are located in locations with rhodic soils [9]. The majority of the sugarcane agricultural regions in KZN are wetlands [11]. As a result, all of these geographic and climatic circumstances must be addressed while designing in order for the design to fulfill its function, which is to solve the challenge outlined in Section 1. Because the rainfall season in KZN is from October to April, the design must be able to perform in wet conditions. Given the annual average wind speed of 15 m/s in KZN, the design must be able to resist the wind speed and its weight must be at least 15 kg [12]. The majority of sugarcane producing areas in KZN have undulating topography, which must be factored into the pest monitoring equipment design.

3.2 Design cost

Another factor to consider is the cost of the pest monitoring system; if the device is more expensive than the losses produced by the insect in sugar, a farmer may decide that purchasing the gadget is unnecessary, and so demand for the design will be minimal. This enables the designer to select low-cost design components and materials, as well as low-cost manufacturing methods, lowering the device's cost and making it more accessible to all South African farmers. Only in KZN was study conducted to calculate the annual net income per hectare for sugarcane in three regions: the Midlands, the Coast, and the Northern region. **Figure 2** shows that in the worst-case scenario, a small-scale farmer with 30 hectares of sugarcane will earn R899 880 per year in the Coastal region, R1 002990 in the Midlands, and R1 956,330 in the Northern region. As a result, the annual average income for all three regions is R1 286,400. With this in mind, their device should not cost more than R100,000 in order for all farmers to be able to buy it, hence increasing demand.

3.3 Convenience and easy to use

Given that there are more small-scale sugarcane farmers in KZN (20,711) than large-scale sugarcane farmers (1126), most of them will have less knowledge of how to use the device, so a less complex control system must be considered so that they do

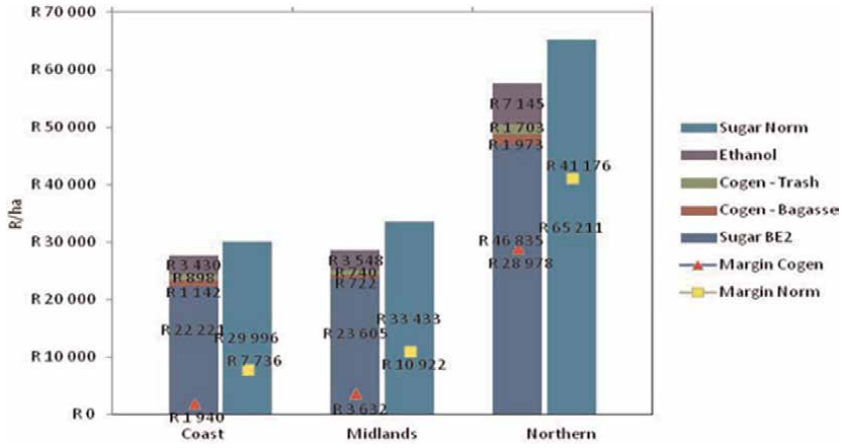

Figure 2.
2020–2022 average annualized income per hectare [13].

not have to hire labor to operate, lowering labor costs. The device must also be serviceable, which means that the design's parts and components must be made locally available.

4. Design methodology

The concept is for an unmanned aerial aircraft to identify the pest on a sugarcane field in the KZN region. The detection system is the principal design function since it is the primary function for solving the problem outlined in Section 1. Infrared thermography revealed the appropriate features needed to address the problem out of six pest detecting sensors. The platform's design, which was chosen to be airborne, serves as a supplementary function. This function was extended to include determining the type of airborne platform, which is the UAV. The hybrid, fixed wing, and rotary wing UAVs were all assessed, and the hybrid was the one that demonstrated the most of the required qualities, such as clear visualization of pest and operation in similar weather conditions in the sugarcane region, as stated in Section 3. Following the conceptual design phase, the preliminary design phase was completed, with the UAV being designed from the wing design forward. A rectangular wing with a one-to-one taper ratio was created. The wing was created with the intention of being a high wing. This was followed by the design of the tail, which was done in the traditional manner. The control surfaces, such as the ailerons, rudder, and elevators, were designed using the wing and empennage proportions. Then came the propulsion system, which consisted of four rotors, each with its own battery. The fuselage was the next in line, and it was designed to fit all of the avionics and other equipment. The landing gear was then designed using computer-aided design (CAD). After the hybrid (VTOL) was designed and assessed (performance analysis), the infrared thermography was created, taking into account the UAV's altitude and cruise speed. Stability, structural stresses, and sustained maximum turning performance were all investigated further. The tilt rotor system was subjected to a rigorous design in order to identify the loads, fatigue, and

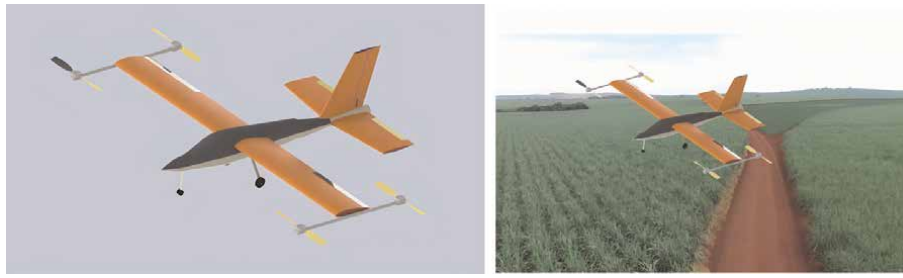

Figure 3.
Final CAD design.

endurance limits. The cost of the entire design was then calculated to see if the farmers could afford it. **Figure 3** depicts the final UAV design.

5. Conceptual design

5.1 Detection system design

5.1.1 User requirements specification

- Requirements
  - The system must detect all types of pests over a $50m^2$ area.
  - The system must be capable of capturing the location of the pests.
  - The device must be able to zoom and capture at least 60 meters away.
  - The system must have a storage capacity of at least 128GB.
  - The system must be self-contained, meaning it must adjust when the detection quality deteriorates.
- Constraints
  - The system must not weigh more than 5 kg.
  - The system must not weigh more than 5 kg.
- Criteria
  - Lower power consumption.
  - High scalability.
  - Low cost
  - Coverage

5.1.2 Concept generation

1. X-ray Imaging

   Two-dimensional projections are possible using this imaging technology. The density affects X-ray absorption. An X-ray source is placed on one side of the object, which is the plants, and an X-ray detector is placed on the opposite side. The X-ray tube emits a short-duration pulse of X-rays, a major portion of which interacts with the investigated object, and some of which pass through the sample and reach the detector, where a radiographic image is created. The degree to which X-rays are attenuated by scattering and absorption within the tissues, where the attenuation properties of tissues range greatly, results in a heterogeneous distribution of X-rays that emerges from the plants.

2. Infrared Thermography

   Infrared thermography (IR) is a technique for determining quantitatively measurable characteristics (temperature) of live organisms. The premise that makes this method virtually universally applicable is that all objects generate IR radiation that is proportional to their temperature due to the movement of molecules, which causes charge displacement and thus electromagnetic radiation in the form of photons. Electromagnetic radiation can be deflected, focussed, or reflected from surfaces that can be utilized with thermo-electronic devices. The wavelength of this radiation ranges from 0.7 to 1000 meters. The IR radiation observed is converted into electrical impulses by IR thermography. Because the majority of infected sugarcane pests are found in the stem, thermal imaging can identify the temperature of the pest by locating the regions where the temperature is high, because the insect's respiration produces heat that is higher than the plant's.

3. Computer Tomography Imaging

   For image processing, computer tomography (CT) uses X-ray radiation, however this approach can create X-ray absorption values by volume elements in the inspected item. It is one of the most useful non-destructive procedures that uses ionizing radiation to provide qualitative and quantitative data. It can visualize the texture and volume fractions of the items under investigation. In a multi-slice CT system, it uses spiral data collecting mode, in which an image reconstruction algorithm calculates 2D pixel values with a third dimension determined by slice thickness.

4. Acoustic Sensor

   The noise level of the pest is used to monitor the noise level as it approaches the predetermined threshold level. It is tuned to capture the pest's lowest sound, such as the sound made by the larva biting the stem. When it detects sound in the calibrated sound level, it must save the position and data. Other sounds, such as those produced by the wind and the equipment that carries it, must also be eliminated.

5. Bioluminescence imaging

   The chemical reaction (oxidation) that causes bioluminescence involves a specific enzyme and light-emitting chemicals. It detects biophoton emission in

response to biotic and abiotic stress, which is thought to be the consequence of endogenous creation of metastable excited states as a result of spontaneous photon emission "representing" the organism's oxidation status. When assessing pest-induced damage, the employment of a monitoring system capable of detecting the biotic stress factor is enabled via spontaneous chemiluminescence. Thus, information about the extent and actual location of the harm caused by hidden pests can be collected indirectly. Physical symptoms must appear on the surface of plant tissues in order to assess the impact of the insect's harm on the entire plant. When the intensity of spontaneous plant autoluminescence is exceedingly low, photomultiplier tubes and photon counting instruments are commonly used.

6. Magnetic Resonance Imaging

The low magnetic nature of hydrogen protons, which have varying behaviors depending on the type of tissue, is used in the magnetic resonance system (MRI). The investigated object is put within a magnet with a magnetic field strength of 0.2–3.0 Tesla (T). Because of the energy absorption, a steady magnetic field is applied by radio-frequency pulses on the suitable resonant frequency, known as the Larmor frequency, generating an excited state of the protons in the sample. These protons emit radio waves, which a receiver coil may detect, resulting in a nuclear magnetic resonance (NMR) signal. The foundation for MR imaging is measuring the intensity of the MR signal, correct spatial placement of signal intensities of various strengths from various sites of the inspected objects, and cross-sectional representation of the signal intensities with greyscale (**Table 2**).

5.1.3 Concept evaluation

Taking into account all of the design requirements, it was discovered that infrared thermography received the highest score, making it the greatest option for visualizing the sugarcane insect.

Criteria	**Max W**	**Concept**											
		X-ray Imaging		**IR Thermography**		**MRI**		**CT Imaging**		**Acoustic Sensor**		**Bioluminescene Imaging**	
		S	**W**	**S**	**W**	**S**	**W**	**S**	**W**	**S**	**W**	**S**	**W**
		(/5)	**S**	(/5)	**S**	(/5)	**S**	(/5)	**S**	(/5)	**S**	(/5)	**S**
Coverage	20	2	8	3	12	3	12	2	8	2	8	3	12
Low Cost	10	3	6	4	8	1	2	2	4	5	10	2	1
Accuracy	30	4	24	4	24	4	24	4	24	3	18	3	18
High resolution	40	4	32	4	32	4	32	4	32	2	16	4	32
Total	100		70		76		62		68		52		66

Table 2.
Detection system evaluation matrix [14].

5.2 Detection platform design

5.2.1 User requirements specification

- Requirements
  - The system must be able to cover at least 50 hectares
  - It must be capable of supporting at least 10 kg the entire mission
- Constraints
  - The system must be able to accommodate the detection system
  - The system must be non-destructive that is it must not interact with the crops
- Criteria
  - Low cost
  - Deployability
  - Maneuverability
  - High ground cover
  - Susceptibility to weather
  - Adaptability
  - Operational complexity

5.2.2 Concept generation

1. Ground Based

   The detection system is carried by the ground-based platform, which functions on the earth's surface in order to produce clear detected data. Handheld cameras (both film and digital), cranes, ground vehicles, tethered balloons, tripods, and even towers are examples. Ground-based devices can give up to 50 meters of raised remote sensing data and are effective for obtaining low-altitude pictures with frequent coverage for dynamic phenomena. These platforms are generally affordable, stable, and give high-resolution data because to their low height.

2. Satellites

   The monitoring system is carried via satellite platforms sent into space. Their orbital geometry and timing can be used to classify them. Geostationary, equatorial, and Sun-synchronous orbits are the three most popular orbits for remote sensing satellites. A geostationary satellite rotates at the same rate as the

Earth (24 hours), therefore it always passes over the same spot on the planet. A satellite in an equatorial orbit circles Earth at a low inclination (the angle between the orbital plane and the equatorial plane).

3. UAV

UAV platforms are aircraft that are controlled remotely by a remote-control operator and do not have an onboard pilot. Unmanned aerial vehicle (UAV), unmanned aircraft systems/vehicles, remotely piloted aircraft (RPA), and drone are all words that are frequently interchanged. According to the Federal Aviation Administration, their weight ranges from 0.2 to 25 kg (FAA).

4. Manned Aircrafts

Aircraft platforms are aerial vehicles that require a pilot to transport the sensor system from one location to another. Low-altitude and high-altitude aircraft are the two types (**Table 3**).

5.2.3 Concept evaluation

After conducting the evaluation process based on the criteria, it is evident that a UAV has shown to be the best solution to the problem.

5.3 UAV platform design

5.3.1 User requirement specifications

- Requirements
    - The design must have maximum take-off weight of at most 30 kg.

Criteria	**Max W**	**Concept**							
		Ground-Based		**Satellites**		**UAV**		**Manned-Aircraft**	
		S	**W**	**S**	**W**	**S**	**W**	**S**	**W**
		(/5)	**S**	**(/5)**	**S**	**(/5)**	**S**	**(/5)**	**S**
Low cost	14.3	4	11.4	1	2.86	4	11.4	2	5.72
Deployability	7.14	3	4.28	2	2.86	4	5.71	2	2.86
Maneuverability	17.9	2	7.16	2	7.16	4	14.3	3	10.7
Sesceptibility to weather	14.3	3	8.58	4	11.4	2	5.72	4	11.4
Adaptability	10.7	2	4.28	2	4.28	3	6.42	2	4.28
High ground cover	17.9	2	7.10	5	17.9	3	10.7	4	14.3
Operational complexity	17.9	4	14.3	1	3.58	5	17.9	2	7.16
Total	100		57.2		50.1		72.2		56.4

Table 3.
Detection system platform evaluation matrix [14].

- The aerial device must aerodynamically support a weight of its components plus the detection system that is at least 15 kg throughout the entire flight envelop.
- The nominal operating altitude must top out 30 metres above the ground level.
- The UAV must have a horizontal stall speed of at most 15 m/s.
- The system must cover a range of at least 50 km and an endurance of at least 1 hr.
- The design must carry a payload of at most 1 kg

- Constraints
  - The UAV must fit a detection system compartment of the dimension 600 mm by 600 mm by 400 mm.
  - The system must be capable of operating autonomously
  - The system must have a wing loading of at most 200 N/m^2.
  - The UAV must have a thrust loading greater than 1
  - Criteria
  - Energy efficiency
  - Field performance required
  - Propeller motion effect on images
  - Turning radius restrictions
  - Easy to maintain
  - Low cost
  - High-speed flight capability

5.3.2 Concept generation

1. Fixed wing UAV

   Fixed-wing Static and fixed-wing aerofoils are predefined for UAVs. To conduct its field performance, this type of UAV requires a take-off and landing field. During the field performance stage, they also have high lift devices such as aps and slats to produce lift. The elevator is used to turn the roll over, the ailerons

are used to pitch, and the rudder is used to produce yaw. The detecting system and autonomous avionics are mounted in the fuselage.

2. Rotary wing UAV

To manage the attitude and position in three-dimensional space, rotary wing UAVs have numerous rotors and propellers pointing upwards, resisting the aircraft's weight, horizontal propulsive force, and other forces and moments. Rotary-winged UAVs exist in a variety of rotor configurations, including helicopters, quadcopters, hexacopters, and other unique designs. The ability to execute vertical take-off and landing (VTOL) as well as hovering and rapid maneuvering are the most distinguishing features of rotary-wing UAVs. The rotors' torque and thrust regulate the UAV's movement, which includes yaw, pitch, roll, and throttle. The detection equipment will be installed beneath the wing.

3. Hybrid UAV

The hybrid UAV is also known as a VTOL UAV since it can take off and land vertically utilizing a rotary mechanism, much like a fixed-wing aircraft. Their control system consists of three controllers: one for horizontal mode, one for vertical mode, and one for transition mode. The detection and control systems are housed within the fuselage.

5.3.3 Concept evaluation

Hybrid This UAV combines the features of a fixed-winged and rotary-winged UAV, making it more suitable for carrying the imaging system, however it is slightly more expensive to produce. As a result of **Table 4**, it is evident that the hybrid UAV outperformed all of their conceptions, and the hybrid UAV will be developed throughout the design development phase.

Criteria	**Max W**	**Concept**					
		Fixed-wing		**Rotary-wing**		**Hybrid**	
		S	**W**	**S**	**W**	**S**	**W**
		(/5)	**S**	**(/5)**	**S**	**(/5)**	**S**
Energy efficiency	14.3	4	11.4	2	5.72	4	11.4
Field performance required	7.14	1	1.43	4	5.71	4	5.71
Turning radius restrictions	17.9	3	10.7	5	17.9	4	14.3
Propeller motion effects on images	25	4	20	2	10	4	20
High speed flight capability	3.57	4	2.86	2	1.43	4	2.86
Easy to maintain	17.9	4	14.3	5	17.9	3	10.7
Low cost	14.3	3	8.58	4	11.4	2	5.72
Total	100		69.3		70.1		70.7

Table 4.
UAV feasibility analysis [14].

6. UAV design development

6.1 Mission requirements and parameter estimation

The flight profile mission must be determined before any design vehicles are considered. Because this vehicle will be classified as a mini-VTOL UAV, the mission profiles will be limited. The UAV's range must be at least 10 kilometers, as estimated by statistical analysis of existing VTOLs such as the Bluebird Skylite, AV RQ-11B Raven, AV Switchblade, and AV UAS: Wasp AE. Hovering is the stage where the aircraft transitions from VTOL to fixed-wing mode. The UAV must be able to cruise at a maximum altitude of 60 meters, as most IR thermographies, such as the Hikvision thermal Bi-spectrum network bullet camera and the Flir Duo Pro thermal camera, have a maximum capturing distance or altitude of 60 meters. The UAV's endurance must also be at least one hour (**Figure 4**).

Initial weight estimation and weight build-up is given as below:

$$W_{TO} = W_{struct} + W_{avi} + W_{prop} + W_{fuel} + W_{misc} + W_{pauload} \quad (1)$$

where W_{struct} is the airframe structures + motor casing + tilt rotor mechanism + the landing gear, W_{avi} is the weight of Servos + Sensors, W_{prop} is the weight of the propulsion system, W_{fuel} is the weight of fuel cells and/or batteries, W_{misc} are the miscellaneous Weights such as in connecting wires, fasteners and $W_{pauload}$ is the payload that is the detection system.

- 15 kg is thought to be the starting weight (without payload). The available options at several internet sites are used to determine avionics, propulsion, fuel, payload, and miscellaneous weights.

- Thrust loading must be greater than one for vertical take-off and landing. Using the stall speed as an example: 1.78 Thrust Loading The aspect ratio has been set to 8.0 to give superior glide performance throughout the cruise and loiter phases, as well as the ability to cruise at low thrust without a large descend angle. To match mission requirements, constraint analysis is performed at a stall speed of roughly 14 m/s. Without lift-enhancing devices, the wing loading is bound by velocity and coefficient of lift, which is typically up to 1.4 (**Figure 5**).

From the constraint analysis the marked region in red is the region of operation at stall. At this region for various speeds of stall the optimum wing loading is around $164 N/m^2$.

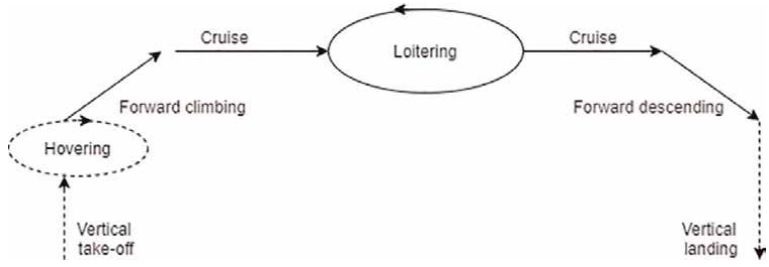

Figure 4.
Mission profile.

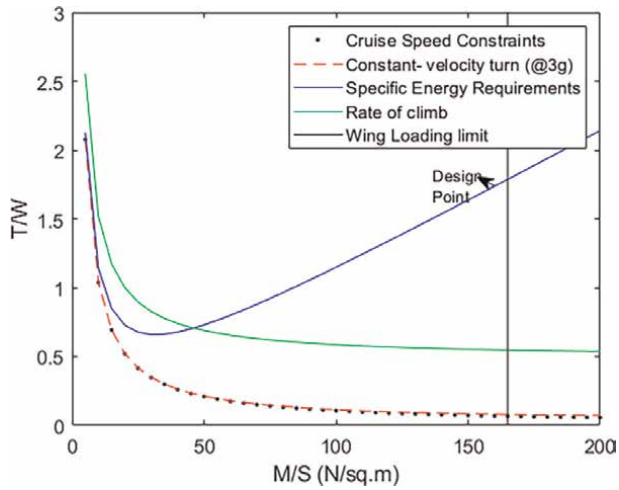

Figure 5.
Constraint analysis.

6.2 Wing design

Dihedral is not necessary because the wing attachment on the UAV is to be high wing and made roll stable. As a result, the dihedral angle is $\mathbf{0^o}$. The UAV is not designed for high speed, and the motor mechanism will be located near the tip of the wing, with a taper ratio of one. The Mach number sweep is 0o since the UAV is not meant to achieve high Mach numbers and does not face drag divergence. The wing loading range obtained yielded a wing surface area of 1.221 $\boldsymbol{m^2}$. The span (b) is 3.127 meters, while the chord (c) is 0.25 meters.

6.2.1 Airfoil selection

The airfoil was chosen by comparing the NACA 4 series to the other NACA series, which are the 5 and 6 numbers, because the NACA 4 series is thought to have a higher maximum lift coefficient, as Raymer proved. As a result, the lift, drag, and pitch moment coefficients of three NACA 4 series airfoils, the NACA 0012, 2412, and 4412, were compared. In the event of an air gale or other disturbance, a negative moment coefficient is desirable to aid maintain level flying. However, if this moment is sufficiently negative, the aircraft may be difficult to control. The NACA 4412 airfoil was ruled out due to its huge negative moment coefficient (**Figures 5** and **6**).

The NACA 2412 airfoil has a relatively small negative moment coefficient at practically all angles of attack, as seen in **Figure 7**. As a result of the analysis, the NACA 2412 has been chosen as the airfoil for the UAV since it possesses the required properties.

6.3 Tail design

The main aim of the empennage is to provide stability and counter moments caused by the wing. Horizontal and vertical stabilizers make up the empennage. A conventional tail was chosen because of its simplicity, which makes it simple to construct, as well as the fact that it meets both longitudinal and directional trim and stability criteria. The tail volume coefficients are used to design the empennage.

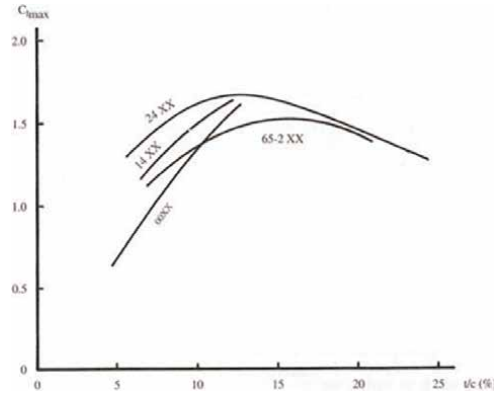

Figure 6.
Clmax vs. percent thickness to chord.

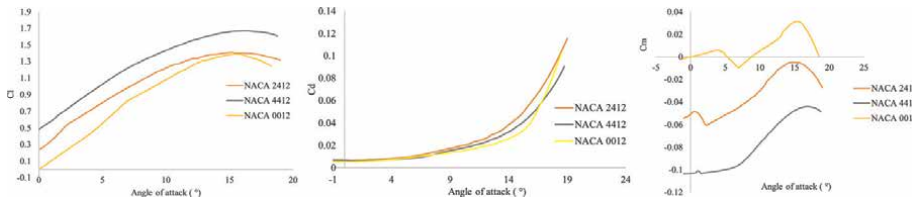

Figure 7.
Airfoil selection parameters.

Vertical tail volume coefficient is given by:

$$V_v = \frac{l_{vt} S_{vt}}{S_w b_w}$$

Horizontal tail volume coefficient is given by:

$$V_h = \frac{l_{ht} S_{ht}}{S_w \bar{c}_w}$$

According to Raymer, the horizontal and vertical tail volume coefficients for an agricultural UAV are chosen to be 0.5 and 0.04 respectively (**Table 5**) [15].

6.4 Control system design

The ranges shown in **Figure 8** were used to size the control system.

6.5 Propulsion system selection

6.5.1 Fuselage design

Given the thickness of the detection system, the diameter was determined to be 500 mm. The detection system (camera), batteries, servos, and control system were all designed to fit inside the fuselage. The fuselage length was then calculated to be 75% of the wingspan, followed by the lofting process. The fuselage is lofted in order to

Parameter	Symbol	Value
Horizontal tail area (m^2)	S_h	1.221
Tail arm	l_h	0.648
Aspect Ratio	AR_h	5.33
span (m)	b_h	1.399
Root chord (m)	C_{r_h}	0.4318
Tip chord (m)	C_{t_h}	0.3455
Mean chord (m)	MAC_h	0.2622
Taper	λ_h	0.8
Sweep (°)	Λ_h	0
Dihedral (°)	Γ_h	0
incident (°)	i_h	−1.26
Parameter	Symbol	Value
Vertical tail area (m^2)	S_v	0.235
Tail arm	l_v	0.648
Aspect Ratio	AR_v	1.5
span (m)	b_v	0.5933
Root chord (m)	C_{r_v}	0.2966
Tip chord (m)	C_{t_v}	0.4944
Mean chord (m)	MAC_v	0.396
Taper	λ_v	0.6
Sweep (°)	Λ_v	35
Dihedral (°)	Γ_v	15
incident (°)	i_v	−1.26

Table 5.
Geometrical parameters of designed empennage.

Control surface	Elevator	Aileron	Rudder
Control surface area/lifting surface area	$S_E/S_h = 0.15–0.4$	$S_A/S = 0.03–0.12$	$S_R/S_V = 0.15–0.35$
Control surface span/lifting surface span	$b_E/b_h = 0.8–1$	$b_A/b = 0.2–0.40$	$b_R/b_V = 0.7–1$
Control surface chord/lifting surface chord	$C_E/C_h = 0.2–0.4$	$C_A/C = 0.15–0.3$	$C_R/C_V = 0.15–0.4$

Figure 8.
*Control surface design parameters (**Table 6**) [16].*

increase the fuselage's overall aerodynamic performance. This entails reducing fuselage drag and generating a reasonable amount of lift from the fuselage. A rounded rectangle was initially chosen because to its ease of fabrication and component housing, however it had a bigger frontal area and wetted surface area, resulting in significant drag. In order to reduce drag and optimize the design, an oval cross-section with a small frontal area was chosen. In addition, an effort was made to limit the amount of wetted surface area. Because there were no components in the aft part of the fuselage,

Parameter	Value
Max thrust /rotor	14 kg
Recommended battery	12SLiPo
Recommended take-off weight / rotor	4.5 to 7.0 kg
Operating temperature	(−10 to 50°
Motor	
Stator size (mm)	100 by 10
KV	120 rpm/V
Propeller	
Diameter (mm)	669.4
Number of blades	2
Weight	0.161 kg
ESC	
Max allowable voltage (V)	52.2
Max allowable current (A)	80
Max peak current (A)	120

Table 6.
Battery and motor specification.

the volume was reduced and a boom was used. This resulted in a large reduction in overall wetted surface area and, as a result, a significant reduction in parasitic drag.

6.6 Tilt rotor mechanism

Unmanned aerial vehicles with vertical take-off and landing capabilities take off and land vertically. It takes off vertically from the ground, then transitions to a stage when the tilt-rotor mechanism is utilized to tilt or rotate the motors about the y-axis (body-fixed frame) in order to take off vertically and cruise like a fixed-wing. To lift the fixed-wing aircraft, the VTOL UAV has four rotors at the tips of the wings. During the take-o_ phase from the leading edge of the, the leading-edge motors face upwards, while the trailing-edge motors face downwards. During the cruise, the rotors in the front operate as tractors, while those in the back act as pushers. The C.G. is located at

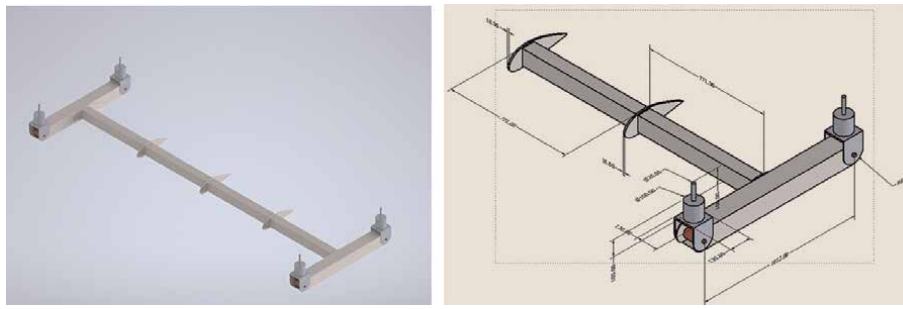

Figure 9.
Tilt rotor mechanism.

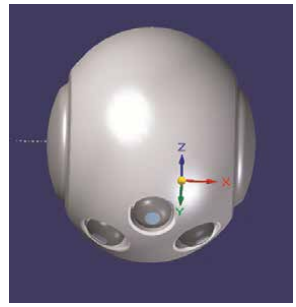

Figure 10.
Camera housing and the FLIR Vue pro R640.

the intersection of motor diagonals, ensuring that no superfluous seconds are generated. Through a spar, the tilt-rotor system is connected to the wing (**Figure 9**).

7. Infrared thermography design

The infrared thermography was created using the UAV's characteristics, such as cruising altitude, turning radius, and cruise speed. The major goal is to get the best detection quality while minimizing flight and picture processing time. The flight parameters of the UAV, such as altitude, image overlap, and flight speed, must be considered to determine the optimum sensor parameters, such as sensor resolution, exposure time, image acquisition rate, focal length, and camera angle, in order to find an adequate compromise between quality and efficiency (determining the field-of-view). All of these factors influence image metrics such as ground resolution and the number of photos required per region. Following the coverage area calculations, the optimum detector size at 60 m was determined to be 614 by 512, with a focal length of 9 mm and pixel size of 11.7 μm, yielding a horizontal field of view (HFOV) of 45.2^0, a vertical field of view (VFOV) of 36.8^0, and a diagonal field of view (DFOV) of 51.80. Thus, the horizontal width was determined to be 175.87 m and the vertical width to be 23.98 m, To achieve this, a thermography with at least 12 Megapixels was discovered to be necessary, and the FLIR Vue Pro R640 camera was proven to be sufficient for visualizing the pest (**Figure 10**).

8. Design analysis

8.1 Aerodynamic analysis

8.1.1 Parasite drag calculation

(**Table** 7)

8.1.2 Drag polar

Because it can be used to determine other performance metrics, the drag polar is important in characterizing and designing a UAV. Eq. (2) describes one form of the drag polar, which is based on the assumption that the least drag occurs at zero lift (**Figure 11**).

Component Name	S_wet (m^2)	L_ref (m)	t/c or d/l	FF	Re	Cf	Q	f (m^2)	D/q
Main Wing	2.350	0.39	0.150	1.331	711,043	0.00477	1	0.0149	0.0122
Fuselage	1.222	2.324	7.789	1.084	4,237,088	0.00346	1	0.00458	0.00375
htail	1.047	0.391	0.118	1.248	713,420	0.00477	1	0.00623	0.00510
vtail	0.460	0.407	0.118	1.248	742,821	0.00473	1	0.00271	0.00223
VTOLArm	0.189	1.1	37.143	1.007	2,005,506	0.00394	1	0.000749	0.000614
[B] Box	0.054	0.1	2.311	1.994	182,319	0.00628	1	0.000673	0.000552
VTMotor	0.0620	0.0265	0.309	0.246	48,314	0.00847	1	0.129	0.000106
MainGear	0.0311	0.253	15.343	1.027	460,896	0.00519	1	0.000166	0.000136
Wheel	0.0413	0.03	0.300	0.269	54,695	0.00822	1	0.0911	7.47E-05
Axle	0.000516	0.05	10.130	1.053	91,159	0.00731	1	0.000004	3.26E-06
FrontGear	0.00591	0.205	20.766	1.017	373,753	0.00541	1	0.000032	2.67E-05
Wheel	0.0110	0.01	0.201	0.878	18,232	0.0108	1	0.104	8.55E-05
Axle	0.000405	0.04	8.104	1.078	72,927	0.00769	1	0.000003	2.75E-06
PropGeom	0.259	0.061	0.500	5.750	110,421	0.0070	1	0.0104	0.00855
								Cd_o	0.027458

Table 7.
Parameters for parasite drag calculation.

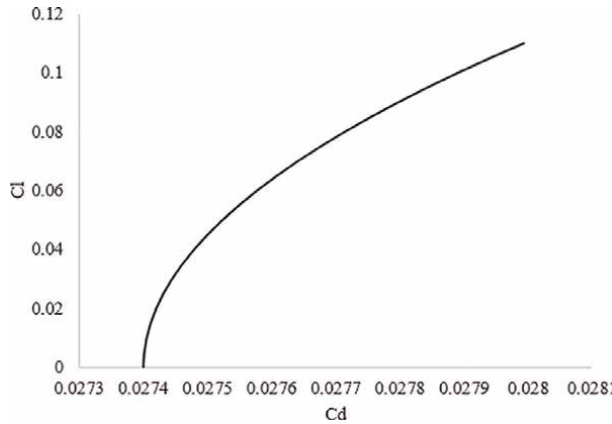

Figure 11.
Drag polar.

8.2 Thrust modeling

8.2.1 Performance analysis

(**Figure 12**)

8.2.1.1 Field performance

Because the UAV is a VTOL, there is no need for a ground roll, but the take-off and landing can be evaluated based on the vertical height gained during take-off and

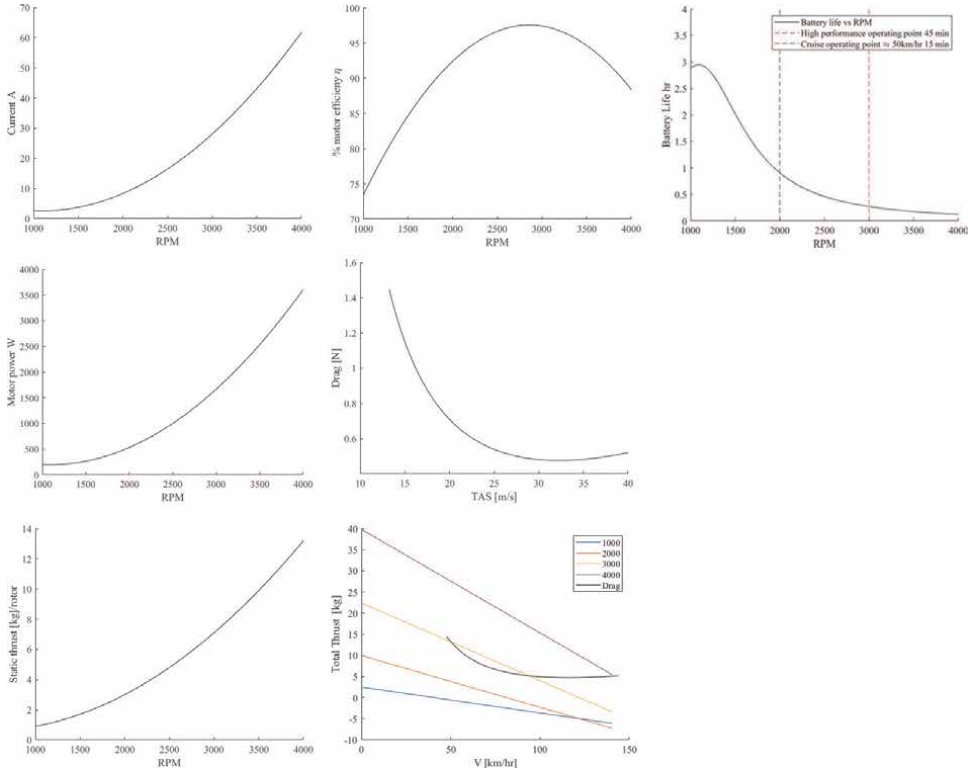

Figure 12.
Thrust modeling graphs.

landing. The equation below was calculated using Newton's equation of motion (**Figure 13**),

$$Z = \left(\frac{T\cos\theta - mg}{2m}\right)t^2 - V_{z_0}t$$

where Z is the vertical distance, T is the thrust, m is the mass and V_{z_0} is the stall velocity (**Figure 13**).

The maximum take-off obstacle height was found to be 293 m, while the maximum landing obstacle height was found to be 187 m, for various throttle settings with a time constraint of 10s.

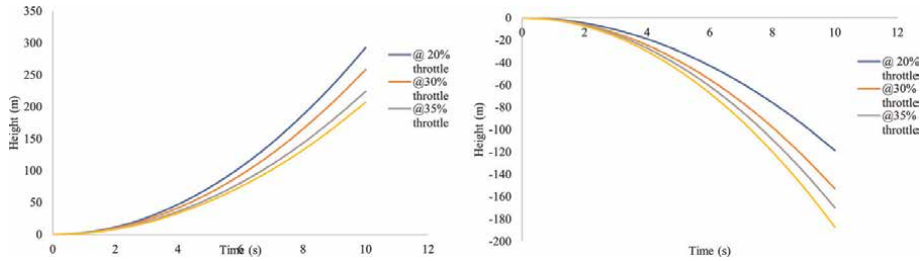

Figure 13.
Take-off performance (left) and landing performance (right).

8.2.2 Transition phase

(**Figure 14**)

8.2.3 Climb performance

$$ROC = \frac{Power_{required} - Power_{available}}{Weight}$$

where $Power_{available}$ is calculated by multiplying the battery efficiency by battery current hour and the voltage that is 0.85 by 48AmpH by 12 respectively. The $Power_{required}$ is the required power for climbing which can be determined by multiplying thrust require by velocity. Thus, from the graph, the optimum rate of climb is 12.58 m/s and the climb speed is 15.08 m/s. **Figure 15** shows the climb performance graphs.

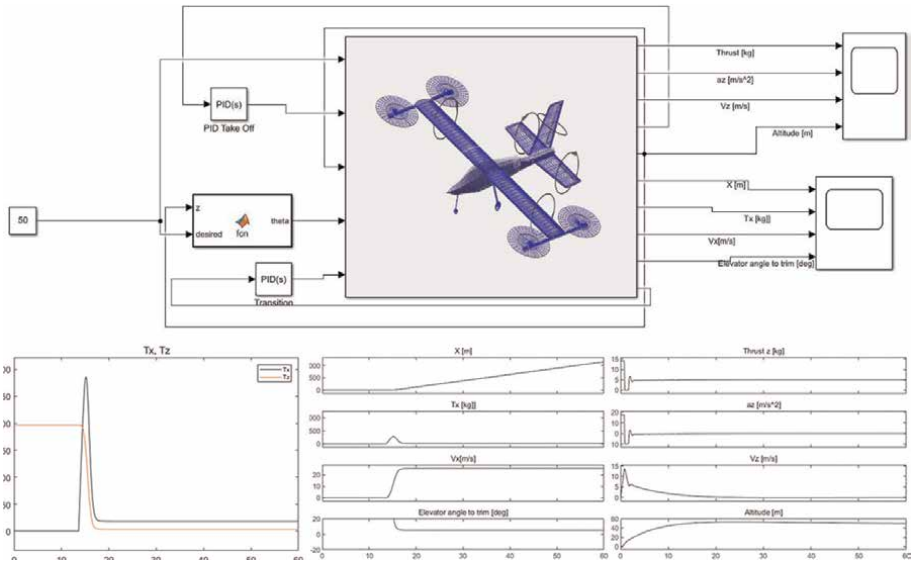

Figure 14.
Simulink model and the transition parameters all against time.

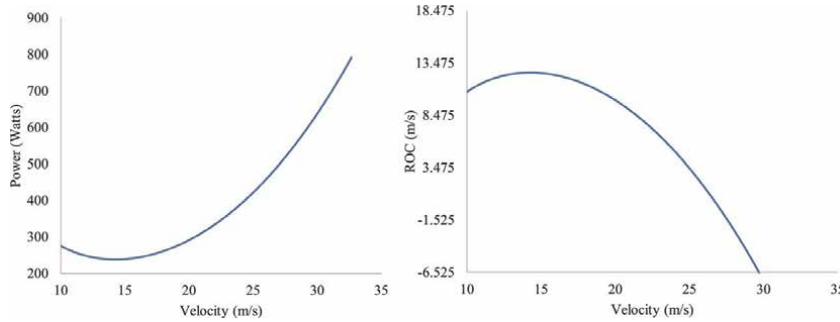

Figure 15.
Climb performance.

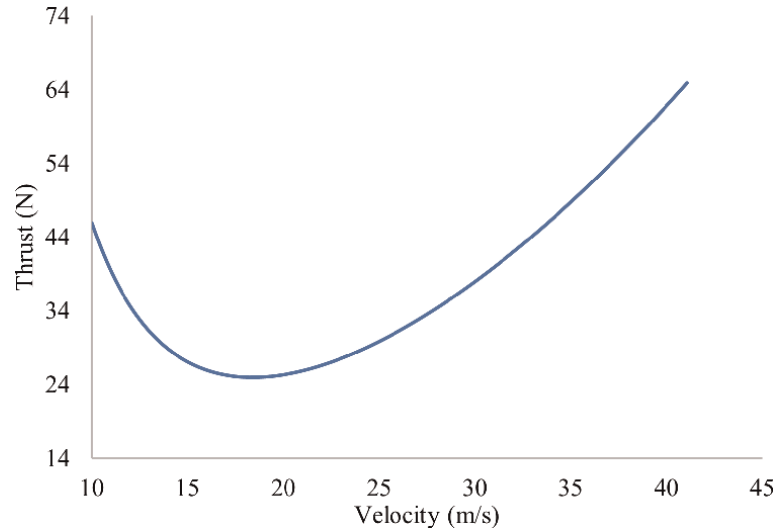

Figure 16.
Thrust against velocity.

8.2.4 Cruise performance

The cruise performance of the design is shown in **Figure 16**. Frome the graph the cruise speed is the at the minimum thrust that is 18.06 m/s.

8.2.5 Range and endurance

The maximum endurance can be determined by:

$$E = \frac{\eta_{batt} \times volt \times Ah}{\frac{1}{2}\rho S_w C_{d0} V^3 + \frac{2KW^2}{V}}$$

that is E = 1.487 h. Range can be calculated by multiplying endurance with velocity which give 96.7 km.

8.2.6 VN diagram

The applied loads during the UAV's operational life flight and ground conditions must be known in order to create the final configuration. The load factor diagram depicts these three restrictions, with each point representing the load condition of the UAV when maneuvering at the true airspeed UAV data required to construct the load factor diagram. The safety flight conditions are provided within the limitations of the load factor diagram. Wind gusts are ascending air motions perpendicular to the ground that affect the angle of incidence and relative speed of the aircraft. Gust loads can be thought of as an increase in the load factor, necessitating the creation of a new safety field. **Figure 17** shows the wind gust load and load factor diagrams. The entire flight envelope diagram is created by superimposing the maneuverings and wind gust diagrams and is used to define the appropriate field in which the UAV can design the building.

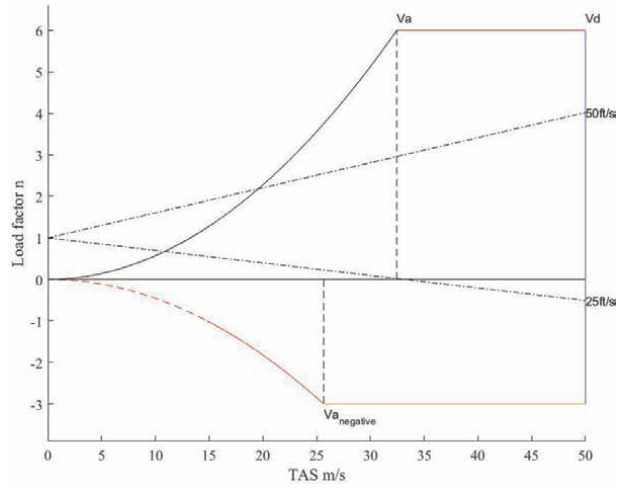

Figure 17.
VN diagram and flight envelop velocities.

8.2.7 SEP chart

The SEP chart was used to determine the design's maximum sustained turning performance for various altitudes and load factors. The SEP lines within the SEP envelope are all positive, indicating that the UAV has extra energy to do maneuvers, climb, or avoid collisions (in most cases). However, this is more power than the mission requires. Thus, boosting efficiency by employing a smaller motor and reducing battery weight while increasing endurance and preserving SEP values would be an improvement in future development. The aircraft can climb at speeds of up to 7000 feet per minute and beyond, well beyond the needed design value (**Figure 18**).

8.3 Stability analysis

It is ideal for the Cg position to be at 20–30 percent MAC because this reduces the required elevator deflection in the most operating range of speeds (cruise). 15 degrees is the elevator angle that is practical to trim during transition because the tail will deflect to trim the aircraft for the UAV to be stable, according to the graph (**Figure 19**) (**Table 8**).

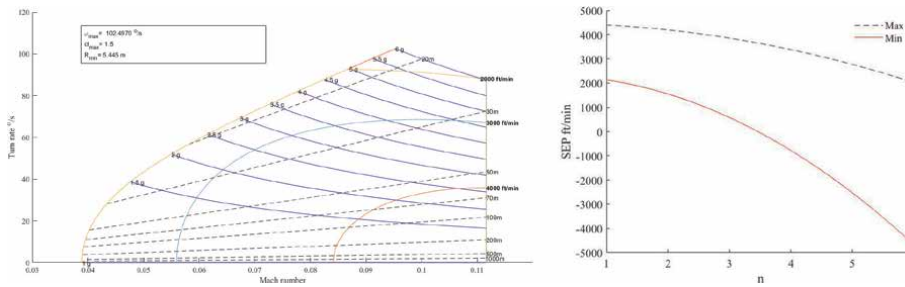

Figure 18.
Maximum and minimum SEP (right) and SEP chart (left).

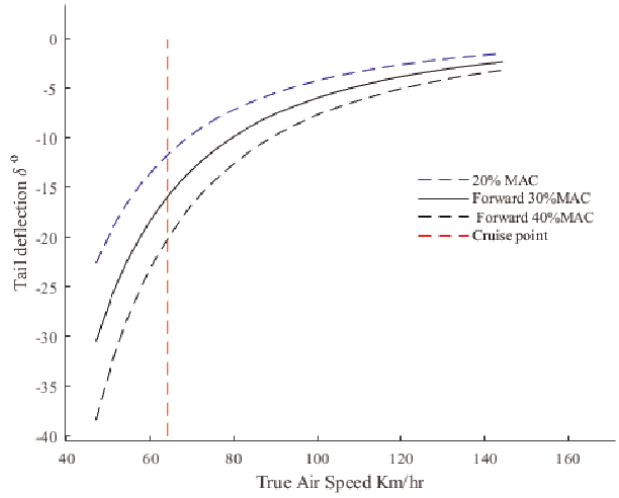

Figure 19.
Trim curves.

9. Cost analysis

Item	Description	Quantity	Cost
Propulsion System			
Battery	12 V 12LiPO	4	R1,200.90
Motor	100*10 mm (stator size)	4	R3,126.96
Propeller blades	Fabrication	4	R1,000.00
Avionics			
Servo	—	9	R651.51
Lidar	—	1	R1,110.00
GPS	IMU magnetometer		R1,120.00
Wheels	Vulcanized rubber	3	R890.00
Structural framework	Fabrication	1	R4,500.00
Payload Components			
Camera	FLIR Vue pro R640	1	R42,595.20
Grand Total			R56,193.67

Table 8.
Bill of materials.

10. Conclusion

In this project, a fixed wing VTOL UAV is successfully deigned (conceptual) and analyzed for its aerodynamic, performance and stability parameters and the results obtained are as per the mission requirements (**Figure 20**) (**Table 9**).

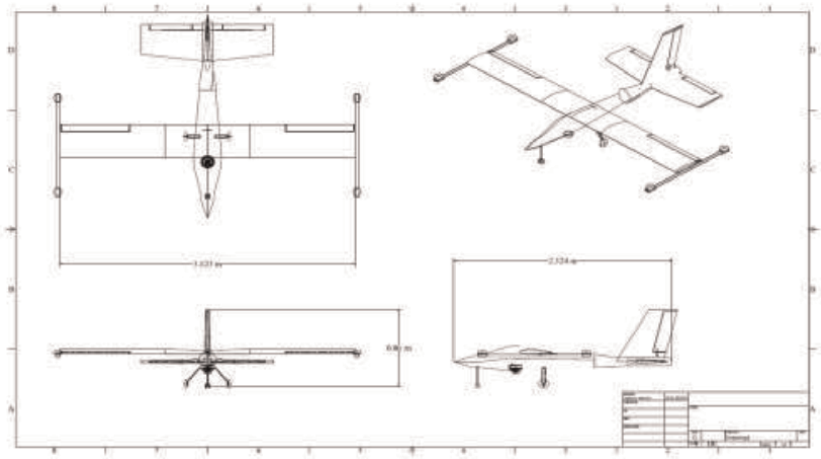

Figure 20.
Three views.

URS	Design	Percentage
Endurance of at least 1 hr	1.487	48.7
Range of at a least 50 km	96.7 km	93.4
Payload of at most 1 kg	2	100
Total weight of at most 30	20.043	−33.19
stall at most 15	13.7	−8.667
Thrust loading at least 1	2.74	174
Altitude of at least 30	60	100

Table 9.
Justification.

Author details

Alphanos Mahachi*, Trymore Aloni and Lucious Mashevedze
The School of Mechanical, Industrial, and Aeronautical Engineering, Wits University, Johannesburg, South Africa

*Address all correspondence to: 1994304@students.wits.ac.za

References

[1] SASA. Where we are Located? Technical Report. Pretoria, South Africa; 2019

[2] Statistics South Africa. Stats SA Releases Census of Commercial Agriculture 2017 Report | Statistics South Africa [Online]. Statssa.gov.za; 2020. Available from: https://www.statssa.gov.za/?p=13144 [Accessed: 1 May 2022]

[3] Nicol RM, Ortmann GF, Ferrer SR. Management decisions on commercial sugarcane farms in KwaZulu-Natal: A focus on choice bracketing behaviour for risk management. Agrekon. 2008;**47**: 116-139. DOI: 10.1080/03031853.2008.9523793

[4] Potgieter J, Vuuren V, Conlong D. Modelling the effects of the sterile insect technique applied to Eldana saccharina Walker in sugarcane. ORiON. 2012;**28** (2):59. DOI: 10.5784/28-2-112

[5] Azfar S, Nadeem A, Basit A. Pest detection and control techniques using wireless sensor network: A review. Journal of Entomology and Zoology Studies. 2015;**3**:2

[6] Wang B et al. Towards detecting red palm weevil using machine learning and fiber optic distributed acoustic sensing. Sensors. 2021;**21**(5):1424-8220. DOI: 10.3390/s21051592

[7] Bioucas-Dias JM et al. Hyperspectral remote sensing data analysis and future challenges. IEEE Geoscience and Remote Sensing Magazine. 2013;**1**(2):6-36. DOI: 10.1109/MGRS.2013.2244672

[8] Monno Y, Kitao T, Tanaka M, Okutomi M. Optimal Spectral Sensitivity Functions for a Single-Camera One-Shot Multispectral Imaging System [Online] Undefined. Tokyo, Japan; 2012. Available from: https://www.semanticscholar.org/paper/Optimal-spectral-sensitivity-functions-for-a-system-Monno-Kitao/d07717d49051fbf7abd80510176acb47624b3507 [Accessed: 1 May 2022]

[9] Matavire MM. Impacts of sugarcane farming on coastal wetlands of the north coast of Zululand, Kwadukuza, South Africa. Technical Report. KwaZulu Natal, South Africa; 2015

[10] Singh RG. Landslide Classification, Characterisation and Susceptibility Modelling in KwaZulu Natal (thesis). Technical Report. Johannesburg: Faculty of Science, University of the Witwatersrand; 2009

[11] Cowan GI. Wetlands of South Africa. Technical Report. Pretoria: Department of Environmental Affairs and Tourism; 1995

[12] Shikwambana L et al. Qualitative study on the observations of emissions, transport, and the influence of climatic factors from sugarcane burning: A South African perspective. International Journal of Environmental Research and Public Health. 2021;**18**(14):7672. DOI: 10.3390/ijerph18147672

[13] Botha D. Unpublished Draft [masters dissertation]. Department Agricultural Economics, Extension and Rural Development, University of Pretoria; 2014

[14] Mahachi A. Agriculture Pest Surveillance UAV. Johannesburg, South Africa: School of Mechanical, Industrial and Aeronautical Engineering, University of the Witwatersrand; 2021

[15] Raymer D. Aircraft Design: A Conceptual Approach. American Institute of Aeronautics and Astronautics, Inc.; 2012

[16] Sadraey MH. Aircraft Design: A Systems Engineering Approach. New Hampshire, USA: Daniel Webster College; 2009

Chapter 2

Review of Agricultural Unmanned Aerial Vehicles (UAV) Obstacle Avoidance System

Uche Emmanuel

Abstract

Unmanned aerial vehicles (UAVs) are being used for commercial, scientific, agricultural and infrastructural enhancement to alleviate maladies. The objective of this chapter is to review existing capabilities and ongoing studies to overcome difficulties associated with the deployment of the agricultural unmanned aerial vehicle in obstacle-rich farms for pesticides and fertilizer application. By review of various literature, it is apparent that the potential for real-time and near real-time exists but the development of technology for quality imagery and rapid processing leading to real-time response is needed. The Infrared, time of flight and millimeter wavelength radar sensors for detecting farm and flight environment obstacles appear promising. The autonomous mental development algorithm, and the simultaneous localization and mapping technology are, however, ahead of others in achieving autonomous identification of obstacles and real-time obstacle avoidance. They are, therefore, found fit for further studies and development for deployment on agricultural unmanned aerial vehicles for obstacle-rich farms.

Keywords: unmanned aerial vehicle, obstacle avoidance, sensors, spraying, obstacle-rich farm

1. Introduction

Topical in Nigeria today is, therefore, the intractable problem of sustainable economic growth whose precursor are people and capital formation. The proximate cause of economic growth is an increase in knowledge and its application in increasing the amount of capital or other resources per head. It is axiomatic that the motivation for agricultural mechanization is to reduce drudgery, increase productivity and return on investment and ultimately enhance capital formation for economic growth. But for a labour surplus, country like Nigeria agricultural mechanization is considered toxic to employment since the sector is responsible for the livelihood of over 70% of the population who are mostly into subsistence agriculture. Today agriculture has become a poverty incubator of the country wherein over 40% of the population are within the poverty bracket earning less than one dollar a day [1]. This is not because farming is not a profitable vocation but the native approach to the business of farming

fall below global best practice creating a poverty trap for 70% of the population with the concomitant avalanche of societal problems such as high crime rate, insurgency, hyper inequality in income distribution and unstable national structure. As Lewis [2] noted, the traditional agricultural sector is characterized by zero marginal labour productivity.

Farmers in more developed climes use sophisticated technologies such as robots, temperature and moisture sensors, aerial imaging, drones and GPS technology in the area of precision agriculture to ensure high productivity, more profit, efficiency, safe and environmentally friendly farming [3]. As a result, only 12–15% of the gainfully occupied population suffice to feed the people in developed countries [2]. In contrast and at the low level of productivity 60–70% of the gainfully occupied population is needed in agriculture for the same purpose in Nigeria. For instance, Ukrainian GDP comes from the agriculture sector that employs just around 20% of its population [4]. It, therefore, becomes imperative that all hands especially those entrusted with the responsibility for defending and building the nation must be on deck to salvage the nation.

A sure step toward this is to unleash the power of modern agricultural technology on this critical sector to free this trapped population to the various value chains of agriculture expected to be induced by higher production and productivity of mechanized farming. More importantly is that the released population will create a huge market for farm produce as they no longer depend on the below optimal subsistence farming to feed and cater for their daily need. Today this tepid population adds nothing to the off-take of agricultural products and services as they can neither afford to buy nor have felt the need for them, choosing instead to live on their meager production or go into crime.

This debilitating state of affairs demands massive attacks from both grounds—tractorization and air-agricultural UAV. The development of advanced electronics, global positioning systems (GPS) and remote sensing have enabled advancements in the practice of precision agriculture whereby agronomic practices are based on variations in soil, nutrition and crop stress [5]. Fortunately, Nigeria is endowed with enormous land resources relative to its population. It will create not only jobs and market up front but also provide the adequate raw material for the various high capacity processing plants doting the country and currently operating far below-installed capacity due to lack of raw materials and limited market. Typical examples abode such as the tomato, sugar cane, rubber, oil palm, breweries, rice mills and other plants which cannot adequately source the local content of their raw material need.

The proper implementation of artificial intelligence (AI) in agriculture will help the cultivation process and create ambiance for the agricultural value chain market. Such development in Nigeria's agriculture sector will boost rural development and rural transformation and eventually result in structural transformation of the national economy.

2. Unmanned aerial vehicles (UAVs)

UAVs come in different forms and for different purposes. Purposes include military and civil applications such as firefighting, reconnaissance for natural disaster, border security, traffic surveillance etc. UAVs are deployed in agriculture in many areas such as spraying and fertilizer application, seed planting and weed recognition, diagnosis

of insect pests and artificial pollination, irrigation assessment, mapping and crop forecasting [6]. Pedestrian classification of UAVs is by use; photography, aerial mapping, surveillance, cinematography, agricultural etc. UAVs are better categorized by type; multi-rotor, fixed-wing, single rotor and fixed wing multi rotor hybrid with varying capabilities on altitude, control range, flight endurance and air speed. UAVs are further classified by their drive to include electric; where electric battery is used, solar; where solar cells are the source of energy and internal combustion engines; where they are driven by gasoline or methanol-fueled combustion engines [7]. For agricultural purposes, Vroegindeweij et al. [8] categorized UAVs into three as—fixed wing, vertical take-off and landing (VTOL) and bird/insect. According to Banjo and Ajayi [9], hybridization resulted in higher flying altitude, wider control range, increased speed and longer flights time, factors which are at variance with the demands on Ag UAVs of low altitude, low speed but agrees with Ag UAVs need of longer flight time and wider control range. Hence, for low altitude remote sensing (LARS), most Ag UAVs are of low cost, low speed, lightweight, low payload weight capabilities and short duration. UAVs for pesticide spraying and fertilizer application, however, need to be of higher payload weight and able to support longer flight endurance [5].

2.1 Agricultural unmanned aerial vehicles (Ag AUV)

The use of aerial system is necessary not only to ensure precision in agriculture for optimum utilization of inputs and efficacy and mitigation of the environmental impact of excess application inorganic agrichemical, but also times the only mechanized means to overcome obstacles limiting ground operations such as terrain, soil compaction, swamp etc. Moreover, with an increasing knowledge-based population inclined more to the mental white-collar job than to physical blue-collar job sourcing farmhands for even routine farm operations as pest and disease control (PDC) is becoming arduous necessitating deployment of agricultural technology to achieve the desired outcome. The innovative UAV platform for farming may lure the youth to rural areas having afforded a comfortable working environment and reduced farm drudgery thereby generating employment opportunities in the rural sector which may address social balance. Piloted aircrafts are used to carry out spraying and aerial imaging on large fields in a short time but these are not readily available in all areas and so UAVs are used especially on smaller fields. UAVs are considered to have high efficiency, low labour intensity and low comprehensive cost [10].

The deployment of UAV platforms for agriculture started in 1983 when the first remote-controlled aerial spraying system (RCASS) was built, followed in 1990 by an R50 helicopter with a payload limit of 20 kg and a laser system for height determination. Currently, low-volume UAV helicopters with fully autonomous unmanned vertical take-off and landing (VTOL) and spraying capacity of up to 7.7 kg, integrated with the flight control system of the UAVs show high potential for vector control in areas not easily accessible by ground services. Some agricultural spraying unmanned helicopters now have plant protection parameters as shown in **Table 1** [7, 11].

Agricultural unmanned vehicles (Ag UAVs) are used to optimize agricultural operations, increase crop production, monitor crop growth, sensor and produce digital imagery and to give a clear picture of the status of farm to a farmer, especially on large farms. Ag UAVs have, therefore, become a prerequisite for precision agriculture toward rapid industrialization of agriculture.

Items	Index
Length of spraying rod	140 m
Spraying height (above crop)	1–3 m
Nozzle number	6pcs
Spraying flow rate	3.0–4.4 liter/min
Agrochemical tank volume	18.0 liter
Spraying time per flight	4–9 min
Spraying width	6–8 m
Covering area of one flight	1.0–1.2 hectare

Table 1.
Plant protection parameter (QF170-18L AgriSpraying Helicopter).

The limited scale adoption of aerial services relative to other methods of farming service tools is not unconnected with the high cost of the service, short flying time, the unreliability of the equipment, the uncertainty of the quality of operations, risk of liquid spray being airborne to unintended targets and the fact that flying of UAVs is under aviation laws [7]. Moreover, most Ag UAVs operations are done through manual remote control rendering the outcome susceptible to the skill level of the operator [5]. It is therefore imperative as a solution, to realize real-time autonomous OA technology to assuage the fears of many farmers on the safety and quality of UAVs services.

The deposition of pesticides on plants with the use of UAVs is the combined effect of the jet of liquid being sprayed and the stream of air generated by the rotors [7]. Hence, the efficacy of aerial spraying depends on the speed, droplet drift, flight altitude, weather, type of pesticide, temperature and terrain, the goal being to achieve blanket spraying or spot spaying of targets. The efficacy of the spaying is therefore subject to the behavior of the UAV airframe. The rush of air from the rotor changes because of the varying operation load of the UAV on the discharge of the spraying mix content of the tank thereby inducing a difference in the concentration of droplets in the air stream between the start, along with and end of spraying operation. Hence, the quality of UAV spraying may not meet that of manned aerial and ground systems [7].

2.2 Agricultural unmanned aerial vehicles (Ag AUV) obstacle avoidance technology

The objective of this chapter is to examine the literature on existing capabilities and ongoing studies to overcome difficulties associated with the deployment of agricultural UAVs on obstacle-rich farms for pesticides and fertilizer application.

Small size, fragmentation, multiple farmlands, undulating, fallow, beast, human and meandering boundary are all characteristics of a typical Nigerian farm holding. Forested areas, tall trees, electric poles and wire, farm structures, birds and some reflecting objects, wireless networks and hot and stormy weather abound in the flying environment. Furthermore, when operating on farmland, Ag UAVs are typically 1–1.5 m above the ground, posing ground operation challenges such as small trees in the middle of the farm, stacking poles, robes, molehills, undulation terrain, out-growths and so on. Flying dust and liquid smudge the spraying farm environment, making it impossible to use visual obstacle avoidance systems. As a result, an

autonomous system is required to manage these complex and constantly changing aerial farm environments and spraying variables.

An agricultural unmanned vehicle obstacle avoidance (Ag UAV OA) technology, according to Wang et al. [12], is the core intelligent technology that allows an agricultural drone to autonomously identify farm obstacles and complete the specified avoidance action. It is an inbuilt capacity for sensing and avoidance (S&A) of threat [13]. In sensing depth, especially of frontal obstacles, studies have been on mimicking biological systems such as motion parallax, monocular cues and stereo vision [14]. An Ag OA UAV functions, therefore, include real-time perception, rapid image analysis, intelligent identification, potential areas detection and decision making on obstacle avoidance. To this end, radar ranging, laser ranging, ultrasonic ranging, monocular and binocular vision are deployed as tools for sensing or detecting obstacles.

Sensor fusion is a process by which data from multi-sensor UAV are fused for computations in multispectral remote imaging in precision agriculture to capture both visible and invisible images of crops and vegetation. The sensors feed the data back to the flight controller which runs on obstacle avoidance algorithms for processing the image data of the scanned surrounding [15]. Many Ag UAV systems use on-site suspension, planned travel routes, and autonomous obstacle avoidance as obstacle avoidance methods after detecting an obstacle. However, Leonetang pointed out [16] that autonomous actions that require the UAVs to evade the algorithm and regenerate the route come at the cost of battery life, which may be insufficient to tackle additional obstacles during route regeneration. In agriculture, as noted earlier UAV have been primarily applied in remote sensing, crop production and protection materials, precision seeding, vegetation testing (NDVI) etc. with various types of obstacle avoidance (OA) systems under remotely or programmed flight control [5]. Initially, there were two main sense and avoid (S&A) technologies—radar that sends out radio waves and measures their reflections from obstacles and light detection and ranging LiDAR optical sensor that uses laser beams instead of radio waves to provide detailed images of nearby features [17]. UAVs control modes are categorized as linear, non-linear and learning-based by Kim et al. [6]. They opined that linear and non-linear control systems based on linear-quadratic (LQ) are used to control UAV and handle wind and weather but not storm and snow. Learning-based controls use a type of fuzzy logic that learned using data obtained from the flight and does not require models.

Many variants of controls and obstacle detection and avoidance devices adorn the UAV shelves and aircraft market today, virtually solving the earlier version of sensors' problems of bulkiness, weight, low energy efficiency and high cost. This includes RTK sensors, ultrasonic sensors, laser sensors, infrared sensing technology, structured light, TOF ranging, millimetre-wavelength radar, monocular visual ranging and binocular stereo vision [7]. The sensors are further supported by a variety of algorithms that enable real-time obstacle perception, rapid analysis and actionable image interpretation. These are broken down into three categories [13] to include a geometric relationship (relative distance, speed, acceleration, angle etc. between the drone and the obstacle), real-time planning (artificial potential field, ANN algorithm—a software-based approach to replicate the biological neurons, artificial heuristic, path-planning etc.) and decision making (Markov and Bayesian decision theory). In the genre of emerging OA technique is the reinforcement learning whereby the UAV selects the actions on the basis of its past experiences (exploitation) and also by new choices (exploration) such as autonomous mental development (AMD) algorithm [13] that simulates the mental development process of a human being using neural

network algorithm [18], online free path generation and navigation system [19], multi-UAVs genetic algorithm [15], and the simultaneous localization and mapping (SLAM) technology which maps in real-time, recognizing own position and identifies obstacles while autonomously traveling or performing tasks [6]. The technique of UAV swarm control is also evolving using linear and nonlinear controls with strong resistance to external influence based on the K-means algorithm (K-means clustering) to prevent collisions and another to map allocated areas. However, as Corrigan pointed out in his paper [15], the challenge of these technologies is accuracy, as measurements must be taken continuously as the UAV moves through its environment and assimilated to update the models and account for noise introduced by both the device's movement and the measurement method's inaccuracy. This task is accomplished by updating the model state variables with measured values. The state variables are updated sequentially i.e. each time an observation is available. Kalman filter is deployed in estimating the states of the systems from the sensor data, estimating variables that are not directly observable and to minimize the noise [20].

The plethora of demands on OA system according to Wang et al. [12] to ensure the safety of agricultural UAV and continuous operations at low altitude and ultralow volume spraying include the following capabilities: action response time and implementation efficiency, autonomous adjustment of flying speed, height and attitude of the drone, re-planning of flight path after obstacle avoidance, deployment of signal loss prevention and anti-magnetic field interference, decision making on single, multiple static or dynamic obstacles.

To achieve the above objectives of all-weather autonomous operation of Ag UAV, multi-sensor obstacle avoidance technology is evolving while the development of auxiliary classification (indirect identification) of farmland obstacles and standardization of UAVs processes is ongoing. In July 2015, the Republic of South Africa became the first country to implement and enforce a comprehensive set of legally binding rules governing unmanned aerial vehicles. By 2016, 15 countries had published dedicated drone regulations. Nigeria is one of the countries with legally binding rules on the use of unmanned aerial vehicles (UAVs) [21].

2.3 Applicability of the various UAV obstacle sensing and avoidance technologies to obstacle rich farmland

2.3.1 Real-time kinematic (RTK)

It is more suitable for building obstacle maps of farmland than real-time obstacle avoidance. The positioning technology has not been fully applied to Ag UAV because of its high cost, difficulty of deployment and time consuming and labour intensive features [12]. However, Global Navigation Satellite System (GNSS) with RTK allows for centimeter level high position accuracy [6].

2.3.2 Ultrasonic sensors

These are used as an auxiliary safety device to get flight altitude parameters, achieve autonomous take-off and landing or fly in complex terrains at very low altitudes. Image processing is used to recognize the position of an obstacle while the ultrasonic determines the distance [22]. The obstacle avoidance principle is based on the sound wave reflected by the obstacle and measuring the echo time difference to determine the distance [16]. On Ag quadrotor UAV the ultrasonic sensors are used to detect objects

and to calculate the distance between the obstacle and the UAV. The effective method is subsequently devised to avoid the obstacle [23]. They are not affected by light intensity, color variation and are of simple structure, low cost and easy to operate. However, its performance is limited by the small range and sound absorption, ambient temperature, humidity, atmospheric pressure and ground effect of grass in addition to losses caused by ultrasonic reflection and crosstalk between sound waves [6]. Further, acoustically, soft materials like cloth may be difficult to detect [9]. Moreover, Gibbs et al. [24] argued that their resolution can be as low as 60 degrees and cannot, therefore, identify the angular location of an obstacle in its view. Their study using two sonar receivers and scalar Kalman filter to reduce the effect of the signal noise was however salutary, especially with the energy and power spectral density metrics (out of the four signal metrics tested). Others being maximum (peak) frequency and cross-correlation of raw data and PSD. Further work by Davies et al. [25] using ultrasonic transit-time flow meters' reveals that the autonomous performance of ultrasonic sensors in-flight instrumentation of UAVs can be improved upon by optimal design of two variables—the mounting configuration and the optimal angle of incidence for the transducer mounting.

2.3.3 LiDAR

It calculates distances and detects objects by measuring the time, it takes for a short laser pulse to travel from the sensor to an object and back using the known speed of light [9]. Laser sensors mainly used in autonomous navigation require optical systems thereby making them unsuitable for liquid, the dusty and smoky farming environments in addition to their weight and production cost, especially for small (sUAV) and micro unmanned aerial vehicles (MAVs). 3D scanning information takes so much time with laser scanners that make them unsatisfactory for real-time obstacle avoidance [26]. However, Huang et al. [5] proffered that light detection and ranging (LiDAR) optical sensor could be configured in a multi-sensor platform for agricultural field survey and crop height profiling.

2.3.4 Infrared (IR)

This sensing technology is based on the principle of triangulation whereby the infrared emitter emits an infrared beam at a certain angle and the light is reflected back on encountering the object. On detection, the object distance is calculated [18]. Output on analogue voltage corresponds to the distance to the reflecting object [15]. It works under all weather conditions including a night to measure distances and describe contours. It must, however, avoid direct sunlight and reflections to evade interference or failure of the OA system [6]. Corrigan [15], however, noted that IR obstacle avoidance sensors work with a specific frequency of infrared produced by the emitter to prevent them from being confused by visible light. Its good concealment and all-time service confer it with unique ability to observe animals in their natural habitats without causing disturbances [9]. On his part, Wang et al. [12] argued that the detection distance is small and the light emitted by the system is easily disturbed by the external environment.

2.3.5 Line structured light

It is emitted from the laser and converged into the light band of different shapes after passing through different lens structures [6]. Through the image acquisition,

processing and calculation, the distance, azimuth and width and other parameter information of front obstacles are extracted [24]. Single camera-based obstacle avoidance systems use structured light to map their environment in 3D without being weighed down by traditional bulky LiDAR [25]. Wang et al. [6] however observed that there are mutual interferences between adjacent structural light sensors with natural light nullifying structured light for the outdoor environment and hence not commonly used in agricultural UAVs.

2.3.6 Millimeter-wavelength radar

It is a detection radar working in a microwave band. It transmits signals with a wavelength that is in the millimeter range—a short wavelength. It, therefore, can detect movements that are as small as a fraction of a millimeter [26]. Due to the complex farmland operating environment ultrasonic and other sensors based on optical principles are easily affected by climatic conditions, whereas millimeter wavelength radars a non-cooperative sensor can work in all weather conditions with strong penetrating ability, large operating distance, reliable detection, and anti-electromagnetic interference [6]. Compared with other ranging sensors the millimeter wavelength radar, however, has low resolution and implemented with discrete components that demand increase power consumption and overall system high cost. It can not only detect parallel distances but also hardly describe the outline of the OA objects as well as their angle in the field of view. It is, therefore, limited to terrain imitation flight systems for agricultural UAVs. Lovescu and Rao [26] noticed that Texas Instrument has solved these challenges with complementary metal-oxide semiconductors (CMOS)-based mmWave radar devices and implemented frequency modulated continuous wave (FMCW) that measures range as well as angle and velocity. This differs from traditional pulse-radar systems which transmit short pulses periodically they noted.

2.3.7 Time of flight (TOF) ranging

It is one of the widely used ranging methods. It works by the round trip flight time whereby its camera illuminates the whole scene including the objects using a pulse or continuous wave light source and then measures the reflected light time using the speed of light to and from the object to obtain the distance and hence the 3D depth range map. It is the quickest technology to capture 3D information, created in a single shot of an area or scene [9]. Compare with other ranging methods, it has the features of low energy consumption and easy deployment and is suitable for applications where high ranging accuracy is required. However, due to the transmission features of the light wave signal non-linear propagation factors such as reflection, refraction, and diffraction can all cause measurement time deviation which will lead to huge distance calculation errors. When applied in agricultural UAVs safety, an auxiliary device derived from the combination of TOF ranging principle and other sensors is more suitable for obstacle avoidance [26]. AMS TOF obstacle detection and avoidance sensors, for example, are based on a proprietary single photon avalanche photodiode (SPAD) pixel design and time to digital converters (TDCs) with extremely narrow pulse width and can measure the time of flight of a laser emitted infrared ray reflected from an object in real-time [7].

2.3.8 Monocular visual ranging

It captures images through a single-lens camera. The constraints of payload due to size, weight and power (SWaP) of both small and micro UAVs favors the use of monocular cameras. It is a 3D depth reconstruction from a single still image. It is simple in structure, mature in technology and fast in computing speed [26], but it cannot directly obtain the depth information of obstacles because both optical flow and perspective cues cannot handle frontal obstacles well [21]. The algorithm deployed to interpret the image data using various cues in the image is what makes monocular vision cameras able to create 3D images, determine distances between objects and detect obstacles [9]. Hence, monocular ranging is difficult to meet the requirements of real-time performance and accuracy of obstacle avoidance for UAVs giving the complexity of the farmland operating environment. However, a relative size cue to detect frontal collisions which work on the knowledge that the size of approaching objects increases with nearness appears promising for real-time frontal obstacle detection using a single camera. According to Mori and Scherer [14], the time to collision can be obtained by measuring the expansion of the obstacle.

2.3.9 Binocular stereo vision sensors

Beginning with identifying an image pixel that corresponds to the same point in a physical scene observed by multiple cameras, stereoscopic vision is the calculation of depth information by combining two-dimensional images from two cameras at slightly different viewpoints. Triangulation using a ray from each camera can then be used to determine the 3D position of a point [15]. Stereo vision technology can recognize and measure the distance between the fuselage and the obstacles due to its good concealment and ability to obtain comprehensive information including color and texture of obstacles as well as 3D depth information. The most serious issue with binocular vision, however, is stereo matching. The effects of lighting changes, scene rotation, object occlusion, low image resolution, interference and even overwhelming of target features all lead to target feature instability and decreased object detection accuracy [6]. It is, therefore, more used in consumer and professional UAVs rather than in agriculture.

3. Conclusion

The attempt was made to situate the topic and review within the milieu of the national discourse on economic development to isolate it from the pool of academic exercise which has become the bane of research in Nigerian Institutions of Learning (NIL). The imperatives of enhanced mechanization of the nation's farm systems as a cardinal strategy to fight poverty and for capital formation and economic growth were highlighted. The role of unmanned aircraft in precision agriculture was x-rayed to include soil and water analysis, planting, crop and spot spraying, crop monitoring, irrigation, farm health assessment and livestock production systems. Based on the three functional compartments of unmanned aircraft system—guidance, navigation and control (GNC) the application of UAV to agriculture was examined to include the two main platforms fixed wing and rotor airframes, the navigations sensors such as real-time kinematic (RTK), ultrasonic sensors, laser sensors, infrared sensing

technology, structured light, time of flight (TOF) ranging, millimetre-wavelength radar, monocular visual ranging and binocular stereo vision and the controls—geometric relationship, real-time planning and decision-making algorithms, the autonomous mental development (AMD) algorithm, online free path generation and navigation system, multi-UAVs genetic algorithm, the simultaneous localization and mapping (SLAM) technology and UAV swarm control and sensor fusion systems. The obstacle avoidance methods of many Ag UAV systems were found to be either by on-site suspension, planned travel route and/or autonomous obstacle avoidance. The merits and the demerits of the available Ag UAV technologies were highlighted and the gap to bridge in airframe technology—cost, payload and flight endurance; in sensors—direct imaging sensors of less cost, size and weight; reliability—in mechanical, electronics and interference; in off-the-shelf devices for rapid remediation, in operation-autonomous take-off and landing, automated computation of flight paths, integrated spray and remote sensing algorithm to direct the operation of spraying and in power for higher and lightweight solar cells were noted.

The objective of the study is to examine the literature pertaining to the use of UAV for pesticides and fertilizer application in obstacle rich farms. The study shows that UAVs platform for agricultural pesticide and fertilizer application needs higher payloads weight that demands enhanced mechanical (especially the landing gears) and integrated electrical structure. Enhanced flight endurance to ensure continuous spraying operation by a unit of task size is important. It was further observed that rotor aircraft with the ability for vertical take-off and landing (VTOL) is better for agricultural operations.

It was also observed that the farm environment is replete with flight obstacles for Ag UAVs. The various types of obstacles were outlined. Nine sensors that are primary to obstacle sensing and avoidance technology were therefore reviewed for their applicability to such environment and their merits and demerits highlighted. None is found completely independent without an assist to achieve the objectives of real-time all-weather autonomous operation. A fusion of multi-sensor data systems is therefore in vogue to complement the shortfall of each other. The potential for real-time and near real-time exists but the development of technology for quality imagery and rapid processing leading to real-time response is needed. The infrared, time of flight and millimeter wavelength radar sensors for detecting farm and flight environment obstacles appear must promising especially with its modern versions for Ag UAV.

The autonomous mental development (AMD) algorithm and the simultaneous localization and mapping (SLAM) technology appear to be ahead of others in achieving autonomous identification of obstacles and real-time obstacle avoidance for agricultural UAVs. They are, therefore, found fit for further studies and development for deployment on Ag UAVs for pesticides and fertilizer application in obstacles in rich farmlands.

Author details

Uche Emmanuel
Faculty of Air Engineering, Air Force Institute of Technology, Kaduna, Nigeria

*Address all correspondence to: eaumie@gmail.com

References

[1] National Bureau of Statistics. Statistic Bulletin. 2020;**3**:70806. Available from: https://www.aljazeera.com-news [Accessed: May 04, 2020]

[2] Lewis A. Theory of Economic Development. London: George Allen and Unwin Ltd; 1977

[3] Agbo J. Precision Agriculture and National Development in The Nation Online. 11th June 2020

[4] Yun G, Mazul M, Pederii Y. Role of unmanned aerial vehicles in precision farming. Proceedings of the National Aviation University. 2017;**70**(1):106-112

[5] Huang Y et al. Development and prospect of unmanned aerial vehicle technologies for agricultural production management. International Journal of Agricultural and Biological Engineering. 2013;**6**:3. Available from: http://www.ijabe.org [Accessed: June 14, 2020]

[6] Kim J et al. Unmanned aerial vehicle in agriculture: a review of perspective of platforms, control and applications. IEEE Access. 2019;**10**:1109. Available from: https://creativecommons.org/licences/by/4.0/ [Accessed: June 14, 2020]

[7] Uche E, Audu S. UAV for agrochemical application: a review. Nigerian Journal of Technology (NIJOTECH). 2021;**40**(5):795-809

[8] Vroegindeweij B, Henten E. Autonomous unmanned aerial vehicles for agricultural applications. In: Proceeding. International Conference of Agricultural Engineering. Zurich; 2014. p. 8

[9] Banjo C, Ajayi O. Sky-Farmers: Applications of Unmanned Aerial Vehicles (UAV) in Agriculture. IntechOpen; 2019. Available from: http://creativecommons.org/licences/by/3.0 [Accessed: June 12, 2020]

[10] He L et al. Optimization of pesticide spraying tasks via multi-UAVS using genetic algorithm. Hindawi Mathematical Problems in Engineering. 2017;**2017**:7139157. DOI: 10.1155/2017/7139157

[11] Chufang H. QF170-18L AgriSpraying Helicopter. 2020 [Accessed: June 14, 2020]

[12] Wang L et al. Applications and prospects of agricultural unmanned aerial vehicle obstacle avoidance technology in China. MDPI. 2019;**19**(3):642. Available from: http://creativecommon.org/licences/by/4.0/ [Accessed: June 14, 2020]

[13] Renke H et al. UAV autonomous collision avoidance approach. Automatika. 2017;**58**(2):195-204. DOI: 10.1080/00051144.2017.1388646

[14] Mori T, Scherer S. First results in detecting and avoiding frontal obstacles from a monocular camera for micro aerial vehicles. In: Proceedings of the IEEE International Conference on Robotics and Automation (ICRA). Karlsruhe, Germany; 2019

[15] Corrigan F. 12 Top Collision Avoidance Drones and Obstacle Detection Explained. DroneZon [Online]. 2020. pp. 1-31. Available from: https://www.dronezon.com/learn-about-drones-quadcopters/top-drones [Accessed: June 10, 2020]

[16] Leonetang W. The Obstacle Avoidance System of Agricultural UAV.

Welkinuav [Online]. 2018. pp. 921-922. Available from: https://www.welkinauv.com [Accessed: June 10, 2020]

[17] Braasch M. Obstacle Avoidance: The Challenge for Drone Package Delivery. The Conversation [Online]. 2016. pp. 1-5. Available from: https://theconversation.com/amp/obstacle-avoidance-the-challenge-for-drone-package-delivery-70241 [Accessed: June 09, 2020]

[18] De Simone M et al. Obstacle avoidance system for unmanned ground vehicles by using ultrasonic sensors. Machines. 2018;**6**:18. Available from: www.mdpi.com/journal/machines [Accessed: June 12, 2020]

[19] Adnan A, Majd A, Troubitsyna E. Online path generation and navigation for swam of UAVs. Scientific Programming. 2020;**2020**:1-15. Available from: http://creativecommon.org/licences/by/4.0/ [Accessed: June 12, 2020]

[20] Gerstberger LJ. State Estimation: KALMAN FILTER. In: Programmierrung & Softwaretechnik. Munchen: Lud wig Maximilians Universtat; 2012. p. 6

[21] Sylvester G. Unmanned Aerial Systems (UAS) in Agriculture: Regulations & Good Practices. E-Agriculture in Action, Drones for Agriculture, Food and Agricultural Organization of the United Nations (FAO). 2016. p. 20

[22] Anis H et al. Automatic quadcopter control avoiding obstacle using camera with integrated ultrasonic sensor. Journal of Physics: Conference Series. 2018;**1011**:012046

[23] Guanglei M, Haibing P. The application of ultrasonic sensor in obstacle avoidance of quadrotor UAV [Online]. In: 2016 IEEE Chinese Guidance, Navigation and Control Conference (CGNCC). 2016. Available from: https://ieeexplore.ieee.org.document [Accessed: June 12, 2020]

[24] Gibbs G, Jia H, Madani I. Obstacle detection ultrasonic sensors and signal analysis metrics. In: International Conference on Air Transport—INAIR 2017 [Online]. 2017. pp. 173-182. Available from: www.sciencdirect.com [Accessed: June 12, 2020]

[25] Davies D, Bolam R, Vagapov Y, Excell P. Ultrasonic sensor for UAV flight navigation. In: 25th International Workshop on Electric Drives: Optimization in Control of Electric Drives (IWED). Available from: http://doi.org/10.1109/IWED.2018.8321389 [Accessed: June 14, 2020]

[26] Lovescu C, Rao S. The Fundamentals of Millimetre Wave Sensors. Texas Instrument [Online]. 2019. Available from: http://www.ti.com/sc/docs/sampterms.htm [Accessed: June 12, 2020]

Section 2

Recent Challanges

Chapter 3

Motion Planning of UAV Swarm: Recent Challenges and Approaches

Muhammad Mubashir Iqbal, Zain Anwar Ali, Rehan Khan and Muhammad Shafiq

Abstract

The unmanned aerial vehicle (UAV) swarm is gaining massive interest for researchers as it has huge significance over a single UAV. Many studies focus only on a few challenges of this complex multidisciplinary group. Most of them have certain limitations. This paper aims to recognize and arrange relevant research for evaluating motion planning techniques and models for a swarm from the viewpoint of control, path planning, architecture, communication, monitoring and tracking, and safety issues. Then, a state-of-the-art understanding of the UAV swarm and an overview of swarm intelligence (SI) are provided in this research. Multiple challenges are considered, and some approaches are presented. Findings show that swarm intelligence is leading in this era and is the most significant approach for UAV swarm that offers distinct contributions in different environments. This integration of studies will serve as a basis for knowledge concerning swarm, create guidelines for motion planning issues, and strengthens support for existing methods. Moreover, this paper possesses the capacity to engender new strategies that can serve as the grounds for future work.

Keywords: UAV, swarm intelligence, motion planning, swarm challenges, flight, aerial mission

1. Introduction

UAV has significance in our lives due to their potential applications. Single UAVs are restricted to limited power, capabilities, sensing, and flight time. This has raised a requisite for employing swarms of UAV systems. UAV swarm conquers the exploitations and restrictions of an unaccompanied UAV and assists larger teams to cooperate for successful aerial missions. Swarm has benefits and brings versatile possibilities as the strength lies in numbers. Many of them are task completion in less time, redundancy, and collaborative task execution.

1.1 Background

Swarming is not a contemporary conception. It existed in nature and was motivated by the cooperation and mutual communication of biological populations [1]. Studying the flocking of birds, movement of the ant colony, cooperation of bees,

schools of fish, and predation of wolves the concept of the swarm of UAVs came into existence. The unity of the animal kingdom makes it possible to achieve a common challenging and complex goal.

Nevertheless, swarming is not restricted to a natural phenomenon. It is also inspired by a military tactic in which many units from multiple axes coverage attack a common target in a coordinated and deliberately structured form [2]. Since the fourth century, swarming has been observed throughout military history. However, today swarming has changed the traditional concepts of command and control into innovative ones. Moreover, a single person is capable to command and control several UAVs at a time.

1.2 Related work

Swarm of UAVs is evolving because of its significant capabilities of long-range operations, enhanced robustness, and flexibility [3]. Swarm intelligence has a high impact on many fields such as technology, science, society, and various systems like inspection, tracking, transporting, and many others [4]. For the motion planning of UAV swarms, many improvements in terms of control designs, path planning algorithms, communication structure, monitoring and tracking architectures, and safe flight protocols are considered in different studies [5].

The researchers combined computational techniques with mathematical models in [6] to examine the communication effects. The modeling process was simplified through this approach, but the process of modeling was slow and run out of memory. In [7] a controller based on a decentralized, leader-follower strategy, and a geometry of the tree-based network were suggested. This study achieved the arrival of multi-UAVs at a common spot with maintained synchronization. Moreover, the suggested design showed flexibility and robust performance. However, this study was bounded to a limited number of UAVs. In [8] researchers developed a framework for novel path planning of UAV swarm. This proposed algorithm resulted in efficient path planning with a reduction in energy and inspection time. Additionally, it provided the guidelines for determining various parameters.

In [9] the study presented an algorithm for computing the control of swarm and modeling their distributed behavior. The examination and simulations have shown the communication latency effects on different scenarios. In [10] an improved algorithm with resilience metric is proposed while considering the limited communication range effects. This strategy is implemented in a surveillance mission, which showed its significance as a more realistic method that can face efficiently the external disturbance and threats. In a recent study [11], the concepts of PIO algorithm, proportional-integral controller, and proportional integral differential controller are employed for the formation control of UAV clusters. This strategy has outperformed the traditional methods and provided a safe flight protocol. Further extensive reflection on how this technology has evolved is in the section of the related survey.

1.3 Motivation and contribution

The motivation for this paper is to gather multiple challenges, which can hinder the performance of a UAV swarm, on a single platform. Moreover, to provide appropriate approaches as the solutions to achieve optimal motion planning. This study can assist researchers in exploring multiple motion planning strategies with their contributions and limitations. The appropriate selection of the motion planning

techniques and models can complete the complex tasks quickly and targets the applications dotage as well. Following are the significant contributions of this paper:

- To provide an explanation of swarm intelligence and the challenges it faces.
- To present a detailed analysis of the motion planning techniques with their contributions and limitations from several research articles from more than the last decade.
- To recommend future directions to guide the researchers.

1.4 Organization of the Paper

The paper is organized into many sections. Section 2 provides the state-of-the-art of UAV swarms. Section 3 evaluates the concept of swarm intelligence. Section 4 presents challenges faced by the UAV swarm. Section 5 reflects on an extensive survey of the techniques and models used to address many challenges concerning the UAV swarm. Section 6 discusses the key findings and limitations. Section 7 gives the conclusion, and Section 8 recommends some future work for further research and development.

2. State-of-the-art

The swarm makes decisions collectively and completes its aerial mission using relatively simple instructions due to the Artificial Intelligence (AI) technology and edge computing [12]. Features like following the leader and missions, path planning, sensing, and avoiding are already developed in the Veronte Autopilot. This advancement in the features makes teamwork possible and ensures task success. Surveillance and attack induction is a milestone event in the swarm globally. This game-changing capability of the swarm of UAVs is benefitting both larger as well as smaller nations. Other significant aspects of swarming include combined decision-making, self-healing, and adaptive formation flying. The swarm of UAVs is still in the progressing phase as further research is being conducted to further enhance the systems. Further focus includes the expansion of capability of artificial swarm intelligence, increase in the autonomy state among the swarm agents, and commodification to reduce the cost impacts.

The most amazing aspect of the UAV swarm is its application for both civilian and military purposes using swarm intelligence [13]. The civilian agencies are using the swarm technology for bigger plans. The National Aeronautics and Space Administration (NASA) is also employing this AI-based swarm technology for climate change analysis [14]. This results in the accomplishment of the required things, which were not possible while using one. Moreover, many developed nations have passed regulations to widespread the commercial application of UAV swarms. The swarm shows tremendous performance in power line and structure inspections, precision agriculture, surveying, search and rescue operations, and others.

However, the swarm of UAVs gained the spotlight for its potential and efficiency in military usage. If in combat, some of the UAVs of the swarm get shot down then still the remaining ones complete the mission with similar tactics, power, and flexibility. Raytheon demonstrated this by employing swarm operation during a field exercise of the US Defense Advanced Research Projects Agency (DARPA) program [15]. The

Raytheon swarm had the communication and coordination ability. Moreover, all the individuals had sensors, cameras, and Tactical Assault Kit (TAK) integration capability for environmental explorations.

The swarm technology is enhancing the capabilities of the military in complex environmental tasks. Many militaries, like the US and China militaries, are in a lead in testing and observing the simulations for swarm operations on the highest levels [16]. Some militaries, like the British military, are using this technology for real-time operations. The UK has also experimented with Leonardo's Brite Cloud for swarming that contained electronic warfare jammers. Similarly, soon Russia aims large UAV swarm induction, "Flock 93," in its army. Moreover, it is trying to fill the gap by 2025. Iran, Turkey, and India are also attempting efforts to mature and proliferate this technology using distributed intelligence and edge computing. Swarms of UAVs are the future of aerial wars, and the future is now [17].

3. Preliminaries of swarm intelligence (SI)

In this world, we observe that all individuals wish to amplify their intelligence. For this goal, they think and prefer working together, like a bee swarm, fish scull, and birds flock together. This is because they believe that they are smarter in a group rather than being alone. A new intelligence that is formed due to the deep interconnection of the real system having feedback loops is known as swarm intelligence [18]. In simple words, a swarm is a brain of all the brains that are smarter than individual ones. Swarm intelligence is an evolving area of bio-inspired artificial intelligence [19].

Moreover, using swarm intelligence, many heads follow a single mind. All the individuals follow clear rules and interact not with each other but with the environment as well. This adaptive strategy requires a large mass of individuals. It is capable of scheduling, clustering, optimizing, and routing a cluster of similar individuals. Swarm intelligence emphasizes the task's relative position in the schedule. It follows the summation evaluation rule for scheduling. A collaboration of all the similar individuals in a swarm is known as clustering. For example, UAVs of a swarm are different from other clusters' UAVs. It is capable to provide the best and low-cost solution from all the feasible outcomes through optimization. Moreover, it has potential capabilities of routing. It imitates the principle of ants in which forward ants gather the information while the backward ants utilize that information [20].

3.1 Aspects of SI

Major aspects of swarm intelligence include distribution, stigmergy, cooperation, self-organization, emergence, and imitating natural behavior [21]. Distribution is the prime characteristic of swarm intelligence as all the individuals are capable to select their actions and perform them. The phenomenon with which the agents interact through environmental alteration indirectly is called stigmergy. This phenomenon provides them with awareness of their surroundings and disconnects the interactions of the individuals. Another significant behavior is the cooperation of all the UAVs in a swarm [22]. UAVs cooperate for solving complex tasks and show their collective behavior using swarm intelligence. Another aspect of swarm intelligence is self-organization. This behavior is based on positive feedback, negative feedback, fluctuations amplification, and different social interactions. Positive feedback is the amplification that gives better outcomes by allocating more UAVs to them. Negative feedback is to stabilize so that not all the UAVs

converge to a similar state. The self-organization phenomena usually observe a tension between both the feedbacks, such as complex networks, markets, cellular automata, and many others. Another characteristic is emergence, which can be weak or strong. The emergence is said to be weak if the individual behavior is traceable from the emergent properties. The emergence is said to be strong if the individual behavior cannot be traced from the properties of emergence. Moreover, a swarm of UAVs is modeled by taking inspiration from natural swarm behavior. Generally, swarm behavior includes foraging, constructing a nest, and moving together in the environment. Hence, imitating these natural swarm behaviors is another key aspect of swarm intelligence [23].

3.2 Levels of SI

There are two levels of swarm intelligence. The first level employs a positive feedback pheromone for marking shorter paths and an entry signal for others. Whereas the second level of swarm intelligence employs a negative pheromone for marking unpleasant routes and no entry signal for others.

3.3 Principles to follow in SI

A swarm follows five principles generally. The proximity principle, the quality principle, diverse response principle, stability principle, and adaptability principle [24]. Following the proximity principle, the basic swarm individuals can easily respond to the environmental variance that is caused by interactions among them. The quality principle allows a swarm to respond to quality factors like location safety only. The diverse response principle enables to design of the distribution in such a way that all the individuals are protected from environmental fluctuations to a maximum level. The stability principle restricts the swarm to show a stable behavior with the changes in the environment. The adaptability principle shows the sensitivity of a swarm as the behavior of the swarm changes with the change in environment. The most widely used principles are attraction between all individuals, collision avoidance, and self-organization. While following attraction they come closer and focus on a similar direction. While following the collision avoidance principle, they keep a particular distance between them to avoid collisions. Whereas, in self-organization rule, they interact with the neighbors but do not trust all.

3.4 Mechanism of SI

The mechanisms of swarm intelligence are regarding the environment, interactions, and activities of the individuals in a swarm. No direct communication takes among the individuals in a swarm [25]. They interact with each other through environmental alterations. Thus, environmental alterations serve as external memory. This simulation of work is done by applying the stigmergy behavior of all the swarm members. Moreover, the individuals choose their actions with an equilibrium between a perception-reaction model and any random model. Then, they react and move according to this perception-reaction model while perceiving and affecting the local environmental properties.

3.5 Languages used for SI

Proto-swarm, swarm, Star-Logo, and growing point are some programming languages for swarm intelligence. The proto-swarm language uses amorphous

medium abstraction to program the swarm [26]. This amorphous medium abstraction is obtained by utilizing a language that is from the continuous space-time model of Proto and a runtime library that estimates the model on the provided hardware. Another language for swarm intelligence is a distributed programming language called a swarm. The basic concept for it is to move the computation rather than the data. Swarm is analogous to the Java bytecode interpreter with a primitive version. Now it is applied as a Scala library. Star-Logo is not only a programming language but also a programmable modeling environment of a decentralized system. By utilizing this programming language, different real-life scenarios can be modeled like market economies, bird flocks, traffic jams, etc. Whereas, to program amorphous computing medium growing point language is essential. This programming language has the capacity of generating pre-specified and complex patterns like the interconnection form of an arbitrary electrical circuit.

3.6 Significance of SI

There is much significance of swarm intelligence; some of them are discussed here. It enables the swarm to be flexible while responding to external challenges and internal disturbances. It completes the tasks with robust performance even with the failure of some agents [27]. It allows the scalability to range from a few to a million individuals in a swarm. No central authority or control lies in the flocking of individuals. It is completely adaptable and provides self-organized solutions only. The propagation of changes is very rapid in the networks. All these are beneficial for clusters of individuals.

4. Swarm challenges

4.1 Swarm control

The basis of a UAV swarm is to control all the individual UAVs during the planned path. To solve the reconstruction, anti-collision, search, and tracking issues in the swarm formations the development of proper control system frameworks and controllers is required [28]. Centralized and distributed are the two major control platforms for the automation-equipped clusters. The main advantage of the centralized platform is achieving higher quality in outputs but with the limitation of limited scalability. Whereas the main contribution of the decentralized platform is its enhanced scalability, which is less complex. The network of the UAV swarm guarantees the nodes' connectivity and simplifies the application designs. Sensor inputs with the environmental and target's prior knowledge are the essentials for the traditional models.

Various research overcome these issues using multi-layer distributed control frameworks. The designing of the controller is crucial in the process design of the UAVs. Many studies suggest using the ANFIS controller for the learning error reduction and quality improvement of the controller. During the movement of UAVs following a specific path, the target tracking performance is directly affected by the control of the airborne gimbal system. Some studies propose the nonlinear Hammerstein block structure for modeling gimbal systems to enhance the efficiency of the model predictive controller (MPC). This also improves the performance of the target tracking under external interference in real-time. Other approaches for formation control are leader-follower strategy, consensus theory, virtual structure method,

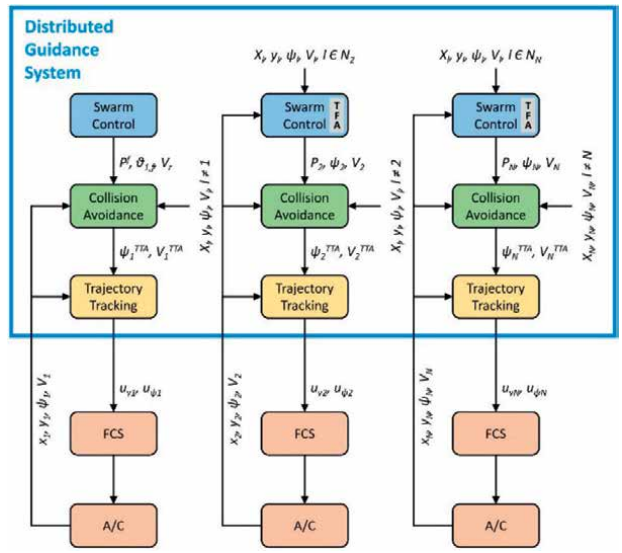

Figure 1.
Distributed guidance model using leader-follower controller.

behavior method, etc. **Figure 1** represents the concept of distributed guidance model using a leader-follower controller as given in [29]. The leader guidance algorithm is given in the first column of this figure, whereas the other two columns represent the followers. The preassigned topology in this model cannot be altered.

4.2 Swarm path planning

The path planning of a UAV swarm is quite challenging [30]. To solve this NP-hard problem many studies suggest path-planning algorithms. These algorithms are categorized into classic algorithms and meta-heuristic algorithms as shown in **Figure 2**. Classic algorithms require environmental information while meta-heuristic algorithms require information on the real-time position and measured environmental elements. Road map algorithm (RMA), A* algorithm, and artificial potential field (APF) method

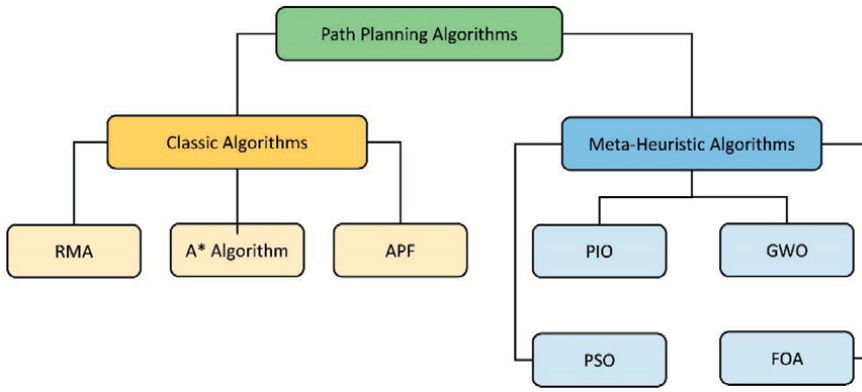

Figure 2.
Path planning algorithms for UAV swarm.

are some examples of classic algorithms as presented in **Figure 2**. Particle swarm optimization (PSO), pigeon-inspired optimization algorithm (PIO), fruit fly optimization algorithm (FOA), and gray wolf optimization algorithm (GWO) are some examples of meta-heuristic algorithms as given in **Figure 2**.

The swarm path planning can be categorized into dynamic path planning, 3D path planning, area coverage path planning, and optimal path planning [31]. Dynamic path planning is essential for the task performance of a UAV swarm in a complex environment. To ensure dynamic path planning many researchers suggest using collision probability with Kalman Filter, the artificial potential field (APF) with the wall-follow method (WFM) method, trail detection, scene-understanding frameworks, and so on. All these methods provide better direction estimation, better performance, and avoid path conflicts. 3D path planning is complicated, but many studies apply meta-heuristic algorithms for dealing with it. Like the GWO algorithm realizes the feasible flight trajectory, the FOA algorithm performs local optimization and PIO optimizes the initial path.

All these algorithms work efficiently for 3D path planning of UAV swarms under threats and emergencies. Path planning in which UAVs can move at all the areas of interest points is area coverage path planning. Many studies suggest a five-state Markov chain model, improved potential game theory, and a cyber-physical system for it. For optimal path planning battery capacity of UAVs, matching performance, and energy consumption are serious considerations. Studies suggest a coupled and distributed planning strategy, mobile crowd perception system (MCS), and energy-efficient data collection frameworks for optimal path planning.

4.3 Swarm architecture

For swarm implementations, the architecture of UAVs is of much importance [32]. Architecture is a combination of design, management, and optimization techniques. Swarm architecture can be based on communication, mission doctrine, control, etc. Communication-based swarm architecture has two forms. Ad-hoc network-based architecture and infrastructure-based swarm architecture. Both are promising architectures and perform well under complex environments.

Considering the operational mission for designing a swarm architecture is also important. Studies consider it imprudent if the mission doctrine is not considered. Current approaches include bottom-up modeling approaches and top-down design approaches for designing swarm systems. Similarly, control-based architectures are also beneficial for the swarm. **Figure 3** gives a mission-based architecture for swarm composability (MASC) as presented in [33]. This framework focuses on the phases, tactics, plays, and algorithms. According to this figure, mission explains the entire task, phases evaluate specific periods, tactics are the individuals' usage in a particular order for task performance, the play describes the swarm behavior and algorithms are the procedures. Moreover, linking distributed behavior control methods with centralized coordination can efficiently work for swarm aerial missions. The aerospace architecture can perform the thinking task, execution task, reaction task, and socialization task efficiently. Moreover, the Internet of Things (IoT) supports swarm architectures and facilitates interactions as well.

4.4 Swarm monitoring and tracking

Another prime challenge for a swarm is monitoring and tracking. All the UAVs' positions, status, and the external environment change concerning time during

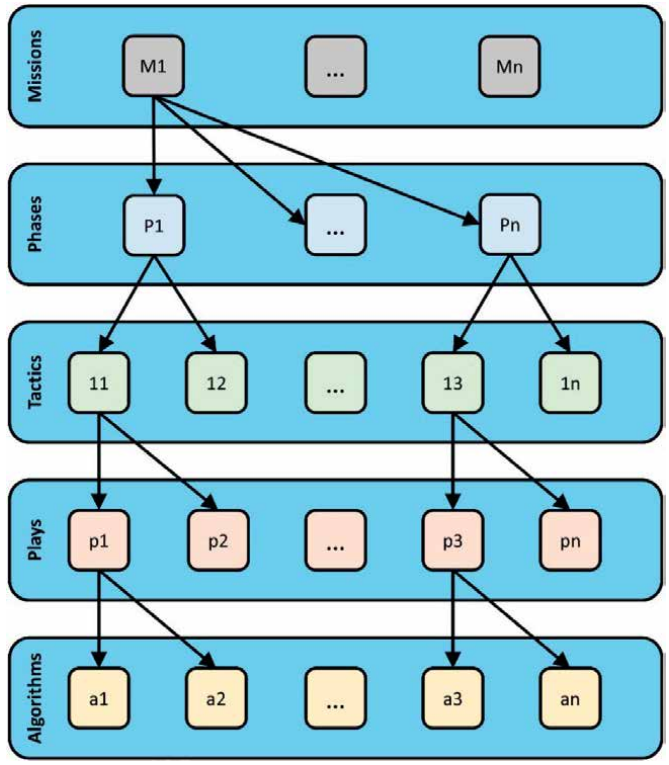

Figure 3.
MASC framework.

a swarm's operation. Moreover, the swarm adapts to these changes and adjusts its behavior accordingly. For this, continuous monitoring and tracking are essential. Many researchers propose different control models, simulation models, and simulation tools for solving monitoring and tracking challenge. Dynamic Data-Driven Application System (DDDAS) is a solution, which assists in the environment and the mission's adaptation [34].

Target searching requires consideration of effective methods and control strategies. If the target knows about the mobility and position of the searcher, then the searching complexity will be enhanced. The distributed strategy also provides solutions to the Automatic Target Recognition (ATR) issue. Many researchers suggest layered detection solutions, learning-edge software, and optimal technology for tracking UAVs in a swarm. **Figure 4** represents spatial distribution using an improved bean optimization algorithm (BOA) that is based on the population evolution model as developed in [35]. In this figure, the swarm space is distributed into three layers, a temporary dispatch layer, an individual layer, and a parent layer. BOA shows effective target search capabilities, emerging group intelligence, and distributed collaborative interaction. The individuals' distribution using BOA can be given as,

$$X_{ij}(t+1) = X_i(t), \text{ if } X_{ij}(t+1) \text{ is a parent} \tag{1}$$

$$G\left(X_i(t)\right), \text{ if } X_{ij}(t+1) \text{ is not a parent} \tag{2}$$

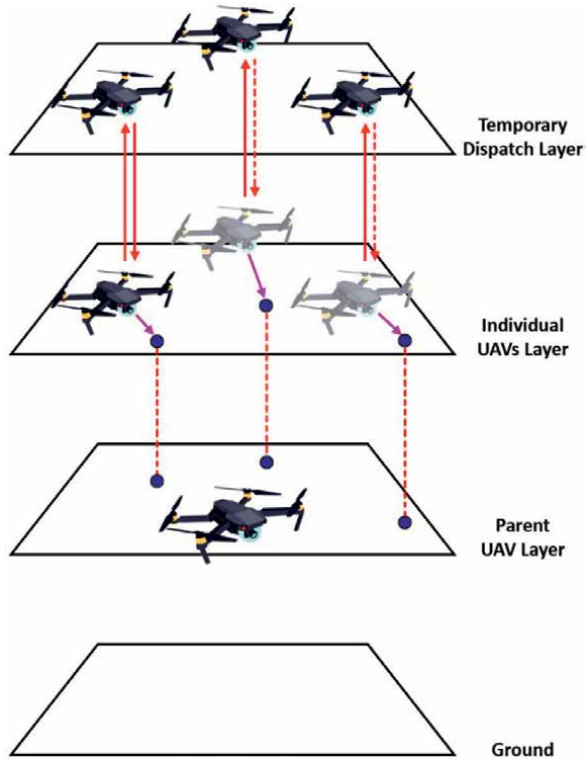

Figure 4.
Spatial distribution of individual UAVs.

Here, the parent i generates the position of individual j and is denoted by $X_{ij}(t+1)$, the $X_i(t)$ denotes the parent i, and $G(X_i(t))$ gives the distributed function.

4.5 Swarm communication

Communication is one of the prime challenges for UAV swarms [36]. Under a noisy and complex environment, a swarm requires accurate and efficient data communication for the task executions. Data communication depends upon an appropriate structured network. **Figure 5** shows that wireless ad-hoc networks are capable to provide efficient communications as presented in [37]. A base station is connected with two UAVs in this figure. Both of these UAVs are further connected to a different group of UAVs. The intraconnection of UAVs is independent but the interconnection is dependent on the base station. Three forms of networks include Flying Ad-hoc Network (FANET), Mobile Adhoc Network (MANET), and Vehicle Adhoc Networks (VANET). FANET network provides a network for communication between a few UAVs with GCS, while the rest of the UAVs communicate with each other. FANET enhances the range of communication as well as the connectivity in areas with limited cellular infrastructure and obstacles. Whereas MANET and VANET are interlinked with FANET. Therefore, FANET possesses similar features to both the other forms except a few ones like mobility, better connectivity, energy constraints,

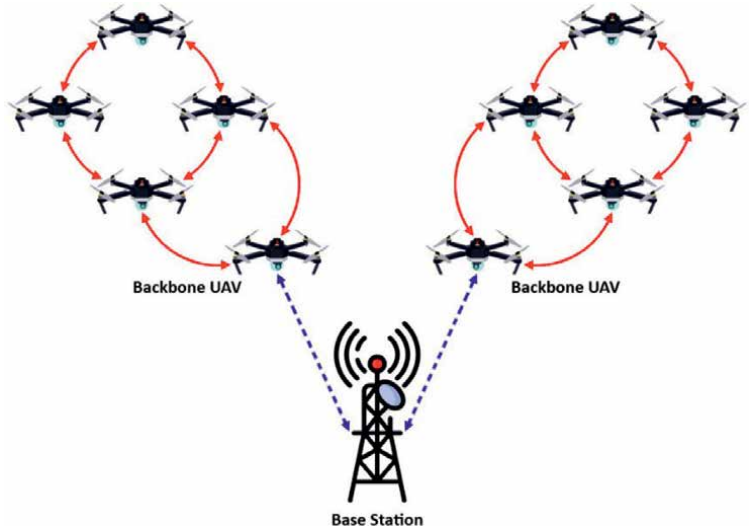

Figure 5.
Ad-hoc network for multi-group UAV.

etc. MANET does not require any support from the infrastructure of the internet and is formed with a required number of mobile devices. Whereas the VANET consists of terrestrial vehicles.

For quick deployment UAVs act as aerial base stations in a swarm to support the infrastructure of the communication. This wireless networking is implemented successfully between UAV and Internet of Things (UAV-IoT), UAV and cellular unloading (UAV-CO), UAV and emergency communications (UAV-EC), and others. These improve transmission efficiency and reduce response delays. Moreover, efficient communication can also solve other challenges like cooperation, control, and path planning. Hence, the foundation of a UAV swarm is effective communication.

4.6 Swarm safe distance protocol

In UAV swarm collaboration, the self-organization behavior becomes essential for each UAV. Transfer of data and communication take place among all the UAVs for appropriate decision-making during self-organizing swarm flights. But there is a risk of collision among UAVs in complex flight conditions. Hence, one of the key challenges is to provide a collision avoidance protocol for safe flights [38]. These protocols are necessary because of the continuous mobility of UAVs, limited resources, and air links instability. All the UAV members of a swarm must know each other's positions using a multi-hop connection. Most of these require a global positioning system (GPS) and in the absence of GPS, the location of a UAV can be estimated using the Euclidean distance formula with three nodes of known positions. Several kinds of research provide safe flight protocols using goose swarm algorithms, Reynolds rule, and pigeon flock algorithm. Other than this, many optimization algorithms can promote the UAV swarm consensus. Reynolds protocol uses three flocking behavioral rules. First is the separation rule in which a UAV attempts to move away from neighboring UAVs in a swarm. Second is the alignment rule in which UAV attempts to align the velocity with the neighboring UAV to avoid collisions. The third is the cohesion rule-following which

the UAV tries to share the same position by coming closer to the neighboring UAVs to form clusters. A self-organized flight model using Reynolds Rules is given using the idea of [39]. All these rules are summarized in the following equation,

$$J_i = V\left(\| s_{ij}(t) \|\right) + \sum_{j \in Ni(t)} \| \dot{si}(t) \|^2 \tag{3}$$

Here N shows the number of UAVs in a swarm, s_{ij} is the position of two UAVs i, and j in time t and $j \in \mathrm{N}i\ (t)$ with V represents an attractive–repulsive potential function with a local minimum. These rules provide a proper safe flight protocol among the UAV swarm but still have limitations, which should be improved to achieve safer trajectory planning.

5. Related survey

Successful motion planning of UAV swarms requires significant optimization algorithms with relevant infrastructures or models. **Table 1** provides a comprehensive exploration of techniques and models applied for the motion planning of a swarm of UAVs. This review will provide a detailed and better understanding of appropriate techniques for challenges faced by UAV flocks used in previous and current studies.

Kim et al. [40] considered the Kalman filter with Covariance Intersection (CI) algorithm and smoothing, and string-matching methodologies to observe the airborne monitoring using a swarm of UAVs. The researchers employed the hidden Markov model (HMM) for path planning and achieved an increment in the tracking accuracy and a reduction in the tracking error. Oh et al. [41] suggested a vector field guidance approach to track the moving objects. The study further introduced a two-phase approach; K-means clustering with Fisher information matrix (FIM) and cooperative standoff tracking method for this purpose. The results showed standoff group tracking successfully, allowed local replanning, and kept all the targets of interest within the sensor's field-of-view (FOV). Sampedro et al. [42] presented Global Mission Planner (GMP) and Agent Mission Planner (AMP) for a UAV swarm. Their proposal gave a complete operative, robust, scalable, and flexible framework that automatically performed many high-level missions.

Yang et al. [43] analyzed eleven swarm intelligence (SI) algorithms for UAV swarm. This research explained the features and principles of these algorithms and analyzed different algorithm combinations and task assignments for multiple UAVs. Hocraffer and Nam [44] performed a meta-examination of the human-system interface concerning human factors. The analysis provided a basis to start research, enhanced situation awareness (SA), and yielded efficient results. Lee and Kim [45] studied multirotor dynamic models with linear and nonlinear controllers for trajectory tracking control of multi-UAVs. The study showed that linear controllers were easily applicable, robust, and provide optimality and some nonlinear controllers were also easily applicable, intuitive, and gave global stability. Yang et al. [46] linked an orthogonal multi-swarm cooperative particle swarm optimization algorithm with a knowledge base model (MCPSO-K). This technique converged faster, avoided premature convergence, lessened the computational costs, and ensured the uniform distribution of particles.

Ref.	Author (Year)	Applied Technique/Model	Challenges Addressed	Contributions	Limitation
[40]	Kim et al. (2010)	Kalman filter with CI and smoothing Boyer-Moore algorithm HMM	Monitoring and tracking	• Enhances the tracking accuracy • Reduces the tracking error by 50%	• Shows weaving behavior • Requires decision-making integrations
[41]	Oh et al. (2015)	Vector field guidance approach Two-phase approach. K-means clustering with FIM and Cooperative standoff tracking method	Target tracking	• Gives standoff group tracking successfully • Allows local replanning and keeps all the targets of interest within the sensor's FOV	• Has many implementation issues • Shows imperfect communication effects and measurement data association effects
[42]	Sampedro et al. (2016)	GMP AMP	Architecture, target detection, and exploration	• Gives a complete operative, robust, scalable, and flexible framework • Performs automatically many high-level missions	• Does not focus on various behavior functionalities • Does not include time-based or autonomy-based optimization approaches
[43]	Yang et al. (2017)	SI	Management and task assignments	• Explains features and principles of many SI algorithms • Analyzes SI combinations and task assignments for multiple UAVs	• Does not consider parameter optimization and swarm robot application • Does not focus on algorithms for computational cost and convergence speed
[44]	Hocraffer and Nam (2017)	Human-system interface	Human-system interfaces	• Focuses on the human-system interface and human factors concerns • Provides a basis to start research and gives efficient results • Enhances SA	• More effective interfaces are required • Requires more research
[45]	Lee and Kim (2017)	Multirotor dynamic models Linear and non-linear controllers	Trajectory tracking control	• Linear controllers are easily applicable, robust, and provide optimality • Some non-linear controllers are easily applicable, intuitive, and give global stability	• Linear controllers require more modification, and some have limited applications • Some non-linear controllers do not work if noise or model error exists and lack robustness

Ref.	Author (Year)	Applied Technique/Model	Challenges Addressed	Contributions	Limitation
[46]	Yang et al. (2017)	MCPSO-K	Cooperation, searching, and path planning	• Converges faster and avoids premature convergence • Lessens the computational costs • Ensures the uniform distribution of particles	• Requires adjustment of information interaction at the swarm level
[47]	Guastella et al. (2018)	Modified A* algorithm	Path planning	• Reduces the computational time • Improves path trajectories • Improves targets' automatic redistribution	• No visible path for the two UAVs
[48]	Duan et al. (2018)	MA with VND	Path planning	• Optimizes the path routing • Gives highly effective results • Solves CVRP even NP-hard problems efficiently	• Does not consider delivery and pickup issues simultaneously
[49]	Koohifar et al. (2018)	EKF Recursive Bayesian estimator CRLB	Localization and path planning	• Plans the future tracking trajectory • Enhances the performance • CRLB and the Bayesian estimator outperform	• Shows higher computational costs • Non-convex optimization can be more significant
[50]	Shao et al. (2018)	RISE-ESO controller Residual estimation error	Trajectory tracking control	• Tackles the lumped disturbance issues • Achieves tracking accuracy, effectiveness, and superiority	• Does not include real-time flight experiment
[51]	Campion et al. (2018)	Cellular mobile infrastructure Machine learning Distributed control algorithms M2M and 5G networks	Communication and control architecture	• Alleviates limiting factors for previous studies • Enhances efficiency of the swarm and commercial usage	• Does not apply practically on a commercial level
[52]	Shao et al. (2018)	ESO-based robust controllers DSC design DOB control techniques	Trajectory tracking control	• Shows effective and superior results in tracking • Shows increased anti-disturbance capability	• Requires further modifications for output feedback–based controllers

Ref.	Author (Year)	Applied Technique/Model	Challenges Addressed	Contributions	Limitation
[53]	Mammarella et al. (2018)	SMPC Guidance algorithm	Trajectory tracking control	• Deals efficiently with noise and parametric uncertainty • Guarantees real-time tracking • Ensures performance with good stability	• May require an onboard fellow computer
[54]	Huang and Fie (2018)	GBPSO	Path planning	• Improves the ability to search and avoids the local minimum • Provides the feasible optimal path with superior quality and speed	• Requires further improvements in terms of accuracy and searching efficiency
[55]	Ghazzai et al. (2018)	Bandwidth hungry and delay-tolerant applications mm-Wave and μ-Wave communication modules Hierarchical iterative approach	Path planning and communication	• Increases the stopping locations • Minimizes the service time	• Does not consider non-orthogonal transmission while applying μ-wave • Requires limiting the interference effect during extra coordination
[56]	Liu et al. (2018)	Distributed formation control algorithm MPC Disturbance estimation method	Control	• Convenient for the formations of arbitrary, time-varying prescribed shapes • Achieves a balanced configuration on a prescribed 2D or 3D shape	• Requires algorithm extension for 3D situations having different obstacles • Needs human operator directions
[57]	Xuan-Mung et al. (2019)	RAS-BSC Lyapunov theory	Trajectory tracking control	• Provides the stability of the closed-loop system • Bounds the tracking errors and ESO errors • Rapid and robust in the uncertainties • Gives superior performance	• Designing of for landing quadrotor in moving platform • Not applicable in multi-agent systems • Slow response time
[58]	Fabra et al. (2019)	MUSCOP	Coordination and synchronization	• Achieves swarm cohesion with a high degree under multiple conditions • Allows least synchronization delays with low position offset errors	• Does not validate the proposed protocol with different formations

Ref.	Author (Year)	Applied Technique/Model	Challenges Addressed	Contributions	Limitation
[59]	Causa et al. (2019)	Multi-GNSS constellation approach Edge cost estimation	Path planning	• Decreases the computation time and entire mission time • Provides a rapid solution to the task assignment issue and planning for offline and in near real-time scenarios	• Has high computational cost
[60]	Brown and Anderson (2019)	Quintic polynomials trajectory generation method OMOPSO Area search radar model	Trajectory optimization and surveillance	• Gives maximum number of better trajectories • Reduces the time to revisit and fuel consumption and enhances the detection probability	• Requires excessive fuel to fly at higher altitudes
[61]	Mehiar et al. (2019)	QRDPSO	Searching and obstacle avoidance	• Provides a more stable, efficient, and quick optimal solution • Avoids obstacles and overcomes the communication constraints • Reaches the global best for search and rescue operations	• Requires more energy conservation and enhanced lifetime
[62]	Wang et al. (2020)	Leader-following model Routh–Hurwitz criterion Consensus protocol MPC	Control and stability	• Predicts the changes in the leader's state • Lessens the consensus achievement time • Keeps the formation shape	• Not extended to nonlinear systems • Does not consider disturbance issue
[63]	Altan (2020)	PSO HHO	Control and path following	• Performs the best for multiple geometric paths • Quickly determines the controller parameters • HHO outperforms and overcomes the stabilization issues • HHO gives the least settling and peak time and overshoot	• Does not focus on model-based controller design

Ref.	Author (Year)	Applied Technique/Model	Challenges Addressed	Contributions	Limitation
[64]	Wang et al. (2020)	NRI model Mapping Table	Trajectory prediction	• Improves the position detection performance • Projects the motion in 3D space into a 2D plane • The designed algorithm predicts the trajectory and gives high accuracy	• Does not consider the height information • Does not include trajectory prediction in 3D space
[65]	Rubí et al. (2020)	BS and FL algorithms NLGL CC algorithms	Path following control	• BS outperforms for yaw error and path distance • CC needs fewer data and proves to be easily applicable for any path type	• Does not consider experimental platform features
[66]	Selma et al. (2020)	ANFIS-PSO	Trajectory tracking control	• Adjusts automatically the ANFIS parameters • Minimizes tracking error by improving the controller quality • Gives high performance	• limitations of classical control laws are solved in the absence of model parameters not found
[67]	Liu et al. (2020)	Kinetic controller The BAT-based topology control algorithm FANET	Control and communication	• Can perform a neighbor selection • Reduces the communication overhead significantly	• Does not consider delay, interference, and other communication constraints
[68]	Madridano et al. (2020)	3D PRM algorithm ROS architecture MavLink protocol Pixhawk autopilot Hungarian method	Control and communication	• Generates optimal solutions using minimum time • Lessens the computational time • Reduces the total traveling distance	• Requires producing a node and developing an MRTA algorithm for allocation efficiently • Does not mount onboard sensors for dynamics obstacles detection
[69]	Zhou et al. (2020)	Hierarchical control framework SI	Decision-making, path planning, control, communication, and application	• Categorizes the major technologies with trends, future research, and limitations	• Requires expensive loads for high performance • Needs to improve safety relation

Ref.	Author (Year)	Applied Technique/Model	Challenges Addressed	Contributions	Limitation
[70]	Wubben et al. (2020)	MUSCOP protocol Ardu-Sim	Resilience and synchronization	• Handles the loss of a leader and backup leaders efficiently • Introduces an ignorable flight times delay	• Does not address swarm split-up situation
[71]	Selma et al. (2020)	Hybrid ANFIS-IACO controller	Trajectory tracking control	• Proves the superior performance • Reduces the errors, MSE and RSE significantly • Allows the UAVs to reach the desired trajectory in a minimum period	• Applicable to only a 2D vertical plane.
[72]	Altan and Hacıoğlu (2020)	Newton–Euler method-based 3-axis gimbal system Hammerstein model MPC	Control and target tracking	• Tracks the target with stability • Shows robustness even under external disturbances	• Does not track an aerial target
[73]	Sanalitro et al. (2020)	Fly-Crane system Optimization-based tuning method Inner or outer loop approach	Control	• Deals with parametric uncertainties • Performs rotating and translating of particular trajectories • Guarantees stability and enhances the performance of $H\infty$	• Needs to keep the motion low • Requires relaxation in the structure
[74]	Chen and Rho (2020)	SI SOMs	Tactical deployment and communication	• Enables self-organization for UAV arrays • Allows reconfiguration of the UAVs into hubs or terminals • Shares information efficiently	• Requires big-data cloud centers to handle huge data
[75]	Qing et al. (2021)	IACO Minimum-snap algorithm ZCBF	Collision avoidance	• Gives optimal results for decision-making in real-time • Evaluates collision-free effectiveness	• Does not perform in the real flight
[76]	Miao et al. (2021)	A multi-hop mobile relay system MSEE maximization transmission scheme BCD SCA Dinkelbach method	Secrecy and energy efficiency, and communication	• Guarantees the convergence • Provides major improvements in energy efficiency and secrecy rate	• Does not include channel models, real-time communications, and unknown nodes' locations

Ref.	Author (Year)	Applied Technique/Model	Challenges Addressed	Contributions	Limitation
[77]	Shao et al. (2021)	Multi-segment strategy IPSO-GPM	Trajectory planning and obstacle avoidance	• Increases obtained solution optimality • Generates high-quality trajectories • Takes minimum running time	• Does not select collocation points • Does not generate trajectory with dynamic obstacles
[78]	Gu et al. (2021)	NIT	Identification	• Gives a quick response, accuracy • Proves to be effective, fault-tolerant, and stable in complex environments	• Sensitive to nuance • Only suitable for high-dimensional trajectories
[79]	Ling et al. (2021)	Out-of-the-box trajectory plotting Multi-round Monte Carlo simulation	Communication, estimation, perception fusion, and path planning	• Works in noise and unstable communication • Proves to be useful for cooperative swarm application	• Does not consider additional mode functionalities and reinforcement learning-based cooperative planning algorithm
[80]	Yao et al. (2021)	Swarm intelligence-based automatic inspection optimization algorithm	Inspection and communication	• Controls the UAVs effectively • Improves the autonomy and inspection efficiency • Minimizes the cost of inspection	• Does not avoid path repetition
[81]	Xia et al. (2021)	MARL-MUSAC	Monitoring and target tracking	• Allows making intelligent flight decisions • Reduces the power consumption • Enhances the tracking success rates • Gives high performances for detection coverage	• Not valid for different formations
[82]	Nnamani et al. (2021)	Grid-structured approach	Communication	• Improves the secrecy rate of ground communications • Improves physical layer security • Evaluates the optimal radius of the eavesdropper's unknown location	• No real-time communications
[83]	Xu et al. (2021)	Communication-aware centralized and decentralized controllers	Trajectory tracking control and communication	• Achieves high waypoint tracking accuracy • Decentralized controller outperforms • Maintains the stability	• Does not suppress Cochannel noise • Does not ignore multipath effects

Ref.	Author (Year)	Applied Technique/Model	Challenges Addressed	Contributions	Limitation
[84]	Sharma et al. (2021)	SI	Environmental knowledge, communication, obstacle avoidance, and target tracking	• PSO has a low computational complexity • ACO possesses good scalability • Firefly utilizes a single operator for solution searching	• Needs to explore an improved, hybrid optimization algorithm with no limitations
[85]	Han et al. (2021)	backscatter communication system MIMO CLT-based approach	Communication	• Performs well to detect parasite devices and separate parasite signals • Reduces the energy consumption • Optimizes the trajectory planning	• Requires a large number of antennas to reduce the channel distribution error
[86]	Zhou et al. (2021)	MTT system Cooperative tracking algorithm Multi-objective Lyapunov optimization model	Target tracking and collision avoidance	• Reduces the execution complexity and energy consumption • Improves the prediction accuracy of trajectory	• Reduces the consumption of energy of the system only if the episodes increase
[87]	Brown and Raj (2021)	Reactive tracking Reactive tracking with predictive pre-positioning	Formation, tracking, and communication	• Shows superior tracking performance	• Requires offsetting the angular orientation of surveillance's adjacent rings for the voids' size-reduction
[88]	Sastre et al. (2022)	Improved CSTH CED_CSTH ArduSim simulator VTOL with KMA	Take-off and collision avoidance	• Allows the computation time optimization • Ensures safe distancing • Improves the time required for take-off • KMA proves to be the most reasonable choice for realistic conditions	• Requires more reduction in take-off time and the number of resulting UAV batches
[89]	Bansal et al. (2022)	SHOTS PUFs Mao Boyd's logic approach Christofides algorithm	Communication, physical security, and scalability	• Achieves scalability • Guarantees physical security • Resists against various attacks • Outperforms and reduces computational costs	• Requires further reduction in the attestation and computation time

Table 1.
A comprehensive review of the motion planning of the swarm of UAVs applying various techniques and models.

Guastella et al. [47] considered operating space as a 3-directional (3D) grid and applied the modified A* algorithm for path planning of multi-UAVs. The researchers found a reduction in computational time, improvement in planned trajectories, and automatic redistribution of targets. Duan et al. [48] gave a novel hybrid metaheuristic approach by linking memetic algorithm (MA) with variable neighborhood descend (VND) algorithm for path planning of multiple UAVs. The results yielded an optimization in routes, gave highly effective results, and solved capacity vehicle routing problems (CVRP) and even Non-deterministic Polynomial-time hard (NP-hard) problems efficiently. Koohifar et al. [49] applied the extended Kalman filter (EKF) with recursive Bayesian estimator, and Cramer-Rao lower bound (CRLB) path planning for UAV swarms. The analysis showed that the proposed method planned the future tracking trajectory successfully. Moreover, CRLB outperformed and enhanced the performance as well.

Shao et al. [50] combined a robust integral of the sign of the error (RISE) feedback controller with an extended state observer (ESO) and used residual estimation error. This strategy tackled the lumped disturbance issues and achieved tracking accuracy, effectiveness, and superiority. Campion et al. [51] studied cellular mobile infrastructure, machine learning and distributed control algorithms, machine-to-machine (M2M) communication, and 5th generation (5G) networks for UAV swarm. This study showed that the applied techniques alleviated limiting factors for previous studies and enhanced the efficiency of the swarm and commercial usage. Shao et al. [52] proposed extended state observer (ESO)-based robust controllers with dynamic surface control (DSC) design and disturbance observer-based (DOB) control techniques. This proposal showed effective and superior results in tracking with increased anti-disturbance capability. Mammarella et al. [53] applied sample-based stochastic model predictive control (SMPC) and guidance algorithm for tracking control of UAV swarm. The applied algorithms dealt efficiently with noise and parametric uncertainty and guaranteed real-time tracking and performance with good stability.

Huang and Fie [54] introduced the global best path with a competitive approach to particle swarm optimization (GBPSO). This developed strategy improved the ability to search, avoided the local minimum, and provided the feasible optimal path with superior quality and speed. Ghazzai et al. [55] suggested applications of bandwidth-hungry and delay-tolerant and exploited typical microwave (μ-Wave) and the high-rate millimeter wave bands (mm-Wave) for trajectory optimization. Further, the research also implemented a hierarchical iterative approach. The dual-band increased the stopping locations and minimized the service time of multi-UAVs. Liu et al. [56] implemented distributed formation control algorithm with a fast model predictive control method and disturbance estimation method. This strategy was convenient for the formations of arbitrary, time-varying prescribed shapes and achieved a balanced configuration on a prescribed 2-directional (2D) or 3D shape.

Xuan-Mung et al. [57] used a robust saturated tracking backstepping controller (RAS-BSC) and Lyapunov theory. The researchers found that the proposed mechanisms provided the stability of the closed-loop system and bounded the tracking errors and extended state observer (ESO) errors. Moreover, it was rapid and robust in the uncertainties and gave a superior performance. Fabra et al. [58] suggested a Mission-based UAV Swarm Coordination Protocol (MUSCOP) for a swarm of UAVs. This study achieved swarm cohesion with a high degree under multiple conditions and allowed the least synchronization delays with low position offset errors. Causa et al. [59] employed a multi-global navigation satellite system (multi-GNSS) constellation approach and edge cost estimation method for path planning of multiple UAVs.

These approaches decreased the computation time and entire mission time providing a rapid solution to the task assignment issue and planning for offline and in near real-time scenarios.

Brown and Anderson [60] applied the Quintic polynomials trajectory generation method, multi-objective particle swarm optimization (OMOPSO) and area search radar model to optimize the trajectories for the UAV swarm. This combination gave a maximum number of better trajectories, reduced the time to revisit and fuel consumption, and enhanced the detection probability. Mehiar et al. [61] developed Quantum Robot Darwinian particle swarm optimization (QRDPSO) for UAV flocks. This optimization algorithm provided a more stable, efficient, and quick optimal solution, avoided obstacles, and overcome communication constraints. Moreover, it reached the global best for search and rescue operations. Wang et al. [62] suggested a Leader-following model, Routh–Hurwitz criterion, a consensus protocol, and a model predictive controller for multiple UAVs. The applied approaches predicted the changes in the leader's state, reduced the consensus achievement time, and kept the formation shape.

Altan [63] proposed metaheuristic optimization algorithms, Harris Hawks Optimization (HHO), and Particle Swarm Optimization (PSO) for UAV swarm. His suggested methods performed the best for multiple geometric paths and quickly determined the controller parameters. HHO outperformed, overcome the stabilization issues, and gave the least settling, peak time, and overshoot. Wang et al. [64] developed Neural Relational Inference (NRI) model along with a Mapping Table between the UAV swarm and the spring particles. The results of the developed method were able to improve the position detection performance. Moreover, it projected the motion in 3D space into a 2D plane and the designed algorithm predicted the trajectory and gave high accuracy. Rubí et al. [65] employed four PF algorithms namely, backstepping (BS) and feedback linearization (FL) algorithms, Non-Linear Guidance Law (NLGL) algorithm, and Carrot-Chasing (CC) geometric algorithms for UAV swarms. In comparing, the results of path following BS outperformed for yaw error and path distance and the CC algorithm needed fewer data and proved to be easily applicable for any path type. Selma et al. [66] used a hybrid controller, adaptive neuro-fuzzy inference system (ANFIS), and PSO algorithms for trajectory tracking of multiple UAVs. The results evaluated that the PSO algorithm adjusted automatically the ANFIS parameters, minimized tracking error by improving the controller quality, and gave a high performance.

Liu et al. [67] suggested a kinetic controller, distributed β-angle test (BAT)-based topology control algorithm, and Flying ad-hoc network (FANET) for UAV flocking. This mechanism could perform neighbor selection and reduce the communication overhead significantly. Madridano et al. [68] applied the 3D probabilistic roadmaps (PRM) algorithm, Robot Operating System (ROS) architecture, Mav-Link protocol, Pixhawk autopilot, and Hungarian method for trajectory planning in 3D. This combination generated optimal solutions using minimum time and lessened the computational time and the total traveling distance. Zhou et al. [69] analyzed the Hierarchical control framework with different SI algorithms. This analysis categorized the major technologies with trends, future research, and limitations. Wubben et al. [70] employed MUSCOP protocol and an emulation tool, Ardu-Sim, to provide resilience to multiple UAVs. This protocol handled the loss of leaders and backup leaders efficiently and introduced an ignorable flight time delay.

Selma et al. [71] applied an adaptive-network-based fuzzy inference system (ANFIS) and improved ant colony optimization (IACO) for controlling trajectory tracking tasks. This strategy proved its superior performance, reduced the mean

squared error (MSE) along with root mean squared error (RMSE) significantly, and allowed the UAVs to reach the desired trajectory in a minimum period. Altan and Hacıoğlu [72] used Newton–Euler method-based 3-axis gimbal system, the Hammerstein model, and the model predictive control (MPC) algorithm for target tracking. This mechanism tracked the target with stability and showed robustness even under external disturbances. Sanalitro et al. [73] suggested a Fly-Crane system with an optimization-based tuning method and an inner or outer loop approach. This system dealt with parametric uncertainties performed by rotating and translating trajectories, guaranteed stability, and enhanced the performance of H∞. Chen and Rho [74] introduced the SI technique with self-organizing maps (SOMs) based on requests from end-users (EUs). This technique allowed self-organization for UAV arrays and reconfiguration of the UAVs into hubs or terminals. Moreover, it shared information efficiently.

Qing et al. [75] applied improved ant colony optimization (ACO), minimum-snap algorithm, and zeroing control barrier function (ZCBF) for multiple swarms. The results evaluated that the proposed algorithms gave optimal results for decision-making in real-time. Moreover, it efficiently provided collision and avoidance-free trajectories. Miao et al. [76] proposed a multi-hop mobile relay system, the minimum secrecy energy efficiency (MSEE) maximization transmission scheme, and generated an algorithm using the block coordinate descent method (BCD), successive convex approximation (SCA) techniques, and Dinkelbach method for multiple UAVs. The results guaranteed the convergence and provided major improvements in energy efficiency and secrecy rate. Shao et al. [77] linked multi-segment strategy with improved particle swarm optimization-Gauss pseudo-spectral method (IPSO-GPM) for UAV swarms. The outcomes evaluated that the applied mechanisms increased obtained solution optimality, generated high-quality trajectories, and took minimum running time.

Gu et al. [78] suggested Network Integrated trajectory clustering (NIT) for determining subgroups of a flock of UAVs. This clustering showed a quick response and accuracy and proved to be effective, fault-tolerant, and stable in complex environments. Ling et al. [79] presented a planning algorithm; out-of-the-box trajectory plotting with multi-round Monte Carlo simulation for UAV swarms. This developed algorithm worked in noise and unstable communication and proved to be useful for cooperative swarm applications. Yao et al. [80] employed swarm intelligence and optimization algorithms for UAV swarms. The results showed that the proposed algorithm controlled the UAVs effectively improved the autonomy and inspection efficiency and minimized the cost of the inspection. Xia et al. [81] suggested multi-agent reinforcement learning (MARL) with multi-UAV soft actor-critic (MUSAC) for the UAV swarm. The suggested mechanism allowed to make intelligent flight decisions, reduced the power consumption, enhanced the tracking success rates, and gave high performances for detection coverage.

Nnamani et al. [82] applied a grid-structured approach to the UAV swarm. The outcomes showed improvement in the secrecy rate of communications and physical layer security and evaluated the optimal radius of the eavesdropper's unknown location. Xu et al. [83] designed communication-aware centralized and decentralized controllers for UAV swarm. Their proposed controllers achieved high waypoint tracking accuracy. Between both controllers, the decentralized controller outperformed and maintained stability. Sharma et al. [84] studied multiple SI algorithms for path planning of UAV swarm. This analysis showed that PSO had low computational complexity, ACO possessed good scalability, and Firefly utilized a single operator for solution searching. Han et al. [85] employed a backscatter communication system

with the massive multiple-input multiple-output (MIMO) and Central limit theorem (CLT)-based approach to analyze the performance and optimize the trajectory. This combination performed well to detect parasite devices and separate parasite signals. Moreover, it reduced energy consumption and optimized trajectory planning.

Zhou et al. [86] used Multi-Target Tracking (MTT) system, an intelligent UAV swarm-based cooperative tracking algorithm, and a multi-objective Lyapunov optimization model. The results showed a reduction in the execution in the complexity and energy consumption with an improvement in the prediction accuracy of trajectory. Brown and Raj [87] applied reactive tracking and reactive tracking with predictive pre-positioning to study the effects of initial swarm formation. The tracking gave a superior performance.

Sastre et al. [88] applied collision-less swarm take-off heuristic (CSTH) with two improvements and Euclidean distance-based CSTH (ED-CSTH) algorithms to analyze the trajectory and batch generations. This study also used the ArduSim simulator and vertical take-off and landing (VTOL) techniques with Kuhn-Munkres Algorithm (KMA) for UAV swarms. The proposed method showed the computation time optimization, ensured safe distancing, and improved the time required for take-off. Whereas KMA proved to be the most reasonable choice for realistic conditions. Bansal et al. [89] proposed a scalable authentication-attestation protocol, SHOTS, with Physical Unclonable Functions (PUFs), Mao Boyd logic approach, and Christofides algorithm for UAV swarms. The authors suggested a lightweight authentication and attestation mechanism for UAV swarms that makes use of Physical Unclonable Functions (PUFs) to ensure physical security as well as the necessary trust in a lightweight manner.

6. Discussion

The significance of multiple UAVs is expanding their cooperative operations and applications in many fields. Swarms are deployed in many environments such as uncertain, indoor, outdoor, traffic, and many others. Findings show that many challenges such as decision-making, control, path planning, communication, monitoring, tracking, targeting, collision, and obstacle avoidance may hinder the motion planning of a UAV swarm. Survey shows that different approaches are adopted in all the research addressing different challenges. Like mission planning architectures provide a complete operative, robust, scalable, and flexible framework. Many controllers whether linear or nonlinear, proves to be easily applicable, intuitive, robust, and provide optimality and global stability. Improved model predictive controllers ensure real-time monitoring and tracking of swarms. Moreover, they enhance the tracking accuracy, effectiveness, and superiority. Machine learning, 5G networking, and other technologies alleviate limiting factors for previous studies and enhance the efficiency of the swarm and commercial usage. Among all these evolving technologies in this chapter, swarm intelligence is determined as an appropriate solution for the reliable and efficient deployment of swarms. Moreover, it enables self-organization, reconfiguration, control, efficient sharing of information, reduction in inspection costs, and improvement in autonomy.

Besides many mentioned advantages of the swarm and technological development, many important and interesting limitations exist that can hinder the swarm performance. Among these restrictions, the manufacturing cost of the large-scale swarm is still high. Existing loads are huge, expensive, and mostly not appropriate for

pursuing high performances. Hence, the lightweight and low-cost loads and platforms are essential for swarm formation. Battery capacity for aerial mission completion is of much significance. Long-lasting batteries are essential for continuous tasks. However, the capacity of the battery can be enhanced by increasing the UAV's weight. And this weight increment will also require an increment in energy consumption. To provide a proper battery solution such systems are essential that can easily and rapidly replace the depleted battery with the supplementary one and are capable to charge other batteries. Another limitation is the privacy protection protocol. This is essential for deploying swarm in sensitive locations safely. Otherwise, it can lead to national security issues.

7. Conclusion

In this chapter, we have presented the state-of-the-art of UAV swarm technology that shows its promising application for different purposes, especially in the military fields. An overview of swarm intelligence, explaining its aspects, levels, mechanisms, followed principles, and significance, is provided in this chapter. Then, the challenges faced by a swarm and approaches given by different researchers are discussed. Moreover, to analyze the motion planning of a swarm, we have studied and compiled multiple kinds of research. All these research papers provide different approaches to counter the challenges faced by a swarm of UAVs. Many of these approaches are based on trending technologies like swarm intelligence and outperform the traditional strategies. All the findings show the significance of using a swarm rather than using a single UAV. Finally, we discuss the key findings of this paper with some limitations and suggest some recommendations for future work.

8. Future work

Although swarm intelligence is in an emerging phase, more progress in this AI-based technology is expected in the upcoming years. Future research can design more intelligent controllers, optimal path planning algorithms, robust architecture, monitoring, target searching strategies, efficient communication structures, and safe flight protocols for swarms. The flight problems and formation maintenance of large-scale swarms still require future explorations. During the modeling process, the size and load of UAVs must be considered to increase the robustness of the swarm control. In the future holistic system, solutions will be provided for integrated task scenarios. Path planning of swarms in a curve requires more efficient algorithms. Moreover, algorithms that can give optimized paths rapidly in any complex environment are future work. The development of low-cost sensors is necessary to address the collective monitoring and target tracking issues but with the capability to provide high accuracy and robustness to noise. More research is required to standardize the communication networking between UAV swarms by upgrading the frequency bands, cooperative countermeasures, and signal distortion monitoring. To enhance the response speed in the threat environments, the focus will be on designing dynamic sensing and powerful safe flight protocols. Considerations are essential for intelligence assisted programs that can meet the next-generation networks. Like 6th generation (6G) network should be used for wireless communication services in swarms. This will extremely enhance the significance of formation, coordination in

tasks, machine-human interactions, and many more. Improvements should be made that can understand and adapt to the environment along with this, and it can respond to user feedback rapidly. This can further improve the systems' agility with the reliability and performance of the network.

Conflicts of interest

The authors declare no conflict of interest.

Abbreviations

Acronyms	Definitions
2D	2-Directional
3D	3-Directional
5G	5th Generation
6G	6th Generation
ACO	Ant Colony Optimization
AI	Artificial Intelligence
AMP	Agent Mission Planner
ANFIS	Adaptive Neuro-fuzzy Inference System
APF	Artificial Potential Field
ATR	Automatic Target Recognition
BAT	β-angle Test
BCD	Block Coordinate Descent
BOA	Bean Optimization Algorithm
BS	Backstepping
CC	Carrot-Chasing
CI	Covariance Intersection
CLT	Central Limit Theorem
CRLB	Cramer-Rao Lower Bound
CSTH	Collision-less Swarm Take-off Heuristic
CVRP	Capacity Vehicle Routing Problems
DARPA	Défense Advanced Research Projects Agency
DDDAS	Dynamic Data-Driven Application System
DOB	Disturbance Observer-based
DSC	Dynamic Surface Control
ED-CSTH	Euclidean Distance-based Collision-less Swarm Take-off Heuristic
EKF	Extended Kalman Filter
ESO	Extended State Observer
EUs	End-users
FANET	Flying Ad-hoc Network
FIM	Fisher Information Matrix
FL	Feedback Linearization
FOA	Fruit Fly Optimization Algorithm
FOV	Field-of-View
GBPSO	Global Best Path with Particle Swarm Optimization
GMP	Global Mission Planner
GPS	Global Positioning System

GWO	Gray Wolf Optimization
HHO	Harris Hawks Optimization
HMM	Hidden Markov Model
IACO	Improved Ant Colony Optimization
IoT	Internet of things
IPSO-GPM	Improved Particle Swarm Optimization-Gauss Pseudo-Spectral Method
KMA	Kuhn-Munkres Algorithm
M2M	Machine-to-Machine
MA	Memetic Algorithm
MANET	Mobile Adhoc Network
MARL	Multi-agent Reinforcement Learning
MASC	Mission-based Architecture for Swarm Composability
MCPSO-K	Multi-swarm Cooperative Particle Swarm Optimization Algorithm with Knowledge
MCS	Mobile Crowd Perception System
MIMO	Multiple-input Multiple-output
mm-Wave	MillimeterWave
MPC	Model Predictive Control
MSE	Mean Squared Error
MSEE	Minimum Secrecy Energy Efficiency
MTT	Multitarget Tracking
Multi-GNSS	Multi-Global Navigation Satellite System
MUSAC	Multi-UAV Soft Actor-Critic
MUSCOP	Mission-based UAV Swarm Coordination Protocol
NASA	National Aeronautics and Space Administration
NIT	Network Integrated Trajectory
NLGL	Non-Linear Guidance Law
NP-hard	Non-Deterministic Polynomial-Time hard
NRI	Neural Relational Inference
OMOPSO	Multi-objective Particle Swarm Optimization
PIO	Pigeon-inspired Optimization
PRM	Probabilistic Roadmaps
PSO	Particle Swarm Optimization
PUFs	Physical Unclonable Functions
QRDPSO	Quantum Robot Darwinian Particle Swarm Optimization
RAS-BSC	Robust Saturated Tracking Backstepping Controller
RISE	Robust Integral of the Sign of the Error
RMA	Road Map Algorithm
RMSE	Root Mean Squared Error
ROS	Robot Operating System
SA	Situation Awareness
SCA	Successive Convex Approximation
SI	Swarm Intelligence
SMPC	Stochastic Model Predictive Control
SOMs	Self-organizing Maps
TAK	Tactical Assault Kit
μWave	Microwave
UAV	Unmanned Aerial Vehicle
UAV-CO	Unmanned Aerial Vehicle-Cellular Unloading

UAV-EC	Unmanned Aerial Vehicle-Emergency Communication
UAV-IoT	Unmanned Aerial Vehicle-Internet of Things
VANET	Vehicle Adhoc Network
VND	Variable Neighborhood Descend
VTOL	Vertical Take-off and Landing
WFM	Wall-follow Method
ZCBF	Zeroing Control Barrier Function

Author details

Muhammad Mubashir Iqbal[1], Zain Anwar Ali[1*], Rehan Khan[2] and Muhammad Shafiq[1]

1 Department of Electronic Engineering, Sir Syed University of Engineering and Technology, Karachi, Pakistan

2 Center of Excellence in Science and Applied Technologies, Karachi, Pakistan

*Address all correspondence to: zainanwar86@hotmail.com

IntechOpen

References

[1] Ali ZA, Zhangang H. Multi-unmanned aerial vehicle swarm formation control using hybrid strategy. Transactions of the Institute of Measurement and Control. 2021;**43**(12):2689-2701

[2] Brust MR, Danoy G, Stolfi DH, Bouvry P. Swarm-based counter UAV defense system. Discover Internet of Things. 2021;**1**(1):1-19

[3] Wilson AN, Kumar A, Jha A, Cenkeramaddi LR. Embedded sensors, communication technologies, computing platforms and machine learning for UAVs: A review. IEEE Sensors Journal. 2021;**22**(3):1807-1826

[4] Gupta A, Afrin T, Scully E, Yodo N. Advances of UAVs toward future transportation: The state-of-the-art, challenges, and opportunities. Future Transportation. 2021;**1**(2):326-350

[5] Khan MTR, Saad MM, Ru Y, Seo J, Kim D. Aspects of unmanned aerial vehicles path planning: Overview and applications. International Journal of Communication Systems. 2021;**34**(10):e4827

[6] Zhu X, Liu Z, Yang J. Model of collaborative UAV swarm toward coordination and control mechanisms study. Procedia Computer Science. 2015;**51**:493-502

[7] Ali ZA, Shafiq M, Farhi L. Formation control of multiple UAVs via decentralized control approach. In: 2018 5th International Conference on Systems and Informatics (ICSAI). IEEE; 2018. pp. 61-64

[8] Monwar M, Semiari O, Saad W. Optimized path planning for inspection by unmanned aerial vehicles swarm with energy constraints. In: 2018 IEEE Global Communications Conference (GLOBECOM). IEEE; 2018. pp. 1-6

[9] James S, Raheb R, Hudak A. UAV swarm path planning. In: 2020 Integrated Communications Navigation and Surveillance Conference (ICNS). IEEE; 2020. pp. 2G3-2G1

[10] Bai G, Li Y, Fang Y, Zhang Y-A, Tao J. Network approach for resilience evaluation of a UAV swarm by considering communication limits. Reliability Engineering & System Safety. 2020;**193**:106602

[11] Tingting B, Bo WD, Ali ZA, Masroor S. Formation control of multiple UAVs via pigeon inspired optimisation. International Journal of Bio-Inspired Computation. 2022;**19**(3):135-146

[12] Ali ZA, Han Z, Masood RJ. Collective motion and self-organization of a swarm of UAVs: A cluster-based architecture. Sensors. 2021;**21**(11):3820

[13] Guitton MJ. Fighting the locusts: Implementing military countermeasures against drones and drone swarms. Scandinavian Journal of Military Studies. 2021;**4**(1):26-36

[14] Rovira-Sugranes A, Razi A, Afghah F, Chakareski J. A review of AI-enabled routing protocols for UAV networks: Trends, challenges, and future outlook. Ad Hoc Networks. 2022;**130**:102790

[15] Wei W, He X, Wang X, Wang M. Research on swarm munitions cooperative warfare. In: International Conference on Autonomous Unmanned Systems. Singapore: Springer; 2021. pp. 717-727

[16] Zieliński T. Factors determining a drone swarm employment in military operations. Safety & Defense. 2021;**1**:59-71

[17] Israr A, Ali ZA, Alkhammash EH, Jussila JJ. Optimization methods applied to motion planning of unmanned aerial vehicles: A review. Drones. 2022;**6**(5):126

[18] Seng KP, Lee PJ, Ang LM. Embedded intelligence on FPGA: Survey, applications and challenges. Electronics. 2021;**10**(8):895

[19] Shafiq M, Ali ZA, Alkhammash EH. A cluster-based hierarchical-approach for the path planning of swarm. Applied Sciences. 2021;**11**(15):6864

[20] Karadimas NV, Doukas N, Kolokathi M, Defteraiou G. "Routing optimization heuristics algorithms for urban solid waste transportation management." wseas transactions on computers. 2008;**7**(12):2022-2031

[21] Cheraghi AR, Shahzad S, Graffi K. Past, present, and future of swarm robotics. In: Proceedings of SAI Intelligent Systems Conference. Cham: Springer; 2021. pp. 190-233

[22] He W, Qi X, Liu L. A novel hybrid particle swarm optimization for multi-UAV cooperate path planning. Applied Intelligence. 2021;**51**(10):7350-7364

[23] Schranz M, Di Caro GA, Schmickl T, Elmenreich W, Arvin F, Şekercioğlu A, et al. Swarm intelligence and cyber-physical systems: Concepts, challenges and future trends. Swarm and Evolutionary Computation. 2021;**60**:100762

[24] Jabbar K. Performance Optimization of Swarm Intelligence-Based Clustering Algorithms." Master's thesis. Itä-Suomen yliopisto; 2021

[25] Shafiq M, Ali ZA, Israr A, Alkhammash EH, Hadjouni M. A multi-Colony social learning approach for the self-Organization of a Swarm of UAVs. Drones. 2022;**6**(5):104

[26] Cybulski P, Zieliński Z. UAV swarms behavior modeling using tracking bigraphical reactive systems. Sensors. 2021;**21**(2):622

[27] Tang J, Liu G, Pan Q. A review on representative swarm intelligence algorithms for solving optimization problems: Applications and trends. IEEE/CAA Journal of Automatica Sinica. 2021;**8**(10):1627-1643

[28] Wu J, Yuanzhe Y, Ma J, Jinsong W, Han G, Shi J, et al. Autonomous cooperative flocking for heterogeneous unmanned aerial vehicle group. IEEE Transactions on Vehicular Technology. 2021;**70**(12):12477-12490

[29] Bassolillo SR, Blasi L, D'Amato E, Mattei M, Notaro I. Decentralized triangular guidance algorithms for formations of UAVs. Drones. 2021;**6**(1):7

[30] Ali ZA, Zhangang H, Hang WB. Cooperative path planning of multiple UAVs by using max–min ant colony optimization along with cauchy mutant operator. Fluctuation and Noise Letters. 2021;**20**(01):2150002

[31] Collins L, Ghassemi P, Esfahani ET, Doermann D, Dantu K, Chowdhury S. Scalable coverage path planning of multi-robot teams for monitoring non-convex areas. In: 2021 IEEE International Conference on Robotics and Automation (ICRA). IEEE; 2021. pp. 7393-7399

[32] Ghulam E. Mustafa Abro, Saiful Azrin BM Zulkifli, Vijanth Sagayan Asirvadam, and Zain Anwar Ali. "Model-free-based single-dimension fuzzy SMC design for underactuated quadrotor

UAV." In Actuators, vol. 10, no. 8, p. 191. MDPI, 2021.

[33] Giles K, Giammarco K. Mission-based architecture for swarm composability (MASC). Procedia Computer Science. 2017;**114**:57-64

[34] Silic M, Mohseni K. Field deployment of a plume monitoring UAV flock. IEEE Robotics and Automation Letters. 2019;**4**(2):769-775

[35] Zhang X, Ali M. A bean optimization-based cooperation method for target searching by swarm uavs in unknown environments. IEEE Access. 2020;**8**:43850-43862

[36] Wang BH, Wang DB, Ali ZA. A Cauchy mutant pigeon-inspired optimization–based multi-unmanned aerial vehicle path planning method. Measurement and Control. 2020;**53**(1-2):83-92

[37] Al-Emadi S, Al-Mohannadi A. Towards enhancement of network communication architectures and routing protocols for FANETs: A survey. In: 2020 3rd International Conference on Advanced Communication Technologies and Networking (CommNet). IEEE; 2020. pp. 1-10

[38] Ali ZA, Zhangang H, Zhengru D. Path planning of multiple UAVs using MMACO and DE algorithm in dynamic environment. Measurement and Control. 2020;**53**(5):1-11

[39] Huang Y, Tang J, Lao S. Collision avoidance method for self-organizing unmanned aerial vehicle flights. IEEE Access. 2019;**7**:85536-85547

[40] Kim S, Żbikowski R, Tsourdos A, White BA. Behaviour recognition of ground vehicle for airborne monitoring by UAV swarm. IFAC Proceedings Volumes. 2010;**43**(16):455-460

[41] Oh H, Kim S, Shin H-s, Tsourdos A. Coordinated standoff tracking of moving target groups using multiple UAVs. IEEE Transactions on Aerospace and Electronic Systems. 2015;**51**(2):1501-1514

[42] Sampedro C, Bavle H, Sanchez-Lopez JL, Suárez Fernández RA, Rodríguez-Ramos A, Molina M, et al. A flexible and dynamic mission planning architecture for uav swarm coordination. In: 2016 International Conference on Unmanned Aircraft Systems (ICUAS). IEEE; 2016. pp. 355-363

[43] Yang F, Wang P, Zhang Y, Zheng L, Lu J. Survey of swarm intelligence optimization algorithms. In: 2017 IEEE International Conference on Unmanned Systems (ICUS). IEEE; 2017. pp. 544-549

[44] Hocraffer A, Nam CS. A meta-analysis of human-system interfaces in unmanned aerial vehicle (UAV) swarm management. Applied Ergonomics. 2017;**58**:66-80

[45] Lee H, Jin Kim H. Trajectory tracking control of multirotors from modelling to experiments: A survey. International Journal of Control, Automation and Systems. 2017;**15**(1):281-292

[46] Yang J, Zhu H, Wang Y. An orthogonal multi-swarm cooperative PSO algorithm with a particle trajectory knowledge base. Symmetry. 2017;**9**(1):15

[47] Guastella DC, Cavallaro ND, Melita CD , Savasta M, Muscato G. 3D path planning for UAV swarm missions. In: Proceedings of the 2018 2nd International Conference on Mechatronics Systems and Control Engineering; 2018. pp. 33-37

[48] Duan F, Li X, Zhao Y. Express uav swarm path planning with vnd enhanced

memetic algorithm. In: Proceedings of the 2018 International Conference on Computing and Data Engineering; 2018. pp. 93-97

[49] Koohifar F, Guvenc I, Sichitiu ML. Autonomous tracking of intermittent RF source using a UAV swarm. IEEE Access. 2018;**6**:15884-15897

[50] Shao X, Meng Q, Liu J, Wang H. RISE and disturbance compensation based trajectory tracking control for a quadrotor UAV without velocity measurements. Aerospace Science and Technology. 2018;**74**:145-159

[51] Campion M, Ranganathan P, Faruque S. UAV swarm communication and control architectures: A review. Journal of Unmanned Vehicle Systems. 2018;**7**(2):93-106

[52] Shao X, Liu J, Cao H, Shen C, Wang H. Robust dynamic surface trajectory tracking control for a quadrotor UAV via extended state observer. International Journal of Robust and Nonlinear Control. 2018;**28**(7):2700-2719

[53] Mammarella M, Capello E, Dabbene F, Guglieri G. Sample-based SMPC for tracking control of fixed-wing UAV. IEEE control systems letters. 2018;**2**(4):611-616

[54] Huang C, Fei J. UAV path planning based on particle swarm optimization with global best path competition. International Journal of Pattern Recognition and Artificial Intelligence. 2018;**32**(06):1859008

[55] Ghazzai H, Ghorbel MB, Kassler A, Hossain MJ. Trajectory optimization for cooperative dual-band UAV swarms. In: 2018 IEEE Global Communications Conference (GLOBECOM). IEEE; 2018. pp. 1-7

[56] Liu Y, Montenbruck JM, Zelazo D, Odelga M, Rajappa S, Bülthoff HH, et al. A distributed control approach to formation balancing and maneuvering of multiple multirotor UAVs. IEEE Transactions on Robotics. 2018;**34**(4):870-882

[57] Xuan-Mung N, Hong SK. Robust backstepping trajectory tracking control of a quadrotor with input saturation via extended state observer. Applied Sciences. 2019;**9**(23):5184

[58] Fabra F, Zamora W, Reyes P, Calafate CT, Cano J-C, Manzoni P, et al. An uav swarm coordination protocol supporting planned missions. In: 2019 28th International Conference on Computer Communication and Networks (ICCCN). IEEE; 2019. pp. 1-9

[59] Causa F, Fasano G, Grassi M. GNSS-aware path planning for UAV swarm in complex environments. In: 2019 IEEE 5th International Workshop on Metrology for AeroSpace (MetroAeroSpace). IEEE; 2019. pp. 661-666

[60] Brown A, Anderson D. Trajectory optimization for high-altitude long-endurance UAV maritime radar surveillance. IEEE Transactions on Aerospace and Electronic Systems. 2019;**56**(3):2406-2421

[61] Mehiar DAF, Azizul ZH, Loo CK. QRDPSO: A new optimization method for swarm robot searching and obstacle avoidance in dynamic environments. Intelligent Automation and Soft Computing. 2019;**20**(10):1-8

[62] Wang Y, Cheng Z, Xiao M. UAVs' formation keeping control based on multi–agent system consensus. IEEE Access. 2020;**8**:49000-49012

[63] Altan A. Performance of metaheuristic optimization algorithms based on swarm intelligence in attitude and altitude control of unmanned aerial vehicle for

path following. In: 2020 4th International Symposium on Multidisciplinary Studies and Innovative Technologies (ISMSIT). IEEE; 2020. pp. 1-6

[64] Wang Q, Zhuang D, Xutao Q, Xie H. Trajectory prediction of uav swarm based on neural relational inference model without physical control law. In: 2020 39th Chinese Control Conference (CCC). IEEE; 2020. pp. 7047-7054

[65] Rubí B, Pérez R, Morcego B. A survey of path following control strategies for UAVs focused on quadrotors. Journal of Intelligent & Robotic Systems. 2020;**98**(2):241-265

[66] Selma B, Chouraqui S, Abouaïssa H. Fuzzy swarm trajectory tracking control of unmanned aerial vehicle. Journal of Computational Design and Engineering. 2020;**7**(4):435-447

[67] Liu C, Wang M, Zeng Q, Huangfu W. Leader-following flocking for unmanned aerial vehicle swarm with distributed topology control. SCIENCE CHINA Information Sciences. 2020;**63**(4):1-14

[68] Madridano Á, Al-Kaff A, Martín D, de la Escalera A. 3d trajectory planning method for uavs swarm in building emergencies. Sensors. 2020;**20**(3):642

[69] Zhou Y, Rao B, Wang W. Uav swarm intelligence: Recent advances and future trends. IEEE Access. 2020;**8**:183856-183878

[70] Wubben J, Catalán I, Lurbe M, Fabra F, Martinez FJ, Calafate CT, et al. Providing resilience to UAV swarms following planned missions. In: 2020 29th International Conference on Computer Communications and Networks (ICCCN). IEEE; 2020. pp. 1-6

[71] Selma B, Chouraqui S, Abouaïssa H. Optimization of ANFIS controllers using improved ant colony to control an UAV trajectory tracking task. SN Applied Sciences. 2020;**2**(5):1-18

[72] Altan A, Hacıoğlu R. Model predictive control of three-axis gimbal system mounted on UAV for real-time target tracking under external disturbances. Mechanical Systems and Signal Processing. 2020;**138**:106548

[73] Sanalitro D, Savino HJ, Tognon M, Cortés J, Franchi A. Full-pose manipulation control of a cable-suspended load with multiple uavs under uncertainties. IEEE Robotics and Automation Letters. 2020;**5**(2):2185-2191

[74] Chen B-W, Rho S. Autonomous tactical deployment of the UAV array using self-organizing swarm intelligence. IEEE Consumer Electronics Magazine. 2020;**9**(2):52-56

[75] Qing W, Chen H, Wang X, Yin Y. Collision-free trajectory generation for UAV swarm formation rendezvous. In: 2021 IEEE International Conference on Robotics and Biomimetics (ROBIO). IEEE; 2021. pp. 1861-1867

[76] Miao J, Li H, Zheng Z, Wang C. Secrecy energy efficiency maximization for UAV swarm assisted multi-hop relay system: Joint trajectory design and power control. IEEE Access. 2021;**9**:37784-37799

[77] Shao S, He C, Zhao Y, Xiaojing W. Efficient trajectory planning for UAVs using hierarchical optimization. IEEE Access. 2021;**9**:60668-60681

[78] Gu, Kongjing, Ziyang Mao, Mingze Qi, and Xiaojun Duan. "Finding subgroups of UAV swarms using a trajectory clustering method." In Journal of Physics: Conference Series, vol. 1757, no. 1, p. 012131. IOP Publishing, 2021.

[79] Ling H, Luo H, Chen H, Bai L, Zhu T, Wang Y. Modelling and simulation of distributed UAV swarm cooperative planning and perception. International Journal of Aerospace Engineering. 2021;**2021**:1-11

[80] Yao Y, Jun-Hua C, Yi G, Zhun F, Zou An-Min X, Biao, and Li Ke. Autonomous control method of rotor UAVs for power inspection with renewable energy based on swarm intelligence. Frontiers in Energy Research. 2021;**9**:229

[81] Xia Z, Jun D, Wang J, Jiang C, Ren Y, Li G, et al. Multi-agent reinforcement learning aided intelligent UAV swarm for target tracking. IEEE Transactions on Vehicular Technology. 2021;**71**(1):931-945

[82] Nnamani CO, Khandaker MRA, Sellathurai M. Gridded UAV swarm for secrecy rate maximization with unknown eavesdropper. arXiv preprint arXiv:2102.03428. 2021;**20**(10):1-8

[83] Xu C, Zhang K, Jiang Y, Niu S, Yang T, Song H. Communication aware UAV swarm surveillance based on hierarchical architecture. Drones. 2021;**5**(2):33

[84] Sharma A, Shoval S, Sharma A, Pandey JK. Path planning for multiple targets interception by the swarm of UAVs based on swarm intelligence algorithms: A review. IETE Technical Review. 2021;**38**(1):1-23

[85] Han R, Bai L, Wen Y, Liu J, Choi J, Zhang W. UAV-aided backscatter communications: Performance analysis and trajectory optimization. IEEE Journal on Selected Areas in Communications. 2021;**39**(10):3129-3143

[86] Zhou L, Leng S, Liu Q, Wang Q. Intelligent UAV swarm cooperation for multiple targets tracking. IEEE Internet of Things Journal. 2021;**9**(1):743-754

[87] Brown J, Raj N. The impact of initial swarm formation for tracking of a high capability malicious UAV. In: 2021 IEEE International IOT, Electronics and Mechatronics Conference (IEMTRONICS). IEEE; 2021. pp. 1-6

[88] Sastre C, Wubben J, Calafate CT, Cano J-C, Manzoni P. Safe and efficient take-off of VTOL UAV swarms. Electronics. 2022;**11**(7):1128

[89] Bansal G, Naren N, Chamola V, Sikdar B. SHOTS: Scalable secure hardware based authentication-attestation protocol using optimal trajectory in UAV swarms. IEEE Transactions on Vehicular Technology. 2022;**71**(6):5827-5836

Section 3

Drones

Chapter 4

Quadrotor-Type UAVs Assembly and Its Application to Audit Telecommunications Relays

Hicham Megnafi and Walid Yassine Medjati

Abstract

Field inspection process of the cellular network infrastructures is an important step during Radio Network Optimization. It allows the collection of all physical data of needed relays to efficiently optimize the network performances. The human-based performed inspection is initiated after the raise of a set of issues. The initiated operation is intended to resolve the cited issues as the errors in physical parameters extraction of relays, human safety issues as burns and falls, etc. This work revolves around an assembly and configuration of quadrotor drones in telecommunication relays inspections because of their easiest construction and their rapidly services. The user of the realized UAV can control and initiate the operation so intuitive thanks to its graphic control interface.

Keywords: telecommunication relay, UAV, configuration, assembly, inspection, quadrotor

1. Introduction

Radio network optimization is one of the main steps to improve the performance of telecommunications cellular networks after deployment and commissioning to solve various problems in order to implement an activity with maximum efficiency and offer a better quality of communication to subscribers [1, 2]. Many operations of radio optimization could be optimized and facilitated with the introduction of drone exploitation as the audit process of cellular networks relays that is used by humans which causes a lot of problems such as taking a lot of time, subject to human error and lacks rapid response in the event of a disaster [3]. Drones also known as unmanned aerial vehicles (UAVs), without human crew on board, and are rather controlled by a person in the field or autonomously via a computer program; the development of drones has led to a change in architecture and operating concepts through the evolution of their features and capabilities [4]. there are so many types of drones that we can easily find in the world and all these drones are working for different applications, the military operations was among the first most common applications of drone technology, because it helps to easily control problems related to surveillance [5], but that does not mean that UAV applications are limited to the military world but also

serve a large part of the economy with advanced mechanisms and impressive capabilities [6], Drones are now working in all fields where humanity operates, for example, used to deliver blood or medical supplies to African countries [7], we can find them also in the agriculture industry [8], personal transportation, Journalism, architectural photography [9], engineering applications [10], Commercial Applications [11] as well as in the world of internet [12]. Currently drones are operating in many fields and, with constant technological advances, these machines will be even more robust and useful [13]. This paper describes a telecommunication's assets inspection process based on the use of autonomous UAVs and human supervised ones capable of overcoming issues related to the human-based classical inspection. Thus, we made a comparative study of both classical and UAV based inspection processes.

The paper is structured as follows: In the second section, we present the concept of quadrotor UAVs. In the third section (section 3), we present the frame design and building of UAVs. In the fourth section we defines the different standard components of quadrotor UAV and its characteristics. In the fifth section, we present the quadrotor assembling methodology. In the sixth section, we present an automated inspection process based on quadrotor UAV. In the seventh section, we present the obtained results validated by the comparative study with the classical inspection process. In the last section, we discuss further perspectives of the process development.

2. Quadrotor UAV concept

The quadrotor consists of a main body having four centrally connected arms and four brushless motors attached to each end of the arm. Four rotors are attached to each engine whose rotation of the propellers/rotors is controlled by radio control. All of these motors are connected to controllers to control the speed of each individual motor. These controllers are connected together in parallel with the power

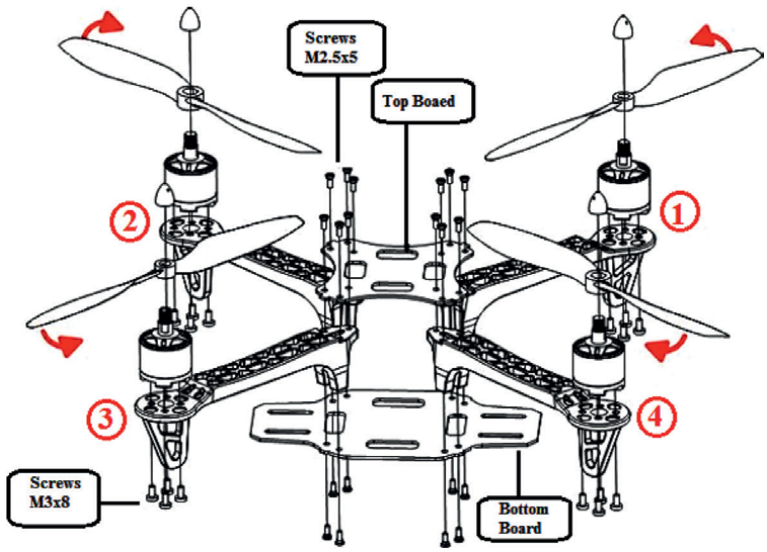

Figure 1.
UAV assembly diagram [13].

distribution board. Further, a battery is used as the power source. The assembly diagram of the quadcopter drone is shown in **Figure 1** [14].

The motor distribution is powered by a battery. In this way, the board evenly distributes power to the four electronically controlled drives, eventually reaching each motor. The accelerometer measures the angle of the quadrotor on the X, Y and Z axes and adjusts and stabilizes the revolutions per minute (RPM) of each motor [14, 15].

The following paragraph describes the components we have selected to make this drone.

3. Frame design and building

The first approach to designing the frame is to mount each arm at a central intersection to provide convenient mounting points and good support for each frame component [16]. The two arms are mounted vertically in the center and fixed by two boards. These boards are the basic support for flight controllers, batteries and distribution boards. Motors are attached to the ends of each arm [14]. The components used to assemble a quadrotor drone are described below.

3.1 Quadrotor SK450 frame

The frame is made of durable fiberglass and the arms are made of light nylon polyamide, with a height of 450 mm and 80 mm.

3.2 Carbon fiber propellers 12 in

Propellers are used to generate aerodynamic thrust. The first pair of propellers rotates clockwise (pusher) and the other pair rotates counterclockwise (puller) [17]. The thrust generated by propellers depends on the density of the air and the speed of the propeller, its diameter, the shape and surface of the blade and its pitch.

3.3 Turnigy multistar 980 Kv motor

The engine has a significant impact not only on flight time, but also on the payload the vehicle can carry. It is imperative to use the same engine throughout the same vehicle, as if pair of engine were of the same brand and model. Also, from the same production, their speeds may be slightly different and it is the air traffic controller who takes care of this [17].

3.4 Electronic speed controller (QBrain ESC)

The electronic speed controller (ESC) controls the speed and direction of the motor by inputting signals from the flight controller. The ESC must handle the maximum current drawn by the motor.

3.5 Pixhawk flight controller

The flight controller is a Pixhawk Mini programmable autopilot microcontroller manufactured by 3dr with enhanced sensors (accelerometer, gyroscope, etc.) that provide excellent flight stability and navigation to specific GPS coordinates.

3.6 Radio remote control turnigy 9X

The radio control receiver sends a wireless input to the vehicle and uses at least four channels connected to the following to control the movement of all vehicles.

1. Pitch (controls the vehicle to forward/backward motion).

2. Roll (moving the vehicle left and right).

3. Yaw (clockwise or counter-clockwise rotation).

3.7 2200 mAh lithium battery

The batteries are lightweight and offer high capacity with high discharge rates. Battery capacity is measured in ampere-hours (Ah), and the larger the capacity, the longer the flight time [18].

4. Configuration and assembly methodology

Assembling a quadrotor requires several steps, from assembling the chassis and the electronic components, to calibrating and finalizing the vehicle. Before explaining, we will present the tools used for assembly. This part describes the interconnection of electronic components and the assembly of the chassis without electronic components [17].

4.1 Connection and wiring of components electronic

Assembling a quadrotor requires several steps, from assembling the chassis and components, to calibrating and finalizing the vehicle. Before explaining, we will present the tools used for assembly. This part describes the interconnection of electronic components and the assembly of the chassis without electronic components as is shown in **Figure 2** [17].

4.2 The assembly frame alone

To assemble the vehicle frame, we follow the steps below:

1. Assemble the four arms with the main board using screws.

2. Mount the skids at the end of each arm.

3. Mount the motors plates at the end of each arm.

4. Mount the upper board.

4.3 Complete assembly with electronic components

This part describes the complete assembly of the sk450 quadrotor frame, including the assembly of the flight controller and electronic wiring.

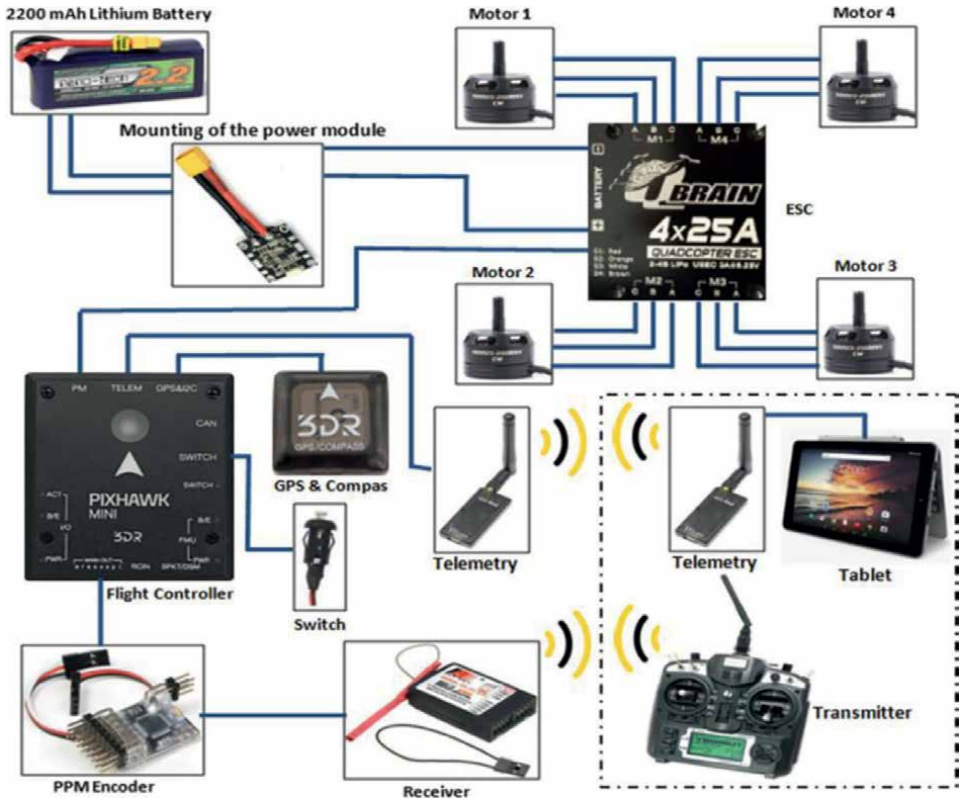

Figure 2.
The wiring diagram of electronic components of quadrotor.

4.3.1 Motors mounting

The motors are mounted in the correct order at the ends of each arm using a motor plate. The rotation of the motor changes according to the choice of user and gives the vehicle certain movements (Take off, landing, Throttle, yaw, pitch, roll, etc.).

4.3.2 ESC mounting

The ESC is mounted on the main board and wired to each motor in the correct order. Signal input is sent from the flight controller to the ESC, which adjusts motor speed. The ESC assembly is shown in the **Figure 3**.

4.3.3 The power module mounting

As shown in **Figure 4**, the power module with four outputs is fixed on the central plate with cable clamp and connected to the electronic flight controller (ESC).

4.3.4 The flight controller mounting

After assembling the chassis upper board, we will use the mounting foams to securely attach the Pixhawk Mini to the chassis center of gravity of the vehicle frame.

Figure 3.
ESC assembly.

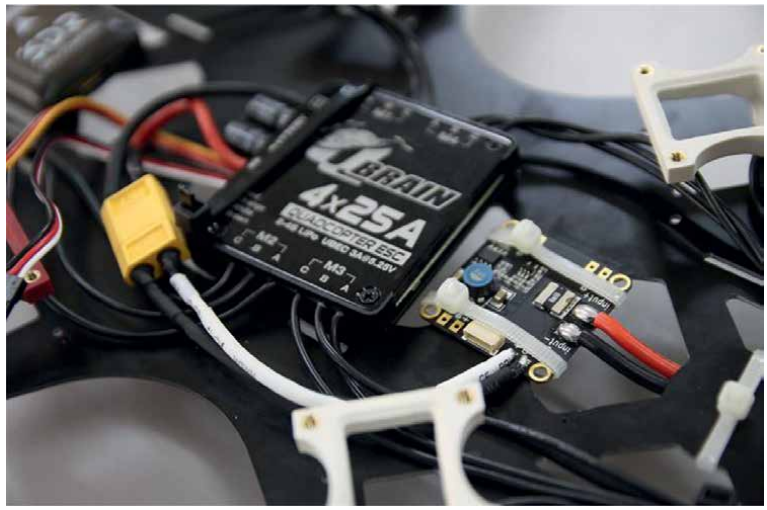

Figure 4.
Mounting of the power module.

These foams act as vibration dampeners that allow the flight controls to operate properly. The flight controller should also point to the front of the vehicle. **Figure 5** shows the Pixhawk mini flight controller mounting:

4.3.5 Wiring the flight controller to the power module

With 6 pin cable. We connect the flight controller to the power module in order to power it when connected to the battery.

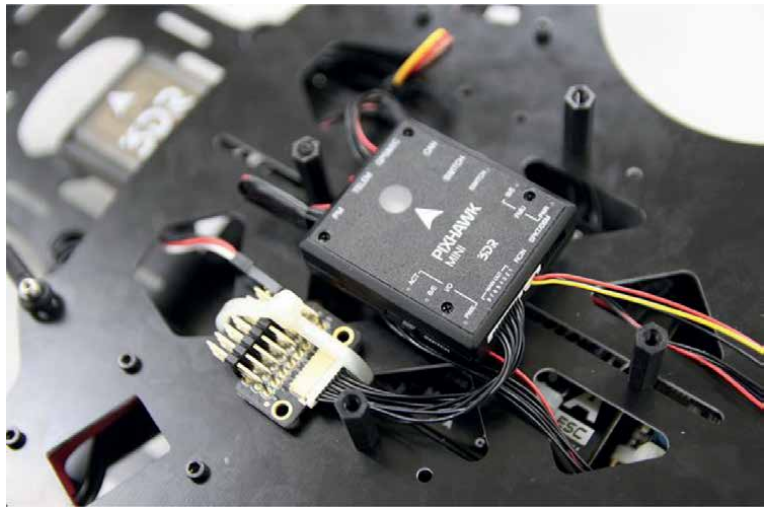

Figure 5.
Pixhawk mini flight controller mounting.

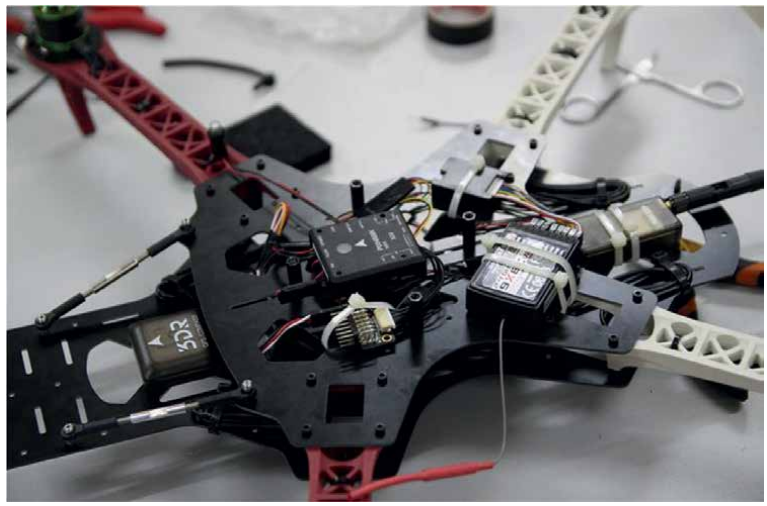

Figure 6.
Assembly of GPS module and radio telemetry.

4.3.6 The GPS module and radio telemetry mounting

As shown in **Figure 6**, the GPS module is mounted and oriented at the front of the vehicle. Then, assemble the wireless telemetry and communicate wirelessly with the vehicle

4.4 Base station installation/configuration

We used Q Ground Control in order to control the vehicle and configure the electronics. This helps you visually change and configure the required settings. It

is open source software, and you can even modify your code to your specific needs. You can also change the lighting mode of UAV (property), such as how it responds to input, low and fast stabilization. The Q Ground Control station is also used to plan missions and provide specific navigation paths based on GPS coordinates.

4.4.1 PX4 firmware implementation

We launch the program Q Ground Control after downloading and installing it on computer by selecting "Firmware" on the sidebar, and then we connect the flight controller to the computer via a USB cable.

After downloading and installing the QGroundControl program on computer. Firstly, we select "Firmware" from the sidebar. Then, we connect the flight controller to the computer using a USB cable and start the QGroundControl program.

4.4.2 Frame selection

The airframe tab displays a multi-frames configuration that can be handled by the autopilot. We select the appropriate chassis configuration. After confirming your selection, the flight controller will restart.

4.4.3 Sensors calibration

The embedded IMU (inertial measurement unit) includes a gyroscope, compass, and accelerometer that must be calibrated to the flight controller can stabilize its flight. Adjust the sensor by manually moving the vehicle in the specified direction.

4.4.4 Radio calibration

After turning on the transmitter, select the appropriate mode and start moving the joystick in the specified direction. We can monitor the transmitter channel, in order to assign a specific channel to a specific input, and use the Q Ground Control software to perform wireless calibration.

4.4.5 Flight modes selection

In flight mode, we can perform autopilot assisted flights and also manual. We configure the receiver to control the following principal flight modes:

1. *Stabilized*: when the sticks are released, the vehicle flight difficulty and stabilizes itself automatically

2. *Altitude*: Takeoff and landing are controlled at maximum speed..

3. *Position*: When you release the joystick, the quadcopter stops and stays in a stationary position.

4.4.6 Flight

When flying a drone, you should first check the following conditions:

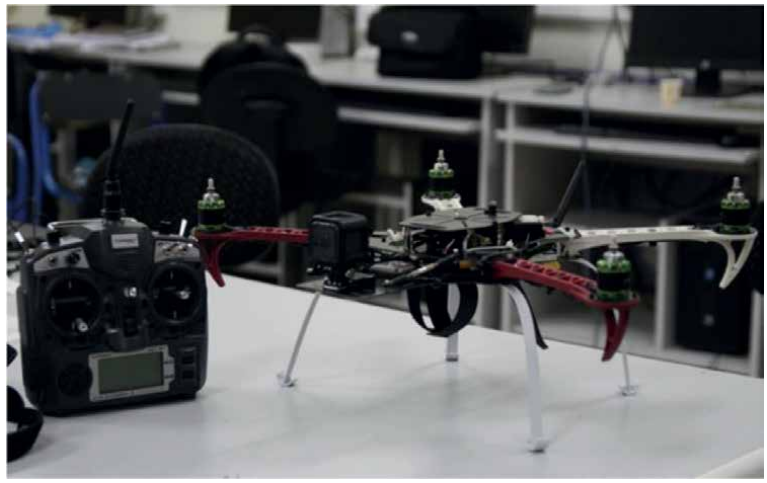

Figure 7.
Quadrotor UAV released.

1. *Choose the right environment*: Drone test flights will initially be conducted in two different environments: indoors (controlled environment) and outdoors (real environment). However, drone test flights are subject to weather conditions (wind, rain, etc.) which may affect the handling of the drone.

2. *Neighborhood*: To set the path and flight plan of UAV, we must take note of the dwellings, objects, trees, surrounding apartments, objects, trees, and streets. However, avoid flying near or in front of the airport.

3. *Flight mode study*: Various modes and settings can affect the ability to control flight and drones. Before flying, you need to configure the drone according to the environment you choose.

4. *Battery check*: Make sure the battery is properly charged to avoid an emergency landing.

After following the predefined steps of the quadrotor assembling and Configuration, The released quadrotor who wears a 4K camera to inspect the transmission part of telecommunication networks is shown in the **Figure** 7.

5. Automated telecommunication relay inspection process

In order to solve the issues related to the human-based inspection process, we designed a new process by introducing a new technique based on the use of autonomous UAVs capable of overcoming the issues faced during such operations. Introducing such a process allows the evaluation of telecommunications relays (NodB) physical state and improves the inspection operation by tackling its major problems such as safety, cost and efficiency. To illustrate our new process we built a quadrotor UAV which provides the needed agility and stability during the flight ensuring a reliable gathering of image/video data.

5.1 Description of the new inspection process

The UAV allows us to gather a set of high quality images and videos from where the physical parameters of all the infrastructure are extracted as (Azimuth, Tilt, Height, Antenna type, etc.) in a short time frame and by eliminating the human intervention. This process will be divided into the following steps:

1. *Site access*: Only one operator is needed to complete the inspection operation. The technician will plan the autonomous flight (route, altitude, coordinate, etc.) without the need to take any safety cautions in case of difficult site accessibility.

2. *Flight planning*: The technician uses the QGroundControl interface in which he inputs the set of informations needed for the autonomous flight of the UAV including the inspection route. The interface will provide a set of flight data and logs during the flight (Battery autonomy, speed, flight mode, etc.).

3. *Pre-flight checks*: Before launching the flight, the UAV operator must go through a list of verifications on the vehicle to ensure its safety and airworthiness for the success of the operation.

4. *Flight*: The operator arms the motors and launches the vehicle take off using the assistance of the radio controller. The vehicle will then follow the designated route to inspect the infrastructure by approaching it. The vehicle is equipped with a 4K camera mounted on the front of the frame and will record images continuously during the whole operation.

5. *End of the operation*: The vehicle will automatically come back to the initial take-off point keeping a constant flight altitude and will then initiate the landing.

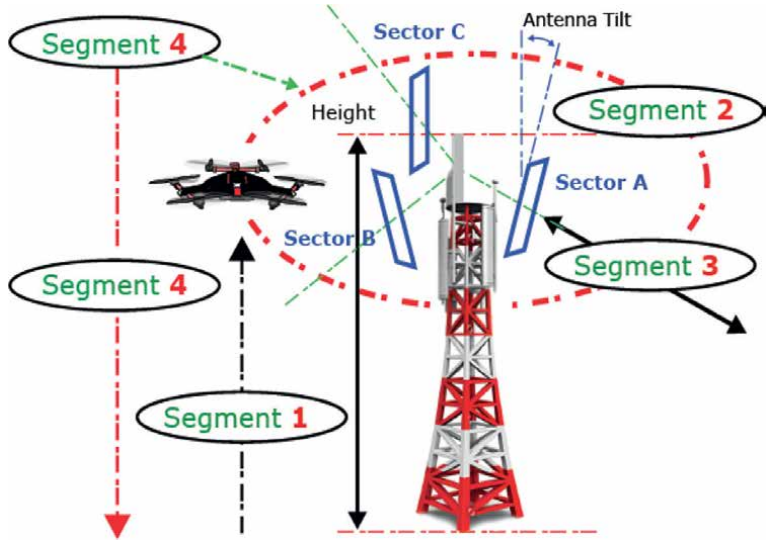

Figure 8.
The automated inspection process scenario.

5.2 The automated inspection process scenario

Figure 8 describes the designed automated inspection scenario. In the 1st segment, the UAV is recording images of the feeder cables state from bottom to top. In the 2nd segment, the vehicle is measuring the height of the antenna and its azimuth, and will then capture 360° panoramic images of the area surrounding the tower. The measurement of the height and azimuth is made using the embedded sensors (GPS, Compass, Accel/Gyro, etc.). In the 3rd segment, the UAV captures a side view of the antenna to measure the tilts and define the type of the antenna. In the 4th segment, a global view of the infrastructure is captured. After completing this, the vehicle initiates the landing.

6. Results and discussion

We have presented and detailed the assembly and configuration process of the UAV and its components. Then, we considered a telecommunication relay inspection operation established by the human being by implementing the technique of using a quadrotor drone. These operations are carried out in order to protect the conditions of activities in order to regulate the operation and management of communication provided by telecommunication operators. Generally, these inspections require climbing and a visual inspection of the structure. Each structural element is checked and verified [19]. The structures examined are usually steel masts, steel and concrete towers, satellite dishes, sector antennas and rooftop telecommunication structures [20, 21], etc.

These inspections are entirely manual, a costly activity for infrastructure companies and cause problems for operators and users, and these inspections are time-consuming. For this and thanks to integrating tools such as 4K cameras, measurement sensors, etc. We have developed an on-site audit technology using a quadrotor drone, capable of inspecting any telecommunications site. These technologies provide detailed measurement and monitoring of the status and operation of critical equipment. However, when the condition of the infrastructure is closely and continuously monitored, the risk due to faulty equipment can be significantly reduced.

The quadrotor was developed to perform checks in hard-to-reach areas and altitudes to troubleshoot any issues. Some of these problems include telecommunication errors, burns and incorrect physical parameters, falls due to climbing the antenna, etc. It is in this context that we have introduced an audit intervention for different heights of telecommunication towers. An inspection operation was triggered for a 20 m high tower, carried out by the radio team of phone operator Mobilis – ALGERIA. During this operation, the aerialist recorded all the necessary time of various measurements of the physical parameters of the relay, namely the tilts, azimuths, heights, type of aerials, etc. Likewise, we considered the same tower, but this time based on a quadrotor drone. As soon as the drone completes its mission, the results obtained are evaluated using a comparative table describing the execution time of the two previous operations as indicated in **Table 1**.

The table details the duration of each step of the inspection process carried out with human support or using a quadrotor drone on a 20 m high tower. The human execution time in the "up turn and check feeders" step is much longer than the time it takes to be executed by the quadrotor drone, similar to the "down turn" step. Tower height determination, GPS (global positioning system) and azimuth points are

Tower inspection steps	Human-based inspection tower (minutes)	UAV inspection tower (minutes)
Checking the feeders and tower climbing	8	2
Determination of tower altitude	5	/
Taking photos of the type of antenna and orientation.	1	1
Measurement of the GPS points and azimuth	2	/
Measurement of antenna tilt	1	1
General site photo	1	1
Tower descending	5	1
Total time	20	6

Table 1.
The execution time of the 20 m tower.

measured when the drone takes over the camera orientation and begins to determine the antenna type, so this does not doesn't take too long. The high sensitivity of the GPS & Compass sensor integrated into the drone allows more precise measurements than the traditional compasses used by the aerialist. The drone inspection time is 6 minutes, while the total time of all human inspection steps is 20 minutes. This means that the drone will save more time and avoid risks that may occur during this process.

The radio team has two towers of 40 and 70 m, to check whether the height can influence the execution time of all the UAV inspection stages or not. We have started a second measurement mission to be carried out. The balances obtained are compared with a histogram showing the execution time of the two operations, as shown in **Figure 9**.

Comparing the two operations, we can see that the 20m tower measured by the antenna operator takes 20 minutes, and the 70m tower takes 45 minutes, and regarding the operation performed by the drone, the 20m tower m took six minutes while that of 70 m is 14 minutes. We notice, at all tower heights, the duration of the UAV-based inspection operation is shorter than the traditional one. It means, the

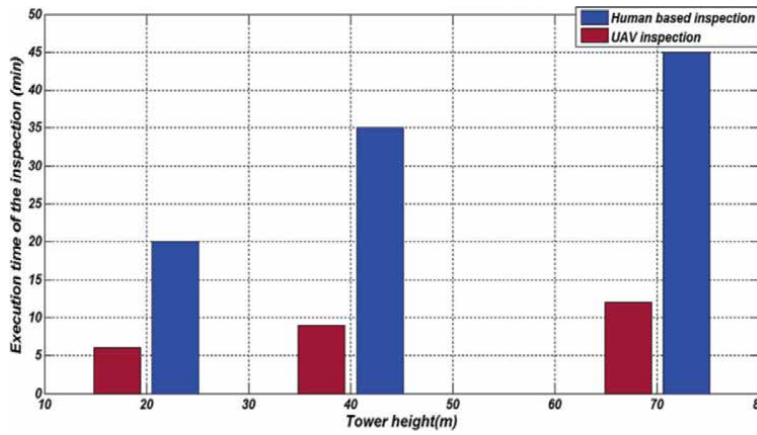

Figure 9.
Comparative histogram of the inspection execution time for each tower.

inspection carried out by the drone gives precision of the measurements, reliability of the information obtained and to save more time in such missions.

The quadrotor drone offers such inspections and thanks to its stability, rapid deployment, a wide angle of view, precision in the physical parameters measured, precious time saving and high quality panoramic images in real-time. In addition to that, all problems that may arise during such operations (burns, human error, falls, etc.) have been eliminated.

7. Conclusion and future scope

This study first showed the purpose of the drone and its possible uses. Next, I explained the concept of the quadrotor drone and the chassis assembly and its electronic components. Next, we introduced the configuration and assembly method of the quadrotor drone. We chose this type of drone because of its stability, superior battery life, reliability, running efficiency and long flight time compared to other types of drones.

Therefore, the future application area of precision quadrotor drones will integrate different sensors for precise measurements, providing different possibilities for the continuation of this project. Integrating machine learning algorithms to make it completely autonomous for more complex communication operations.

Author details

Hicham Megnafi[1]* and Walid Yassine Medjati[2]

1 Higher School in Applied Sciences Tlemcen, Tlemcen, Algeria

2 Airbus Operations GmbH, Hamburg, Germany

*Address all correspondence to: h.megnafi@essa-tlemcen.dz

References

[1] Nam T, Padro TA. Conceptualizing smart city with dimensions of technology, people, and institutions. In: Proceedings of the 12th Annual International Digital Government Research Conference: Digital Government Innovation in Challenging Times. USA: College Park Maryland; 2011. pp. 282-291

[2] Shakhatreh H, Sawalmeh AH, Al-Fuqaha A. Unmanned aerial vehicles (UAVs): A survey on civil applications and key research challenges. IEEE Access. 2019;**7**:48572-48634. DOI: 10.1109/access.2019.2909530

[3] Vang T, Li Z, Zhang F. Panoramic UAV surveillance and recycling system based on structure-free camera array. IEEE Access. 2019;**7**(7):25763-25778. DOI: 10.1109/ACCESS.2019.2900167

[4] Hayat S, Yanmaz E, Muzaffar R. Survey on unmanned aerial vehicle networks for civil applications: A communications viewpoint. IEEE Communications Surveys and Tutorials. 2016;**18**(4):2624-2661. DOI: 10.1109/COMST.2016.2560343

[5] Zhong Y, Zhang Y, Zhang W. Robust actuator fault detection and diagnosis for a quadrotor UAV with external disturbances. IEEE Access. 2018;**6**:48169-48180. DOI: 10.1109/ACCESS.2018.2867574

[6] Abdellaoui G, Megnafi H, Bendimerad F. A novel model using Reo for IoT selfconfiguration systems. In: 2020 1st International Conference on Communications, Control Systems and Signal Processing (CCSSP). El Oued, Algeria: IEEE; 2020. pp. 1-5

[7] Fethalla N, Saad M, Michalska H. Robust observer-based dynamic sliding mode controller for a quadrotor UAV. IEEE Access. 2018;**6**:45846-45859. DOI: 10.1109/ACCESS.2018.2866208

[8] Megnafi H, Medjati WY. Study and assembly of quadrotor UAV for the inspection of the cellular networks relays. In: Hatti M, editor. Artificial Intelligence and Renewables Towards an Energy Transition. ICAIRES 2020. Vol. 174. Cham: Springer. DOI: 10.1007/978-3-030-63846-7_62

[9] Satici AC, Poonawala H, Spong MW. Robust optimal control of quadrotor UAVs. IEEE Access. 2013;**1**(1):79-93. DOI: 10.1109/ACCESS.2013.2260794

[10] Tian B, Ma Y, Zong Q. A continuous finite-time output feedback control scheme and its application in quadrotor UAVs. IEEE Access. 2018;**6**:19807-19813. DOI: 10.1109/ACCESS.2018.2822321

[11] Lin X, Yu Y, Sun C. Supplementary reinforcement learning controller designed for quadrotor UAVs. IEEE Access. 2015;**7**:26422-26431. DOI: 10.1109/ACCESS.2019.2901295

[12] Liu Z, Liu X, Chen J. Altitude control for variable load quadrotor via learning rate based robust sliding mode controller. IEEE Access. 2019;**7**:9736-9744. DOI: 10.1109/ACCESS.2018.2890450

[13] Bhatia AK, Jiang J, Zhen Z. Projection modification based robust adaptive backstepping control for multipurpose quadcopter UAV. IEEE Access. 2019;**7**:154121-154130. DOI: 10.1109/ACCESS.2019.2946416

[14] Wang Z, Yu J, Lin S. Distributed robust adaptive fault-tolerant mechanism for quadrotor UAV real-time wireless network systems with random

delay and packet loss. IEEE Access. 2019;**7**:134055-134062. DOI: 10.1109/ACCESS.2019.2936590

[15] Amaldi E, Capone A, Malucelli F. UMTS radio planning: Optimizing base station configuration. In: Proceedings of the IEEE 56th Vehicular Technology Conference. Vancouver, Canada: IEEE; 2002. pp. 768-772

[16] Wood RJ, Avadhanula S, Steltz E. An autonomous palm-sized gliding micro air vehicle. IEEE Robotics & Automation Magazine. 2007;**14**(2):82-91. DOI: 10.1109/MRA.2007.3 80656

[17] Chellal AA, Lima J, Gonçalves J, Megnafi H. Dual coulomb counting extended kalman filter for battery SOC determination. In: International Conference on Optimization, Learning Algorithms and Applications. Vol. 1488. Cham: Springer; 2021. pp. 219-234. DOI: 10.1007/978-3-030-91885-9_16

[18] Chellal AA, Gonçalves J, Lima J, Pinto V, Megnafi H. Design of an embedded energy management system for Li–Po batteries based on a DCC-EKF approach for use in mobile robots. Machines. 2021;**9**(12):313. DOI: 10.3390/machines9120313

[19] Burggräf P, Martínez ARP, Roth H, Wagner J. Quadrotors in factory applications: Design and implementation of the quadrotor's P-PID cascade control system. SN Applied Science. 2019;**1**(7):722. DOI: 10.1007/s42452-019-0698-7

[20] Megnafi H, Abdellaoui G, Haddouche K, Boukli-Hacene N. Analysis and evaluation of the radio link by developing an application under MapBasic. In: 2021 Conférence Nationale sur les Télécommunications et ses Applications (CNTA 2021). Algérie: Ain-Témouchent; 2021

[21] Megnafi H. Frequency plan optimization based on genetic algorithms for cellular networks. Journal of Communication Software System. 2020;**16**(3):217-223. DOI: 10.24138/jcomss.v16i3.1012

Chapter 5

Robust Control Algorithm for Drones

Parul Priya and Sushma S. Kamlu

Abstract

Drones, also known as Crewless Aircrafts (CAs), are by far the most multi - level and multi developing technologies of the modern period. This technology has recently found various uses in the transportation area, spanning from traffic monitoring applicability to traffic engineering for overall traffic flow and efficiency improvements. Because of its non-linear characteristics and under-actuated design, the CA seems to be an excellent platform to control systems study. Following a brief overview of the system, the various evolutionary and robust control algorithms were examined, along with their benefits and drawbacks. In this chapter, a mathematical and theoretical model of a CA's dynamics is derived, using Euler's and Newton's laws. The result is a linearized version of the model, from which a linear controller, the Linear Quadratic Regulator (LQR), is generated. Furthermore, the performance of these nonlinear control techniques is compared to that of the LQR. Feedback-linearization controller when implemented in the simulation for the chapter, the results for the same was better than any other algorithm when compared with. The suggested regulatory paradigm of the CA-based monitoring system and analysis study will be the subject of future research, with a particular emphasis on practical applications.

Keywords: crewless aircrafts (CA), dynamic controller, adaptive controller, robust controller, LQR, PID, ANN

1. Introduction

Crewless Aircrafts (CAs) are becoming more common in a variety of industries, including reconnaissance, aerial reconnaissance, rescue operations missions as first responders, and industrial automation. CAs outperform their competitors due to their small size and strong manoeuvrability, allowing them to easily navigate complex trajectories. A CA is a mechanism featuring 6-D-o-F however and four control inputs: the rotor speeds. Individual rotor speeds are adjusted to provide the thrust as well as torques needed to propel the CA. The axis of a CA have to be skewed with respect to the vertical to accomplish propulsion in a specific direction [1]. CA kinematics and control are thus complicated since the CA's translational motion is connected with its angular orientation.

Prior to controller design, mathematical modelling is perhaps the most important stage in understanding system dynamics. The Newton–Euler and Euler–Lagrange

approaches are used to derive the differential equations that govern CA dynamics. Due to modelling limitations, complex interactions such as blades flapping but also rotors stiffness effects are frequently overlooked [2]. CA control is primarily concerned with two types of issues: attitude stability and trajectory tracking. There are three types of controllers used for this purpose: linear controls, model-based nonlinear controllers, and learning-based controllers. Multirotor stand out among CAs for their manoeuvrability, stability, and payload. Initially, the goal of these vehicles' research was to find controllers capable of maintaining their attitude, as well as the fastest and most powerful dynamics [3]. Backstepping, Feedback-linearization, Sliding Mode, optimum regulation, PID, adaptive control, learning-based control, and other strategies have been used to tackle the stabilisation control problem for the specific instance of a CA.

The difficulty for CAs nowadays is trajectory controls, fault - tolerance control, path planning, or obstacle avoidance, given that stability control has been extensively explored. The trajectory control problem, which is defined as getting a vehicle to follow a pre-determined course in space, can be solved using one of two methods: a trajectory tracking controllers and perhaps a path following controller [4]. A reference described in time is tracked about the trajectory tracking issue, where the path's references are provided by something like a temporal evolution from each spatial coordinate. Path following (PF) provides a solution of following the path with no pre-assigned timing information, removing the problem's time dependence [5].

Because the quantity, as well as the complexity of implementations for such systems, is increasing on a daily basis, the control techniques used must likewise improve to provide improved performance and versatility. Considering computational ease and reliable hover flight, simple linear control algorithms were previously used. However, with improved modelling techniques and faster on-board processing capabilities, real-time implementation of comprehensive nonlinear techniques has become a reality. Nonlinear techniques promise to improve the performance and robustness of these systems quickly. This chapter discusses various ways to CA automatic control [6]. The system dynamics are used to design specific linear and nonlinear control strategies.

1.1 Motivation

CA support to various ground domains or terrestrial networks has lately been identified as a critical success factor for a large number of jobs that require significant enhancement of timeframe, connectivity, and flexibility. As a result, a really well notion of this paradigm must be precisely specified while taking into account the various CA criteria. This enables CAs to better support ground-users (GUs) and complete their assigned tasks. CAs can overcome communication gaps in ground networks and monitor hostile settings or disaster zones [3]. Aside from the traditional CA difficulties, a number of new ones, including such technical and standardisation considerations, societal privacy and safety, and mobility optimization, require further attention. The possible benefits of CAs raise the following concerns:

- What are the control methodologies and advantageous for establish a CA flight control across a terrestrial flight?

- What is the best number of CAs and mobility models to use in a particular scenario?

- How can CAs improve ground network performance as well as better serve GUs?

Inspired from the afforested questions, we present a full overview of CA's extant achievements and control mechanisms in this chapter.

1.2 Classification

CAs differ in terms of weight, size, kind, altitude, payload, and a variety of other characteristics. According to their type and height, they can be divided into two broad categories (**Figure 1**). Both category have their own set of benefits and drawbacks. Various sorts of CAs are utilised depending on the application scenario. **Table 1** shows the classification of CAs.

Classification based on the weight of UA (Unmanned Aircraft) as follows:

- Micro: less than 2 kilogrammes (<2 kg).

- Mini: Greater than 2 kilogrammes and less than 20 kilogrammes (2–20 kg).

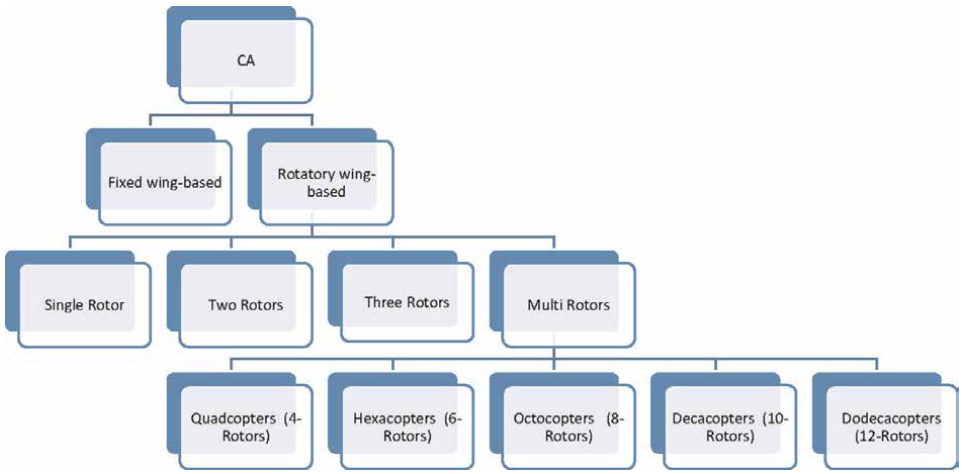

Figure 1.
Classification of CAs on the basis of the design.

	Advantages	**Limitations**
Fixed wing-based	• Comparatively Simpler Design • Simpler maintenance mechanism • Aerodynamically steady • Improved energy efficiency - Longer flight times with less energy and cost	• For take-off and landing, need a runway or a launcher. • must go forward in a steady moving pace and cannot hover in one place
Rotary wing- based	• Able to Vertical take-off and landing (VTOL) • No need for Landing/Takeoff plot • Capable for manoeuvring for agile functioning and hover • Rigour flying	• Aerodynamically not very steady and needed on-board computers • Comparatively complicated programming and structure • Low at energy efficacy

Table 1.
Classifications of CA.

Take-off weight	6–16 lb
Airframe weight	5–9 lb
Wing span	5–7 ft
Fuselage length	4–8 ft
CA speed	20–30 mph
Payload	5–10 lb
Flight endurance	10–25 h
Rating of electric motor	1 kW or 1.35 HP (some CAs use gasoline engine, while others use an electric motor)
Take-off speed	15–20 mph
Landing speed	15-20mph
Runway length	40–60 ft
Maximum climb speed	16 ft./s
Turn radius	35–50 ft
Flight altitude	50–6000 ft.(max)
Radio control range	3–5 km

Table 2.
Technical parameters of CAs.

- Small: Greater than 20 kilogrammes and less than 150 kilogrammes (20–150 kg).
- Large: Greater than 150 kilogrammes (>150 kg).

Typical physical parameters of small CAs for commercial applications can be summarised as follows as in **Table 2**.

2. State of art in CA

CA, sometimes known as drones, has had robust growth in the previous 5 years all over the world. The model UAS fleet is expected to grow from 1.25 million entity to about 1.39 million by 2023, according to the study aerospace projection fiscal years 2019–2039, while the non-model CA fleet is expected to rise from 277,000 CA to over 835,000 CA by 2023. CA's beneficial applications have the potentiality for saving lives, improving safety and efficiency, and allow for more impactful engineering as well as research [7]. Designers experimenting with small CA for a variety of purposes such as aerial surveillance as well as personal recreational flying, entrepreneurs exploring parcel and medical supply delivery, and search and rescue missions are just a few examples.

While CA have their origins in military uses, they have recently become more helpful towards scientific and commercial purposes [8, 9]. Remote sensing, georeferencing, cartography, customs and border protection, investigation, rescue operations, fire espial, agronomic imaging, traffic surveillance systems, and package delivery are just a few of the applications they have recently discovered around the world.

Due to the rapid growth of CA technology, the extensive usefulness of CAs for numerous applications has been recognised, ranging from transportation services to disaster search and rescue.

While many current control systems still rely heavily on the availability of precise mathematical models (e.g., Model-Predictive-Control (MPC) [10], linear quadratic Gaussian [11, 12], backstepping [13], as well as gain scheduling [14]), this article evaluates extra versatile and intelligent approaches by emphasising the value of evolutionary computation to resolve the actual constraints of model-based control systems.

When building a robust flight control system, there are a few things to keep in mind. The first issue is the closed-loop control's robustness in the presence of uncertainties [11], including unpredictably extremely high air passes (e.g., violent wind gusts) and modelling errors. A small CA's mobility can be extremely vulnerable to wind gusts, which might cause the system to deviate from its intended trajectories. This phenomenon can also result in large overshoots and tracking offsets, both of which are undesirable in terms of safety and efficiency.

While many current dynamic control systems still rely significantly on mathematical equations of the subsystems (e.g., gains scheduling [14] as well as feedback linearization strategies), these approaches may be excessively complex or unworkable in some cases. Gain scheduling control, for example, has been considered one of the most historically dominant adaptive control approaches, but it has a number of technical flaws. Because it significantly leans on the linearization technique of the aviation dynamics over numerous places in the performance envelope, as well as several joint interpolation approaches, the system is extremely mathematical and time-consuming. It could potentially result in a system that lacks global property. Furthermore, in the absence of thorough mathematical models, feedback linearization could be impractical.

Despite the positive results, MBC-based designs face a hurdle in that they rely on the correctness of the mathematical model of a real plant. According to imprecise system information and omnipresent exogenous disruptions, a poorly developed or described model might have a negative impact on later controller synthesis, resulting in inadequate performances or even instability. Uncertainties and disturbances of this nature can be categorised as follows:

- Parametric uncertainties: These are typically caused by incorrect modelling and/or system depreciation (e.g., inertia changes as well as mass, etc).

- Stochastic dynamics: These are difficult-to-model, ill-defined, and purposefully neglected components of a nonlinear model, such as sophisticated aerodynamic effects such blade flapping [15], airflow effect [16], ground and ceiling impact [11, 12], and so on.

- Disruptions and noise: Disturbances might include things like gusty winds and turbulence, whereas noise mostly relates to sensor noise. Because the statistical features of sensor noise are typically non-Gaussian in actuality, the assumptions considered may not be realistic.

To address these issues, a variety of modern control systems have been offered, each with its own set of benefits, restrictions, and drawbacks. Gain Scheduling (GS) [10], for example, is a frequently used strategy that shows good capabilities in dealing

with parametric variations and nonlinearities, but frequent and fast changes in the controller gains might make the system unstable [13]. Furthermore, as noted in [14], the cost of implementation rises with the frequency of functioning points. Robust control, on the other hand, is effective when dealing with constrained parametric uncertainties, but it has drawbacks when dealing with boundless ones or stochastic dynamics [17, 18]. Adaptive control is a potential method for managing parametric uncertainties (because to its real-time adaptation strength); nonetheless, there are few commonly acknowledged approaches here to robust adaptive control issue so far [19]. The sliding control technique has been demonstrated to be resistant to modelling mistakes and parameter uncertainty, however frequent controller switches can cause chattering. Furthermore, when exogenous disruptions occur, the insensitivity to parameter changes characteristics may cause problems with self-stabilisation. Last but not least, thanks to using a continually updated model, namely an ultra-local model, Model-Free Control (MFC) approaches that have arisen to tackle stochastic dynamic behaviour as well as ambiguities of nonlinear systems have exhibited outstanding adaptation and estimating capabilities. However, for the time being, this methodology is confined to system dynamics that can be turned into Single-Input Single-Output (SISO) subsystem. There are other issues with analytic stability and evidence of convergence. ANNs have been used to analyse complicated control systems in order to solve the previously mentioned limitations of MBC-based solutions. This is primarily due to ANNs' perceived advantages in structural analysis and controller design [14, 20], which include their ability to recognise stochastic and multinomial systems [21, 22], their capacity to adapt in real-time, and their relatively simple computation methodology and hardware implementation.

As a result of these characteristics, ANNs are a fantastic tool for building the systems underneath prototype of high accuracy and low sophistication, even if it is distorted by uncertainties and disturbances, as well as for facilitating the implementation process and improving real-time performance. Regardless, there are still obstacles owing to their data-driven essence that limit their industrial applications, to some extent, due to various: a need for huge datasets of training data; the tendency to learn spurious relationships, which can lead to poor generalisation functionalities [23]; dearth of readability due to their own black-box characteristics [24]; and the lack of a structured method for pertaining ANN architecture designs [25] (In other words, given a certain ANN design, the number of hidden layers and synapses, the sort of perceptron, weight update algorithms, and so on are often decided haphazardly than in a structured manner).

3. Dynamic model of CA

Quad-rotor CA systems typically have a cross "X" or plus "+" structure with four rotors attached to each side of the structure. When at the time all of four rotors revolve in the likewise direction, the quad rotor produces a vertical upward lift force, allowing it to move in landing positions, pitch, hover, yaw, roll, take-off.

Two frames, a reference Earth frame as well as a quad-rotor frame, can be used to define and characterise quad-rotor dynamics. Rotational and translational dynamics with 6 degrees of freedom (DoF) are common.

The following is a summary of the deciding set for 6DoF equation that describe the dynamic model of a conventional CA including a longitudinal axis of symmetry treated as a rigid body (**Figure 2**).

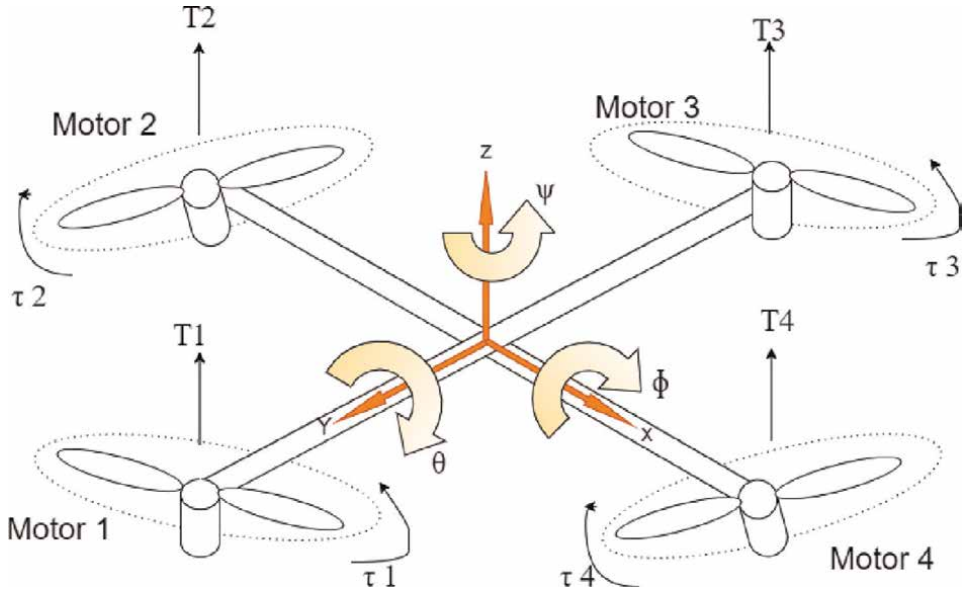

Figure 2.
CAs' movements and angles description.

$$\begin{cases} X = m[u + qw - rv] \\ Y = m[v + ru - pw] \\ Z = m[w + pv - qu] \end{cases} \tag{1}$$

$$\begin{cases} L = I_{XX}p + (I_{ZZ} - I_{YY})rq + I_{XZ}(r + pq) \\ M = I_{YY}q + (I_{XX} - I_{ZZ})rp + I_{XZ}(r^2 - p^2) \\ N = I_{ZZ}r + (I_{YY} - I_{XX})qp + I_{ZX}(p - qr) \end{cases} \tag{2}$$

$$r = R_b^u V_b^g = \begin{bmatrix} \cos\theta\cos\psi & -\cos\theta\sin\psi + \sin\phi\sin\theta\cos\psi & -\sin\sin + \cos\sin\cos \\ \cos\theta\sin\psi & \cos\phi\cos\psi + \sin\phi\sin\theta\sin\varphi & -\sin\phi\cos\psi + \cos\phi\sin\theta\sin\psi \\ -\sin\theta & \sin\phi\cos\theta & \cos\phi\cos\theta \end{bmatrix} \tag{3}$$

$$\begin{bmatrix} \varphi \\ \theta \\ \psi \end{bmatrix} = \begin{bmatrix} 1 & \sin\varphi\dfrac{\sin\theta}{\cos\theta} & \cos\varphi\dfrac{\sin\theta}{\cos\theta} \\ 0 & \cos\varphi & -\sin\varphi \\ 0 & \sin\varphi\dfrac{1}{\cos\theta} & \cos\varphi\dfrac{1}{\cos\theta} \end{bmatrix} \begin{bmatrix} p \\ q \\ r \end{bmatrix} \tag{4}$$

The aforementioned differential equations are nonlinear, linked, which means that each differential equation is dependent on variables that are represented by other nonlinear equations. In most cases, the analytical answers are unknown, and the only way to solve them is numerical. The free motion of a solid body subject to extrinsic forces $F_b = [X \ Y \ Z]^T$ and moments) $M_b = [L \quad M \quad N]^T$ is described by 12 states. These variables are known as state variables in control system design because they entirely characterise the state of a physical system at any given moment. For completeness, the state variables are presented in **Table 3**.

State-variable	Definition
$r = [r_x \quad r_y \quad r_z]^T$	CA's inertial position vector and its components
$V_b^g = [u \quad v \quad w]^T$	Body frame, the components of inertial velocity vector is settled.
$[\phi \quad \theta \quad \psi]$	Euler angles describe the position of body frame in relation to inertial ref. frame.
$w = [p \quad q \quad r]^T$	Body-fixed frame, angular inertial rates are settled.

Table 3.
6DoF equations of motion state variables.

3.1 Problem statement

Nonlinear rotational dynamics can cause hindrance in actuated control torques when paired with modest imperfections in rotating alignments and propeller defects. With the help of internal feedback control scheme for the quadrotor attitude can eliminate the influence of these. External disturbances such as gusty winds, aerodynamic interacts with neighbouring structures, and ground impacts can all be compensated for using the same attitude controller.

In order to create and deploy robust control mechanisms for quadrotor CAs, the following technical difficulties must be explored in a research.

1. How to develop a dynamic inversion models to improve the performance of a PID controller.

2. How to include a LQR into the responsive method of improving controller resilience in the context of nonlinearities, variable incompatibility, and wind perturbations.

3. Application of the LQR-based dynamical inversion control system in practise.

4. Control strategies

The most significant component of the control system is the controller. It is in charge of the control system's performance. It is a mechanism or method that works to keep the amount of the process variable at a predetermined level.

Based on the input(s), a control method can direct its output(s) to a specific value, complete a sequence of events, or execute an action if the terms are met. The controllers are useful for a variety of purposes, including:

- Controllers increase steady-state accuracy by lowering steady-state error [4, 26].

- With the improvement in accuracy for the steady-state, so does the stability [2].

- Controllers also aid in decreasing the system's undesired offsets [27].

- The maximum overrun of the system can be controlled using controllers [28, 29].
- Controllers can aid in the reduction of noise signals generated by the system [2, 30].
- Controllers can help boost an overdamped system's slow reaction.

In this section, we'll go through the most prevalent path-following control schemes and algorithms. The algorithms are divided into subsections and compared qualitatively. Several control techniques have been implemented due to the CA's dynamics. Fuzzy logic, LQR (LQG), NN, Proportional Integral Derivative (PID), Sliding Mode Control (SMC), and other control systems can be employed [31, 32]. To deal with parameterized uncertainties and external disturbances, robust control systems are extensively developed. Several methods for CA or unsupervised robot path planning have been proposed in recent years. CA translational and rotational restrictions are rarely taken into account by these methods, hence they are rarely useful in practise [33]. Population-based genetic operators have made significant progress recently as a result of developments of swarm intelligence technology [34], and they continue to have a strong ability to find the best answer in a somewhat more efficient and adaptable manner. Using this strategy, an increasing number of researchers have focused on CA path planning. Artificial bee colony approach (ABC), ant-colony-approach (ACO), genetic-algorithm (GA), and particle swarm algorithm are the most often utilised algorithms (PSO) [35]. The necessity about a robust nonlinear controller in multirotor CAs is dictated by uncertainties originating through propeller rotation, blade flap, shift in propeller rotational speed, and centre of mass position [36]. Each control system, as one might imagine, has certain set of advantages and disadvantages. There were both linear as well as non-linear control designs employed.

One of the control techniques is linear (LQG), whereas the other two are nonlinear (Dynamic feedback and dynamic n-version having nil-dynamics stabilisation provide perfect linearization and non-interacting control [37]). There are several similarities made between these control strategies.

4.1 PID

A diverse variety of controller applications have used the PID-controller. It is, without a doubt, the most widely used controller in industry. The traditional PID linear controllers has the advantages of being easy to alter parameter gains, being simple to construct, and having strong resilience. However, non-linearity connected with both the precise mathematical and the imprecise character of the model to determine to unmodeled or faulty mathematical modelling of a few of the dynamics are two of the CA's key issues [38]. As a result, using a PID-controller on the CA reduces its performance. The attitude stabilisation of a CA was done with a PID-controller, while the altitude control was done with a Dynamic-Surface-Control (DSC). Researchers were able to verify that all CA signals were uniformly ultimately confined using Lyapunov stability criteria. This signified that now the CA was sturdy enough to hover. The PID-controller, on the other hand, appears to been performed better in pitch angle tracking, although substantial steady-state errors were noted in roll angle tracking [39], according to the model and the experimental plots. The PID-controller was successfully used to the CA, however with significant limitations, according to the literature.

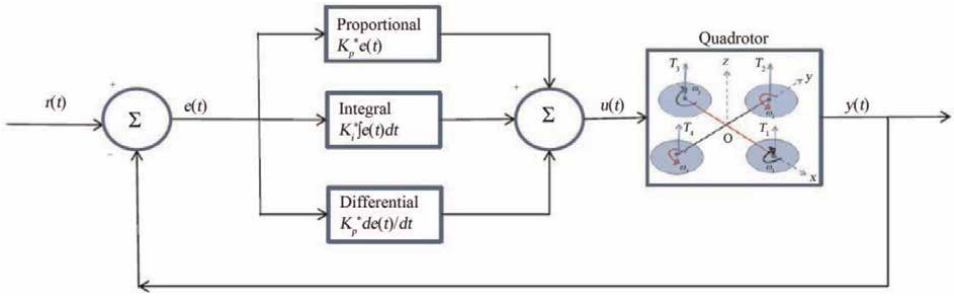

Figure 3.
Depicts the PID-controller bock diagram.

Tuning the PID-controller might be difficult because it must be done around the equilibrium position, which would be the hover point, in order to achieve better results (**Figure 3**).

The time domain outcome of such a PID controller, that is equivalent to the control signal to the plant, is computed from the feedback inaccuracy as follows:

$$u(t) = K_p e(t) + K_i \int e(t)dt + K_d \frac{de}{dt} \tag{5}$$

First, using the diagram shown above, examine how the PID controller operates in a closed-loop system. The tracking error is represented by the variable (e), which is the gap between the actual actual output (Y) and the desired output (r). This error signal (e) is sent into the PID controller, which computes for both derivative and integral of the error function with respect to time. The proportional gain (K_p) times of the magnitude of the difference adds the integral gain (K_i) repeats the integration of the error in addition of the derivative gain (K_d) times of the derivative for error equals the control signal (u).

The plant receives this control signal (u) and produces the new output (Y). The new output (Y) is then sent back into the loop and evaluated to the reference signal to determine a new error amplitude (e). The controller uses the new error signal to update the control input. This process continues as long as the controller is active.

The Laplace transform of Expression (5) is used to calculate the transfer function for such PID controller.

$$K_p + \frac{K_i}{s} + K_d s = \frac{K_d s^2 + K_p s + K_i}{s} \tag{6}$$

4.2 LQR

By minimising a suitable cost function, the LQR optimal-control method manages a dynamic system. Boubdallar and colleagues tested the LQR-algorithm on a CA and compared it to the PID-controller's performance. The PID been used on the CA's simplified kinematics, whereas, LQR is used on the entire model. Both of approaches produced not so good results, but it seemed evident, the LQR strategy performed better attributed to the reason that it has been implemented to a more comprehensive dynamic model [40]. Upon the comprehensive dynamic system of the CA, a basic trail

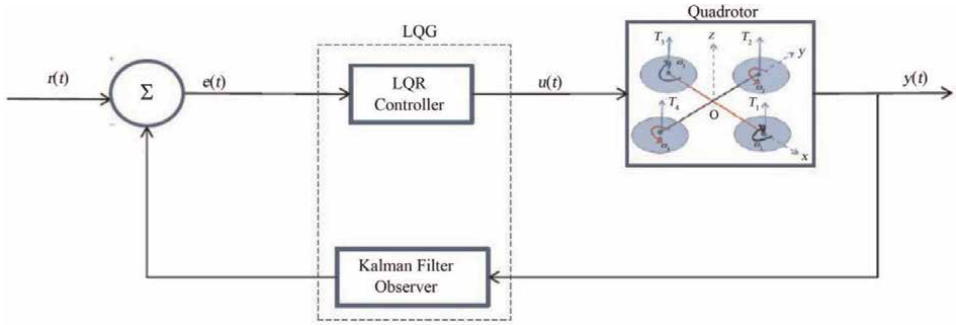

Figure 4.
Schematic representation of a CA's LQG controller.

LQR controller was deployed. Despite the existence of gust and other disturbances, accurate pathway following been demonstrated using simulation utilising of optimal real-time trajectory (ies). After evading a barrier, the controller appeared to lose track. Its effectiveness in the face of several challenges was still being studied.

The LQR technique becomes the Linear-Quadratic-Gaussian (LQG) when combined including a Linear-Quadratic-Estimator (LQE) as well as a Kalman Filter. Considering systems having Gaussian noise and partial state information, this approach is used. In hover mode, the LQG using integral action was used to stabilise the inclination of a CA with good results. The upside of the whole LQG controller is that it can be implemented without having entire state information (**Figure 4**).

If output is to reflect reference r, therefore adding an integrator and specifying error state (e) is integrator output, with is difference between system input and output:

$$\left.\begin{aligned} \dot{x} &= Dx + Eu \\ y &= Gx \\ u &= -K'x + k_I'e \\ \dot{e} &= r - y = r - Gx \end{aligned}\right\} \tag{7}$$

Equation (7) describe a dynamic system.

$$\begin{bmatrix} \dot{x} \\ \dot{e} \end{bmatrix} = \begin{bmatrix} D & 0 \\ -G & 0 \end{bmatrix} \begin{bmatrix} x \\ e \end{bmatrix} + \begin{bmatrix} E \\ 0 \end{bmatrix} u + \begin{bmatrix} 0 \\ I \end{bmatrix} r \tag{8}$$

4.3 Linearization of feedback

Through a change in variables, feedback-linearization control scheme convert a complex nonlinear model into more of an equivalent linear-system. The reduction of granularity due to linearization and the need for a specific set for implementation are two drawbacks of feedback-linearization [41]. On a CA with having dynamic changes in its centre of gravity, feedback-linearization was used as an adaptive control approach for stabilisation and trajectory tracking. When the CA's centre of gravity shifted, the controller proved able to stabilise and reorganise it in real time [42, 43]. In

order to develop a path-following controller, feedback-linearization as well as input dynamic inversion had been used. This allowed the designer to describe the control performance and yaw angle as more of a function as displacement anywhere along path. Two simulation scenarios were evaluated, with the CA cruising at varying speeds throughout the course. The airspeed and yaw angle convergence was seen in both circumstances. In, adaptable sliding mode control was compared to feedback-linearization [14, 44]. The feedback controller proved very vulnerable to sensor noise but not robust, even with simplified dynamics. Under noisy conditions, the SMC operated effectively, and adaptability was able to anticipate uncertainty including ground effect [17]. As a result, nonlinear feedback-linearization control has good-tracking yet poor-disturbance rejection. However, when feed-back-linearization is combined with that another approach that is less sensitive to noise, good results are obtained.

4.4 Intelligent adaptive control (artificial-neural-networks and fuzzy-logic controller)

Two simulation scenarios were evaluated, with the CA cruising at varying speeds throughout the course. The airspeed and yaw angle convergence was seen in both circumstances. In, adaptable sliding mode control was compared to feedback-linearization. The feedback controller proved very vulnerable to sensor noise but not robust, even with simplified dynamics. Under noisy conditions, the SMC operated effectively, and adaptability was able to anticipate uncertainty including ground effect [45]. As a result, nonlinear feedback-linearization control has good tracking yet poor disturbance rejection [46]. However, when feed-back linearization is combined with another approach that is less sensitive to noise, good results are obtained. The use of a trial and error strategy to tune input variables was, however, a key shortcoming of this study. The strategy was shown to be more effective in terms of achieving the target attitude as well as reducing weight drift [47]. To learn the whole dynamics of the CA, including unmodeled dynamics, outputting feedback control been implemented on a CA employing NN for leader-follower CA generation. From four control inputs, a virtual NN control was used to govern all 6DoF. In the context of a sinusoidal disturbance, an adaptive neural network approach was used to stabilise CAs. Decreased error function and so no weight drifts were achieved using the proposed technique of two simultaneous single hidden layers (**Figures 5** and **6**).

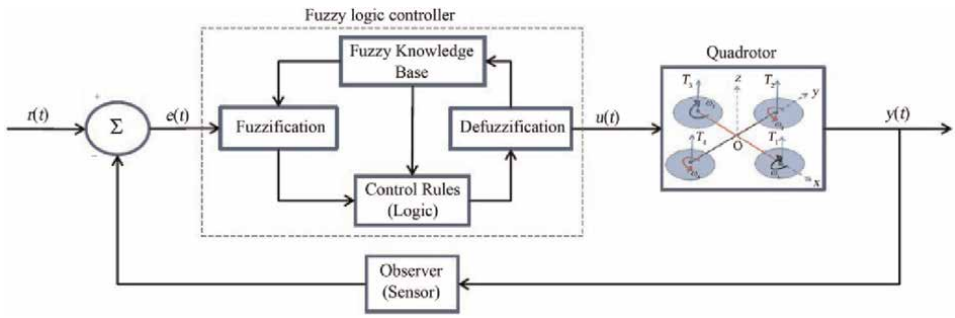

Figure 5.
On the CA, a schematic representation of FLC.

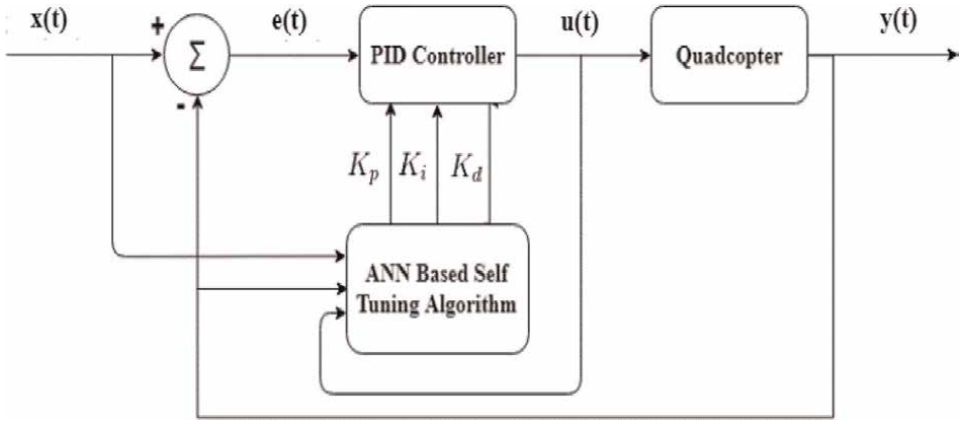

Figure 6.
On the CA, a schematic representation of ANN.

5. Matlab-simulink result and comparison

In this chapter, we display the Mat lab-Simulink findings and discuss the divergence between the various controllers shown above. The step-response of the endogenous variable x, y, z and ψ is shown for each control, followed by the double circular or elliptical trajectories along the simulated outcomes.

With LQR control is utilised, some distinctive characteristics of the step-response are shown using **Table 4** (**Figures 7** and **8**).

Table 5 depicts the exact linearization position and yaw response with no interfering control by dynamic-feedback to a step-input (**Figure 9**).

Table 6 Exhibits some typical features from the step response, while using dynamic inversion using zero-dynamics stabilisation control.

5.1 Comparison

Whenever different Controllers are used, the step-response of the dependent variable x, y, z, and ψ is shown in the diagram below (**Figure 10**).

Tables 7-10 demonstrate some of the step response's characteristic parameters, where D-FBL denotes Dynamic-Feedback-Linearization and S-FBL denotes Static-Feedback-Linearization.

	x(t)	y(t)	z(t)	(t)
RT[s]	00.75	00.75	00.72	00.08
OS[m]	04%	04%	04.3%	00%
ST[s]	02.3	02.3	02.60	01.75

Table 4.
Distinctive characteristics of the step-response.

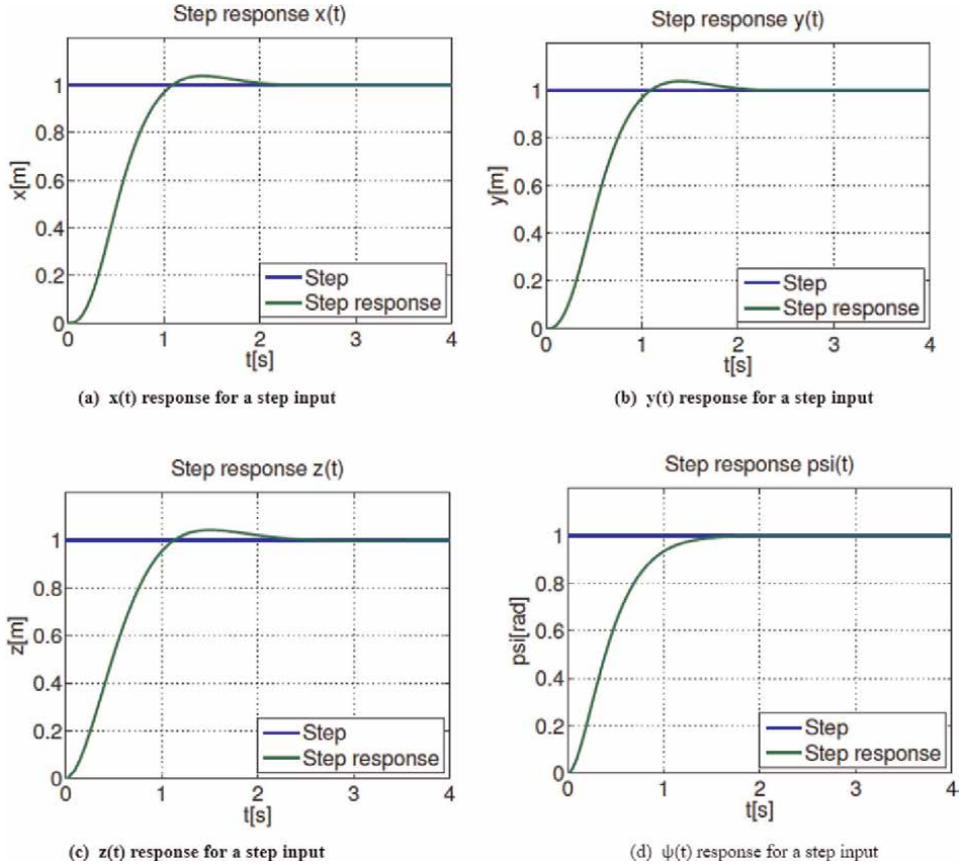

Figure 7.
The LQR's Yaw and position for a step-input response.

We can deduce the following from the information shown in these tables:

- The LQR's control is slower and has a low overshoot value.
- Although the dynamic inverting with zero-dynamics stabilisation control is faster, it has a higher overshoot value.
- Because the related linear-system shows the fourfold integrators after feedback-linearization, dynamic inversion of zero-dynamics stabilisation control is slower to dynamic inversion of zero-dynamics stabilisation control.

6. Conclusion

The dynamic model of a crewless aircraft is discussed in this chapter, as well as a comparison of linear or nonlinear control algorithms and the t, S Trajectories control challenge, which can be handled using a track follower or trajectory controlling tracking algorithm. The CA's dynamic theory is obtained using the Newton-Euler

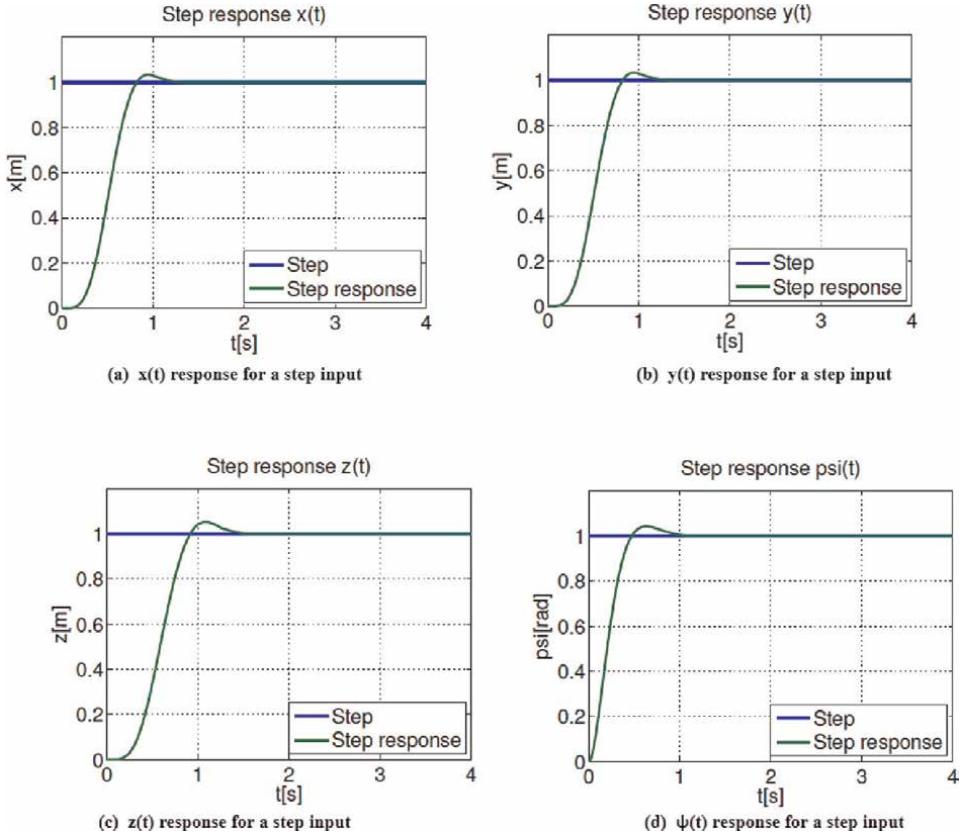

Figure 8.
Exact linearization position and yaw response with no interfering control by dynamic-feedback to a step-input.

	x(t)	y(t)	z(t)	(t)
RT[s]	00.4	00.4	00.47	00.301
OS[m]	04%	04%	05.20%	04.20%
ST[s]	01.3	01.3	01.54	01.70

Table 5.
Distinctive characteristics of the step-response.

method. The 'RT', 'OS', and 'ST' of any and all three controllers were all investigated. When applying the Feedback-linearization controller, the best results are attained. Path-following control strategies are a concept that has been defined. All simulations in this study were conducted under the assumption that the CA's whole motion happens at a significant altitude from the ground, and also that the CA does not perform take-off or landing. Another issue is that due to the complexity of modelling uncertainties like wind velocities as well as ground impacts, the proposed theoretical model does not include them. The controllers must be made resilient so that they can deal successfully with external disturbances that were not taken into account during the modelling process. A next step towards achieving is to design a controller which can deal with the malfunction with one or more rotors.

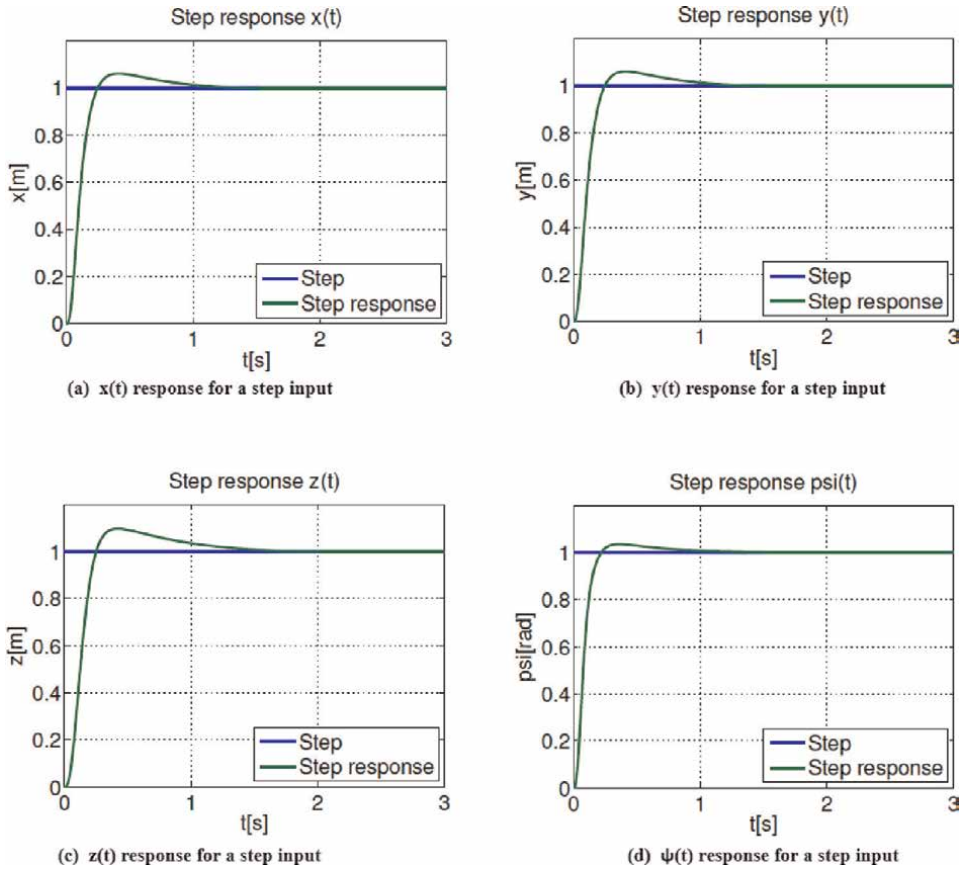

Figure 9.
Dynamic inversion's position and yaw response to a step input with zero-dynamics stabilisation.

	x(t)	y(t)	z(t)	(t)
RT[s]	00.02	00.02	00.02	00.15
OS[m]	07%	07%	09%	04%
ST[s]	01.4	01.4	01.7	01.5

Table 6.
Distinctive characteristics of the step-response.

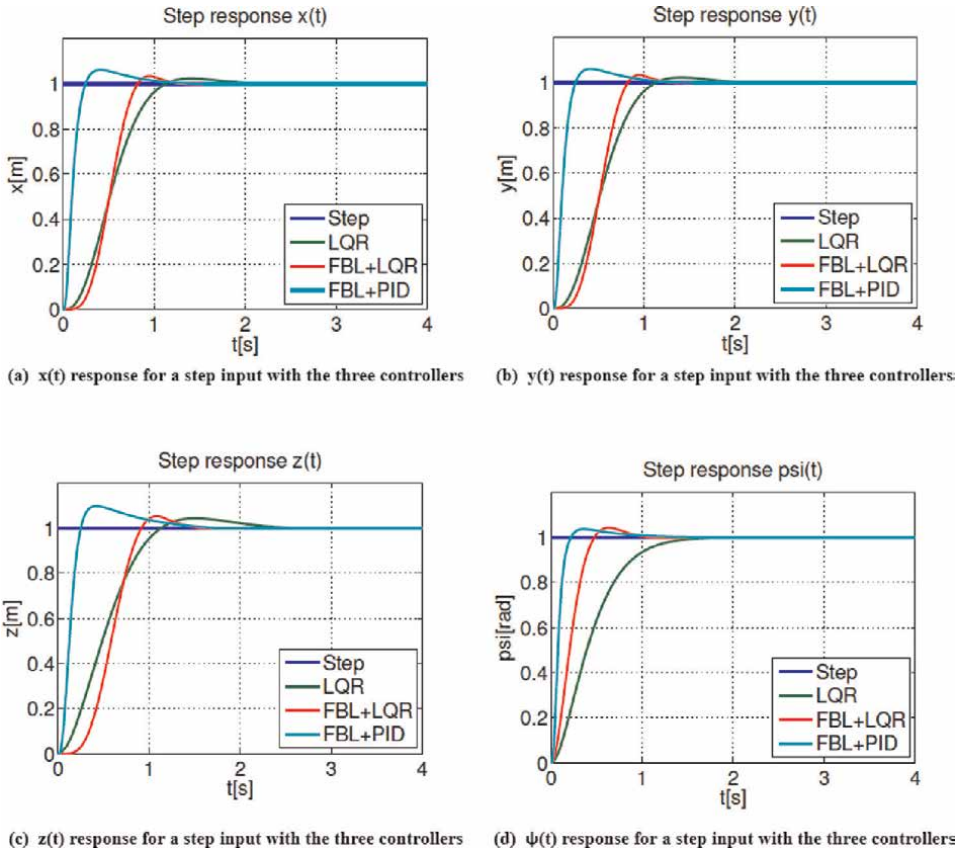

(a) x(t) response for a step input with the three controllers

(b) y(t) response for a step input with the three controllers

(c) z(t) response for a step input with the three controllers

(d) ψ(t) response for a step input with the three controllers

Figure 10.
The three controls' position and yaw responses to a step-input.

x(t)	LQR	D-FBL	S-FBL
RT[s]	00.75	00.04	00.02
OS[m]	04%	04%	07%
ST[s]	02.3	01.3	01.4

Table 7.
Using the control techniques discussed above, assign distinguishing attributes for a step response to x (t) variable.

y(t)	LQR	D-FBL	S-FBL
RT[s]	00.75	00.04	00.02
OS[m]	04%	04%	07%
ST[s]	02.3	01.3	01.4

Table 8.
Using the control techniques discussed above, assign characteristic attributes for a step input to y (t) variable.

z(t)	LQR	D-FBL	S-FBL
RT[s]	00.72	00.47	00.02
OS[m]	04.3%	05.2%	09%
ST[s]	02.6	01.54	01.4

Table 9.
Using the control techniques discussed above, assign characteristic attributes for a step input to z(t) variable.

(t)	LQR	D-FBL	S-FBL
RT[s]	00.08	00.31	00.15
OS[m]	00%	04.2%	04%
ST[s]	01.75	01.7	01.7

Table 10.
Using the control techniques discussed above, assign characteristic attributes to a step input to (t) variable.

Conflict of interest

The authors declare no conflict of interest.

A. APPENDIX

RT	Rise Time
OS	Overshoot
ST	Settling Time
K_p	Proportional-Gain
K_i	Integral-Gain
K_d	Derivative-Gain.

Table A1.
List of abbreviations used for parameters.

DOI: http://dx.doi.org/10.5772/intechopen.105966

Author details

Parul Priya* and Sushma S. Kamlu
Department of Electrical and Electronics Engineering, Birla Institute of Technology, Mesra, India

*Address all correspondence to: parulpriya.ee@gmail.com

IntechOpen

References

[1] Kanellakis C, Nikolakopoulos G. Survey on computer vision for UAVs: Current developments and trends. Journal of Intelligent and Robotic Systems. 2017;**87**(1):141-168

[2] Han D, Gwak DY, Lee S. Noise prediction of multi-rotor UAV by RPM fluctuation correction method. Journal of Mechanical Science and Technology. 2020;**34**:1429-1443

[3] Fotouhi A, Qiang H, Ding M, Hassan M, Giordano LG, Garcia-Rodriguez A, et al. Survey on UAV cellular communications: Practical aspects, standardization advancements, regulation, and security challenges. IEEE Communications Surveys & Tutorials. 2019;**21**(4):3417-3442

[4] Atyabi A, Mahmoud-Zadeh S, Nefti-Meziani S. Current advancements on autonomous mission planning and management systems: An AUV and UAV perspective. Annual Reviews in Control. 2018;**46**:196-215

[5] Bonna R, Camino JF. Trajectory tracking control of a UAV using feedback linearisation. Proceedings of the XVII International Symposium on Dynamic Problems of Mechanics DINAME-2015.-2015, February; 2015

[6] Bouabdallah S, Noth A, Siegwart R. PID vs LQ control techniques applied to an indoor micro UAV. Proceedings of the 2004 IEEE/RSJ International Conference on Intelligent Robots and Systems, 2004. (IROS 2004), IEEE; Vol. 3, 2004; pp. 2451-2456

[7] Song H, Srinivasan R, Sookoor T, Jeschke S. Smart Cities: Foundations, Principles and Applications. Hoboken, NJ: Wiley; 2017

[8] Zhou G, Ambrosia V, Gasiewski AJ, Bland G. Foreword to the special issue on unmanned airborne vehicle (UAV) sensing systems for earth observations. IEEE Transactions on Geoscience and Remote Sensing. 2009; **47**:687-689

[9] Nex FC, Remondino F. UAV for 3D mapping applications: A review. Applied Geomatics. 2013;**6**:1-15

[10] Singh L, Fuller J. Trajectory generation for a UAV in urban terrain, using nonlinear MPC. In: Proceedings of the American Control Conference, Vol. 3; June 2001. pp. 2301-2308

[11] Santoso F, Liu M, Egan G. *H*2 and *H*∞ robust autopilot synthesis for longitudinal flight of a special unmanned aerial vehicle: A comparative study. IET Control Theory and Applications. 2008; **2**(7):583-594

[12] Santoso F, Liu M, Egan G. Optimal control linear quadratic synthesis for an unconventional aircraft. In: Proceedings of the 12th Australian International Aerospace Congress (AIAC), March 2006

[13] Azinheira JR, Moutinho A. Hover control of an UAV with backstepping design including input saturations. IEEE Transactions on Control Systems Technology. 2008;**16**(3):517-526

[14] Hernández-García RG, Rodríguez-Cortés H. Transition flight control of a cyclic tiltrotor UAV based on the gain-scheduling strategy. In: Proceedings of the International Conference Unmanned Aircraft System (ICUAS), June 2015, pp. 951-956

[15] Santoso F, Garratt MA, Anavatti SG. State-of-the-art intelligent flight control

systems in unmanned aerial vehicles. IEEE Transactions on Automation Science and Engineering. 2018;**15**(2):613-627

[16] Das A, Subbarao K, Lewis F. Dynamic inversion with zero-dynamics stabilisation for UAV control. IET Control Theory and Applications. 2009; **3**(3):303-314

[17] Arisoy A, Temeltas H. Attitude control of a UAV. Fourth International Conference on Recent Advances in Space Technologies, 2009. RAST'09, June, IEEE; 2009. pp. 722–727

[18] Lee D, Jin Kim H, Sastry S. Feedback-linearization vs. adaptive sliding mode control for a UAV helicopter. International Journal of Control, Automation and Systems. 2009; **7**(3):419-428

[19] Li L, Sun L, Jin J. Survey of advances in control algorithms of UAV unmanned aerial vehicle. 2015 IEEE 16th International Conference on Communication Technology (ICCT), October, IEEE; 2015. pp. 107-111

[20] Luukkonen T. Modelling and control of UAV, independent research project in applied mathematics, Espoo. 2011

[21] Sabatino F. UAV control: Modeling, nonlinear control design, simulation, 2015

[22] Slotine JJE, Li W. Applied Nonlinear Control; Vol. 199(1). Prentice-Hall, Englewood Cliffs, NJ. 1191

[23] Ramon Soria P, Arrue BC, Ollero A. Detection, location and grasping objects using a stereo sensor on UAV in outdoor environments. Sensors. 2017;**17**(1):103

[24] Xiao B, Yin S. Exponential tracking control of robotic manipulators with uncertain dynamics and kinematics. IEEE Transactions on Industrial Informatics. 2018;**15**(2):689-698

[25] Yang C, Jiang Y, Na J, Li Z, Cheng L, Su CY. Finitetime convergence adaptive fuzzy control for dual-arm robot with unknown kinematics and dynamics. IEEE Transactions on Fuzzy Systems. 2018;**27**(3):574-588

[26] Jamisola RS Jr, Mastalli C, Ibikunle F. Modular relative jacobian for combined 3-arm parallel manipulators. International Journal of Mechanical Engineering and Robotics. 2016;**5**(2):90-95

[27] Jamisola RS, Kormushev PS, Roberts RG, Caldwell DG. Task-space modular dynamics for dual-arms expressed through a relative jacobian. Journal of Intelligent and Robotic Systems. 2016;**83**(2):205-218

[28] Chen S, Laefer DF, Mangina E. State of technology review of civilian UAVs. Recent Patents on Engineering. 2016; **10**(3):160-174

[29] Dupont QF, Chua DK, Tashrif A, Abbott EL. Potential applications of UAV along the construction's value chain. Procedia Engineering. 2017;**182**:165-173

[30] Otto A, Agatz N, Campbell J, Golden B, Pesch E. Optimization approaches for civil applications of unmanned aerial vehicles (UAVs) or aerial drones: A survey. Networks. 2018; **72**(4):411-458

[31] Gaffey C, Bhardwaj A. Applications of unmanned aerial vehicles in cryosphere: Latest advances and prospects. Remote Sensing. 2020;**12**(6):1-40

[32] Huo X, Huo M, Karimi HR. Attitude stabilization control of a UAV by using backstepping approach. Mathematical Problems in Engineering. 2014;**2014**:1-9

[33] Mahony R, Kumar V, Corke P. Multirotor aerial vehicles: Modeling, estimation, and control of UAV. Robotics Automation Magazine. 2012; **19**:20-32. DOI: 10.1109/MRA.2012.2206474

[34] Lee B-Y, Lee H-I, Tahk M-J. Analysis of adaptive control using on-line neural networks for a UAV. Thirteenth International Conference on Control, Automation and Systems (ICCAS), 20-23 October 2013; 2013. pp. 1840-1844

[35] Diao C, Xian B, Yin Q, Zeng W, Li H, Yang Y. A nonlinear adaptive control approach for UAVs. Proceedings of the 8th Asian Control Conference (ASCC), Kaohsiung, 15-18 May 2011. 2011. pp. 223-228

[36] Palunko I, Fierro R. Adaptive control of a UAV with dynamic changes in the center of gravity. Proceedings of the 18th IFAC World Congress, Milan, 28 August-2 September 2011; 2011. pp. 2626-2631

[37] De Monte P, Lohmann B. Position trajectory tracking of a UAV helicopter based on L1 adaptive control. Proceedings of the 2013 European Control Conference (ECC), Zurich, 17-19 July 2013. 2013. pp. 3346-3353

[38] Jung W, Lim S, Lee D, Bang H. Unmanned aircraft vector field path following with arrival angle control. Journal of Intelligent Robotic & Systems. 2016;**84**(1):311-325. DOI: 10.1007/s10846-016-0332-5

[39] Kaminer I, Yakimenko O, Pascoal A, Ghabcheloo R. Path generation, path following and coordinated control for time-critical missions of multiple UAV s. In: 2006 American Control Conference, Proceedings of the American Control Conference. Vol. 1-12; 2006. p. 4906. Doi: 10.1109/ACC.2006.1657498

[40] Klausen K, Fossen TI, Johansen TA, Aguiar AP. Cooperative path-following for multirotor UAVs with a suspended payload. In: 2015 IEEE Conference on Control and Applications (CCA 2015); 2015. pp. 1354-1360

[41] Kokotovic PV, Sussmann HJ. A positive real condition for global stabilization of nonlinear-systems. Systems and Control Letters. 1989;**13**(2):125-133

[42] Kukreti S, Kumar M, Cohen K. Genetically tuned Lqr based path following for CAs under wind disturbance. In: 2016 International Conference on Unmanned Aircraft Systems (ICUAS); 2016. pp. 267-274. Doi: 10.1109/ICUAS.2016.7502620

[43] Hoffmann G, Huang H, Waslander S, Tomlin C. Quadrotor helicopter flight dynamics and control: Theory and experiment. In: AIAA Guidance, Navigation and Control Conference and Exhibit; 2007. p. 6461

[44] Conyers SA, Rutherford MJ, Valavanis KP. An empirical evaluation of ground effect for small-scale rotorcraft. 2018 IEEE International Conference on Robotics and Automation (ICRA); 2018. pp. 1244-1250

[45] Kothari M, Postlethwaite I, Gu DW. A suboptimal path planning algorithm using rapidly-exploring random trees. International Journal of Aerospace Innovations. 2009;**2**:93-104

[46] Ali ZA, Wang D, Aamir M. Fuzzy-based hybrid control algorithm for the stabilization of a tri-rotor UAV. Sensors. 2016;**16**(5):652

[47] Espinoza-Fraire T, Saenz A, Salas F, Juarez R, Giernacki W. Trajectory tracking with adaptive robust control for quadrotor. Applied Sciences. 2021; **11**(18):8571

Section 4

Military Crafts

Chapter 6

Military Aircraft Flight Control

Cătălin Nae, Ilie Nicolin and Bogdan Adrian Nicolin

Abstract

This chapter presents major stages in the evolution of military aircraft flight control systems. As the flight speed steadily increased, it was necessary to develop new flight control systems to replace the old pilot control with mechanical connections to the control surfaces. The first major step is the pilot with a side stick/rudder pedal or an autopilot, who sends commands converted to electrical signals to a flight control computer and, in turn, interprets and sends wired electrical commands to the electrohydraulic actuators of each control surface and receives electrical signals from the motion transducer of each control surface. This stage of development of aeronautical technologies has been called the fly-by-wire flight control system. The latest major step in the evolution of military aircraft flight control systems is the replacement of copper wires with the fiber-optic cables, which have a much lower weight and a much higher capacity to carry digital information (light or photons). The command imposed by the pilot with a side stick/rudder pedal or autopilot is converted into light signals to the flight control computer and to the electrical or electrohydraulic actuators of each control surface and receives light signals from the motion transducer of each control surface. The latest flight control system is called fly-by-light system.

Keywords: flight control system, fly-by-wire, fly-by-light, military aircraft

1. Introduction

The flight control system of a military aircraft is determined by the control surfaces installed on the airplane body that are balanced movements coordinated by a flight control system that drives an aircraft around the three axes of motion, as shown in **Figure 1** [1, 2]:

- Yaw
- Pitch
- Roll

Main forces acting on a military aircraft in straight and level flight or any other type of aircraft in straight and level flight [3] are shown in **Figure 2**.

To take off and to keep in flight, a military aircraft must meet the following conditions: the **lift** forces must be bigger than the **weight** of the aircraft and the **trust** must

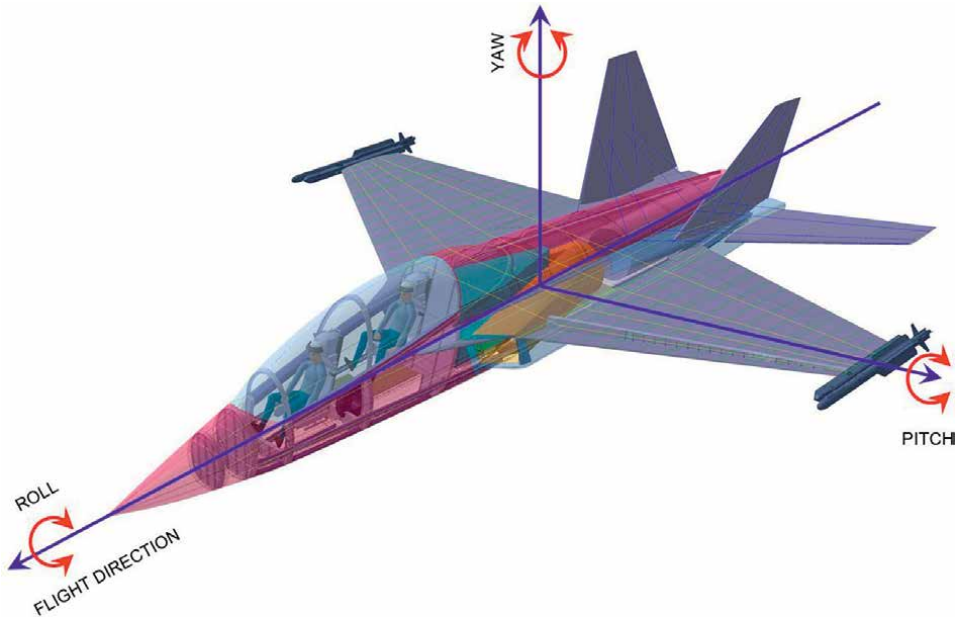

Figure 1.
Axes of motion of a military aircraft.

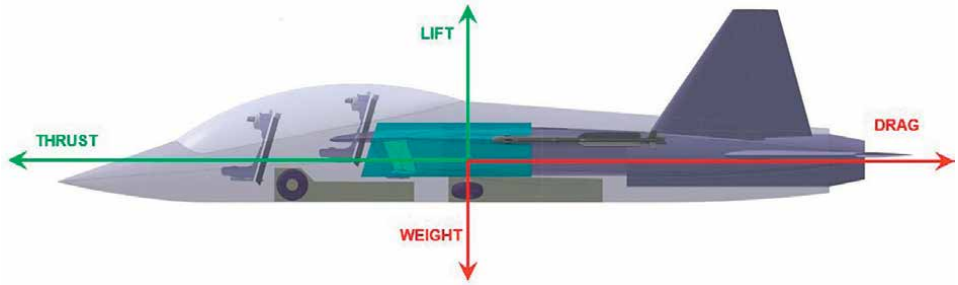

Figure 2.
Main forces acting on a military aircraft.

be bigger than the **drag** forces (the aerodynamic forces that oppose a military aircraft's movement through the air). If the lift is less than the weight, then the aircraft falls, and if the trust is less than the drag, the aircraft slows down, especially when the aircraft maintains the same altitude [3].

Primary flight control surfaces of a modern military aircraft are shown in **Figure 3**.

Flaperons are flight control surfaces on the rear wing of a military aircraft used as flaps during takeoff and landing maneuvers when the aircraft has a low speed. Flaperons are also used as ailerons to roll aircraft; therefore, the flaperons combine the functions of flaps and ailerons.

Leading-edge slats are used to increase the aircraft lift during takeoff and landing maneuvers when the aircraft has a low speed.

The horizontal stabilizer provides stability for the military aircraft, and it can be slowly rotated to act as an elevator (both for pitch control).

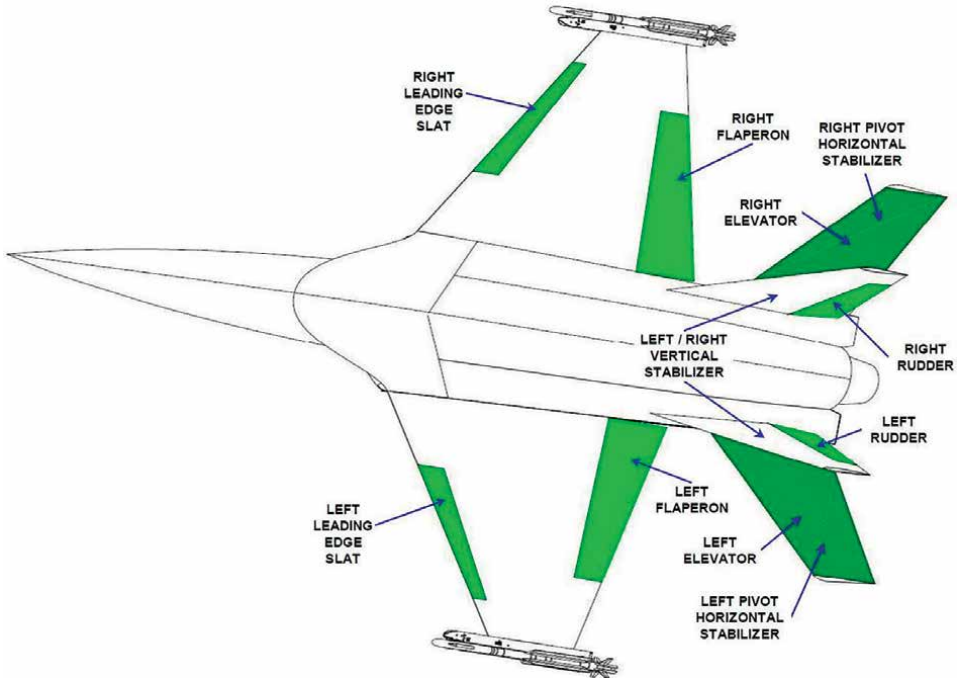

Figure 3.
Primary flight control surfaces of a modern military aircraft.

The two vertical stabilizers provide the stability of the military aircraft around the vertical axis. The two rudders ensure the control of the yaw movement of the military aircraft.

As the flight speed of military aircraft has increased continuously, it was necessary to develop new flight control systems. The old flight control system with mechanical links from the pilot control column (yoke) and rudder pedals to the control surfaces is using the power of the pilot's arms and legs to directly move the control surfaces.

The first major step in the development of flight control systems for military aircraft is the fly-by-wire (FBW) flight control system [2, 4], which is designed as a multiredundant system. The command imposed by the pilot with a side stick/rudder pedal or by autopilot is converted into electrical signals to a flight control computer (FLCC), which interprets and sends wired electrical commands to the electrohydraulic actuators of each control surface and receives electrical signals from the motion transducer of each control surface. To increase flight safety, each flight control computer has a flight envelope embedded in it (a computer program made by specialized engineers) that eliminates dangerous maneuvers for the aircraft structure and the life of the crew on board while maintaining the aerodynamic stability of the aircraft in any situation or maneuvers allowed by the flight envelope.

The latest major step in the evolution of military aircraft flight control systems is the fly-by-light (FBL) flight control system consisting of the replacement of copper wires with fiber-optic cables, which have an even much lower weight and a much higher capacity to carry digital information (light or photons). The command imposed by the pilot with a side stick/rudder pedal or by autopilot is converted into light signals to the flight control computer and from here to the electrical or electrohydraulic actuators of each control surface and receives light signals as feedback from the motion transducer

of each control surface. The flight computer of the fly-by-light flight control system has a flight envelope embedded in it, which eliminates dangerous maneuvers for the aircraft structure and the life of the crew on board while maintaining the aerodynamic stability of the aircraft in any situation or maneuvers allowed by the flight envelope [2, 5]. The Fly-by-Light flight control system is designed as a multi redundant system.

2. Flight control systems for military aircraft

2.1 The fly-by-wire system

The old pilot-control flight control system with mechanical links is shown in **Figure 4**. The pilot directly moves all the control surfaces using the control column (yoke) or rudder pedals with the strength of his arms or his legs. The pilot also feels the resistance to the movement of all these control surfaces.

As the flight speed of a new military aircraft increased continuously from subsonic velocities to supersonic velocities, and the aircraft was designed aerodynamically unstable to increase their maneuverability in the air, it was necessary to continuously develop new and modern flight control systems.

The first major step in the development of aeronautical technologies for flight control systems of military aircraft is the fly-by-wire (FBW) flight control designed as a multiredundant system. The command imposed by the pilot with a side stick/rudder pedal or by autopilot is converted into electrical signals sent by copper wires to a flight control computer, which interprets and sends wired electrical commands to the electrohydraulic actuators of each control surface and receives (feedback) electrical signals from the motion transducer of each control surface to provide self-corrective action, as shown in **Figure 5**. Initially, the data sent by copper wires were analog, but later these were transformed into digital signals to avoid any communication errors.

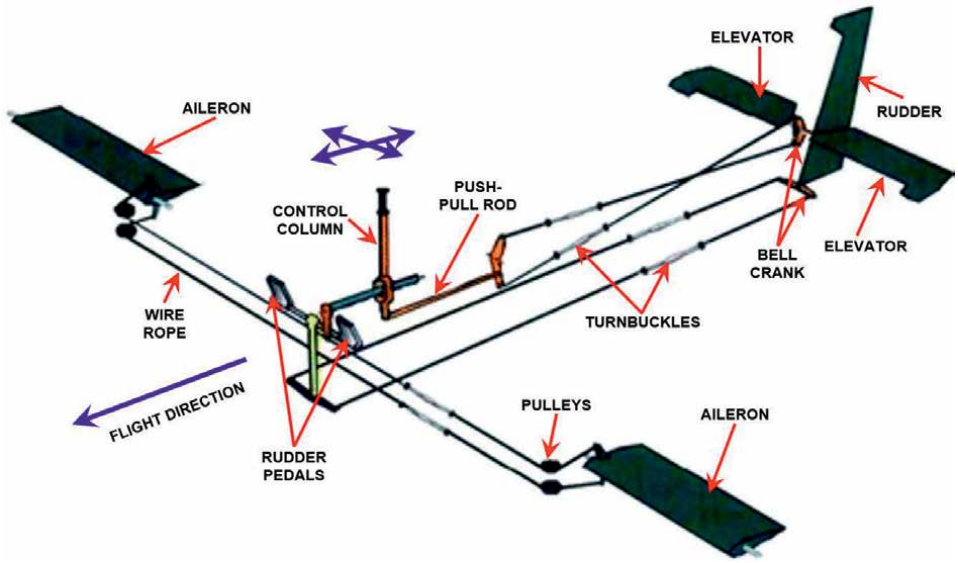

Figure 4.
Pilot-control flight control system with mechanical links.

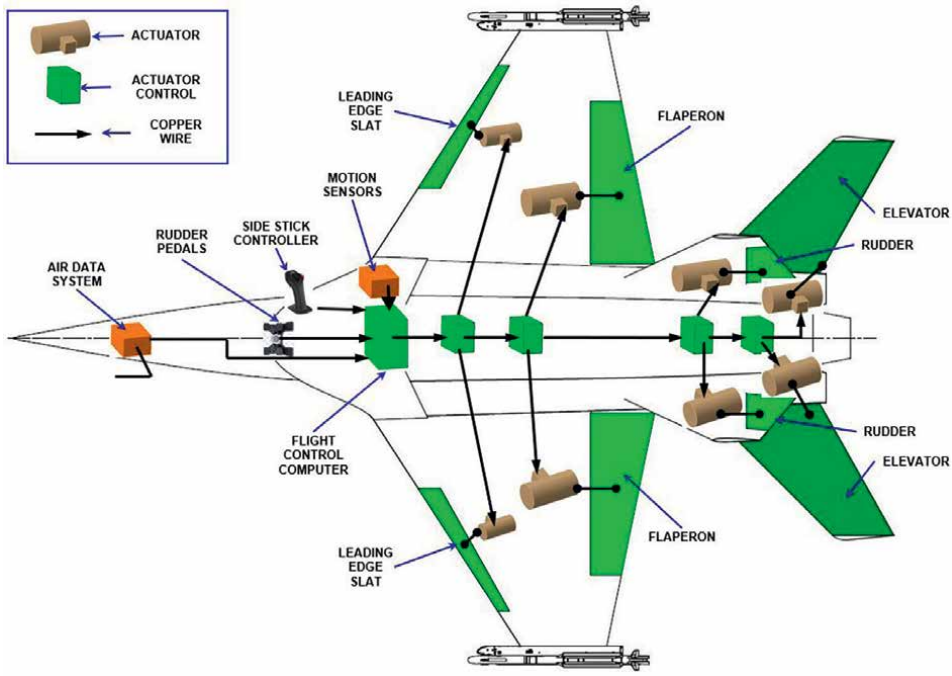

Figure 5.
Fly-by-wire flight control system for a military aircraft.

The fly-by-wire flight control system has a much lower weight than the previous flight control system because all the mechanical connections have been replaced by thin copper wires. Other advantages of this new control system are lower weight, better reliability, damage endurance, and very efficient control of a high-speed very maneuverable military aircraft designed unstable just to increase its maneuverability [2].

The fly-by-wire system is the flight control system that processes the flight control inputs made by the pilot or autopilot using flight computers and submits suitable electrical signals by copper wires to each actuator of the flight control surfaces [2]. The fly-by-wire system means that the pilot inputs do not directly move the control surfaces as explained above, but the pilot must have an effort simulator when moving the side stick/rudder pedal to feel the command. Instead, the inputs are read by a computer, which, in turn, determines how to move the control surfaces to perform the pilot's maneuvers as well as possible, controlled by the active flight envelope containing flight control laws implemented in it by specialized engineers [2, 5], as shown in **Figure 5**.

Another definition of fly-by-wire is a flight control system of an aerospace vehicle in which information is completely transmitted by electrical means via copper wires [2, 4].

The flight envelope refers to the properties of use in the safe parameters of a military airplane. The airplane is manufactured to fly at different parameters of all the kinds of different natures set exactly in advance by engineers. These parameters refer, for example, to the maximum speed, the maximum altitude, the maximum climb rate, etc [5–9].

In the past, there have been aircraft near-accidents or even crashes due to malfunctioning sensors that have transmitted incorrect data to the flight control

computer. That is why it is very important to consider multiredundant sensor circuits in the design process to compare provided information. Overall, it should be noted that the introduction of automation and computers onboard aircraft has significantly reduced the possibility of human error.

The protection software included in the flight envelope automatically prevents pilots' unsafe actions and helps them stabilize the airplane. The fly-by-wire flight control system ensures the suppression of air disturbance and, consequently, reduces the fatigue loads and increases the comfort of the crew on board and ensures an optimized trim setting and, consequently, drag reduction.

In 1972, at NASA's Dryden Flight Research Center, the first digital fly-by-wire flight control system without a mechanical backup was successfully utilized.

Neil Armstrong, a former research pilot at Dryden, played an important role after his historic Apollo 11 lunar landing. NASA's DFBW program consisted of 210 flights and lasted 13 years [2, 10–15].

The Dryden DFBW program has changed the way engineers design and pilots fly commercial and military aircraft. Aircraft equipped with fly-by-wire systems are safer, more reliable, easier to fly, more maneuverable, and more fuel-efficient while having lower maintenance costs [2, 10, 14–19].

The second major step in the development of the fly-by-wire system is the F-16 Fighting Falcon, originally developed by General Dynamics (now Lockheed-Martin) and is a proven compact, single-engine, multirole fighter airplane and the World's first fly-by-wire combat airplane [14, 20, 21] presented in **Figure 6**.

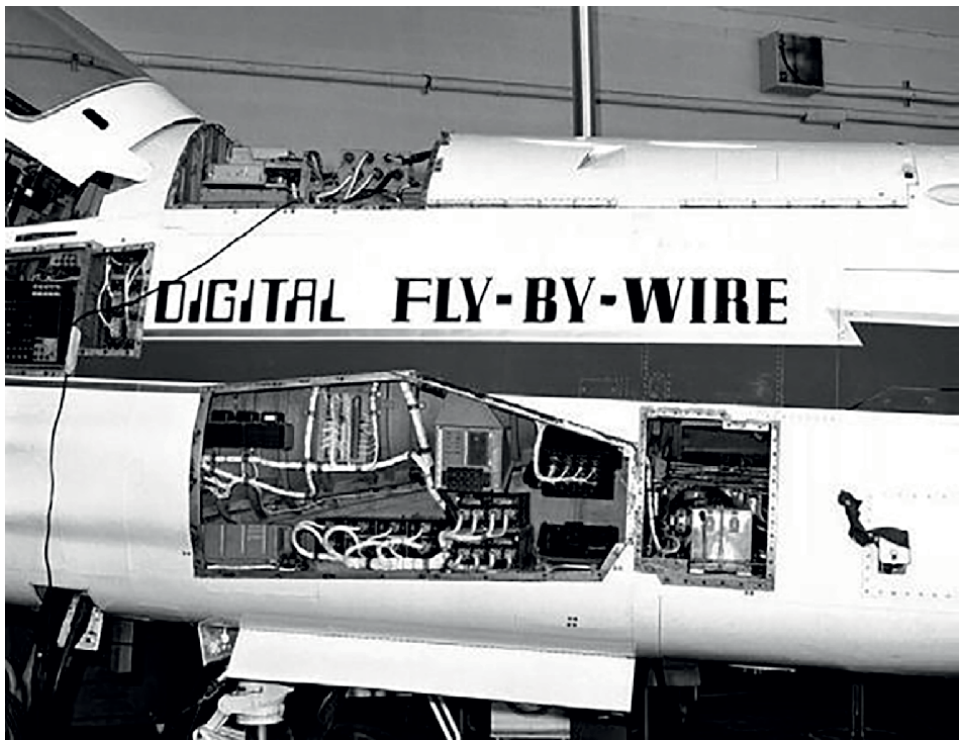

Figure 6.
Digital fly-by-wire system [14].

Since the F-16A's first flight in December 1976, this highly maneuverable air-to-air combat and air-to-surface attack airplane has provided mission versatility and high performance for the U.S. and allied nations at a relatively low cost. The F-16 pilot maintains excellent flight control through the airplane's fly-by-wire system. The pilot sends electrical signals via a side stick/rudder pedal to flight computers and then to the actuators of flight control surfaces, such as ailerons and rudders. The flight computers constantly adjust the inputs to enable stability in level flight and high maneuverability in combat, inside the flight envelope. The side stick/rudder pedal allows the pilot to easily and accurately control the airplane during high G-force of combat maneuvers [14, 20, 21].

The F-16 was the first production airplane to use fly-by-wire technology. To improve maneuverability, the F-16 was designed to be aerodynamically unstable or to have relaxed static stability (RSS). To make the flight of this lightweight fighter airplane smoother, the F-16 has a flight control computer (FLCC) that manages the flight control system [14, 22].

2.2 The fly-by-light system

The fly-by-light (FBL) system installed on military aircraft, using fiber-optic cables, has multiple advantages highlighted below, which provide tactical and safety advantages for the military aircraft and its crew [23].

The structure of a fiber-optic cable [24, 25] is presented in **Figure 7**.

- The fiber core is made of very high-purity optical glass or special plastic, and its thickness (9 μm/50 μm/62.5 μm), depending on the desired transmission spectrum, is less than the thickness of the human hair (about 70 μm).
- The cladding of an optical fiber has a thickness of 125 μm.
- The coating of an optical fiber has a thickness of 250 μm.
- The strengthened layer of an optical fiber has a thickness of 900 μm, which contains a tight buffer wrapped in aramid yarn.
- The outer jacket of an optical fiber has a diameter of 1.2 mm/1.6 mm/2.0 mm/3.0 mm.

Owing to their qualities, fiber-optic cables are extensively used in telecommunications and data networks (Internet). In recent years, more and more countries and companies have implemented the FBL system for military and commercial aircraft [23].

The fiber-optic cables are used in fly-by-light (FBL) flight control systems of the aircraft, and they replace the copper cables previously used in fly-by-wire (FBW) flight control systems [26–28].

For this reason, the advantages of using optical fibers are highlighted, as shown in **Figure 8** and the following explanations [27, 29].

The fiber-optic cable provides a multitude of benefits and redundancy too. The flight control computer has also a flight envelope embedded in it (a computer program made by engineers) that eliminates dangerous maneuvers for the aircraft structure and the life of the crew on board while maintaining the aerodynamic stability of the aircraft in any situation or maneuvers allowed by the flight envelope.

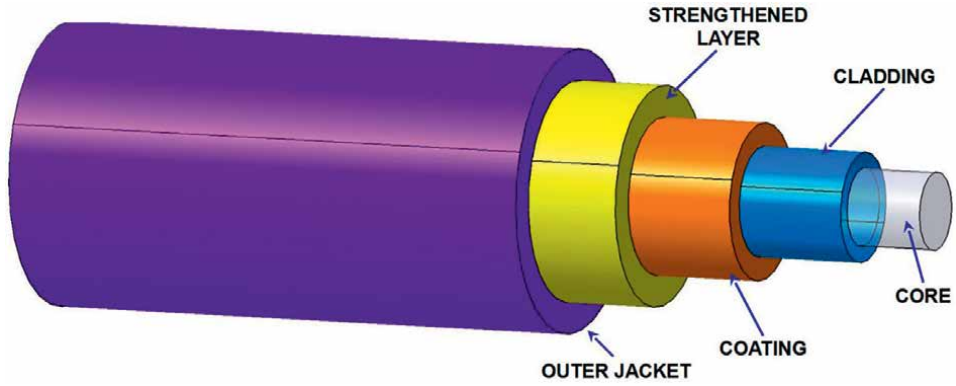

Figure 7.
Fiber-optic cable structure [23].

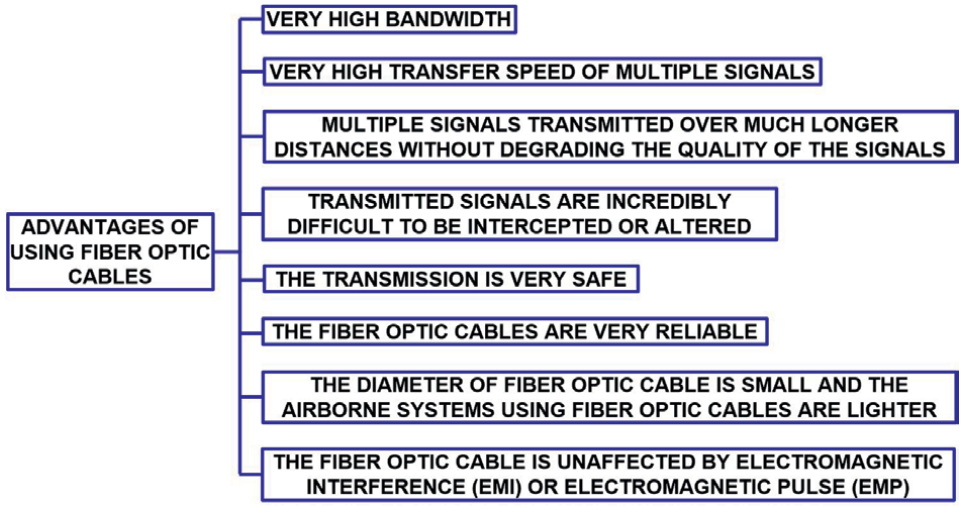

Figure 8.
Advantages of using fiber-optic cables [23].

The fiber-optic cable has a **much higher bandwidth** compared to a copper wire, meaning that it can carry multiple signals on one cable instead of a single signal on a copper wire.

The use of a fiber-optic cable to replace the copper wire will significantly reduce the weight of the new fly-by-light system, and therefore, it will reduce the weight of the entire aircraft.

Fiber-optic cables are characterized by the **very high transfer speed of multiple signals**, with the speed of light through the glass, while the copper wire can carry a single signal at a much lower speed, namely, the speed of electric current through the copper wire.

Multiple light signals can be carried by the fiber-optic cable over much longer distances, without degrading the quality of the multiple light signals, since the signal sent through the optical fiber is much less likely to be altered during transmission, compared to the copper wire.

The core of fiber-optic cables is made of glass, which makes it **incredibly difficult to intercept the signal** without sectioning the cable, even in the case of very qualified people. This makes transmission through fiber-optic cables **very safe**, compared to the copper wire, which can be intercepted very easily, even by less qualified people.

The fiber-optic cables are **very reliable** because they only transmit light signals, without the risk of fire, while the copper wires heat up when transmitting electrical signals; in addition, the transmitted electrical signal can be altered by environmental conditions (severe weather conditions such as lightning, elevated temperature, high humidity, etc.).

The diameter of the fiber-optic cable is smaller than the copper wire, because the fiber-optic cable allows the transmission of multiple signals without affecting the speed or quality of the signals, while the transmission of the electrical signal through the copper wire is strictly dependent on the size of the wire.

Consequently, the weight of a flight control system using fiber-optic cables (FBL) is significantly reduced compared to the FBW system.

The fiber-optic cables do not heat up because they transmit only light signals (photons).

The fiber-optic cable is **unaffected by electromagnetic interference** (EMI) or **electromagnetic pulse** (EMP) [27] generated by nuclear detonation and, therefore, does not need protective shielding like the copper wire (which can be affected by its electromagnetic field, by the electromagnetic frequency given by military electronic jamming devices, other existing electronic devices in the aircraft or even lightning).

The fly-by-light (FBL) system installed on military aircraft, using fiber-optic cables, has multiple advantages highlighted above, which provide tactical and safety advantages for the military aircraft and its crew.

The architecture of the fly-by-light (FBL) flight control system for a modern military aircraft is presented in **Figure 9** [23], and it is like the structure of an FBW system, but there are significant differences between the two systems (FBL and FBW) [29], as presented below:

- The fiber-optic cable is replacing the copper wires.
- The fiber-optic cable does not heat up because it transmits only light signals (photons).
- The fiber-optic cable has a high bandwidth; therefore, the number of cables is reduced, and the weight of the flight control system is also reduced.
- The fiber-optic cable is unaffected by electromagnetic interference (EMI); therefore, the cables can be positioned near electronic devices, near weapons, or even fuel tanks in the aircraft.
- The fiber-optic cable is unaffected by electromagnetic pulse (EMP) generated by nuclear detonation, and the FBL system recovers in a few minutes after explosions that generated strong radiation; therefore, the aircraft can be used in the war zone if the mentioned explosions did not hit the aircraft directly.
- The flight control computer has a high capacity, and it is designed with open architecture for both components, that is, hardware and software, so that it can be easily adapted depending on the tactical situation, the type and quantity of weapons loaded, the type of missions, etc.

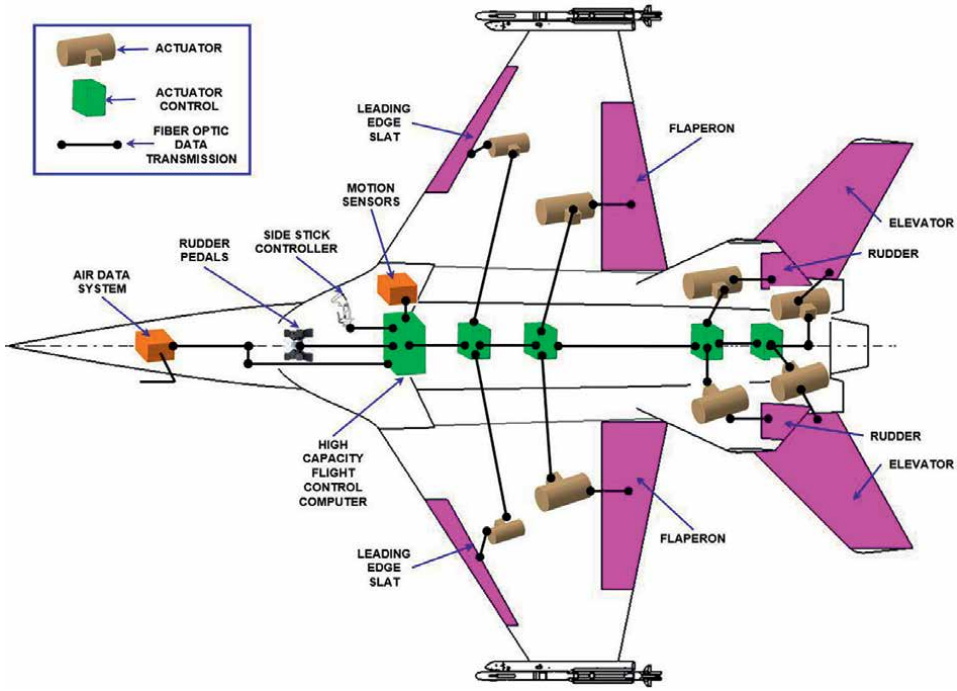

Figure 9.
The fly-by-light flight control system for a modern military aircraft [23].

A list of known aircraft using the fly-by-light system is presented below.

The A-7D test aircraft, equipped with the complete fly-by-light system flew first on February 7, 1975 and then on March 24, 1982, in California, USA [23].

The Kawasaki XP-1, a Japanese maritime reconnaissance aircraft, had its first flight in September 2007, and it has the distinction of being the first operational aircraft in the world to use a fly-by-light (FBL) flight control system [23].

On March 18, 2018, Gulfstream demonstrates the fly-by-light aircraft control system, during a nearly 75-minute flight [26].

China intends to use the fly-by-light (FBL) flight control system for the sixth-generation fighters [28].

India is developing research to use the fly-by-light (FBL) flight control system for the sixth-generation fighters for the Advanced Medium Combat Aircraft (AMCA), an Indian program to develop fifth- to sixth-generation fighter aircraft for the Indian Air Force and the Indian Navy [23].

Many companies, such as Boeing and Airbus, are interested in implementing the fly-by-light (FBL) flight control system on new aircraft or if they have the opportunity when modernize existing aircraft [23].

2.3 About this research

Flight control systems for military aircraft have had and still have a very rapid evolution based on the needs of the air force in each country, on the rapid scientific and technical evolution that allows new and new improvements of military flight control systems. As presented, military aircraft are designed to be aerodynamically

unstable to give them superior maneuverability in training or during air combat with enemy armed forces.

During the air maneuvers, the aerodynamic forces developed on the control surfaces and the fuselage of the military aircraft are very large, which requires strong, very fast, but also very safe flight control systems, considering the huge cost of these aircraft.

To make the flight control systems very secure, they are designed as multiredundant systems, and the actuators with which the control surfaces are operated are dimensioned to exceed the aerodynamic forces in any situation.

Of all the systems presented and analyzed, the most advanced, the lightest, and with increased protection from electromagnetic interference (EMI) and electromagnetic pulse (EMP) is the fly-by-light (FBL) flight control system.

In addition, the fiber-optic cable used in the fly-by-light flight control system has a much higher bandwidth, and a very high transfer speed of multiple signals, with the speed of light, it is incredibly difficult to intercept the signal without sectioning the cable, and finally, the diameter of the fiber-optic cable is smaller, which makes it possible to design a multiredundant flight control system without significantly increasing the weight of military aircraft.

The best flight control system for military aircraft is by far the fly-by-light (FBL) system, due to its extraordinary features highlighted above.

3. Conclusions

From the creation of the first aircraft (the Wright brothers, in [30]), or even earlier, pioneer inventors used empirical mechanical flight control systems to take off, fly, and land with aircraft designed by them. Since then, flight control systems have evolved continuously, at a very fast pace, as flight speed has steadily increased and the sound barrier has been overcome several times nowadays.

The fly-by-wire flight control system is much lighter than the previous flight control system because all the mechanical connections have been replaced with thin copper wires. Other advantages of the control system are lower weight, better reliability, damage resistance, and highly efficient control of a high-speed and highly maneuverable military aircraft, unstable designed to increase its maneuverability.

The fly-by-light flight control system uses fiber-optic cables and is widely used in data and telecommunications networks. Recently, glass has been replaced with special clear plastic that helps reduce weight even more significantly. Due to its major advantages, the fly-by-light flight control system is increasingly used in military aircraft as well as in commercial aircraft [16, 31–33].

Because the fly-by-light system has low weight, high bandwidth, compact size, and resistance to electromagnetic interference (EMI) and electromagnetic pulses (EMP), it is expected to become the next generation of flight control systems as it offers immunity to new more hostile military environments.

Acknowledgements

The work was carried out within contract no. 8 N/2019, code PN 19 01 04 01, supported by the Romanian Ministry of Research, Innovation, and Digitalization.

Conflict of interest

The authors declare no conflict of interest.

Author details

Cătălin Nae, Ilie Nicolin* and Bogdan Adrian Nicolin
INCAS - National Institute for Aerospace Research "Elie Carafoli", Bucharest, Romania

*Address all correspondence to: nicolin.ilie@incas.ro

References

[1] Sutherland JP. Fly-by-Wire Flight Control Systems. Ohio: Air Force Flight Dynamics Laboratory, Wright Patterson Air Force Base; 1968

[2] Nicolin I, Nicolin BA. The Fly-by-Wire system. INCAS Bulletin. 2019;**11**(4):217-222 (P) ISSN 2066-8201, (E) ISSN 2247-4528. DOI: 10.13111/2066-8201.2019.11.4.19

[3] Forces on an Airplane - NASA Glenn Research Center. Available from: https://www.grc.nasa.gov/www/k-12/airplane/forces.html

[4] InterConnect Wiring. Available from: https://www.interconnect-wiring.com/aerospace/what-does-Fly-by-Wire-mean/

[5] Fly-by-Wire, SKYbrary. 2017. Available from: https://www.skybrary.aero/index.php/Fly-by-Wire

[6] Angulo D. Fly-by-Wire. 2019. Available from: https://aertecsolutions.com/2019/03/11/Fly-by-Wire/?lang=en

[7] Fehrm B. Flight control. 2016. Available from:https://leehamnews.com/2016/03/11/bjorns-corne.r-flight-control/

[8] Pope S. Fly-by-Wire Fact versus Science Fiction. 2014. Available from: https://www.flyingmag.com/airplane/jets/Fly-by-Wire-fact-versus-science-fiction/

[9] Fly by Wire. Available from: http://elektromot.com/tag/Fly-by-Wire-advantages/

[10] Moir I, Seabridge A. Aircraft Systems, Mechanical, Electrical, and Avionics Subsystems Integration. 3rd ed. The Atrium, Southern Gate, Chichester, West Sussex, England: John Wiley & Sons Ltd.; 2008

[11] Twombly JI. How it works: Fly-by-Wire, Flight Training Magazine. 2017, Available from: https://www.aopa.org/news-and-media/all-news/2017/july/flight-training-magazine/Fly-by-Wire

[12] Airplane Systems – Lecture Notes, Chap. 6 Flight Control System, Milano. 2004. Available from: https://www.academia.edu/3805511/POLITECNICO_DI_MILANO_-_DIPARTIMENTO_DI_INGEGNERIA_AEROSPAZIALE

[13] Cloer L. What Is Fly-by-Wire? Vol. 12014 Available from: https://duotechservices.com/what-is-Fly-by-Wire

[14] Creech G. Digital Fly-by-Wire: Airplane flight control comes of age. NASA Dryden Flight Research Center, September. 2007;**30** Available from: https://www.nasa.gov/vision/earth/improvingflight/fly_by_wire.html

[15] Tomayko EJ. In: Levine J, editor. The Story of the Self-Repairing Flight Control System. NASA Dryden Flight Research Center; 2003

[16] Digital Fly-by-Wire, "The All-Electric Airplane", TF-2001-02 DFRC, NASA Dryden Flight Research Center. 2003. Available from: https://www.nasa.gov/pdf/89222main_TF-2001-02-DFRC.pdf

[17] Fly-by-Wire. NASA Technology. Available from: https://spinoff.nasa.gov/features/dfbw.html

[18] Digital Fly-By-Wire (Apollo 11). Available from: https://wehackthemoon.com/tech/digital-fly-wire

[19] Bellm D. How the F-16 Became the World's First Fly-by-Wire Combat Airplane. 2009. Available from: http://www.f-16.net/articles_article13.html

[20] Ferguson B. The F-16 Fighting Falcon. 2018. Available from: https://airman.dodlive.mil/2018/02/12/f-16-fighting-falcon/

[21] Kämpf P. Fighter Jets Are Designed To Be Inherently Unstable. 2014. Available from: https://aviation.stackexchange.com/questions/8049/are-fighter-jets-designed-to-be-so-inherently-unstable-that-a-human-cant-fly-o

[22] Nicolin I, Nicolin BA. The Fly-by-Light system for military aircraft. INCAS Bulletin. 2022;**14**(1):237-241 (P) ISSN 2066-8201, (E) ISSN 2247-4528. DOI: 10.13111/2066-8201.2022.14.1.19

[23] Urban J. Anatomy of a Cable – Optical Fiber. Available from: https://blog.biamp.com/anatomy-of-a-cable-optical-fiber/,05.09.2013

[24] Nelson RC. Flight Stability and Automatic Control. Second ed, International Editions. Singapore.: WCB/McGraw-Hill; 1998

[25] Pope S. Gulfstream Testing Fly-By-Light Controls, Available from: https://www.ainonline.com/aviation-news/aviation-international-news/2008-04-01/gulfstream-testing-fly-light-controls [Accessed: January 4, 2008]

[26] Tooley M, Wyatt D. Aircraft Electrical and Electronic Systems. Elsevier Ltd.; 2009 ISBN: 978-0-7506-8695-2

[27] China's Fly-By-Light Flight Control System to be Used on 6th-Gen Fighters, Available from: https://www.china-arms.com/2021/01/china-fly-by-light-flight-control/

[28] Garg A, Linda RI, Chowdhury T. Evolution of aircraft flight control system and fly-by-light flight control system. International Journal of Emerging Technology and Advanced Engineering, ISSN 2250-2459, ISO 9001:2008. 2013;**3**(12)

[29] Padfield D. The birth of flight control: An engineering analysis of the Wright brothers' 1902 glider. The Aeronautical Journal. 2003;**1**(2854):697-718

[30] Garg A et al. Evolution of airplane flight control system and fly-by-light flight control system. International Journal of Emerging Technology and Advanced Engineering, Website: www.ijetae.com ISSN 2250-2459, ISO 9001:2008 Certified Journal. 2013;**3**(12)

[31] Garg A et al. Application of fiber optics in airplane control system & its development. In: International Conference on Computer Communication, and Informatics (ICCCI -2014). 2014 Coimbatore, India

[32] Spitzer RC. Digital Avionics Handbook. Second ed. Williamsburg, Virginia, U.S.A.: CRC Press, Taylor & Francis Group; 2007. ISBN: 10:0-8493-8441-9

[33] Tooley M, Wyatt D. Airplane Electrical and Electronic Systems. Elsevier. Linacre House, Jordan Hill, Oxford, UK: Elsevier; 2009. ISBN: 978-0-7506-8695-2

Section 5

Modeling and Simultion

Chapter 7

Simulation of a Mathematical Model of an Aircraft Using Parallel Techniques (MPI and GPU)

Peter Kvasnica

Abstract

This chapter is focused on creation, accuracy, and simulation of two-parameter control of a mathematical model of motion of aircraft in a flying simulator. We are discussing many of the important advances in applied aircraft modeling. Modeling on various computer architectures (central, distributed, parallel) has an impact on a structure of a mathematical model of aircraft. An important part is the way of description of a numerical method and its accuracy, use of distributed memory system, and shared memory system are presented in the chapter. Motivation of this research is implementation of the general-purpose message passing interface and graphics processing units as inexpensive arithmetic-processing units bring a relevant amount of computing power to desktop personal computers. The chapter is focused on exploitation of parallel techniques of simulation features, computation time of parallel methods of implementation, and improved simulation of a continuous mathematical model of aircraft motion in a flying simulator. The use and application of modeling methods and parallel simulation techniques determine the structure of the mathematical model used in the flying simulator. The effectiveness of our solution is confirmed by providing simulation results obtained by two-parameter control of the mathematical model of aircraft motion.

Keywords: mathematical model, block structured model, message passing interface, parallel architecture of modeling, graphics processing unit

1. Introduction

Mathematical models are mostly used in natural sciences (physics, chemistry, earth science) and engineering disciplines (computer science, biological science, genetic engineering), as well as in social sciences. Substantial stages of implementation (creation, design, simulation, and visualization) of a continuous mathematical model of aircraft motion in a flying simulator were described in many papers. The one-parameter control of a distributed mathematical model of motion of aircraft with all phases of implementation in a flying simulator was described in the published paper [1, 2].

Motivation of this research is using a mathematical model of an object, which in practice and the real world often can be determined analytical otherwise. For this reason, it is necessary to design mathematical models characterized for this problem statement. The more accurate the mathematical model of the object we create, the more accurate the results of its simulation.

The mathematical model of motion of aircraft can be simulated using central computer architecture, which can be based on single-processor systems. The simulation of structured mathematical model of an aircraft can be implemented using central computer architecture, a distributed memory system (DMS) using a message interface (MPI) architecture; they are identified as node computers or shared memory system (SMS) and graphics processing unit (GPU) architectures [3]. The parallel computer architecture may be based on multiprocessors; each processor has a multicore architecture. Multiprocessor systems are computationally more efficient than such systems compared with the central computer architecture, see [4].

As known from specialized literature, creation of mathematical models of motion of aircraft consists of the following phases: definition of a physical base for creation of a mathematical model, selection of notation of a mathematical model, implementation of a mathematical model and others. The Laplace transformation, computation of parameters of aircraft for a selected flight phase, determination and computation of coefficients, numerical integration, programming, and simulation on a computer, etc. are used in our problem statement and proposed solution.

According to current knowledge, the effort made to create mathematical models of motion is aimed at improvement and extension of a field of view of simulation of mathematical models on the different computer architectures. The solution of large and complex mathematical models of aircraft problems leads to considerable demand for parallel computing and strategies [5]. We can confirm the most frequent use of the following phases: creation, design, implementation, and simulation of mathematical models. The parallel computing tools guarantee an impressive reduction of computing time [6].

A block structure mathematical model of motion of aircraft can be integrated numerically using parallel computer architecture. This architecture can be motivation for using a central processing unit (CPU)-based implementation with multiprocessor systems and a graphics processing unit (GPU); see [7]. Likewise, a computer system fitted with a GPU accelerator and a software application designed and created for this architecture is also suitable for simulation of a block mathematical model of aircraft motion. From our point of view, the following three principles are important for proposed solution:

- representation by solution architecture, i.e., the migration of codes of a mathematical model of motion of aircraft toward parallel computers.
- low-cost distributed platforms, combined suitable software tools that open very demanding perspectives.
- use GPU to speed up calculations.

Accordingly, in the chapter, we explain how to implement a compute unified device architecture (CUDA) algorithm of computation of a block structure mathematical model of motion of aircraft so as to achieve peak speed. The efficiency is

demonstrated by discussing two-parameter control of aircraft, throttle control stick (fuel supply), and aircraft elevator control stick (angle of attack).

2. Description of aircraft mathematical model

The unstable characteristics such as aero elasticity impact, fuel density, changing geometry of aircraft, and some other parameters support complexity of our design mathematical models in simulation. The mathematical models of motion interact with intervening pilot's control of aircraft and real equipment respond to the pilot's interventions, data on equipment the flying aircraft are observed by the pilot. We can use a continuous simulation method to solve differential equations in mathematical models of motion of aircraft created this way. Aerospace engineers often use Newton's laws of motion in design and creation of a mathematical model of motion of aircraft described by differential operators.

According to Newton's third law, there is always the same opposite reaction to every action, or the interaction of two bodies on each other always leads to opposite parts. The basic system of equations has the form [8]:

$$\dot{x}_1 + f_i(x_1, \ldots, x_n; u_1, \ldots, u_m; \xi_1, \ldots, \xi_\gamma) = 0, (i = 0, 1, \ldots, p) \tag{1}$$

where $x_1, \ldots, x_n$ are object coordinates, $u_1, \ldots, u_m$ are elements of control, and $\zeta_1, \ldots, \zeta_\gamma$ are failure functions. The problems of simulation and synchronization of mathematical models on computers is know, where the accuracy of a linear motion model is used [9]. The accuracy between the transient response results of nonlinear mathematical models compared with linear mathematical models from in terms of human accuracy can be neglected [10].

2.1 Equations numerical integration of mathematical model

The proposed solution based on the presented analysis of the state model space does not contain any discontinuity in either $f_i(\boldsymbol{x}, \boldsymbol{u}, t)$ or in any of higher derivatives, $x_i(t)$ itself is a continuous function of time. Currently used methods of numerical integration are used to find numerical approximations to solutions of ordinary differential equations (ODEs). The name, also known as numerical integration, represents a broad family of algorithms for calculating the numerical value of a particular integral. The methods of numerical integration can generally be described as combining evaluations of the integrand to get an approximation to the integral. The integrand is evaluated on a finite set of points called integration points, and the weighted sum of these values is used to approximate the integral [11]. This method of calculation is often used for polynomial functions, and these are suitably used on computers. Our proposed solution deals with creation of such functions, i.e., integration of mathematical models.

Two most basic algorithms, Euler (forward and backward) and Taylor series, are motivation for this research in our solution for numerical integration. A numerical stability domain is introduced as a pillar to characterize an integration algorithm and a general procedure to find the numerical stability domain of any integration scheme, see [11]. The mathematical model in state space has the following form:

$$\dot{\mathbf{x}}(t) = \mathbf{f}(\mathbf{x}(t), \mathbf{u}(t), t), \tag{2}$$

where $\boldsymbol{x}$ is a state vector, $\boldsymbol{u}$ is an input vector, and t represents time, with a set of initial conditions:

$$\mathbf{x}_{(t=t_0)} = \mathbf{x_0}. \tag{3}$$

Let $x_i(t)$ represents the ith state trajectory as a function of simulated time t. As long as the state-space model does not contain any discontinuity in either $f_i(\boldsymbol{x}, \boldsymbol{u}, t)$ or any of higher derivatives, $x_i(t)$ is itself a continuous function of time. Such function can be approximated by any desired precision by a Taylor series expansion of any given point along its trajectory. Let t^* denote a point in time, about which we wish to approximate the trajectory using Taylor series, and let $t^* + h$ be the point in time, at which we wish to evaluate the approximation [11]. The trajectory at that point can then be given as follows:

$$x_i(t^* + h) = x_i(t^*) + \frac{dx_i(t^*)}{dt} \cdot h + \frac{d^2x_i(t^*)}{dt^2} \cdot \frac{h^2}{2!} + \cdots. \tag{4}$$

Different integration algorithms differ in how they approximate the higher-order derivatives and in the number of Taylor series members that they take into account in the approximation [10].

If the term $n + 1$ of the Taylor series is considered, the approximation accuracy of the second derivative $d^2x_i(t^*)/d^2t = df_i(t^*)/dt$ should be of order $n - 2$, since this factor is multiplied by h^2. The accuracy of the third state derivatives should be of the order $n - 3$, since this factor is multiplied by h^3, etc. In this way, the approximation is correct up to h^n. N is therefore called the *approximation order* of the integration method, see [11].

Many engineering simulation applications require a global relative accuracy of approximately 0.002. If the *local integration* error is of size e_l, then the *per-unit-step integration error* assumes the value of $e_{p.u.s} = e_l/h$. The *global integration error* is proportional to the per-unit-step integration error, as long as the integration error does not accumulate excessively across multiple steps.

In accordance with the previously made observation, this corresponds to an algorithm with an approximation order of h^4 for the local integration error. We should require, for example, a local accuracy of 0.0001 [11]. In a digital computer, a real number can only be represented with a finite precision, 32-bit numbers, and double precision for 64-bit numbers. This type of error is called *round-off error*. It occurs in one of the two main general formats that have become common and called *floating point.* The most common problems due to a rounding error occur when multiple steps are rounded in each step.

3. An appropriate structured mathematical model of motion in state space

These practical requirements are determined to using linear models in a process of analyzing general processes [12]. For writing of mathematical models of motion of aircraft in a simulator, we can use state-space description. We define a linear controlled unobserved dynamic system based on the current state, see [13]:

$$\begin{aligned} \dot{\mathbf{x}}(t) &= \mathbf{A}\mathbf{x}(t) + \mathbf{B}\mathbf{u}(t), \\ \mathbf{y}(t) &= \mathbf{C}\mathbf{x}(t), \\ \mathbf{x}(t) &= \mathbf{x}_0 \end{aligned} \tag{5}$$

where $\boldsymbol{A}$, $\boldsymbol{B}$, $\boldsymbol{C}$, $\boldsymbol{x}$, $\boldsymbol{u}$, and $\boldsymbol{y}$ have dimensions $(n\ x\ n)$, $(r\ x\ n)$, $(l\ x\ n)$, $(n\ x\ l)$, $(m\ x\ l)$, and $(r\ x\ l)$ are defined matrices, see the description of items [2]. The task easier that we will focus on the control object, the first and second equation from the system (5) can have a general shape:

$$\begin{aligned}\dot{\mathbf{x}} &= \mathbf{A}\mathbf{x} + \mathbf{B}\mathbf{u},\\ \mathbf{y} &= \mathbf{C}\mathbf{x}.\end{aligned} \tag{6}$$

Eq. (6) in matrix form represents a complex aircraft dynamic system of a mathematical model of aircraft motion comprising in a process of simulation of 11 state variable sensors of information, 18 state variables-coordinates of performing elements in the system. These are two parts and the remaining 38 state variables are divided into variables that represent unmeasured noise and sensor disturbances [9]. The differential equations of mathematical model of aircraft motion have two-parameter control the form [14]:

$$\begin{aligned}&\Delta\dot{V} + a_x^V\Delta V + a_x^\alpha\Delta\alpha + a_x^\theta\Delta\theta = a_x^{\delta M}\Delta\delta_M\\ &\Delta\theta + a_y^V\Delta V + a_y^\alpha\Delta\alpha + a_y^\theta\Delta\theta = a_y^{\delta M}\Delta\delta_V\\ &\Delta\dot{\omega}_z + a_{mz}^V\Delta V + a_{mz}^\alpha\Delta\alpha + a_{mz}^{\dot{\alpha}}\Delta\theta + a_{mz}^{\omega z}\Delta\omega_z = a_{mz}^{\delta V}\Delta\delta_V\\ &\Delta\upsilon = \omega_z, \Delta\upsilon = \Delta\theta + \Delta\alpha.\end{aligned} \tag{7}$$

Four parts represent a state matrix of mathematical models of motion of aircraft expressed by the state vector $n = 4$. Coefficients c_i and e_j represent aerodynamic parameters, their computation, in accordance with (Eq. (7)), we get [14]:

$$\begin{aligned}&\Delta\dot{V} + a_x^V\Delta V + a_x^\alpha\Delta\alpha + a_x^\theta\Delta\theta + a_x^H\Delta H = a_x^{\delta M}\Delta\delta_M\\ &\Delta\theta + a_y^V\Delta V + a_y^\alpha\Delta\alpha + a_y^\theta\Delta\theta + a_y^H\Delta H = a_y^{\delta M}\Delta\delta_V\\ &\Delta\dot{H} - \sin(\theta_0)\Delta V - \cos(\theta_0)\Delta V = 0; \Delta\dot{\upsilon} = \omega_z, \Delta\upsilon = \Delta\theta + \Delta\alpha.\end{aligned} \tag{8}$$

Items ΔV, $\Delta\alpha$, $\Delta\theta$, ΔH, $\Delta\delta_M$, and $\Delta\delta_V$ are defined in [2]. The following items: $a^V{}_x\ \Delta V$, $a^\alpha{}_x\ \Delta\alpha$, $a^\theta{}_x\ \Delta\theta$, $a^H{}_x\ \Delta H$ for flight speed ΔV, $a^V{}_y\ \Delta V$, $a^\alpha{}_y\ \Delta\alpha$, $a^\theta{}_y\ \Delta\theta$, $a^H{}_y\ \Delta H$ for thumb angle, and other parameters of aircraft motion. Transfer functions have the form [14]:

$$\begin{aligned}&\Delta V(s) = -G_{V/\delta M}(s)\Delta\delta_M(s) - G_{V/\delta V}(s)\Delta\delta_V(s)\\ &\Delta\alpha(s) = -G_{\alpha/\delta M}(s)\Delta\delta_M(s) - G_{\alpha/\delta V}(s)\Delta\delta_V(s)\\ &G_{V/\delta M}(s) = a_x^{\delta M}\left(\Delta_{11/}\Delta\right); G_{V/\delta V}(s) = a_y^{\delta M}\left(\Delta_{21/}\Delta\right) + a_{mz}^{\delta V}\left(\Delta_{31/}\Delta\right);\\ &G_{\alpha/\delta M}(s) = a_x^{\delta M}\left(\Delta_{12/}\Delta\right); G_{\alpha/\delta V}(s) = a_y^{\delta V}\left(\Delta_{22/}\Delta\right) + a_{mz}^{\delta V}\left(\Delta_{32/}\Delta\right).\end{aligned} \tag{9}$$

where Δ_{ij} is the subdeterminant of the ith row and the jth column. Our problem and the proposed solution are described in the following. The first member (Eq. (9)) of the system is employed to describe the change of the aircraft speed ΔV; also the equation describing displacement of the speed aircraft depending on the displacement of throttle engine lever $G_{V/\delta M}(s)$ and the displacement of elevator angle $G_{V/\delta V}(s)$ is employed. The items of second (Eq. (9)) describe the change of aircraft attack of

angle of the system $G_{\alpha/\delta M}(s)$ and $G_{\alpha/\delta V}(s)$. The third row of the system (Eq. (9)) defines how to compute these changes of two parameters for a change of aircraft speed, and fourth row of the system (Eq. (9)) defines how to compute these changes of two parameters for a change of an aircraft angle of attack. For the meaning of coefficients $a^{\delta M}{}_x$, $a^{\delta M}{}_y$, $a^{\delta V}{}_y$, $a^{\delta V}{}_{mz}$ and $\Delta_{ij}(s)$, see the paragraph after (Eq. (20)). In our problem solution, the flight of the aircraft is steady and without any random interferences (wind, storm, or other outer interferences) [12].

3.1 Structure-defined mathematical model of an aircraft motion in a simulator

At present, matrix notation of a mathematical model in the state space, which we mentioned in the previous section, is very often used. We should express the first equation from (Eq. (6)) next [15]:

$$\begin{pmatrix} \dot{x}_1 \\ \dot{x}_2 \\ \dot{x}_3 \\ \dot{x}_4 \end{pmatrix} = \begin{pmatrix} a_{11} & a_{12} & a_{13} & a_{14} \\ a_{21} & a_{22} & a_{23} & a_{24} \\ a_{31} & a_{32} & a_{33} & a_{34} \\ a_{41} & a_{42} & a_{43} & a_{44} \end{pmatrix} \begin{pmatrix} x_1 \\ x_2 \\ x_3 \\ x_4 \end{pmatrix}. \tag{10}$$

The described solution is relatively simple due to description of the analyzed system using equations (Eq. (10)), see [5] for more. Let us divide the mathematical model of aircraft motion into four subsystems. The first will be a subsystem of state variable sensors, the second and third will be subsystems of power elements (two systems), the fourth will measure noise and system faults. Thus, the subsystems have the order $n_1 = 1$, $n_2 = 1$, $n_3 = 1$, $n_4 = 1$. The state space is divided into four parts:

$$\mathbf{x} = (x_1, x_2, x_3, x_4)^T = (x_1x_1, x_1x_2, x_1x_3, \ldots, x_4x_4), \tag{11}$$

where $\boldsymbol{x_ix_j}$ represent the items of a state vector. If i represents order relevancy n, i.e., the number of the subsystem, then j – stands for sequential number of the item in the given subsystem. The research architecture of the discussed system matrix $\boldsymbol{A}$ in the state space can be formed after multiplying the following shape, see [15]:

$$\begin{aligned} \dot{x}_{11} &= a_{11}x_1x_1 + a_{11}x_1x_2 + a_{11}x_1x_3 + a_{11}x_1x_4, \\ \dot{x}_{12} &= a_{12}x_1x_1 + a_{12}x_1x_2 + a_{12}x_1x_3 + a_{12}x_1x_4, \\ &\vdots \\ \dot{x}_{44} &= a_{44}x_1x_1 + a_{44}x_1x_2 + a_{44}x_1x_3 + a_{44}x_1x_4, \end{aligned} \tag{12}$$

Then we divide 16 subsystems into four parts called isolated subsystems. The above decomposition process is performed by matrix and vector operations. The sixteen blocks A_{11}, A_{12}, ..., A_{43}, A_{44} of matrix $\boldsymbol{A}$ are marked in the order, where:

$$\begin{aligned} \dot{x}_{11} &= A_{11}x_{11} + A_{11}x_{12} + A_{11}x_{13} + A_{11}x_{14}, \\ \dot{x}_{12} &= A_{12}x_{11} + A_{12}x_{12} + A_{12}x_{13} + A_{12}x_{14}, \\ &\vdots \\ \dot{x}_{44} &= A_{44}x_{11} + A_{44}x_{12} + A_{44}x_{13} + A_{44}x_{14}. \end{aligned} \tag{13}$$

The mathematical description of isolated subsystems has then the following form:

$$\dot{x}_1 = A'_{11}x_1, \dot{x}_2 = A'_{22}x_2, \dot{x}_3 = A'_{33}x_3, \dot{x}_4 = A'_{44}x_4, \tag{14}$$

where:

$$A'_{11} = \begin{pmatrix} A_{11} \\ A_{12} \\ A_{13} \\ A_{14} \end{pmatrix}, \; A'_{22} = \begin{pmatrix} A_{21} \\ A_{22} \\ A_{23} \\ A_{24} \end{pmatrix}, \; A'_{33} = \begin{pmatrix} A_{31} \\ A_{32} \\ A_{33} \\ A_{34} \end{pmatrix}, \; A'_{44} = \begin{pmatrix} A_{41} \\ A_{42} \\ A_{43} \\ A_{44} \end{pmatrix}. \tag{15}$$

The mutual relations between the first and second isolated subsystems are described by $l_{12}(x)$ meaning that the equation of the first and second isolated subsystem is:

$$l_{12}(x) = A'_{11} \begin{pmatrix} x_1 \\ x_2 \\ 0 \\ 0 \end{pmatrix} = (A_{11}, A_{12}, A_{13}, A_{14})^T \begin{pmatrix} x_1 \\ x_2 \\ 0 \\ 0 \end{pmatrix}. \tag{16}$$

The state of solution method is known and well described in the reference [5]. The capability of being decomposed can be calculated by means of incidental matrices that can be utilized in cases when the mathematical model of the system is defined. The units in random matrix are positioned as its elements are permuted or transformed so that they can be placed diagonally.

4. Structured mathematical model of speed and angle of attack aircraft in a flight simulator

Current computer technologies allow formulation and solutions to a new intricate problem, which depends on construction of structured mathematical models of aircraft and methods of their solution. Achieving an accurate solution to this problem requires simultaneous solution of the whole complex of physical and geometric problems, which is based on considerable computational resources [16]. Our proposed solution is supported by the above approach, where there are, complex requirements for properties and parameters affecting the design process of a structured mathematical model of aircraft motion on computers.

To create a system of differential equations, it is necessary to know the aerodynamic coefficients, mathematical model of aircraft systems, and other parameters of the aircraft [1, 2]. The contribution in Laplace transform creates a structured mathematical model of aircraft motion in a flight simulator, see [5, 15].

Action of an aircraft elevator control stick angle and throttle control stick displacement on aircraft motion—two control parameters (**Figure 1**) are discussed below. **Figure 1** is a block diagram of already mentioned two-parameter control of a structured mathematical model of motion of aircraft on a flight simulator, which will be the subject of research.

The process of simulation experiments requires finding solutions for individual tasks defined at the beginning of the previous subchapter. The simulation program

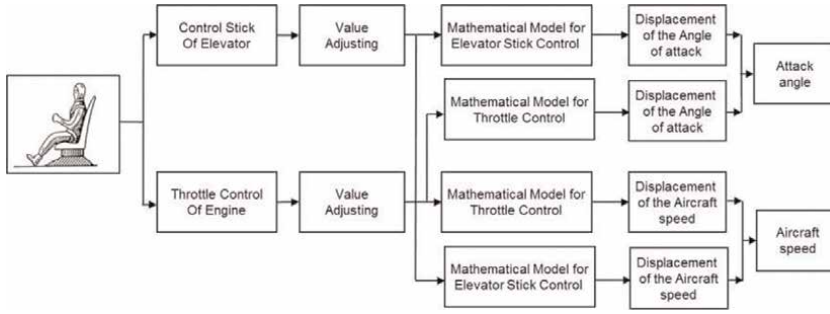

Figure 1.
Block diagram of a structured mathematical model of control of aircraft motion – speed and angle of attack.

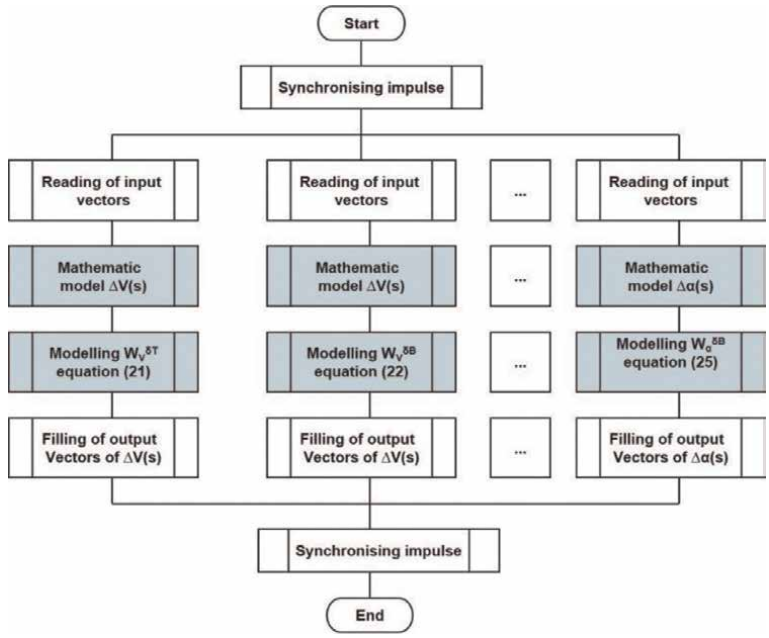

Figure 2.
Parallel simulation algorithm of simulators' models.

expresses the time factor in the form of an explicit simulation time and changes the state of model. Two opposite methods of working with simulation time are implemented in the programming technique. In the constant time step method, it is necessary to select a constant real-time interval, which is considered as a unit of simulation time. The structured mathematical models of all simulators need to process the simulation run—the simulating step during this time unit (**Figure 2**).

4.1 Structure-defined mathematical model of the aircraft speed in a flight simulator

The input values are represented by a change of an aircraft elevator control stick angle and a throttle control stick of engine. The values are adjusted as required and

forwarded to the input of the structured mathematical model of aircraft motion-speed. The aircraft speed displacement equation $\Delta V(s)$ defines a change in fuel supply and the change in the aircraft elevator angle [14]:

$$\Delta V(s) = -G_{V/\delta M}(s)\Delta\delta_M(s) - G_{V/\delta V}(s)\Delta\delta_V(s), \tag{17}$$

where $G_{V/\delta M}(s)$ defines a mathematical model of speed—transfer function for fuel supply, $\Delta\delta_M(s)$ is an input function for fuel supply in Laplace transform, $G_{V/\delta V}(s)$ is a mathematical model of speed—transfer function for an aircraft lift, and $\Delta\delta_V(s)$ means the input function of an aircraft pitch angle in the Laplace transform. Derivation of equations of a structured mathematical model of speed increment is a suitable description of the problem. Information about mathematical solution of these equations is known [13]. The expression $A = s^4 + 1.134s^3 + 62.798s^2 + 28.659s + 4.093$, is the same in all equations. The items for $l_{12}(x)$ defined by the Eq. (16) are as follows:

$$A_{11} = 5\frac{s^3 + 1.12s^2 + 62.782s + 25.32}{A}, x_1 = \Delta\delta_M(s). \tag{18}$$

$$A_{12} = \frac{-0.11 \cdot (9.81s + 620.973) - 0.42 \cdot (-9.81s - 10.006)}{A}, x_2 = \Delta\delta_V(s). \tag{19}$$

In Eq. (17), $G_{V/\delta M}(s)$ is the mathematical model of aircraft speed (a transfer function) depending on the fuel supply, $\delta_M(s)$ is the fuel supply, $G_{V/\delta V}(s)$ is a mathematical model of aircraft speed depending on the elevator angle, $\delta_V(s)$ is the aircraft elevator angle. The mathematical model of aircraft speed in the longitudinal direction, the fuel supply, and angle of attack can be determined, see [14]:

$$G_{V/\delta M}(s) = -a_x^{\delta M}\frac{\Delta_{11}}{\Delta}, G_{V/\delta V}(s) = -a_y^{\delta V}\frac{\Delta_{21}}{\Delta} - a_{mz}^{\delta V}\frac{\Delta_{31}}{\Delta}, \tag{20}$$

where $a^{\delta M}{}_x$ is a speed coefficient with respect to the fuel supply, $a^{\delta V}{}_y$ is a pitch coefficient with respect to the elevator angle, $a^{\delta V}{}_{mz}$ is the coefficient of the speed angle with respect to the elevator angle, $\Delta(s)$—a determinant of the transfer function, $\Delta_{11}(s)$, $\Delta_{21}(s)$, $\Delta_{31}(s)$—algebraic additions to the determinant $\Delta(s)$, see paragraph (Eq. (9)). The fuel supply transfer function (Eq. (17)) can be calculated using the following equation:

$$\begin{aligned}\Delta V_{V/\delta M}(s) &= G_{V/\delta M}(s) * \Delta\delta_M(s) \\ &= 5\frac{s^3 + 1.12s^2 + 62.782s + 25.32}{s^4 + 1.1338s^3 + 62.7975s^2 + 28.6585s + 4.09291}\Delta\delta_M(s).\end{aligned} \tag{21}$$

The transfer function of the elevator (Eq. (17)) is given by:

$$\begin{aligned}\Delta V_{V/\delta V}(s) &= G_{V/\delta V}(s) * \Delta\delta_V(s) \\ &= \frac{-0.11 \cdot (9.81s + 620.973) - 0.42 \cdot (-9.81s - 10.0062)}{s^4 + 1.1338s^3 + 62.7975s^2 + 28.6585s + 4.09291}\Delta\delta_V(s).\end{aligned} \tag{22}$$

4.2 Structure-defined mathematical model of the angle of aircraft attack in a flight simulator

From description angle of aircraft attack $\Delta\alpha(s)$, we can derive that the equation of angle of aircraft attack displacement defines a change aircraft throttle control (of fuel supply) and a change in the angle of aircraft elevator [10]:

$$\Delta\alpha(s) = -G_{\alpha/\delta M}(s)\Delta\delta_M(s) - G_{\alpha/\delta V}(s)\Delta\delta_V(s), \tag{23}$$

where stability determined by zeroes of a characteristic equation is used as a numerator in the structured mathematical model of aircraft motion; see [2]. Next, we define permutation and transformation with regard to (Eq. (16)) and have coefficients for $l_{21}(x)$:

$$A_{21} = 5\frac{0.002s^2 - 0.252s - 0.1}{A}, x_1 = \Delta\delta_M(s). \tag{24}$$

$$A_{22} = \frac{-0.11\cdot(-s^3 + 0.886s^2 + 0.0124s - 2.453) - 0.42\cdot(-s^2 - 0.414s - 0.025)}{A}, \tag{25}$$

$$x_2 = \Delta\delta_V(s).$$

The equations Eq. (18) and Eq. (24) will use a step change of throttle control stick (fuel supply) in Laplace transformation $\Delta\delta_M(s) = 1/s$. Eqs. (19) and (25) will use a step change of aircraft elevator control (angle of attack) in Laplace transform $\Delta\delta_V(s) = 1/s$. The problem statement of a mathematical model of motion in a flying simulator is conditioned by identification of its stability. The roots of the characteristic equation, the denominator equation (Eq. (18)), (Eq. (19)), (Eq. (24)) and equation (Eq. (25)), see [1].

In Eq. (17), $G_{\alpha/\delta V}(s)$ is the calculated mathematical model angle of aircraft attack (a transfer function) depending on the fuel supply, $\delta_M(s)$ is the fuel supply, $G_{\alpha/\delta V}(s)$ is the calculated mathematical model angle of aircraft attack depending on the angle of the elevator, $\delta_V(s)$ is the angle of the elevator. A mathematical model of an angle of aircraft attack in the longitudinal direction, fuel supply, and the angle of attack can be determined; see [14]:

$$G_{\alpha/\delta M}(s) = -a_x^{\delta M}\frac{\Delta_{12}}{\Delta}, G_{\alpha/\delta V}(s) = -a_y^{\delta V}\frac{\Delta_{22}}{\Delta} - a_{mz}^{\delta V}\frac{\Delta_{32}}{\Delta}. \tag{26}$$

The transfer function of fuel supply (Eq. (23)) can be calculated using the following equation:

$$\begin{aligned}\Delta\alpha_{\alpha/\delta M}(s) &= G_{\alpha/\delta M}(s) * \Delta\delta_M(s)\\ &= 5\frac{0.002s^2 - 0.2518s - 0.1}{s^4 + 1.1338s^3 + 62.7975s^2 + 28.6585s + 4.09291}\Delta\delta_M(s).\end{aligned} \tag{27}$$

$$\begin{aligned}&\Delta\alpha_{\alpha/\delta V}(s) = G_{\alpha/\delta V}(s) * \Delta\delta_V(s)\\ &= \frac{-0.11\cdot(-s^3 + 0.886s^2 + 0.0124s - 2.453) - 0.42\cdot(-s^2 - 0.414s - 0.025)}{s^4 + 1.1338s^3 + 62.7975s^2 + 28.6585s + 4.09291}\Delta\delta_V(s).\end{aligned} \tag{28}$$

5. Visualization of results of parallel simulation of mathematical models

Initial or limiting restricting conditions in the given flight phase affect the form of equations of the system depending on which phase of aircraft motion they are calculated [17]. Visualization of results has an impact on quality simulation and simulation

tries to obtain the information about the properties of a real system by means of an experiment, the so-called simulation model [18]. "Computer simulation of flying simulator is employed as enlargement or replacement of a structured mathematical model of aircraft motion for which an analytical solution is difficult of even impossible. [19]".

The sequential program of the mathematical model program is characterized by the equations of simulation of aircraft motion in a single computer time in equidistant moments. The disadvantage of this method is the limitation of the power of the processor, which calculates mathematical models of aircraft motion [20]. For presentation of more accurate simulation results, we need a higher-quality simulation system and a visualization generator providing artificial surrounding of required quality; this surrounding is a three-dimensional scene, see **Figure 3**.

The first term according to Eq. (17) or Eq. (23) represents the transfer function (structured mathematical model of aircraft motion) of speed displacement shift depending on the fuel supply of the aircraft and transfer function (structured mathematical model of aircraft motion) of the angle of attack depending on the aircraft fuel supply. In the polynomial expression of the transfer function, we derive the following form for the transfer function of increase in speed calculated from the change in fuel supply in meters per second and calculated displacement angle of attack shift depending on fuel supply in radians:

$$-G_{V/\delta M}(s)\Delta\delta_M(s) = -5\frac{s^3 + 1.12s^2 + 62.782s + 25.32}{A}\frac{M}{s}. \tag{29}$$

$$-G_{\alpha/\delta M}(s)\Delta\delta_M(s) = -5\frac{0.002s^2 - 0.252s - 0.1}{A}\frac{M}{s}. \tag{30}$$

If displacement of the speed is considered in Eqs. (29) and (30) and this is conditioned by the step of change in fuel supply (unit step).

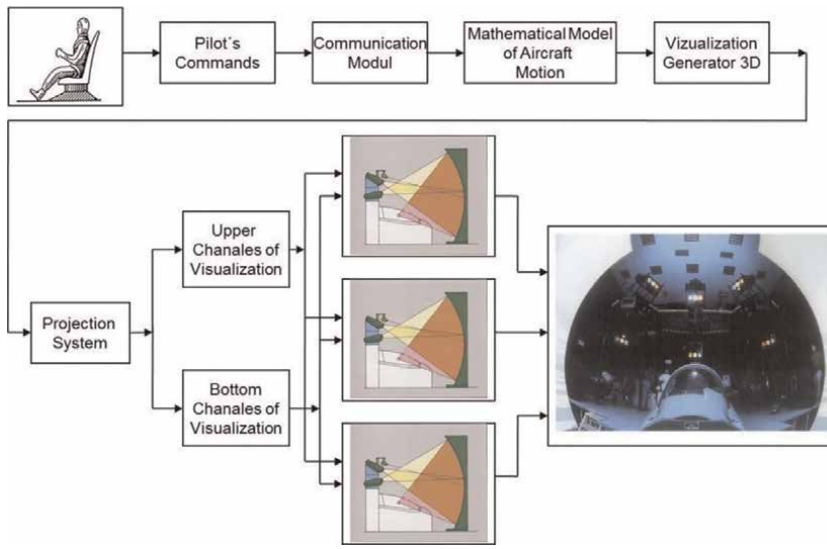

Figure 3.
Principle of a pilot's activity and its visualization in a projection system.

The second member according to Eq. (17) or Eq. (23) represents the transfer function of the speed increment depending on the angle of the aircraft elevator and represents the transfer function of the angle of attack depending on the angle of the aircraft elevator. In polynomial expression of the transfer function, we derive the following form for the transfer function of the increase in speed calculated from the change of aircraft elevator in meters per second and of calculated displacement of angle of attack from the aircraft elevator in radians:

$$-G_{V/\delta V}(s)\Delta\delta_V(s) = -\frac{-0.11\cdot(9.81s+620.973)-0.42\cdot(-9.81s-10.006)}{A}\frac{V}{s}. \quad (31)$$

$$-G_{\alpha/\delta V}(s)\Delta\delta_V(s) = -\frac{-0.11\cdot(-s^3+0.886s^2+0.0124s-2.453)-0.42\cdot(-s^2-0.414s-0.025)}{A}\frac{V}{s}. \quad (32)$$

The displacement of the elevation is considered in the Eq. (31) or Eq. (32) respectively, and this is conditioned by the step of elevator angle (unit step). The design and compilation of processes of a structured mathematical model of aircraft motion movement in the fuel supply to aircraft engines and angle of the aircraft elevator must be accurate. The simulation in our solution takes 30 s, and the intermediate data is sent in periodical time to the processor's core or node processing recorded simulated data and creating a graphical form of calculated results after the end of simulation.

5.1 Parallel simulation of a structure-defined mathematical model of an aircraft using MPI

The sequential program of a mathematical model program is characterized by the calculation of equations in a single computer time. The code operations are performed sequentially in that order. The disadvantage of this method is the energy consumption of the processor that counts the models [20]. The state of the art of parallel system based on the standard MPI can be introduced as the first one.

5.1.1 Principle of parallel message passing interface

The simulation parallel program computers in distributed computer systems are referred to as node computers [21]. They usually consist of a primary message input queue, one or more equivalent processors, and necessary equipment for communicate over the interconnectors. The threads operate in either serial or parallel modes.

The MPI facilitates this approach by providing many ways to call open-source industrial MPI implementations such as MPICH and LAM-MPI. The send/receive commands are implemented to change messages in the source code application and are added to run on nodes. We use two basic functions to send and receive messages [22]:

- MPI_Send (parameters)
- MPI_Recv (parameters).

5.1.2 The program application created using MPI

There are n nodes, which consist of the processor P_i and the local memory M_j. The nodes communicate with each other using lines and an interconnection network. When executing a given program, the program is divided into concurrent processes, each of which is executed in a separate processor. This simultaneous execution of the same task on multiple processors is used to obtain results faster.

Distributed architecture was realized as connection of five nodes: one is a central computer, and the others are computing nodes (**Figure 4**). One node (N_1) is designed as a central computer, and the others are computational nodes, and each of them computes only one mathematical model. The MPI provides alternative methods for communication and movement of data among multiprocessors. There is no global memory, it is necessary to move data from one local memory to another by means of message passing [23].

Where the *MPI_Send()* function on a side of the sender is responsible for sending messages. The corresponding *MPI_Recv()* function is inserted into a target process to receive messages. The simulation takes 30 seconds, and the intermediate data are sent in periodical time to the node that presents the received data in a graphical form.

5.1.3 The distributed modeling

The implementation MPICH2 is a portable, high-performance implementation of the entire MPI-2 standard and consists of a library of routines that can be called from the program. The TOOLKIT is an integrated set of tools that supports measurement, analysis, assignment, and presentation of application performance for sequential and parallel programs [24].

As follows from the expression, the structured mathematical model of aircraft defined by Eq. (18) $A_{11} * x_1$ is simulated by the computer N_2 on the second node, (Eq. (19)) $A_{12} * x_2$ is simulated by the computer N_3 on the third node, structured mathematical model of aircraft defined by Eq. (24) $A_{21} * x_1$ is simulated by the computer N_4 on the fourth node, and Eq. (25) $A_{22} * x_2$ is simulated by the computer N_5 on the fifth node.

From the graphical output of the central node, we get **Figure 5** as a result of the simulation. The simulation of a structured mathematical model of aircraft motion using a flight simulator cluster technology is done according to Eqs. (18) and (19) or Eqs. (24) and (25).

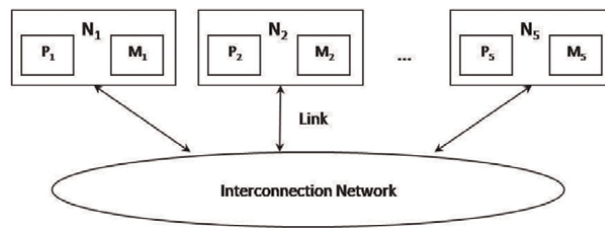

Figure 4.
Message passing interface – architecture, Ni – node-computer, Pi – processor, Mi – local memory.

5.1.4 Simulation results from MPI

The simulation results are in **Figure 5**, the upper left figure shows a graphical presentation of the aircraft speed increase depending on the fuel supply, and it is equal to 31.0192 [m/s], it is identical to the figure in **Figure 6**. The figure on the top right shows the aircraft speed increment depending on from the elevator, and it is equal to −15.6142 [m/s]. The figure at the bottom left shows a graphical representation of the increment angle of the aircraft attack depending on the fuel supply and is equal to −0.1237 [rad], it is identical to the presentation in **Figure 7**. The figure at the bottom right shows the increment angle of the pitch depending on the rudder and is equal to −0.0714 [rad]. The simulation time is set depending on the value of the integration error, which is less than 0.002 with these distributed simulation methods.

Modeling of the parallel aspect of the decomposed flight simulator subsystems in the form of mathematical notation was performed in accordance with Eqs. (18) and (19) or Eqs. (24) and (25). The strengths of this model are the combination of both the advantages: efficiency (memory savings) and ease of programming of a shared-memory method and scalability of a distributed-memory method.

5.2 Parallel simulation of a structure-defined mathematical model of an aircraft using GPU

Computer simulation a structured mathematical model of aircraft motion is used for modeling of aircraft characteristics in such cases [25]. The numerical integration

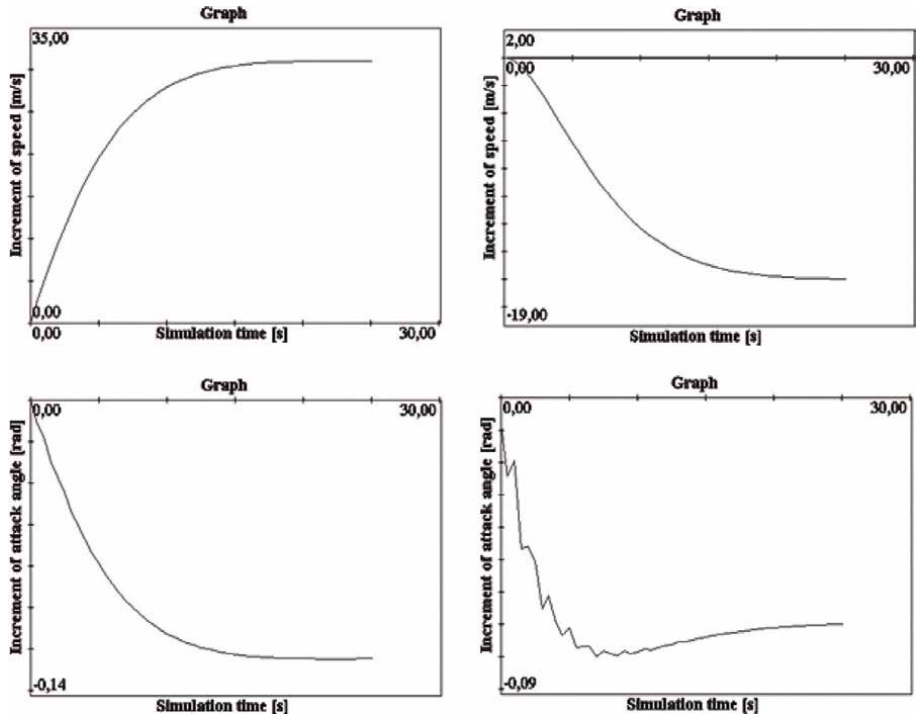

Figure 5.
Simulation results of (Eq. (18)) – upper left, (Eq. (19)) – upper right, (Eq. (24)) – bottom left, (Eq. (25)) – bottom right.

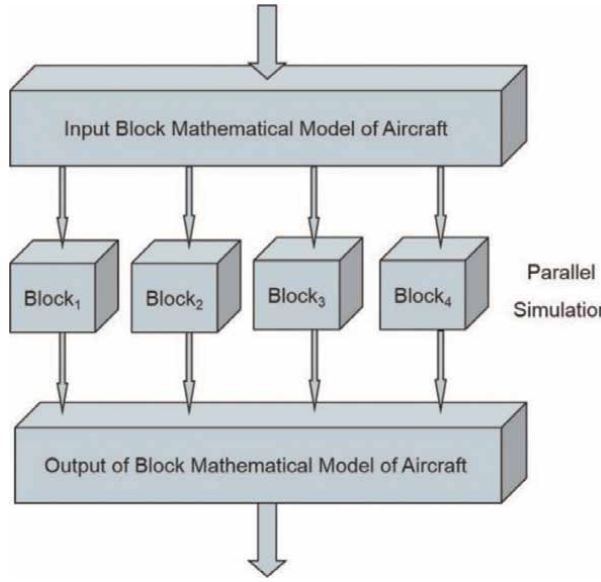

Figure 6.
A block diagram of simulation of a mathematical model of aircraft motion on the GPU computation.

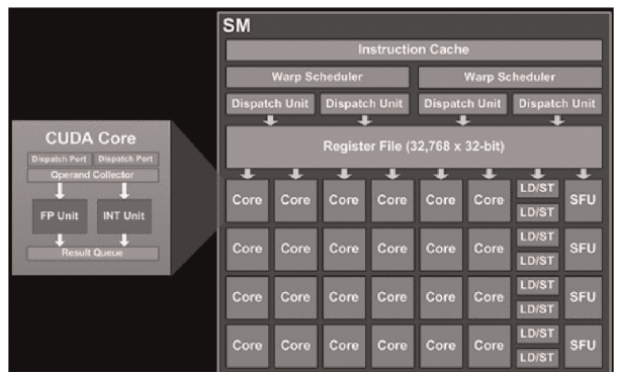

Figure 7.
GeForce 560 GPU block scheme of Streaming Multiprocessors (SM), Load (LD), Store (ST), Special Function Unit (SFU).

must be available in real time, in single computer time in equidistant moments. The above, two-parameter control of a block structured mathematical model of motion is performed by controlling the throttle lever of the engine and throttle rudder, which cause a change in the movement of the aircraft and the angle of attack of the aircraft. Parallel codes running on GPU hardware can yield results equivalent to the performance of dozens of traditional CPUs.

Input of block mathematical model represents control values of block structured mathematical model of aircraft motion—the fuel supply or the elevator angle. *Output of block mathematical model* represents simulated values of block structured mathematical model of aircraft motion—the speed or the attack angle. A given system can simulate multiple computers or processors. When several processors of a simulator system are connected ($Block_1$, $Block_2$, ..., $Block_n$), they communicate with each other via SMS; see **Figure 8**.

```
void ComputeFlightGPU (float* GPUc, float* GPUch, float* t)
{
        …
        // Part 1. Allocate memory device
        cudaMalloc ((void **) &GPUch, size);
        cudaMemcpy (GPUc, GPUch, size, cudaMemcpyHostToDevice);

        // Part 2. Kernel invokes code
        ...
        BlockSimulationModelGPU (float* GPUb, float* GPUm, float* t);
        ...

        // Part 3. Copy from the memory device
        cudaMemcpy (GPUc, GPUch, size, cudaMemcpyDeviceToHost);
        cudaFree (GPUch);
        …
}
```

Figure 8.
Outline of a revised host code ComputeFlightGPU ()

Control values of block structured mathematical models of aircraft motion—fuel supply and an aircraft elevator angle represent an input in a block diagram and an output in a block diagram, next figure.

5.2.1 Approach to CPU block mathematical model of an aircraft

The GPU blocks ($Block_1$, $Block_2$, ..., $Block_4$) count and each of them numerically counts only one block of the mathematical model of aircraft motion. According to our solution, the algorithm of the block structured mathematical model of aircraft motion is the most suitable for implementation in a GPU-enabled manner [2, 26].

In proposed solution, CPU system communicates with GPU by means of an SMS. The CPU is designed with fewer processor cores that have higher clock speeds, allowing them to complete series of tasks very quickly. The CPU is the brain of operation that is responsible for providing instructions to the rest of system. On the other hand, a GPU has much larger number of cores and is designed for a different purpose; it has parallel processing architecture that allows it to perform multiple calculations across streams of data simultaneously. The GPU has a massive parallel architecture consisting of thousands of smaller, more efficient cores [26].

5.2.2 Achievements of implementation of structure-defined mathematical models of an aircraft using CUDA

In our solution, the user can monitor the simulation process in real time using the GPU (**Figure 9**). Parallel simulation is one of the areas of simulation optimization and global optimization, which are implemented by the method of estimating the differences between continuous and discrete versions. The division of the structured mathematical model of aircraft motion into blocks is the motivation of this research with the definition of the relationships between the created blocks of the mathematical model.

```
__global_ void  BlockSimulationModelGPU (float* GPUc, float* GPUch, float* pResult)
{
        …
        // We set it to 2 threads per block, with 2 thread blocks per grid row
        int tid = (blockIdx.y * 2 * 2) + blockIdx.x * 2 + threadIdx.x ;
        // Each thread only multiplies one data element
        …

        pGPUch[tid] = SimModelGPU (pGPUc[tid], ptime) ;
}
```

Figure 9.
The CUDA kernel of BlockSimulationModelGPU() function.

The design of a block structure of mathematical model of aircraft motion is realized by various methods of simulation software systems, and one of them is CUDA computing. The application programming interface (API) improves computing performance with a graphics card for numerical calculation in simulations, and it is standardized layer that allows applications to take advantage of software or hardware services and features. The CUDA includes C/C++ software development tools, function libraries, and a hardware abstraction mechanism that hides the GPU hardware from developers [22].

5.2.3 Basic software solution of computation on the GPU

The *ComputeFlightGPU (…)* function is essentially an outsourcing agent that sends input data to the device, activates the execution of the simulation on the device, and collects the results from the device [28]. To perform a simulation of a block structure mathematical model of aircraft motion on a GPU core, the programmer musts allocate the required memory by calling the *cudaMalloc (…)* function on the device. To transfer the relevant data from the host memory to the allocated device memory, we call *cudaMemcpy (…)* function, see **Figure 10**—Part 1.

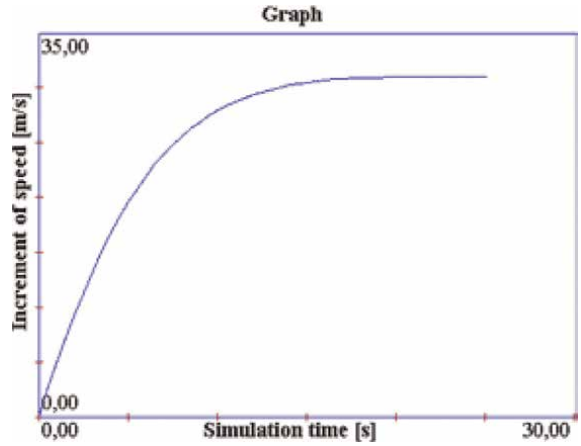

Figure 10.
Screenshot of simulation results based on (Eq. (18)), horizontal axes – time, vertical axes – speed increment.

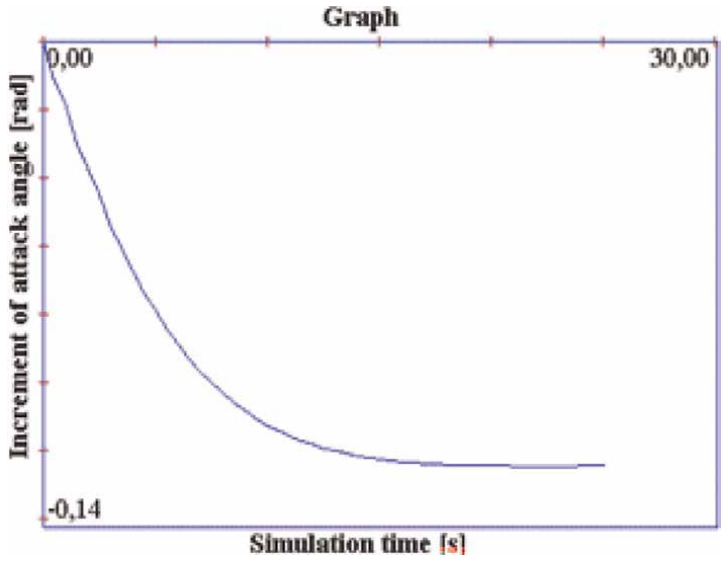

Figure 11.
Screenshot of simulation results based on (Eq. (24)), horizontal axes – time, vertical axes – angle of attack increment.

After completing the simulation, the programmer must transfer results from the device memory back to the host memory by calling function *cudaMemcpy (…)* and free the device memory by calling function *cudaFree (…)*, see **Figure 10** – Part 3. The CUDA kernel provides API simulation functions running as programmer-defined functions [27]. This core function determines the function of the block structure mathematical model of aircraft motion to be performed by all threads during the parallel simulation phase, see **Figure 10**—Part 2.

Parallel programming in C/C++ supports a CPU computer and the GPU card supports programming in C [28]. The inner loop in the CUDA implementation disappears, because the *ComputeFlightGPU* calculation is performed in parallel by CUDA threads, see previous figure. Our presented solution was simulated on a personal computer that consists of a CPU Intel Quad Core Q9650 processor with 4 cores, 3.00 GHz each, cache 12 MB L2, bus speed 1333 MHz (FSB), 4GB RAM DDR3, and GPU accelerator NVIDIA GeForce GTX 560 Ti.

The first thing to notice is the *__global__* keyword, see **Figure 11**. This simply means that this function can be called either from host computer or the CUDA device. Each thread runs the same block mathematical model of aircraft motion, so the only way to differentiate yourself from other threads is to use their *threadIdx* and your *blockIdx* [29].

The index in the thread array is calculated and determined by the block and thread ID. Each thread uses its own *threadIdx.x* and *threadIdx.y* to identify the elements of a block mathematical model of aircraft **motion** defined by the system of equations (Eq. (17)) and (Eq. (**23**)). The expression *blockIdx.y* × *2* × *2* equals the number of threads in all grid rows above the current thread position. The expression *blockIdx.x* × *2* equals the number of all columns in the current grid row. Finally, *threadIdx.x* equals the number of threads above the current block.

The function *BlockSimulationModelGPU()* calculates a unique ID in the *Idx* register variable, which is then used as an identifier in the array and in the aircraft motion simulation calculation model.

5.2.4 Simulation results from CUDA

As follows from the expression, the block of the structured mathematical model of the aircraft is defined by Eq. (18) $A_{11} * x_1$ and is simulated by the GPU block $Block_1$, the block structure of the mathematical model of the aircraft is defined by Eq. (24) $A_{21} * x_1$ and is simulated by the GPU block $Block_2$. From the obtained graphical output, **Figures 6** and 7, which are the results of the numerical integration of the block structure of the mathematical models of aircraft motion.

Graphically, the course of **Figure 6** shows the increase in aircraft speed as a function of fuel delivery not exceeding 31.0174 [m/s]. **Figure 7** shows the angle of increment of the aircraft attack as a function of the change in the position of the rudder, at which it does not exceed −0.1247 [rad].

The CUDA memory model consists of different memory spaces, which differ significantly in latency times [30]. Results from comparing of the simulation of block structured mathematical model of aircraft motion on the CPU and on the GPU are in **Table 1**.

In the number of block mathematical models column, the number means the number of block structure of mathematical model of aircraft motion simulated in parallel. The times achieved from the measurement of the simulation of mathematical aircraft models on the CPU are in CPU runtime column and on the GPU in the GPU runtime column. The last column is the acceleration of the calculation on the GPU compared on the CPU.

The table shows the performance acceleration obtained by simulating a different number of block structured mathematical models of motion of aircraft. The columns show the number of block mathematical models, the CPU run time, GPU run time, and acceleration. Decreasing the simulation speed of a block structure of mathematical models of aircraft motion on the GPU with an increasing number of simulated mathematical models is caused by an increasing the time required to read or retrieve data from or to the host computer.

This subchapter presents GPU calculation and CUDA programming with an explanation of how to implement an efficient GPU application. The subchapter aims to offer data obtained by simulating the block structure of a mathematical model of aircraft motion using the GPU. Even a non-optimized parallel implementation of the block structured mathematical model of aircraft motion on the GPU can lead to a significant reduction in computational time compared with the implementation to the CPU.

Number of block mathematical models	CPU Runtime [ms]	GPU Runtime [ms]	Speed-Up
1	1,60	0,07	22,72
2	3,10	0,14	22,01
5	7,08	0,33	21,74
10	13,82	0,65	21,22
20	25,37	1,24	20,44
50	47,39	2,37	20,02

Table 1.
The performance obtained from simulation different members of the mathematical models of aircraft motion.

6. Conclusions

The results from simulation help to overcome the physical and architectural limitations of computational power that can be achieved with a single-processor system. It is then very convenient for the application to use a more powerful processor, a faster cache, and faster access to the RAM with higher transfer capacity. The results obtained in the simulation of structured mathematical models of aircraft motion and the use of this method appear to be effective and pragmatic according to the requirements of the integration algorithm given in the chapter.

In general, in accordance with the proposed solution, it is also possible to run the program faster due to factors such as the availability of better bandwidth for communication within node. Greater bandwidth provides additional communication with the interface to transfer message between nodes and the higher performance of the graphics processing unit.

The described design of a structured mathematical model of aircraft motion to perform simulation on the GPU, this simulation was chosen as an example of an algorithm confirming the proposed solution. The presented problem of simulation methods of block structure of mathematical models of aircraft motion was solved by predetermined known procedures. The advantages of the methods are a combination of both the features: the efficiency of computer system programming and the scalability of a GPU computational method.

Based on knowledge gained in design of the block structure of mathematical models of aircraft motion, we can say that the graphics card can be used in multiple and parallel simulation, which confirms high speed of computations. The advantage of faster simulation can sometimes be obtained at the earliest defined quality. These facts and accuracies are well suited for use in real-time simulation and a virtual reality imaging system. The results of the simulation of such designed structured mathematical model of aircraft motion show very fast calculation and confirm the effectiveness of such a structure of the mathematical model of aircraft for the proposed system of the simulator, which was the motivation of our research.

Acknowledgements

The part of solving the chapter was supported by the Slovak Grant Agency for Science, by the VEGA 4/0330/09 grant.

DOI: http://dx.doi.org/10.5772/intechopen.105538

Author details

Peter Kvasnica
Alexander Dubcek University of Trencin, Trencin, Slovak Republic

*Address all correspondence to: peter1.kvasnica@gmail.com

References

[1] Kvasnica P. Visualization of aircraft longitudinal-axis motion. Computing and Informatics. 2014;**33**(5): 1168-1190

[2] Kvasnica I, Kvasnica P. Accuracy of mathematical models in simulator distributed computing. Computer Modeling in Engineering and Sciences. 2015;**107**:6

[3] Raeth PG. Parallel MATLAB using standard MPI implementations. In: Proceedings of High Performance Computing Modernization Program Users Group Conference (HPCMP-UGC). 2010. pp. 438-441

[4] Duncan SH, Gordon PL, Zaluska EJ, Edwards SI. Parallel Processing in High Integrity Aircraft Engine Control. Berlin: Springer-Verlag; 1994

[5] Blakelock JH. Automatic Control of Aircraft and Missiles. New York: John Wiley & Sons. Inc; 1991

[6] McCormic BW, Papadakis MP. Aircraft Accident Reconstruction and Litigation. New York: John Wiley & Sons. Inc; 2003

[7] Chapman B, Jost G, Van der Pas R. Using OpenMP - Portable Shared Memory Parallel Programming. Massachusetts, USA: The MIT Press; 2007

[8] Composite authors, Applied mathematics, Part II (in Czech). Praha, Czech Republic: SNTL; 1978. pp. 1158–1161, 1193

[9] Bajborodin JV. Board Systems of Navigation Control (In Russian). Moskva, Russia: Transport; 1975

[10] Rolfe JM, Staples KJ. Flight Simulation. Cambridge, USA: Cambridge University Press; 1986

[11] Cellier FE, Kofman E. Continuous System Simulation. Basic Principles of Numerical Integration. New York: Springer; 2006. pp. 25-32

[12] Driels M. Weaponeering Conventional Weapon System Effectiveness. USA: McGraw-Hill Inc; 2004. p. 155

[13] Clark RN. Control System Dynamics. 2nd ed. New York: Cambridge University Press; 2005

[14] Krasovskij AA. Automatic Systems Control of Flight and Their Analytic Designing (In Russian). Moskva, Russia: Nauka; 1980

[15] Lazar T, Adamčík F, Labún J. Modelling Characteristics of the Aircraft Control (In Slovak). Slovak Republic: University of Technology Košice; 2007

[16] Tereshenko V, One tool for building visual models. Proceedings of Computational Intelligence, Modelling and Simulation, 2009. CSSim '09. International Conference in Brno, Czech Republic; 2009. pp. 59-62

[17] McCormic BW. Aerodynamics, Aeronautics and Flight Mechanics. 2nd ed. New York: John Wiley & Sons, Inc; 1995

[18] Yuan M, Baker J, Brews F, Neiman L, Meilander W. An efficient associative processor solution to a traffic control problem. In: Parallel and Distributed Processing, Workshops and Phd Forum (IPDPSW), 2010 IEEE International Symposium, Atlanta, USA. 2010. pp. 3-8

[19] Stevens BL, Levis FL. Aircraft Control and Simulation. USA: John Wiley & Sons, Inc.; 2003

[20] El-Rewini H, Abd-El-Barr M. Advanced Computer Architecture and Parallel Processing. New York, USA: John Wiley & Sons, Inc.; 2005

[21] Martincová P, Grondžák K, Zábovský M. Programming in Kernel of Operating System Linux. Slovak Republic: University of Žilina; 2008

[22] Huges C, Huges T. Parallel and Distributed Programming Using C++. The Safari Press; 2003

[23] Mmpich2. MPICH2 is a high performance and widely portable implementation of the Message Passing Interface (MPI) standard. [Internet]. 2009. Available from: http://www.mcs.anl.gov/mpi/mpich2 [Accessed: November 08, 2014]

[24] Chevance RJ. Server Architectures: Multiprocessors, Clusters, Parallel Systems, Web Servers and Storage Solution. Burlington, USA: Elsevier; 2005

[25] Adhianto L, Banerjee S, Fagan M, Krentel M, Marin G, Mellor-Crummey J, et al. HPCTOOLKIT: Tools for performance analysis of optimized parallel programs. Concurrency Computatation: Practical Experience. 2010, 2010;**22**:685-701

[26] Garland M, Le Grand S, Nickolls J, et al. cuda parallel programming model. IEEE Micro. 2008;**28**:13-27

[27] Kvasnica I, Kvasnica P. Application of CUDA computing principles in automatic flight control simulation. In: Proceeding 8th EUROSIM Congress on Modelling and Simulation, "EUROSIM 2013". Cardiff, Wales, United Kingdom. 2013. pp. 528-543

[28] Pena AJ, Reano C, Federico S, et al. A complete and efficient CUDA-sharing solution for HPC clusters. Parallel Computing. 2014;**40**:574-588

[29] Farber R. CUDA Application Design and Development. Elsevier: Morgan Kaufmann; 2011

[30] Kvasnica P. A comparing simulation results of a structure defined mathematical model of aircraft. Archives of Electrical Engineering. 2017;**66**(4): 867-878

Chapter 8

Modeling and Simulation of APU Based on PEMFC for More Electric Aircraft

Jenica-Ileana Corcau, Liviu Dinca and Ciprian-Marius Larco

Abstract

The current challenge in aviation is to reduce the impact on the environment by reducing fuel consumption and emissions, especially NOX. An open research direction to achieve these desideratums is the realization of new electric power sources based on nonpolluting fuels, a solution being constituted using fuel cells with H_2. Reducing the impact on the environment is aimed at both onboard and aerodrome equipment. This paper proposes the simulation and analysis of an auxiliary power source APU based on a fuel cell. The auxiliary power source APU is a hybrid system based on a PEM-type fuel cell, a lithium-ion battery, and their associated converters. The paper presents theoretical models and numerical simulations for each component. The numerical simulation is performed in MATLAB/SimPower Sys. Particular attention is to the converter system that adapts the parameters of the energy sources to the requirements of the electricity consumers on board the MEA-type aircraft. Power management is performed by a controller based on fuzzy logic.

Keywords: auxiliary power source, hybrid source, nonpolluting fuels, Dc to Dc converter

1. Introduction

Aeronautics has become an important tool for economic growth, leading to an overall increase in demand for air transport services. This increase is accompanied by operational hazards, adverse environmental effects, and unsustainable operating expenses. Air transport is estimated to carry more than 2.2 billion passengers a year and the current fleet of commercial aircraft will be doubled by 2050. In addition, the demand for air transport is expected to increase by 4–5% per year over the next 20 years. This projected increase in aeronautics has significant effects on the global environment. Noise, local air quality, and climate change are one of the key areas to be addressed in aeronautics and their impact on the environment [1–3] (**Figure 1**).

The expected annual growth rate of 4.7–4.8% over the next 20 years in air transport would mean that, in the future, aeronautics could have a greater negative impact on the environment. The challenge will be for more aircraft to operate longer, but to have a lesser negative impact on the environment compared to the current situation. This

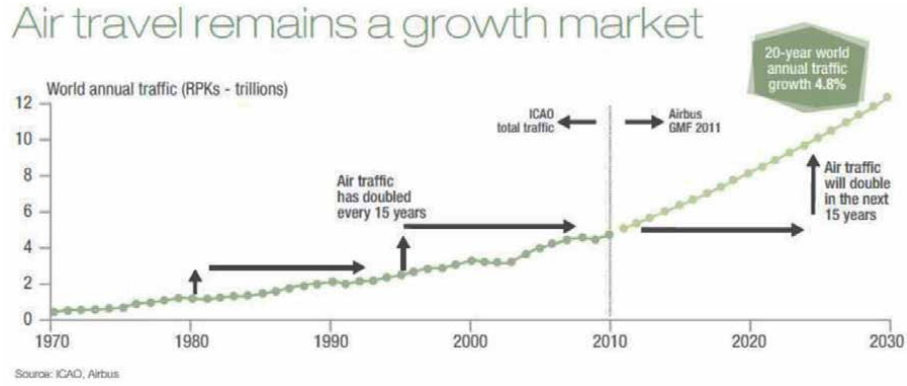

Figure 1.
The evolution of air travel [2].

is how the project Advisory Council for Aeronautics Research in Europe (ACARE) became a priority, which has the following objectives: besides the year 2000, there exists a 50% reduction in the noise level, there is also a reduction in CO_2 emissions per passenger kilometer of 50%, and an 80% reduction in NOx emissions too. All these factors do not affect just the operation way of the aircraft but the design and the construction of the aircraft too. An essential role in improving the air traffic, determined by the following conditions: more efficient aircraft, efficient engines, and the improvement of air traffic management, was detected by ACARE [4, 5]. To achieve the conditions above, new technologies in order to fulfill key functions on the aircraft are introduced, with the review of the entire system of aircraft architecture being required. Nowadays, conventional civil aircraft is characterized by four different secondary energy distribution systems: mechanical, hydraulic, pneumatic, and electrical. This involves a complex onboard power distribution network and a necessity for adequate redundancy of each. To reduce this complexity and improve efficiency and reliability, the aircraft manufacturers' trend is toward the concept of More Electric Aircraft (MEA) and All Electric Aircraft.

Recently, with the increase in fuel costs and the emphasis on greener aircraft technologies, there has been a particular emphasis on the design and production of more MEA (More Electric Aircraft). An aircraft with all electrically powered secondary power systems can be considered an All Electric Aircraft (AEA). Nowadays, MEA aircraft use electricity in the drive systems of aircraft subsystems, which were previously powered by pneumatic, hydraulic, or mechanical power systems, including flight control systems, air conditioning, anti-icing, and various other small systems. **Figure 2** shows the evolution over time of the electrical system on board aircraft [6]. In modern electrical systems, various voltage values are preferred, which consist mainly of the four voltage classes: 235 V VF (variable frequency), 115 VAC CF (constant frequency), 28 VDC, and ± 270 VDC. Many electricity distribution units are also needed to supply electricity to aircraft. Such systems further reduce the mass by reducing the size of electrical wiring [6–11].

The goal of the MEA concept is to replace nonelectric power with electrical energy. This idea was first applied to military aircraft. Over time, the issue of implementing this concept for civil aircraft has also been raised. The rapid development of power electronics has led to a flexible transmission of electricity from sources to loads. Power electronics are used throughout the electrical system, including power

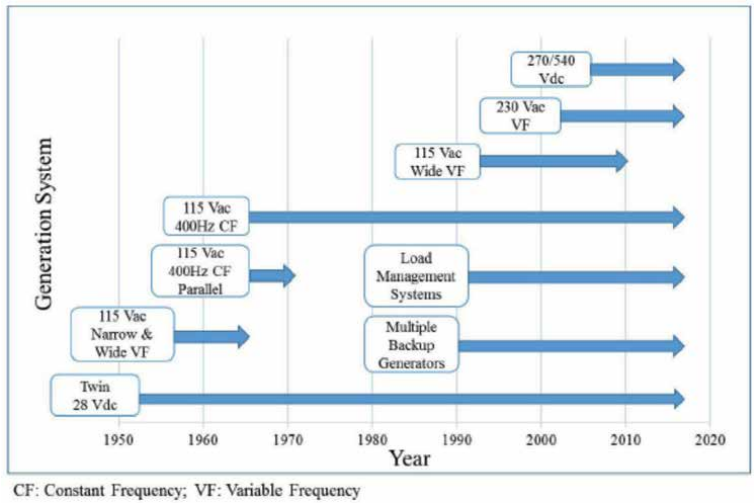

Figure 2.
Electric generation systems' evolution.

generation, conversion, and distribution. The trend in the construction of such complex electrical power systems on aircraft is to obtain more and more efficient subsystems and integrate them into the energy system of the aircraft. This can reduce design costs as well as design time.

The use of high-power electric motors and the addition of new loads have greatly increased the demand for power. In addition, the increase in household load on transport aircraft by almost 500 W per passenger and on entertainment by almost 100 W per seat has reached a total of up to 350 kW for a transport aircraft, which is also added to the power demand.

It is well known that several aircraft incorporate MEA models; however, it is widely acknowledged that the two programs, which have really integrated the MEA concepts, are the Boeing 787 and Airbus A380 commercial aircraft [6]. These aircraft are characterized by intensive electrification because loads such as the Environmental Control System-ECS (for B787) and electro hydrostatic flight control actuators (for A380) are powered. As a result, their power generation capacity is an order of magnitude larger than all other aircraft. Both the B787 and the A380 have replaced the traditional generating system that uses the Integrated Drive Generator-IDG with Variable Frequency Generator-VFG coupled directly to the motors. The B787's main power generation is based on four 250 kVA VFGs (two for each main engine), while the A380 uses four 150 kVA VFGs (one for each engine) [6].

The transition to a more electric architecture, the adaptation of energy-efficient engines and the rigorous use of lightweight composite materials bring the contribution to a substantial reduction in B787's operating costs compared to its predecessor, B767-300/ER. Especially (based on airline data), the reduction in block hourly operating costs is around 14% [6].

The increasing pressure to reduce fuel consumption, noise emissions, and pollution, along with the new requirements for aircraft operating systems, has led directly to the search for new cleaner technologies, so the fuel cells have great potential. To increase efficiency, flexibility, and interoperability, aeronautics engineers have made great efforts in recent years to make the transition from pneumatically and hydraulically

operated systems to electrical systems. Due to the increasing consumption of electricity during the flight, conventional electric generators have undergone a change, becoming larger and more powerful to compensate for the excess energy needed for the flight [12].

Several studies have shown that the conventional auxiliary power unit (APU) plays an important role in aircraft pollution emissions. This has led to the replacement of fuel cell APUs, with special focus on proton exchange membrane fuel cells (PEM-FC) and solid oxide fuel cells (SOFCs). By using this technology, the ecological efficiency can be increased, knowing that these fuel cells do not pollute the environment. Eco-efficiency is one of the main goals of the aerospace industry. First, a "green" aircraft saves the money for the airlines, due to the forecasts of the increase in the fuel prices in the future; second, environmental pollution will become a growing problem for human society. Therefore, the importance of reducing emissions is not only affected by financial reasons. During ground operations, auxiliary power sources, classic APUs, or turbogenerators (TGs) as they are also known in the literature, generate electricity used for the automatic start of aircraft engines, thus resulting in pollution gases. Much of the emissions from airports are produced by these auxiliary turbo-generators. In the future, airlines will have to pay taxes for polluting emissions from airports, according to European Union regulations.

The use of fuel cells in aircraft has attracted the attention of the aeronautics industry, they have formed working groups for the direct development of lines using fuel cell systems for civil aircraft applications. The Society of Auto Engineers (SAE) has collaborated with the European Organization for Civil Aeronautics Equipment (EUROCAE) In 2008, to form the WG80/AE 7AFC Working Group, this group contributed to the support and development of hydrogen fuel cells for large civil aircraft, through standardization and certification. The WG80/AE 7AFC Group has implemented two standard documents to support the use of PEMFC systems [12, 13].

The first document was published in 2013, and it provides basic information on the use and installation of hydrogen PEMFCs on board aircraft for the purpose of generating auxiliary power without the use of separate ground supply systems [12]. And the second document followed 4 years later in 2017, which defined technical guidelines for testing, integration, validation, certification, and development in a secure environment of PEMFC systems for high-capacity civil aircraft, including storage and the distribution of fuel, and the integration of electrical systems in aircraft. In 2015, US Federal Aeronautics Administration of the US Department of Transportation funded The Fuel Cells-Energy Supply Aeronautics Rulemaking Committee. This team concentrates on the use of PEMFCs and SOFCs. The principal objective of this team is to reduce and even eliminate the uncertainties surrounding the safety and application of hydrogen fuel cells in commercial aircraft [12–16].

Here, this chapter discusses the simulation and analysis of an auxiliary power source APU based on fuel cells. The following sections dealt in detail with fuel cell, modeling of APU based on the fuel cell with its simulation, and, finally, with the energy management system that can be used successfully for the applications with the high pulsed loads and transient power requirements.

2. Fuel cell

Hydrogen will become the raw material for various industries such as petrochemicals, amino acids, methanol, hydrogen peroxide, the food industry, and the transportation industry. But due to its high calorific value, research continues to find new uses. In the

1960s, the hydrogen engine was designed to launch missiles. In 1968, the first model to appear in the United States was launched.

This technology will facilitate the success of the Ariane rocket and is considered a forerunner of the hydrogen energy era.

The electrochemical conversion, i.e., the direct, nonpolluting, and silent transformation of the chemical energy contained in a wide variety of substances, into electrical energy is an alternative direction of obtaining electricity. A class of devices in which this conversion takes place is fuel cells.

After the Volta battery was built, it was used by Nicholson and Carlisle to decompose water into hydrogen and oxygen, and by Davy in 1807 to decompose alkalis. Daniel and Faraday continued their brilliant experiments in these new energy sources in the first half of the last century. Although the first fuel cell was invented in 1839 by WR Grower, the evolution of these devices did not take place until the 1960s, because of the development of space programs and especially after 1980 when programs for the implementation of "clean" technologies were imposed in the production of electricity. The fuel cell is a galvanic cell in which the free energy of a chemical reaction is converted into electricity. In the case of a conventional fuel cell, which runs on hydrogen and oxygen, the reaction that takes place is:

$$H_2 + \frac{1}{2}O_2 \rightarrow H_2O. \quad (1)$$

The reaction, a chemical combustion, takes place in a cell composed of two electrodes separated by an electrolyte and takes place in a temperature range between 70 and 1000°C. Whatever the types of batteries studied, the general principle remains the same **Figure 3**. Only the electrolyte, electrodes, and temperature change. There are currently 5 types of cells, **Table 1**.

PEMFC and SOFC have a much longer lifespan than other types of batteries, much more compactness, moderate cost, and offer interesting long-term prospects. Unlike PEMFC, SOFC is a very underdeveloped type of fuel cells. Having a solid electrolyte, like the first one, it is differentiated by the level of the operating temperature: between 650 and 1000°C. This feature gives it a higher resistance to impurities and especially an overall efficiency (electrical + thermal) of the order of 80%, due to the high-temperature level and heat dissipation that allow recovery in combined cycles.

High-temperature fuel cells offer other advantages, already used in fixed installations; we can mention a few generators delivered by Rolls-Royce, especially in North America. In fact, the large manufacturer has recently set up a specialized

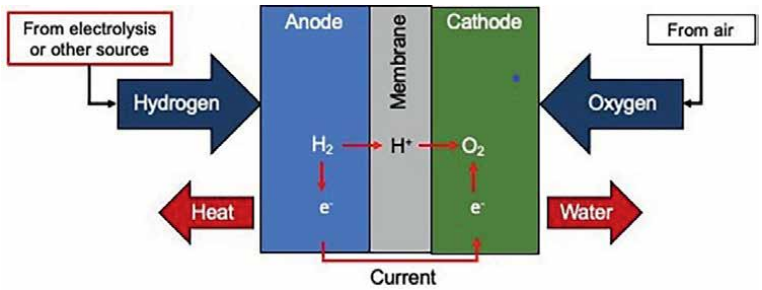

Figure 3.
Schematic diagram of a fuel cell [17].

Cell type	Electrolyte	t[°C]	Field of use
Alkaline (AFC)	Potassium (liquid)	80	in space, transportation Range: 1–100 kW
Polymer acid (PEMFC and DMFC)	Polymer (solid)	80	Portable and stationary applications, transportation Range: 1 W–1 MW
Phosphoric acid (PAFC)	Phosphoric acid (liquid)	200	Stationary applications, transports Range: 200 kW – 10 MW
Liquefied carbonate (melted) (MCFC)	Melted salts (liquid)	650	Stationary applications Range: 500 kW–10 MW
Solid oxides (SOFC)	Ceramic (solid)	700–1000	Stationary applications, transports Range: 1 kW–10 MW

Table 1.
Types of fuel cells.

subsidiary of Rolls-Royce Fuel Cell Systems Ltd. (RRFCS) and will develop a specialized research Centre at the University of Genoa, Italy. This industrialization will lead to a sharp reduction in the cost of the elements of a high-temperature fuel cell. In the short term, these applications will focus on auxiliary generating sets (APUs) for land vehicles, but also for aircraft. Boeing has adopted this solution for its future 777 model. APU-FC ensures the generation of electricity with a level of safety that allows the elimination of hydraulic systems, thus bringing a gain in terms of weight and a reduction in energy required for engine systems, which translates into a reduction in consumption of the order of 15%.

3. Auxiliary power source based on the fuel cell

The proposed auxiliary power source contains the following energy sources: Proton Exchange Membrane (PEM) fuel cells, battery system, DC to DC boost converter connected to the PEMFC output terminals, DC to DC boost converter connected to the battery package, DC to DC Buck converter used for providing the charging/discharging path between the PEMFC and battery, as in **Figure 4**.

The dynamic characteristics of the two types of power sources make the hybrid power system more complicated. Therefore, it is essential, very important, and necessary to ensure efficient energy management. Energy management strategies determine the allocation of power between different energy sources and promote the energy efficiency and life of the hybrid power system. The energy stored in the battery systems offers a double benefit, keeping the life of the fuel cell and obtaining a better dynamic response to load variation. The goals of this hybrid configuration are presented in detail in [15].

3.1 Modeling of PEMFC

A PEM fuel cell stack model was chosen from the MATLAB/Simulink, SimPowerSystems (SPS) Toolbox library. The MATLAB/Simulink model implements a generic hydrogen fuel cell stack. The model has two options: a simplified model and a detailed model.

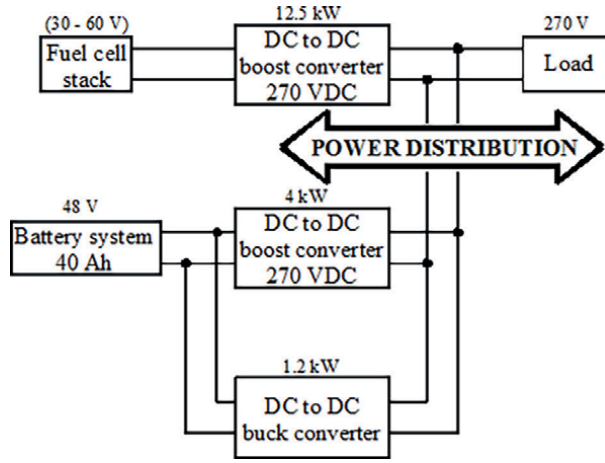

Figure 4.
Block diagram of hybrid fuel cell/battery.

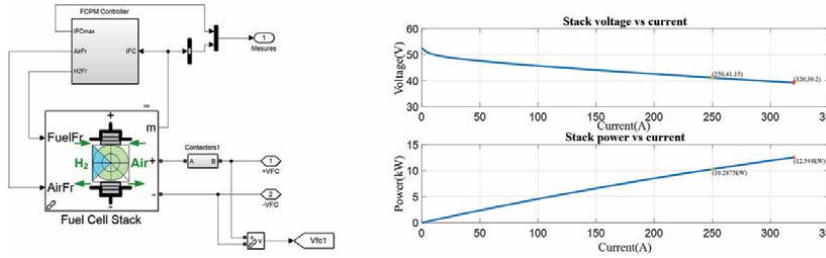

Figure 5.
The dynamic behavior of a PEMFC.

The simplified model shows a particular fuel cell stack operating at nominal conditions of temperature and pressure. **Figure 5** presents the dynamic behavior of a PEMFC and **Table 2** shows fuel cell model parameters. The stack is supplied by liquid hydrogen and compressed air [15].

3.2 Modeling of batteries

The batteries chosen in order to realize this study are lithium-ion types as they have proved to exhibit a high energy density and efficiency in comparison to other battery types like lead-acid, NiCd, or NiMH. This makes them more attractive for aircraft applications. The battery output voltage is given by [15].

$$V_{batt} = E_0 - K\frac{Q}{Q - \int idt} - R{\cdot}i + Aexp\left(-B\int idt\right) \tag{2}$$

where i is the battery current [A], E_0 is the battery constant voltage [V], K is the polarization voltage [V], A is the exponential zone amplitude [V], Q is the battery capacity [Ah], B is the exponential zone time constant inverse $[Ah]^{-1}$, $\int idt$ is the actual battery charge [Ah], R is the internal resistance [Ω], and V_{batt} is the battery no load voltage [V].

Fuel cell model input parameters	
The voltage at I = 0A and I = 1A [V_0(V), V_1(V)]	[52.5, 52.46]
The current and the voltage at nominal operating point [*Inom*(A), *Vnom*(V)]	[250, 41.15]
The current and the voltage maximum operating point [*Iend*(A), *Vend*(V)]	[320, 39.2]
Number of cells	[65]
Nominal stack efficiency (%)	[55]
Operating temperature (Celsius)	[45]
Nominal Air flow rate (lpm)	[732]
Nominal supply pressure [Fuel (bar), Air (bar)]	[1.16,1]
Nominal composition (%) [H2 O2 H2O(Air)]	[99.95, 21,1]

Table 2.
Fuel cell parameters.

The characteristics of the chosen battery are presented in **Figure 6** and the parameters of the above model are shown in **Table 3**. The state-of-charge (*SOC*) of the battery is between 0 and 100%. The *SOC* is calculated as

$$SOC = 100\left(1 - \frac{Q \cdot 1.05}{\int idt}\right) \tag{3}$$

3.3 Modeling of a DC-to-DC converter

Relying on load profile, APU consists of the following: 12.5 kW (peak), 30–60 V PEM (Proton Exchange Membrane) FCPM – Fuel Cell Power Module, with nominal power of 10 kW; 48 V, 40 Ah, lithium-ion battery system; 12.5 kW fuel cell DC to DC boost converter, with regulated output voltage and input current limitation; two DC

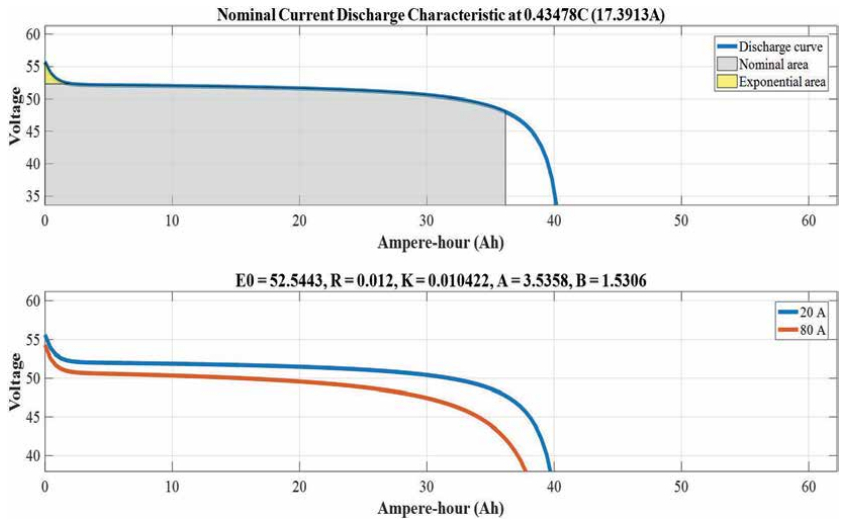

Figure 6.
The dynamic behavior of a battery.

Battery model input parameters	
Maximum capacity (Ah)	[40]
Cut-off Voltage (V)	[36]
Fully charged voltage (V)	[55.8714]
Nominal discharged current (A)	[17.3913]
Internal resistance (Ohms)	[0.012]
Capacity (Ah) at nominal voltage	[36.1739]
Exponential zone [Voltage (V), Capacity (Ah)]	[52.3, 1.96]

Table 3.
Battery parameters.

to DC converters for discharging (4 kW boost converter) and charging (1.2 kW buck converter) the battery system.

Two classical types of DC-to-DC converters are selected for the proposed hybrid battery/fuel cell system (**Figure 4**) to stabilize the output profile of the auxiliary power source system. During transient conditions, the battery supplies electric power for the essential loads on the aircraft electric network until PEM-FC warms up. Moreover, the fuel cell is the one that provides all requested power for the essential loads when the synchronous generator is shut down. Therefore, the DC-to-DC converter of the battery must ensure a bidirectional flow. The battery system during transitional periods provides electric power to the emergency loads, so the converter operates in the boost mode, increasing the output voltage to its standard value at 270 VDC using a feedback control system.

The DC-to-DC boost converter controls the fuel cell. Bi-directional DC to DC boost converter controls the battery. These converters are also output voltage regulated with current limitations. The fuel cell DC to DC converter system is 30–60 V DC input, 270 V DC, 9.2 A output. The battery DC to DC converter system includes 2, 40–58.4 V DC input, 270 V DC, 7 A output, and these DC to DC isolated boost converters are connected in parallel. Alongside 1, 240–297 V DC input, 48 V DC, 20 A output, DC to DC isolated buck converter. The converters used in this study contain the average value model.

Figure 7 shows DC to DC boost converter model realized in Simulink/SimPowerSystems (SPS) [15].

3.4 Power management strategy of APU based on fuel cell

The most common schemes presented in the literature include the following techniques: the state machine control strategy, the rule-based fuzzy strategy, the classical PI control strategy, and the equivalent consumption strategy ECMS [18–25].

The energy management strategy is designed based on: keeping the fuel cell lifetime by avoiding an insufficient supply of reactants (fuel cell starvation); the fuel cell current slope of 40A/s; fuel cell power: $Pfcmin$ = 1 kW and $Pfcmax$ = 10 kW; battery power: $PBattmin$ = 1.2 kW and $PBattmax$ = 4 kW [15]; also, in order to operate the battery system efficiently, it is requested always keeping the battery SOC above 40%. The fuel cell power is caused by the battery state of charge and the required load power ($Pload$). The bus voltage is stabilized through the battery converters for energy management system strategies. The output of the algorithm is the reference for the

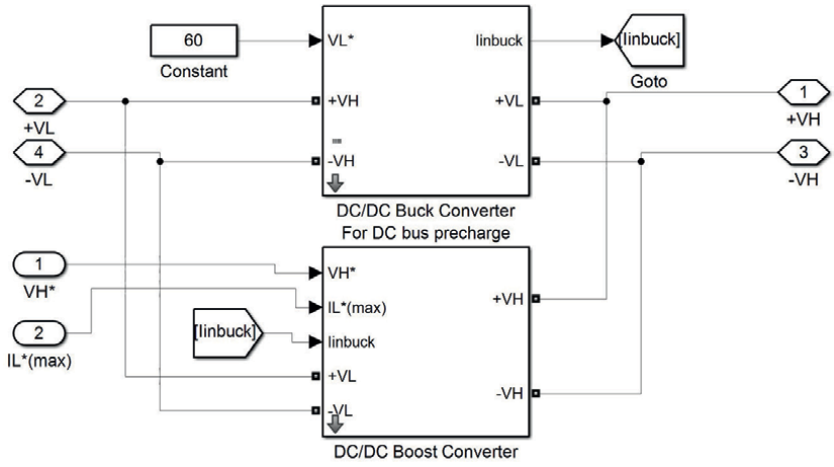

Figure 7.
DC to DC converter model in Simulink/SimPowerSystems (SPS).

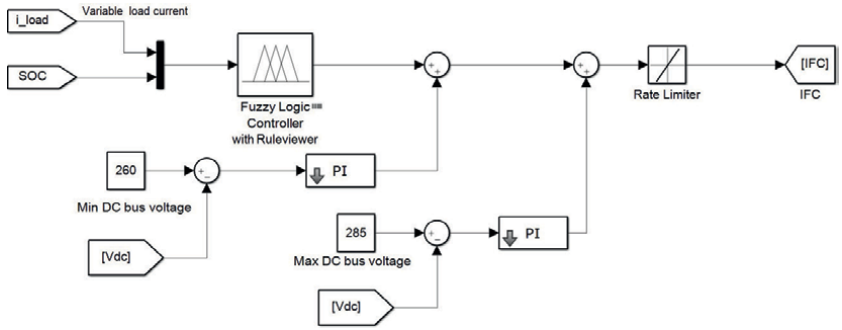

Figure 8.
Schematic of the power management strategies [15, 26].

fuel cell power, as it can be seen in **Figure 8**. This quantity relative to the fuel cell voltage and from the efficiency of the DC-to-DC converter has resulted in the value of the fuel cell reference current [15, 26]. A detailed description of the controller based on fuzzy logic is presented in [15, 26].

4. Implementation in MATLAB/Simulink APU based on fuel cell

Figure 9 shows the simulation scheme made in MATLAB/Simulink. It contains the sources, converters, and the source management system. The performance management scheme proposed in this paper was tested by numerical simulations. The energy management system block outputs the control signals required by DC-to-DC converter. The fuel cell power is identified by the battery state of change and the required load power (*Pload*). The bus voltage is stabilized through the battery converters for energy management system strategies. The management system was tested using an electric load profile, presented in the **Figure 10**. **Figure 11** shows the time variations of the voltage and current of the fuel cell, **Figure 12** shows the time variations of the voltage and current of the converter related to the fuel cell, and **Figure 13** shows the

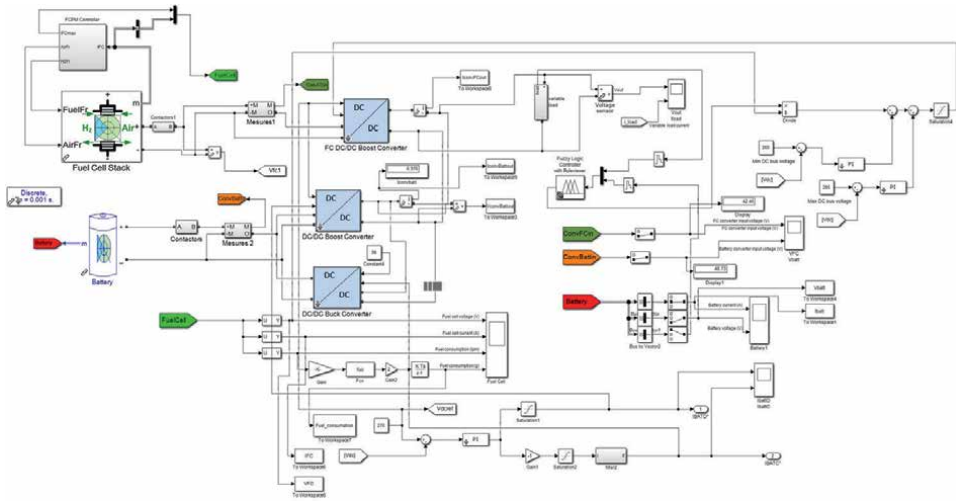

Figure 9.
The APU based on fuel cell model in MATLAB/Simulink.

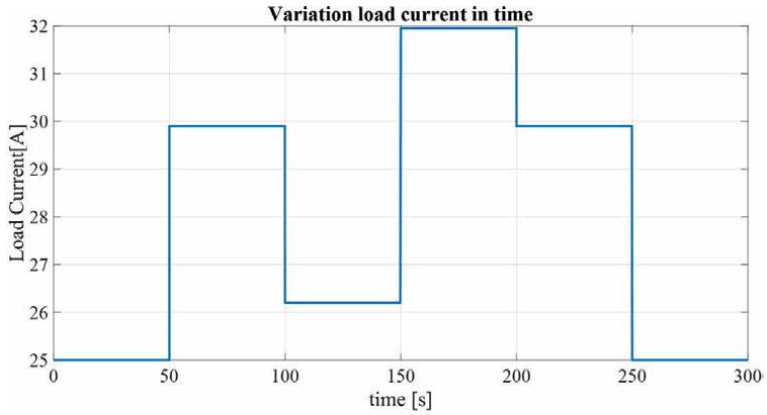

Figure 10.
Load profile used in numerical simulations.

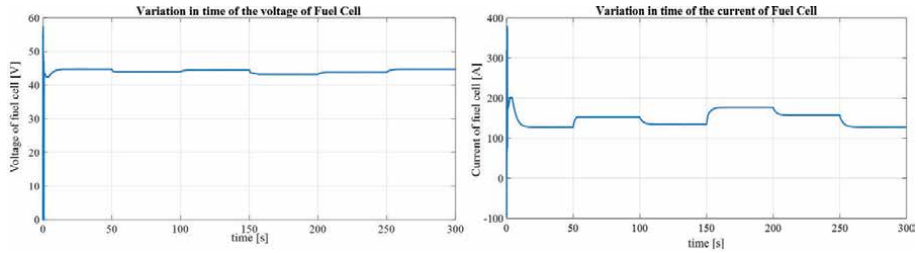

Figure 11.
Variation in time of the voltage and current corresponding to the output terminals of fuel cell.

time variation of fuel consumption. **Figure 14** shows the time variations of battery voltage and current, and **Figure 15** shows the time variations of battery converter voltage and current.

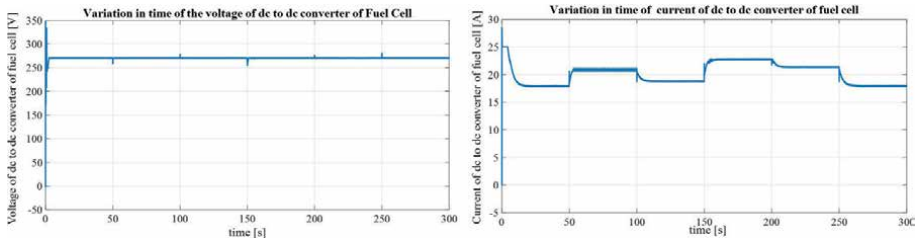

Figure 12.
Variation in time of the voltage and current of DC-to-DC converter connected to the fuel cell.

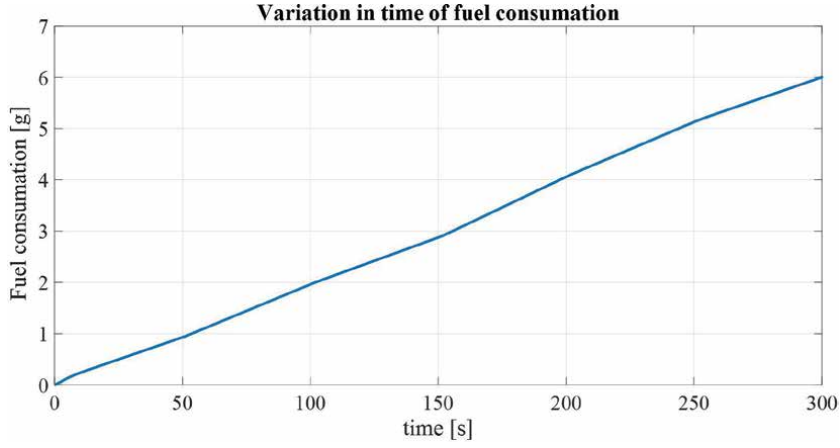

Figure 13.
Variation in time of fuel consumption.

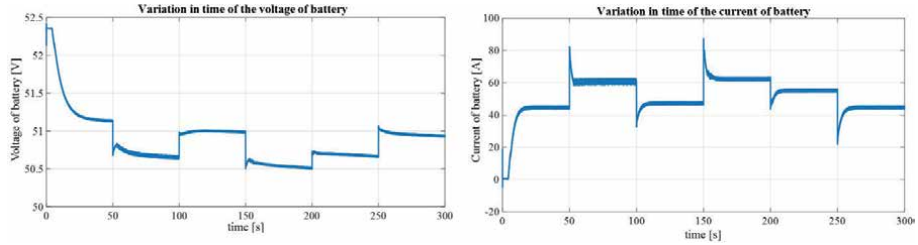

Figure 14.
Variation in time of the voltage and current corresponding to the output terminals of a battery.

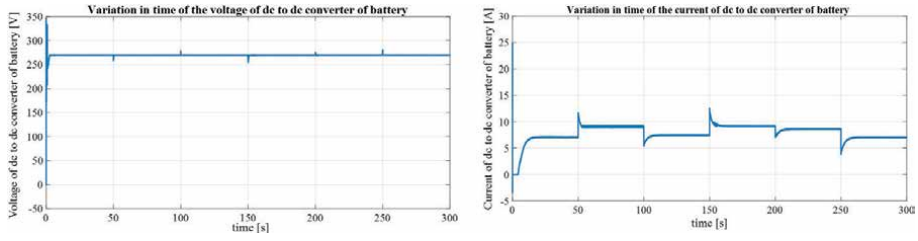

Figure 15.
Variation in time of the voltage and current of DC-to-DC converter connected to the battery.

5. Conclusions

Several studies have shown that classical APU plays an important role in pollution emissions. This has led to the search for new cleaner technologies, so fuel cells have great potential. Major aircraft manufacturers have shown great interest in replacing conventional auxiliary power sources with auxiliary power sources based on fuel cells. In this paper, an auxiliary power source based on the PEM-type fuel cell is proposed. This hybrid source contains fuel cells, batteries, converters, and source management system. The results obtained from the numerical simulation of the proposed auxiliary power source show that it offers a higher peak power than each individual component while maintaining a power density, which is vital for an aircraft. It is also observed on time variations of the battery and battery output currents that the power flow is well managed between the fuel cell and the battery. Another advantage of the hybrid power source is that during the process of starting and transient charging of the system the battery will reliably support the electrical network of the aircraft. The slow performance of the PEM fuel cell during start-up/charge/discharge operations is offset by the fast battery dynamics. If the charging power is subject to sudden changes, the battery is the one that responds immediately so that the electrical system remains in normal operating conditions.

The energy management system proposed in this paper can be used successfully for the applications with high pulsed loads and transient power requirements.

Acknowledgements

Source of research funding in this article: Research, program of Electrical, Energetic and Aerospace Engineering Department financed by the University of Craiova and Military Technical Academy "Ferdinand I".

Author details

Jenica-Ileana Corcau[1*], Liviu Dinca[1] and Ciprian-Marius Larco[2]

1 Department of Electrical, Energetic and Aerospace Engineering, University of Craiova, Romania

2 Department of Aviation, Integrated Systems and Mechanics, Military Technical Academy "Ferdinand I", ATM, Bucharest, Romania

*Address all correspondence to: jcorcau@elth.ucv.ro

References

[1] Seresinhe R. Impact of aircraft systems within aircraft operation: A MEA trajectory optimization study [PhD thesis]. School of Aerospace, Transport and Manufacturing Centre for Aeronautics Aerospace Engineering Division; 2014

[2] AIRBUS DELIVERING THE FUTURE. Global market Forecast 2011-2030, Blagnac Cedex, France, 2011

[3] Waitz I et al. Report to the United States Congress—Aeronautics and the Environment—A National Vision Statement. In: Framework for Goals and Recommended Actions. 2004

[4] Clean Sky. Aeronautics & Environment. Clean Sky. 2013. Available from: http://www.cleansky.eu/content/homepage/aeronautics-environment

[5] ICAO. Aeronautics statistics & data: A vital tool for the decision making process. In: ACI Airport Statistics and Forecasting Workshop London. 2011

[6] Vincenzo M, Giangrande P, Galea M. Electrical power generation in aircraft: Review, challenges, and opportunities. IEEE Transactions on Transportation Electrification. 2018;**4**:646-659

[7] Corcau JI, Dinca L. Onboard Electrical Systems for "More Electric Aircraft". Craiova, Romania: Publishing SITECH; 2014

[8] Emandi A, Ehsani M. Aircraft power systems: Technology, state of the art and future trends. IEEE AES Systems Magazine. 2000;**15**:28-32. DOI: 10.1109/62.821660

[9] Maldonado MA, Shah NM, Cleek KJ, Walia PS, Korba GJ. Power management and distribution system for a more-electric aircraft (MADMEL) – program status. In: Proc. of 32nd Intersociety Energy Conversion Engineering Conference. 1997. pp. 274-279. DOI: 10.1109/IECEC.1997.659198

[10] Weimer JA. Past, present & future of aircraft electrical power systems. In: 39th AIAA Aerospace Sciences Meeting & Exhibit, Nevada. 2001

[11] Moir I. More-electric aircraft-system considerations. In: IEE Colloquium. 1999. pp. 1-9. DOI: 10.1049/ic:19990839

[12] Fernandes MD, Andrade ST, Bistritzki VN, Fonseca RM, Zacarias LG, Goncalvesc H, et al. SOFC-APU systems for aircraft: A review. International Journal of Hydrogen Energy. 2018;**43**:16311-16333

[13] EUROCAE/SAE WG80/AE-7AFC. Hydrogen Fuel Cells Aircraft Fuel Cell Safety Guideline AIR6464 [Online]. 2013. Available from: https://doi.org/10.4271/AIR6464

[14] EUROCAE/SAE WG80/AE-7AFC. Installation of Fuel Cell Systems in Large Civil Aircraft AS6858. 2017. Available from: https://doi.org/10.4271/AS6858

[15] Corcau J, Dinca L. Fuzzy energy management scheme for a hybrid power sources of high-altitude pseudosatellite. In: Modelling and Simulation in Engineering. 2020

[16] Corcau J, Dinca L, Adochiei I, Grigorie TL. Modeling and simulation of an aerodrome electrical power source based on fuel cells. In: The 7th IEEE International Conference on E-Health and Bioengineering. 2019

[17] Available from: https://en.wikipedia.org/wiki/File:Hydrogen_fuel_cell_schematic.jpg;

[18] Aschilean I, Varlam M, Culcer M, Iliescu M, Raceanu M, et al. Hybrid electric powertrain with fuel cells for a series vehicle. Energies. 2018;**11**(1294):1-12. DOI: 10.3390/en11051294

[19] Motapon S, Dessaint LA, Al-Haddad KA. A comparative study of energy management schemes for a fuel-cell hybrid emergency power system of more-electric aircraft. IEEE Transactions on Industrial Electronics. 2014;**61**:1320-1334

[20] Thounthong P, Chunkag V, Sethakul P, Sikkabut S, Pierfederici S, Davat B. Energy management of fuel cell/solar cell/supercapacitor hybrid power source. Journal of Power Sources. 2011;**196**:313-324

[21] Motapon SN. Evaluation of energy management schemes. In: Design and Simulation of a Fuel cell Hybrid Emergency Power System for a More Electric Aircraft, Montreal. 2013

[22] Zhang X, Liu L, Dai Y. Fuzzy state machine energy management strategy for hybrid electric UAVs with PV/fuel cell/battery power system. International Journal of Aerospace Engineering. 2018:1-17. DOI: 10.1155/2018/2852941

[23] Bradley TH. Modeling, design and energy management of fuel cell systems for aircraft [PhD dissertation]. Georgia: Georgia Institute of Technology, School of Mechanical Engineering; 2008

[24] Jeong KS, Lee WY, Kim CS. Energy management strategies of a fuel cell/battery hybrid system using fuzzy logics. Journal of Power Sources. 2005;**145**(2):319-326. DOI: 10.1016/j.jpowsour.2005.01.076

[25] Savvaris A, Xie Y, Malandrakis K, Lopez M, Tsourdos A. Development of a fuel cell hybrid-powered unmanned aerial vehicle. In: 2016 24th Mediterranean Conference on Control and Automation (MED), Athens, Greece. 2016. pp. 1242-1247

[26] Corcau JI, Dinca L, Grigorie TL, Tudosie AN. Fuzzy energy management for hybrid fuel cell/battery systems for more electric aircraft. In: 1st International Conference on Applied Mathematics and Computer Science (ICAMCS), Rome. 2017

Section 6

Aviation

Chapter 9

Role of Human Factors in Preventing Aviation Accidents: An Insight

Kamaleshaiah Mathavara and Guruprasad Ramachandran

Abstract

Flight is one of the safest modes of travel even today. However, nearly 75 percent of civil and military aviation accidents around the globe have been attributed to human errors at various levels such as design, drawing, manufacturing, assembly, maintenance, and flight operations. This paper traces the civil aviation accidents that have occurred during the last eight decades and brings out the vital factors leading to the disaster by considering a few representative cases. The concept of human factors is introduced, and the various models that have been in use to understand the root causes leading to aviation accidents are presented. An example of the application of human factors analysis and classification system (HFACS) framework is narrated. It is found that majority of recent civil aviation accidents have occurred during the landing and approach phases, and it is possible to minimize the accidents by suitably maintaining situational awareness. Considering the growth of air traffic that is expected to double in the next 10–15 years, the role of human factors in preventing aviation accidents is even more relevant. A new model for human factors is proposed. Way forward to even safer skies is presented.

Keywords: human factors, aviation accidents, pilot fatigue, aircraft maintenance, crew resource management, air traffic control, aircraft inspection, work pressure, safety management system, aviation safety, SHEL model, Swiss-cheese model, PEAR model, dirty dozen, HFACS, seven-segment model

1. Introduction

Man has been fascinated by the flight of birds since the time immemorial. The science of flight from dream to reality was realized by Wright brothers in the year 1903. It was the first instance in the history of aviation that a powered, sustained, and controlled flight of airplane under the control of the pilot was achieved. One can see the tremendous progress made by man in the field of aviation in a short span of about 120 years; from small two-seat ab-initio trainer aircraft such as Cessna 152, to the large wide-body aircraft such as the Airbus A380 and the Boeing 777x, capable of carrying hundreds of passengers at transonic speeds, and Concorde, the first supersonic passenger-carrying commercial airplane.

Aircraft design and production encompass diverse areas such as aerodynamics, flight mechanics and controls, material science, power plant, landing gear and hydraulics, electrical and avionics, stress analysis, vibration, manufacturing techniques, special processes, nondestructive testing, metrology, quality control, assembly, integration, static testing, flight testing, certification aspects, and so on. A set of drawings that provide unambiguous and complete information to manufacture the aircraft is the starting point. It is through these drawings that the ideas of the designer are conveyed to the manufacturer. Manufacturing drawings are further translated into a set of "process sheets" by specialists in methods engineering, and these provide a step-by-step procedure in a lucid manner to the shop floor technicians to execute the work. Likewise, airplane flight manual and quick reference handbooks are made available to the flight test crew. Aircraft maintenance manuals contain clear information about periodic procedures to be adhered to, while carrying out aircraft maintenance activities.

To err is human. It is quite possible that human errors, in some form or the other, can creep into design, manufacturing, flight operation, and maintenance phases in the aviation sector. The error may go unnoticed due to various reasons and can result in catastrophic accidents endangering precious lives of passengers and crew. Nearly 75 percent of civil and military aviation accidents around the globe have been attributed to human errors at various levels. It is, therefore, pertinent to go through the aircraft accident databases available in open literature and bring out the vital factors leading to the disaster.

Aircraft designs have evolved over a period of time, as a result of the lessons learnt from the past accidents and incidents. This is also true when we consider corresponding improvements to airport infrastructure and maintenance facilities. It was during the early 1970s that the discipline of human factors began to draw the attention of international aviation community. Pioneering work has since then been done in the field of human factors to understand why aircraft accidents happen. Human factor models have also undergone continual improvements and adaptations to suit the ever-growing needs of air traffic.

Aviation accident database available in open literature has been used in the current work. Human factor analysis models currently in use have been studied. A new model for human factors analysis is proposed, keeping in view the likely improvements in aircraft designs and potential growth in air traffic in the years to come.

This book chapter is organized as follows. To begin with, summary of civil aviation accidents that have occurred during the last eight decades is presented. This is followed by a few representative case studies to bring out the root cause of the accident. The concept of human factors is introduced, along with brief description of various models in use, to understand the root causes leading to aviation accidents. An example of the application of human factors analysis and classification system (HFACS) framework is narrated. A new "seven-segment" concept is proposed to systematically analyze human factors. Way forward to even safer skies is presented.

2. Civil aviation accidents during the last eight decades

According to Federal Aviation Administration (FAA), an aircraft accident is defined as an occurrence associated with the operation of an aircraft, which takes place between the time any person boards the aircraft with the intention of flight and all such persons have disembarked, and in which any person suffers death or serious injury, or in which the aircraft receives substantial damage [1]. Incident refers to

an occurrence other than an accident, associated with the operation of an aircraft, which affects or could affect the safety of operation; occurrence is an abnormal event, other than an incident or accident. Until an event (for example, low-speed abort) can be identified as an incident, it is regarded as an occurrence. An aviation accident is defined by the Convention on International Civil Aviation Annex 13 as an occurrence associated with the operation of an aircraft, which takes place from the time any person boards the aircraft with the intention of flight until all such persons have disembarked, and in which a) a person is fatally or seriously injured, b) the aircraft sustains significant damage or structural failure, or c) the aircraft is missing or is completely inaccessible [2].

The first fatal accident involving a powered aircraft was the crash of a Wright aircraft at Fort Myer, Virginia, in the United States on September 17, 1908, injuring its co-inventor and pilot, Orville Wright, and killing the passenger, Signal Corps Lieutenant Thomas Selfridge [3]. Orville later determined that the crash was caused by a stress crack in the propeller. The Wrights soon redesigned the Flyer to eliminate the flaws that led to this accident.

Table 1 summarizes the number of fatal civil airliner accidents from 1945 through February 2022 [4]. At 864, United States is the country with the highest number of fatal civil airliner accidents, followed by Russia, Canada, Brazil, and Colombia. At 43, Argentina has the least fatalities.

Figure 1 shows the distribution pattern of the number of civil aircraft accidents from the year 1918 through 2022 [5]. **Figure 2** shows the distribution pattern of the number of fatalities for the same period. A total of 28,442 aircraft accidents have resulted in 1,58,798 fatalities. Maximum peak is observed during 1940s, and there is a gradual decrease in the number of accidents from the year 1978. Considering the period between 2001 and 2022, a total of 3769 aircraft accidents have resulted in 20,172 fatalities. Fitting a linear trend line for the data between 2001 and 2022 would indicate a theoretical possibility of aircraft accidents tending to near-zero by mid 2040s.

Apart from potential fatalities, aircraft accidents may result in partial damages to the airframe, or even complete loss of hull, making the aircraft non-airworthy. A recent example is the fatal accident of a domestic passenger aircraft Boeing 737-89P on March 21st, 2022 in China with 123 passengers and nine crew members onboard [5]. The aircraft, whose file photo is shown in **Figure 3**, was scheduled to fly from Kunming to Guangzhou, but plunged midflight and crashed in Wuzhou, in the Guangxi region. All the 132 persons onboard the aircraft were killed in the accident, and the aircraft fully destroyed by the impact. Accident investigation is on. Black boxes of this aircraft are found in a severely damaged condition, making data retrieval a challenge by itself. According to media reports, a preliminary assessment by the US officials has ruled out any mechanical or technical faults with the aircraft, and the aircraft is suspected to have been intentionally put into a nose-dive [6].

On May 29, 2022, a Twin Otter aircraft operated by Tara Air was on a scheduled domestic flight from Pokhara Airport to Jomsom Airport, Nepal. The aircraft lost contact with air traffic controllers about 12 minutes after take-off and crashed in mountainous Mustang district of Nepal, killing all the 19 passengers and three crew members. Black box of the aircraft has been retrieved and accident investigation is ongoing.

In addition to fatalities, as many as 81 aircraft are reported to have gone missing and remain untraced till date [7]. According to a report released by Boeing [8], in the early days of flight, approximately 80 percent of accidents were caused by the machine and 20 percent were caused by human error. The trend has since then

Sl. No.	Country/Region	Number of fatal Accidents
1	USA	864
2	Russia	539
3	Canada	191
4	Brazil	190
5	Colombia	184
6	UK	110
8	Indonesia	106
7	France	105
9	Mexico	102
10	India	95
11	China	76
12	Venezuela	69
13	Italy	68
14	D. R. Congo	66
15	Ukraine	64
16	Bolivia	62
18	Germany	62
17	Peru	61
19	Philippines	61
20	Spain	56
21	Australia	51
22	Atlantic Ocean	51
23	P. N. Guinea	49
24	Kazakhstan	45
25	Argentina	43

Table 1.
Countries/regions with the highest number of fatal civil airliner accidents since 1945.

reversed, and now approximately 80 percent of the airplane accidents are caused due to human error (pilots, air traffic controllers, mechanics, etc.) and the remaining due to equipment failures. According to an analysis of 75 fatal airplane accidents carried out [9], over 70 percent of the accidents involved pilot factors mostly related to poor judgment and decision-making.

3. Case studies

Typical life cycle of an aircraft can broadly be classified into three stages. The first stage comprises activities covering design and manufacturing, signaling its "birth." Second stage comprises "active flying years" during which the aircraft is put into operational service. The aircraft is maintained in fully airworthy condition by

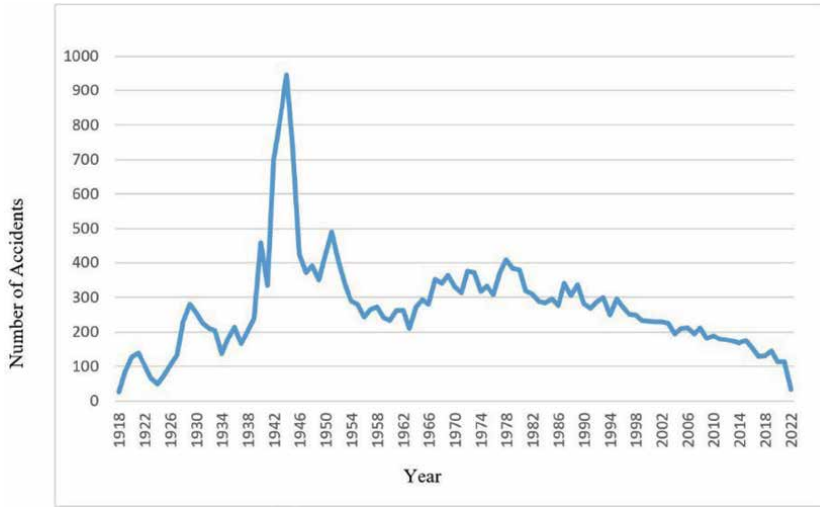

Figure 1.
Distribution pattern of civil aircraft accidents from 1918 through 2022.

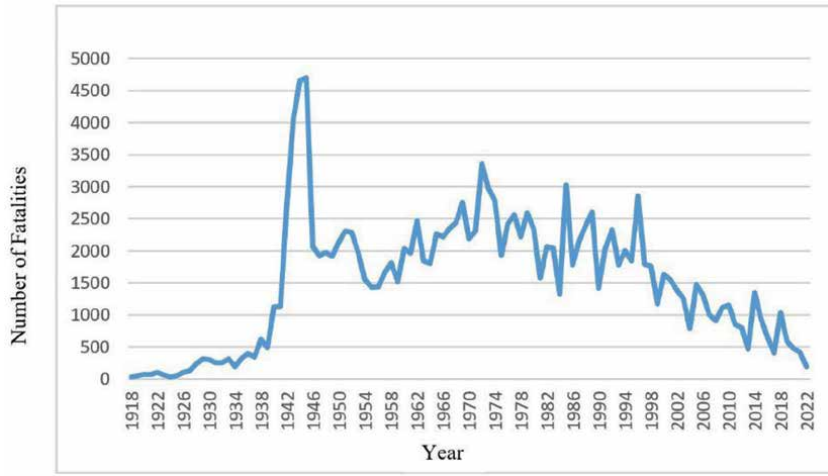

Figure 2.
Distribution pattern of civil aircraft accident fatalities from 1918 through 2022.

following approved Maintenance, Repair, and Overhaul (MRO) procedures. Once the aircraft completes its intended service life, it is eventually grounded or phased out and sent to boneyards. This corresponds to the third stage.

Some of the valuable components are dissembled from the aircraft and depending on their technical condition, are inspected, repaired or overhauled by approved facilities in the aerospace sector, prior to reuse in other aircraft. Some of the retired aircraft find their way into educational institutions or museums for display.

Aircraft accidents can be attributed to one or more of a combination of causes identifiable in the above three stages and usually comprise human factors and technical failures. Generally, occurrences due to experimental test flights, terrorism, hijacking, sabotage, and direct military action are not considered for analysis of airplane

Figure 3.
File photo of Boeing 737-89P aircraft B-1791. (photo credits: CWong, https://www.jetphotos.com/photo/10528109).

accidents. Analysis of the data from aviation accidents throws light on several vital factors that eventually resulted in respective accidents. Let us look at a few typical examples of aircraft accidents from history. Statistical analysis and summary of commercial aviation accidents for the last 60 years are documented in [10, 11].

3.1 Crash of a Boeing 707-321C airplane

A Boeing 707-321C airplane crashed on May 14th, 1977, in Zambia, Africa, [12]. The accident occurred in daylight and in good weather, and on approach to landing, killing all the six people onboard. The complete right-hand horizontal stabilizer and elevator assembly of the aircraft had separated from the aircraft during flight and was found 200 meters behind the aircraft wreckage. Subsequent investigation of the fractured horizontal stabilizer revealed that the accident was caused by a loss of pitch control following the in-flight separation of the right-hand horizontal stabilizer and elevator as a result of a combination of metal fatigue and inadequate failsafe design in the rear spar structure. Shortcomings in design assessment, certification, and inspection procedures were contributory factors.

3.2 Crash of a Boeing 747: 200 freighter

A Boeing Model 747–200 freighter (El Al Flight 1862) crashed on October 4th, 1992 during climb out from Schiphol Airport, Amsterdam, Netherlands [13]. All four people onboard as well 43 others on the ground were killed in the accident. The aircraft experienced the separation of both engines from the right wing (inboard engine 3 and outboard engine 4), resulting in loss of control of the aircraft and subsequent crash. Subsequent investigation revealed that the inboard engine and strut (engine 3)

had separated from the wing and impacted the outboard engine (engine 4). The lessons learnt from this crash led to changes in the strut design philosophy across the aerospace industry.

3.3 Crash of an airbus 380: 842 airplane

An Airbus 380–842 Qantas Flight 32 suffered significant damages due to engine failure on November 4th, 2010, minutes after taking off from Changi Airport, Singapore, on a scheduled passenger flight to Sydney, Australia [14]. The flight carried 469 passengers and crew. Pilots managed to land the aircraft back at Changi Airport and there were no reported injuries to the passengers and crew onboard. Accident investigation revealed that the probable cause of engine failure was a manufacturing error involving an internal oil feed pipe. The oil feed pipe was manufactured with a reduced wall thickness that eventually cracked and resulted in the accident.

3.4 Crash of a Boeing 747 SR-100 aircraft

A Boeing 747 SR-100 flight 123 operated by Japan Airlines crashed on August 12th, 1985 when flying from Tokyo-Haneda to Osaka [15]. In total, 520 out of 524 people on board the aircraft were killed in what is dubbed as the worst ever single aircraft accident in the history of aviation. When the aircraft was cruising at an altitude of about 24,000 ft., decompression occurred due to rupturing of the rear pressure bulkhead, causing serious damage to the rear of the plane. The airplane became uncontrollable and struck a ridge, bursting into flames. Investigations revealed that the probable reason for the initiation and propagation of fatigue cracks in the rear pressure bulkhead was attributable to improper repairs of this bulkhead and lapses in maintenance inspection.

3.5 Crash of an Airbus model 330: 243 aircraft

On August 24th, 2001, Air Transat Flight TSC236, an Airbus Model 330–243 aircraft, was on a scheduled flight from Toronto, Canada, to Lisbon, Portugal [16]. A fuel leak in the right engine was not detected by the flight crew. Right engine eventually flamed out, followed by the left engine too. The flight crew initiated a diversion from the planned route for a landing at Lajes Airport on Terceira Island in the Azores. Assisted by radar vectors from Lajes air traffic control, the crew carried out an all-engine out visual approach and landing at night, in good visual weather conditions. Sixteen passengers and two cabin-crew members received injuries during the emergency evacuation. The aircraft suffered structural damage to the fuselage and to the main landing gear. The accident investigators determined that the fuel leak was caused by fuel line cracking that resulted from interference between the fuel line and a hydraulic line on the right engine. The interference was caused by an incomplete service bulletin incorporation creating a mismatch between the fuel and hydraulic lines during replacement of the right engine.

3.6 Collision between an Illushin IL-76 and a Boeing 747

On November 12th, 1996, Kazakhstan Airlines Flight 1907, an Ilyushin Il-76 coming from Shymkent, Kazakhstan, was to land in Delhi [17]. In the meantime, Saudi Arabian Airlines Flight SV763, Boeing 747, had departed from Delhi for a passenger flight to Dhahran. Both aircraft collided, plummeted down in flames, and crashed in

an arid farming area, resulting in 312 fatalities. The root and approximate cause of the collision was the unauthorized descending by the Kazak aircraft to FL140 and failure to maintain the assigned FL150. This is attributed to inadequate knowledge of English language of Kazak pilot, resulting in wrong interpretations of ATC instructions; poor airmanship and lack of proper CRM (Crew Resource Management) skill on the part of Pilot-in-Command, compounded by leadership quality lacking in him; casual attitude of the crew and lack of coordination in the performance of their respective duties by crew of Kazak aircraft; and absence of standard callouts from any crew member.

3.7 Crash of a Boeing 757: 200 airplane

On October 2nd, 1996, Boeing 757–200 aircraft departed from Lima-Jorge Chávez Airport on an international regular service to Santiago de Chile, carrying 61 passengers and a crew of nine [18]. After 29 minutes of flight, it impacted with the sea 48 nautical miles from the airport, with the total loss of the aircraft and all of its occupants. Investigation revealed that the maintenance staff had not removed the protective adhesive tape from the static ports. This tape was not detected during the various phases of the aircraft's release to the line mechanic, its transfer to the passenger boarding apron and, lastly, the inspection by the crew responsible for the flight (the walk-around or pre-flight check), which was carried out by the pilot-in-command. Both the pilot-in-command and the copilot had made errors by not complying with the ground proximity alarms.

3.8 Crash of Convair 580

As many as 10 recent air crashes, including the American Airlines disaster in New York in November 2001, could have been linked to a newly uncovered scam by which old and faulty aircraft parts were sold as new [19]. Parts illegally salvaged from crashes, counterfeit parts, and other substandard components regularly find their way into the world's air fleets, sold at bargain prices, often with falsified documents about their origin or composition. The worst confirmed accident occurred on Sept. 8, 1989, when at 22,000 feet over the North Sea, the tail section of a Convair 580 turboprop plane began vibrating violently and tore loose [20]. The charter aircraft, carrying 55 people from Oslo to Hamburg, splattered over 3 1/2 miles of sea. Everyone onboard died. Norwegian investigators painstakingly dredged up 90% of the 36-year-old plane and found the cause: bogus bolts, bushings, and brackets.

3.9 Twin accidents involving Boeing 737 max

A Boeing 737-Max airplane (Lion Air Flight 610) took off from Jakarta, Indonesia, on October 28th, 2018 and crashed into the Java Sea soon after takeoff, killing all 189 passengers and crew. Five months down the line, another Boeing 737-Max airplane (Ethiopian Airlines Flight 302) took off from Addis Ababa, Ethiopia, on March 10th, 2019 and crashed near the town of Bishoftu in Ethiopia, killing all 157 people in the aircraft. The aircraft contained a new feature called the Maneuvering Characteristics Augmentation System (MCAS) in its flight control computer [21]. Crash of these two Boeing 737max airplanes raised eyebrows about the technical design flaws, faulty assumptions about pilot responses, and management failures by both Boeing and the FAA.

4. Human factors

Case studies in the preceding section have shown that human errors can cause catastrophic aircraft accidents. We have heard of the popular saying, "to err is human," meaning that it is normal for people to make mistakes. Analogous to manufacturing tolerances that are used to control the inherent variations in aircraft parts to ensure greater consistency, interchangeability, and intended performance, we can think of human error as a deviation from an intended action that does not lead to undesirable consequence. An intentional deviation would amount to violation. In this section, we will introduce the concept of human factors and the various models that have been in use to understand their role in aviation accidents.

In the FAA, Human Factors are defined as a "multi-disciplinary effort to generate and compile information about human capabilities and limitations and apply that information to equipment, systems, facilities, procedures, jobs, environments, training, staffing, and personnel management for safe, comfortable, and effective human performance" [22].

The concept of human factors can be understood by referring to the SHEL model, developed by Edwards and modified by Hawkins as shown in **Figure 4**. The SHEL model is represented by five blocks whose edges are not simple and straight. The most critical and flexible component is in the center of this model and corresponds to Liveware (human). This is flanked by four blocks corresponding to Software, Hardware, Environment, and Liveware. Achieving proper matching of each of these peripheral blocks with that in the center is vital, as any mismatch can be a source of human error [23]. **Table 2** lists the relevance of blocks in the SHEL model.

The PEAR Model is one of the popular concepts related to the science and practice of Human Factors, especially for developing aviation maintenance activities. This mnemonic comprises four key elements, namely People who do the job; Environment in which they work; Actions that they perform; Resources that are necessary to carry out the job [24]. **Table 3** lists the parameters addressed in the PEAR model.

While there are over 300 conditions that can result in human error [25], the aerospace industry very frequently uses a set of 12 (called the "dirty dozen") when discussing human factors. The elements of this set are "lack of communication," "complacency," "lack of knowledge," "distraction," "lack of teamwork," "fatigue," "lack of resources," "pressure,' "lack of assertiveness," "stress," "lack of awareness," and "norms" [26]. Although primarily used in aircraft maintenance programs, this

Figure 4.
SHEL model as modified by Hawkins.

Block	Relevance
Software	Rules, procedures, written documents etc., which are part of the Standard Operating Procedures
Hardware	Air Traffic Control suites, their configuration, controls and surfaces, displays and functional systems
Environment	the situation in which the L-H-S system must function, the social and economic climate as well as the natural environment
Liveware	the human beings – the controller with other controllers, flight crews, engineers and maintenance personnel, management and administration people – within in the system

Table 2.
Relevance of blocks in the SHEL model.

Key element	Parameters addressed
People	Physical (physical size, gender, age, strength, sensory limitations), Physiological (nutritional, health, lifestyle, fatigue, dependency on chemical), Psychological (workload, experience, knowledge, training, attitude, mental or emotional state) and Psychosocial factors (interpersonal conflicts, personal loss, financial hardships, recent divorce)
Environment	Physical (Weather, location inside/ outside work space, shift, lighting, sound level, safety) and Organizational (personnel, supervision, labour-management relations, pressures, crew structure, company size, profitability, morale, corporate culture)
Actions	Steps to perform a task, sequence of activity, number of people involved, communication requirements, information control requirements, knowledge requirements, skill requirements, attitude requirements, certification requirements, inspection requirements
Resources	Procedures/ work cards, technical manuals, other people, test equipment, tools, computers/ software, paperwork/ signoffs, ground handling equipment, work stands and lifts, fixtures, materials, task lighting, training, quality systems

Table 3.
Parameters addressed in the PEAR model.

concept has been extended to all areas of the aviation industry and has enhanced aviation safety. Factors associated with pilot errors have been discussed in [27, 28].

The Swiss-Cheese model of accident causation, originally proposed by James Reason, likens human system defenses to a series of slices of randomly holed Swiss-cheese arranged vertically and parallel to each other with gaps in-between each slice [29, 30]. The Swiss-cheese model, adapted from [29], is shown schematically in **Figure 5**. Each slice of cheese represents the defense of an organization against failure. Holes in each slice represent individual weaknesses in individual parts of the system and have a dynamic nature. It means that the holes vary continually in both size and position on the slice. A limited window of accident opportunity is created when the holes in all the slices align momentarily. This in turn facilitates a hazard to pass through all the holes leading to an accident.

Boeing has used procedural event analysis tool (PEAT) to help the airline industry effectively manage the risks associated with flight crew procedural deviations. Similarly, Boeing has used maintenance error decision aid (MEDA) to help airlines shift from blaming maintenance personnel for making errors to systematically investigating and understanding contributing causes [31]. A variety of operators have witnessed substantial safety improvements, and some have also experienced significant economic benefits because of reduced maintenance errors.

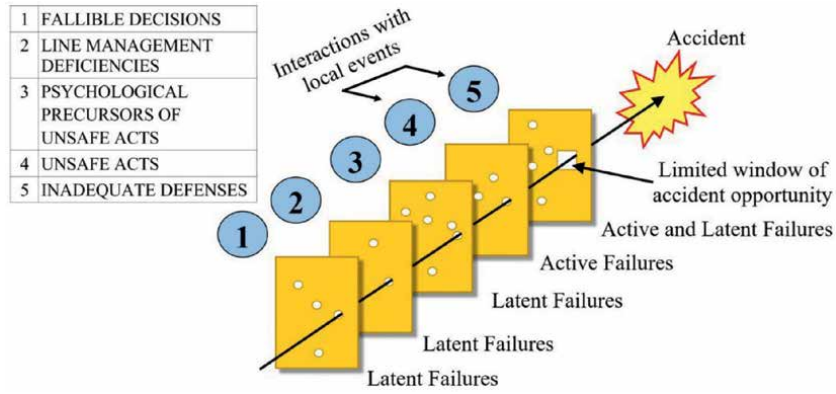

Figure 5.
Concept of Swiss-cheese model developed by reason.

5. Human factors analysis and classification system framework

5.1 HFACS basics

Although the concept of Swiss-cheese model changed the way aviation and other accident investigators view human error, it did not provide the level of detail necessary to apply in the real world. There was a need to have a comprehensive tool for investigating and analyzing human error associated with accidents and incidents. This necessitated the development of the Human Factors Analysis and Classification System (HFACS) [32].

The HFACS framework adapted from [33] is shown in **Figure 6**. The HFACS framework has a total of 19 causal categories identified within the four levels of human failure. By using the HFACS framework for accident investigation, organizations are able to identify the breakdowns within the entire system that allowed an accident to occur. HFACS can also be used proactively by analyzing historical events to identify recurring trends in human performance and system deficiencies. Both of these methods will allow organizations to identify weak areas and implement targeted, data-driven interventions that will ultimately reduce accident and injury rates.

Most accidents can be traced to one or more levels of failure related to organizational influences (three causal categories), unsafe supervision (four causal categories), preconditions for unsafe acts (seven causal categories), and the unsafe acts themselves (five causal categories).

5.2 Application of human factors knowledge to aviation accidents

HFACS provides a structure to review and analyze historical accident and safety data. By breaking down the human contribution to performance, it enables the analyst to identify the underlying factors that are associated with an unsafe act. The HFACS framework may also be useful as a tool for guiding future accident investigations in the field and for developing better accident databases, both of which would improve the overall quality and accessibility of human factors accident data. Common trends within an organization can be derived from comparisons of psychological origins of the unsafe acts or from the latent conditions that allowed these acts within

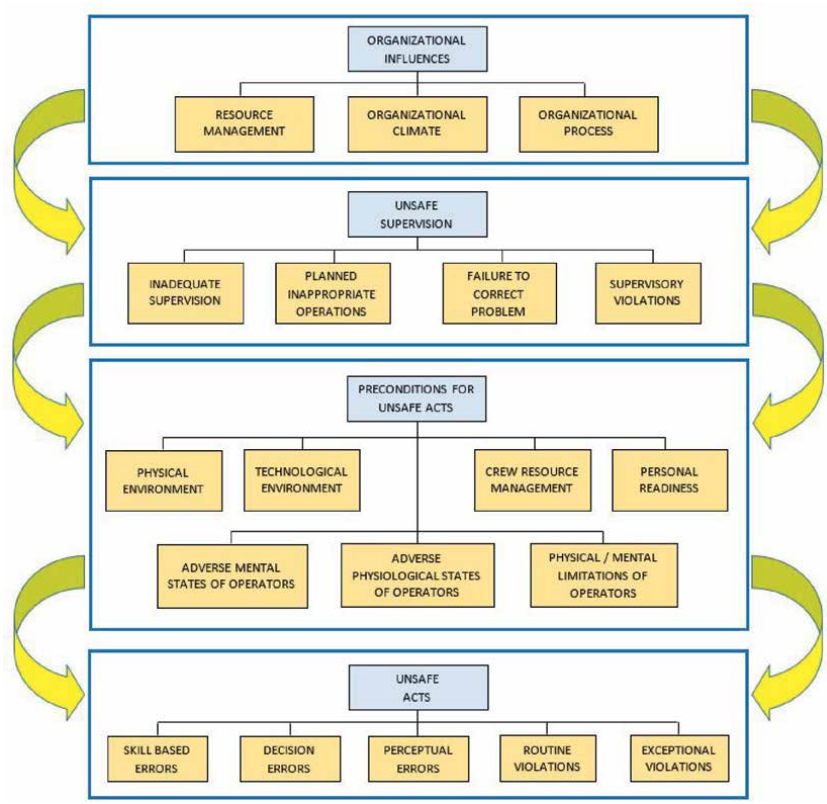

Figure 6.
The HFACS framework.

the organization. Identifying those common trends supports the identification and prioritization of where intervention is needed within an organization.

By using HFACS, an organization can identify where hazards have arisen historically and implement procedures to prevent these hazards resulting in improved human performance and decreased accident and injury rates. The HFACS framework has been successfully applied to analyze accidents in military, commercial, and general aviation sectors [33–39].

An example of analysis using HFACS is shown in **Figure 7** from the data available in [36], considering a total of 1020 aircraft (181 carrier aircraft and 839 commuter aircraft) accidents involving aircrew or supervisory error for the period 1990–2002. Accidents classified as having "undetermined causes" and those that were attributed to sabotage, suicide, or criminal activity are not included in the analysis. Commercial aviation accident data obtained from the NTSB databases were used in the analysis. Numbers 1 through 18 on the abscissa represent the 19 causal categories in the HFACS framework. Note that routine and exceptional violations have not been shown separately, but as a single number represented as 18 on the abscissa.

The HFACS framework has been applied by several researchers to analyze and understand the cause of accidents in aviation and a number of other domains such as rail, maritime, construction, mining, and nuclear power. A consolidated review is available in [40], where the authors conclude that HFCAS can help in analysis to

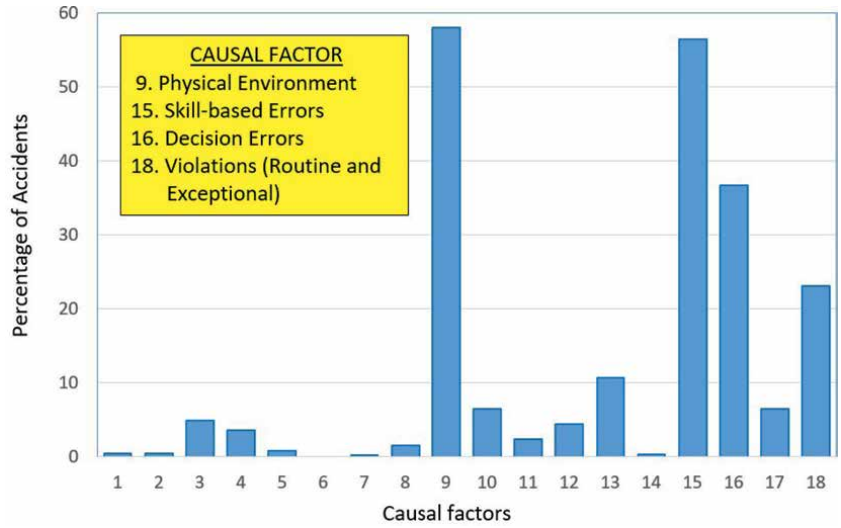

Figure 7.
Example of HFACS analysis applied to 1020 commercial aviation accidents.

identify both latent and active factors underpinning accidents. The development history of 29 different accident causation models and a new 24Model that discusses linear as well as nonlinear accident causation methods is presented in [41]. In 24Model, the cause of the accident is attributed at individual and organizational levels to immediate cause, indirect cause, radical cause, and root cause.

6. A relook at human factors

In this section, we try to look at human factors and their role in the prevention of aviation accidents from a different perspective. Referring to **Figure 8**, the total environment within which aviation accidents happen is marked by the largest circle and represents the overall domain. The seven smaller circles within this domain represent seven possible sources from where the "holes in the cheese" can get triggered or generated. Each of these seven segments also needs to have closely knit coordination with rest of the segments to ensure that human errors are minimized and do not propagate through the system resulting in accidents and fatalities. A brief description of the seven segments is provided in the following paragraphs.

6.1 The seven-segment model

6.1.1 Design organization

This segment covers all the activities commencing from conceptual design of an aircraft till its certification. Design drivers are based on market demand, customer preferences, requirement of reduction in carbon emissions, increase in traffic growth, profit margins, and design modifications to existing aircraft as well. Design organization coordinates and interacts mainly with regulatory body and production organization in achieving its objectives.

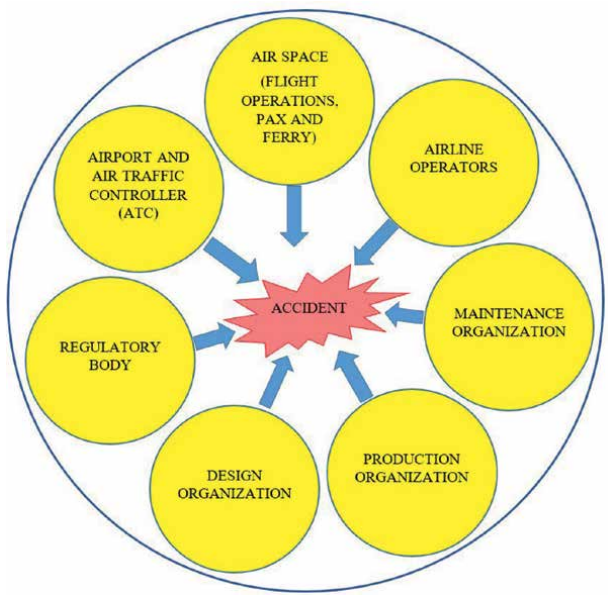

Figure 8.
The seven-segment model.

6.1.2 Production organization

This segment covers all the activities connected with manufacturing of aircraft commencing from conceptual design to certification of aircraft, including both prototype and production versions. It also includes Original Equipment Manufacturers (OEMs) connected with engines, propellers, and line replaceable units (LRUs). Production organization coordinates and interacts with design organization, OEMs, sub-contract vendors, and regulatory body in achieving its objectives.

6.1.3 Maintenance organization

This segment covers all the activities connected with maintenance, repair, and overhaul of aircraft in order to maintain the aircraft in airworthy condition. Maintenance organization coordinates and interacts with airline operators, production organization, design organization, and regulatory body in achieving its objectives.

6.1.4 Airline operators

This segment covers all the relevant activities carried out by companies providing air transport service for transport of people and freight through air navigation. Airline operators coordinate and interact with airports, regulatory bodies, and maintenance organizations in achieving their objectives.

6.1.5 Air space (flight operations, pax and ferry)

This segment covers all the activities connected with low-speed and high-speed taxy checks of aircraft, test flights for certification of aircraft, commercial operations of aircraft for transporting people and freight. It also covers rest of the air space.

These include the space populated by helicopters, other commercial aircraft, drones, trainer aircraft, cargo aircraft, flying cars, birds, and natural phenomena such as thunderstorms, lightning, heavy rains, poor visibility, and so on. It is here that the pilots and crew members play their role and interact with air traffic controller, design organization, and regulatory body.

6.1.6 Airport and air traffic controller (ATC)

This segment covers all the activities connected with management of airport operations, right from fueling the aircraft, pre-flight inspection, clearance for taxying out to the runway, clearance for flight take off, continual monitoring of hundreds of aircraft that are cruising at various flight altitudes, clearance for landings including emergency landings, etc. The ATC coordinates and interacts with the flight crew, design organization, and regulatory body as necessary in achieving its objectives.

6.1.7 Regulatory body

This is an extremely important segment and covers regulation of transport services from source to destination, enforces civil aviation regulations, air safety, and airworthiness standards. It also plays a key role in auditing of design, production, and maintenance organizations, participates in the certification process of aircraft, maintains an aircraft register, and issues certificate of registration to aircraft. It also plays a key role in accident investigation and subsequent issue of advisory circulars/ airworthiness directives as applicable to prevent future recurrence.

6.2 Man and environment

Aircraft accidents happen essentially due to a mismatch in the interaction between man and the environment. This means that there must be an issue either with the man or the environment, or a combination of both. For the purpose of discussion, environment is defined to include all such factors outside of the human system. The word "man" is not gender-specific, but is retained for generic description of personnel. The concept is shown in **Figure 9** illustrating a safe zone, two "potentially unsafe" zones and an unsafe zone. These four zones represent four possible combinations arising out of man-environment interaction. These are elucidated in the following paragraphs.

6.2.1 Safe zone

This is the target zone that every safety-conscious organization strives for and would like to remain in this zone forever. The requirement to reach and sustain in this zone requires fully fit personnel and an ideal/flawless environmental condition. Fitness of the personnel includes physical, physiological, psychological, and psychosocial factors and his interaction with the environment. Ideal environment includes adequate funding, infrastructure, resources, feasible time schedules, healthy work environment, and so on.

6.2.2 Potentially unsafe zone with flawed environment

This zone represents situations wherein fully fit personnel perform their work in environments that are deficient of certain factors and are hence "flawed." An example for this situation is personnel being pressurized to perform aircraft maintenance

Figure 9.
Safe, potentially unsafe, and unsafe zones.

within a short notice, although it is practically not feasible. This may trigger personnel to take a few shortcuts in the maintenance procedures and has potential to create "holes in the cheese," which may remain latent till the bubble bursts. Sometimes it may so happen that the personnel are able to meet the short notice requirements without any error (for example, by resorting to overtime work); however, there is a danger of setting a precedent for the future and the management may demand even more output from the personnel working in a flawed environment. This may gradually result in stretching the capacity of the personnel beyond the normal limits and may lead to errors and violations in subsequent work that they are assigned.

6.2.3 Potentially unsafe zone with ideal environment

This zone represents situations wherein the management has provided ideal environment for the personnel to carry out their duties, but the fitness of the personnel who are carrying out the tasks is far from satisfactory. Hence the personnel may not be able to carry out the duties assigned to them, without committing errors. The reasons for errors or violations committed in this zone are internal to the person, attributable to his/her physical, physiological, psychological, or psychosocial condition. An example is that of a person who had some serious argument with his family members before coming to work, or a person who did not have adequate rest before coming to work, and so on. The work carried out under such a situation can lead the output to potentially unsafe zone.

6.2.4 Potentially unsafe zone with ideal environment

This is a very dangerous zone that every safety-conscious organization tries not to enter. If personnel, not adequately fit to undertake the activity, are made to work

under flawed environments, the end result is a disaster, resulting in loss of precious lives, or hull, or both. All the aviation accidents that have hitherto taken place can be attributed a combination of human errors and environmental factors. Pilots alone cannot be blamed for the accidents, but the latent errors that have crept into the system from the potentially unsafe zones will also have to be considered.

6.3 Modified HFACS model

The HFACS framework adapted from [33] and shown in **Figure 6** is suitably modified by adding additional layer to account for external influences such as market demand, economic and profit motives, inter-segment coordination, and political pressures. The modified HFACS framework is shown in **Figure 10**. To cite an example, due to an increased market demand, aircraft manufacturers may hike up the production rate of aircraft without adequately enhancing the resources required to achieve the targeted production. This will result in additional work pressure and can result

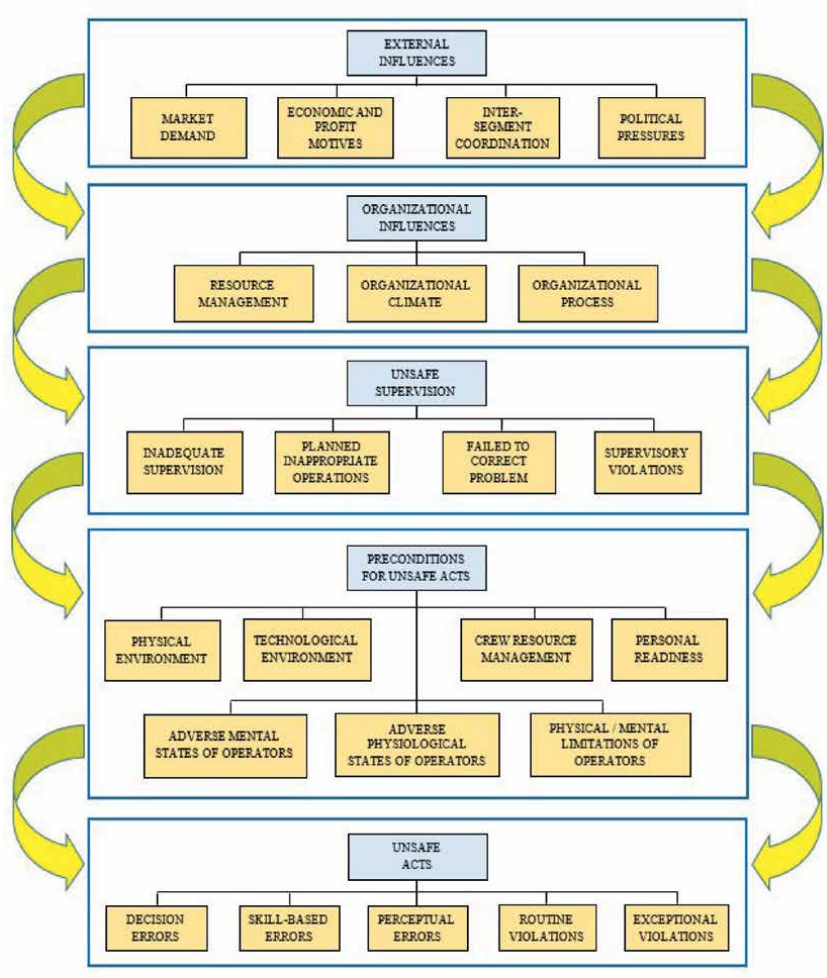

Figure 10.
Modified HFACS framework.

in human errors. In the process of increased competition from other aircraft manufacturers, aircraft design agencies may resort to suggesting quick modifications to an already existing design in order to save time and money. Many a times, there may be lack of coordination between the various segments in the seven-segment model. There may also be situations where a VIP overrules the suggestions given by the pilot and pressurizes him to fly the aircraft. In all these cases, holes are added to the cheese in the system, thus increasing the probability of accidents.

Figure 11 shows schematic of modified HFACS framework for a sample segment 1 and its mutual interaction with rest of the segments 2 through 7. The same concept is applicable to every other segment, and the mutual interaction for the complete domain is depicted in **Figure 12**. It is necessary to cover all the segments

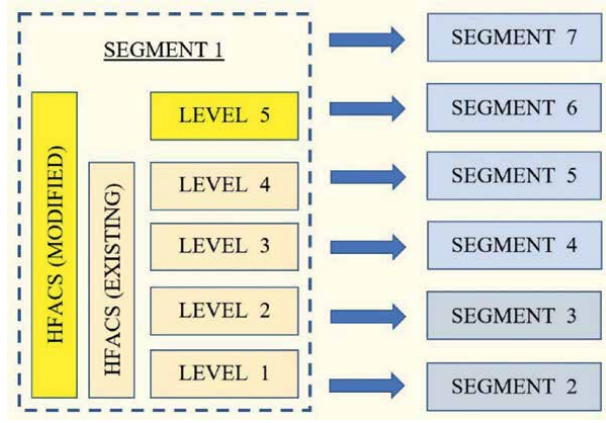

Figure 11.
Modified HFACS framework for a sample segment.

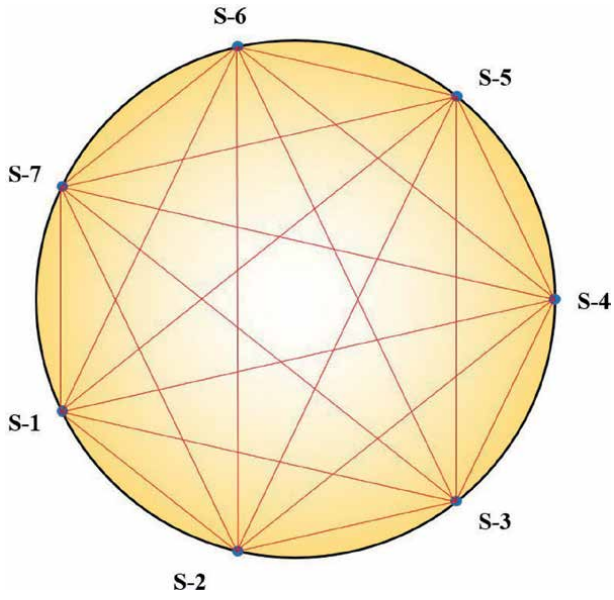

Figure 12.
Mutual interaction paths in the seven-segment model.

during aircraft accident investigation in order to converge onto the root cause(s) for the accident.

7. Way forward for even safer skies

Newer technologies as well as materials available today and in the years to come will result in novel designs of new aircraft configurations as we march towards the zero-emission target. The air space is going to get even more populated with thousands of newer flying machines. This will mean that the way to safer skies begins right from the commencement of the new airplane configuration design. It is right from this stage that the required human factor elements should be embedded into the aircraft projects/programs. Human-to-machine interface designs such as flight deck design will require a relook in view of the new technologies. Also, the concept of design for maintainability and in-service support should be kept in mind. Customer inputs are also to be considered in areas such as passenger cabin design and flight deck design. Human factor experts should review the whole system before the project is taken up. The assessment ideally requires human factors specialists to assess the vulnerability to human error of the response tasks.

In order to achieve and maintain the goal of zero fatalities in commercial operations over the next couple of decades, five specific high-risk categories (HRCs) of occurrences have been identified by ICAO, based on analysis of hitherto aircraft accidents and incidents [42]. These five are Runway excursion (RE), Midair collision (MAC), Loss of control in-flight (LOC-I), Controlled flight into terrain (CFIT), and Runway incursion (RI). Reduction of operational safety risks is a must in order to achieve the goal of zero fatalities, and top management commitment to safety plays an important role in this direction. Continually evolving regulatory procedures must be respected and followed at all times.

Top managements must establish a conducive work environment to prevent the staff of the organization from getting into physical or mental tension. It is not uncommon for anyone subjected to emotional factors such as pressure, distraction, fatigue, and stress to suffer from making judgment errors in the work they carry out. Management should encourage error reporting and honesty among working staff. Many staff may not disclose unintentional errors that have been committed by them for the fear of losing their jobs.

Top managements must identify and implement independent and multiple inspections in critical areas covering design, drawing, raw material inward inspection and storage, fabrication, assembly, integration, aircraft inspection, ground testing, flight testing, servicing of Line Replaceable Units (LRUs), and so on. Design, manufacturing, and flight testing agencies must work with mutual coordination. Human factors will play a key role in every aspect of aircraft life cycle from drawing board till the end of its service life. Organizations that take up aircraft improvisation programs and/or new aircraft development programs will need to first do their homework regarding the feasibility of achieving the project goals within the committed time and funding. Ambitious and impractical goals may land the organization itself into a swirl of external pressures from the stakeholders and funding agencies and result in human errors creeping into the design, development, and manufacturing stages of the program, leading to costly and irreversible consequences.

Pilot familiarization and refresher training including simulator and CRM is an essential element for ensuring flight safety. Training of pilots in competencies such

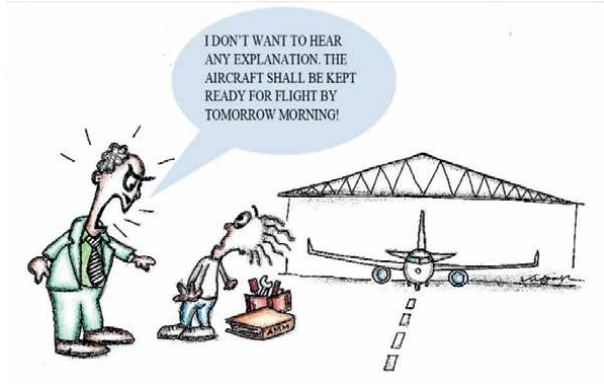

Figure 13.
Aircraft technician under undue time pressure from top management. (illustration credits; Vidya Kamalesh).

as communication, aircraft flight path management (both manual and automated), leadership and team work, problem-solving and decision making, application of procedures, work load management, emergency procedures, situational awareness and knowledge, fatigue and sleep duration, intoxication, checklist verification is a must on continual basis.

Aircraft maintenance activities will increase in the next few decades due to the increase in the number of aircraft as well as number of flights. It is important to integrate human factors into Safety Management System (SMS) in MROs. Some of the bare minimum aspects to be considered in this process are hazard identification, risk assessment and mitigation, management of change, design of systems and equipment, training of operational personnel, job and task design, safety reporting and data analysis, incident/accident investigation. Bullying by the bosses may have significant adverse consequences and may jeopardize the safety of flight. **Figure 13** depicts a typical scenario wherein an aircraft technician is instructed by the top management, to keep the aircraft ready for flight at short notice.

Uniformity should be maintained in all final reports pertaining to aviation accidents especially with respect to various human factors and root causes leading to the accident. This will facilitate use of powerful tools such as Watson Analytics and Cognos Analytics for analysis of airplane crash patterns and also to find possible solutions to make continual improvements in flight safety [43]. An advanced method of reporting system for integrating human factors into safety management system in aviation maintenance is described in [44, 45]. Trust, communication, and transparency are at the heart of an appropriately human-centered design process and, in combination, can have a powerful impact on the successful and safe use of advanced automated technologies [46].

8. Conclusions

The dream of man to fly became a reality with the successful flight of the Wright Flyer in 1903. In a short span of about 120 years, aircraft and power-plant designs have undergone continual improvements to cater to the ever-growing air

traffic requirements. Innovations in design and analysis tools, material sciences, manufacturing processes, electronics, and communication have made flying easier than ever before and reduced the pilot workload. However, the possibility of human error creeping its way into the aircraft cannot be ruled out. If the human error is left unnoticed, it may result in fatal accidents. Vital factors leading to civil aviation accidents have been brought out by quoting a few examples. Various models used for the analysis of human factors have been discussed. A seven-segment model for identifying causal factors based on modified HFACS has been presented.

Most of the accidents in the last two decades have occurred during approach and landing phases of flight. Human-machine interface designs such as flight deck design should be revisited in light of the new technologies. Uniformity should be maintained in all final reports pertaining to aviation accidents especially with respect to various human factors and root causes leading to the accident. This will facilitate use of powerful tools such as Watson Analytics and Cognos Analytics for analysis of airplane crash patterns and also to find possible solutions to make continual improvements in flight safety. Safety Culture has to be established in the complete aviation industry setup, covering aircraft design, production, flight operations, and maintenance. This is even more important in view of the expected increase in air traffic in the coming years. Commitment of top management to safety is very important. Documented procedures should not just remain on paper, but shall be followed in both letter and spirit. Use of Integrated Vehicle Health Management (IVHM) concepts in aircraft design will result in improving the overall safety of the aircraft, while reducing both operation and maintenance costs. Also, the concept of design for manufacturing, maintainability, and in-service support should be kept in mind. CRM refresher at regular intervals including simulator training to handle flight exigencies is a must.

Air traffic will continue to grow increasing airspace congestion and pose challenges for bringing down the number of aircraft accidents. Use of Artificial Intelligence and Big Data can help improve utilization of airspace safely and efficiently. Human factors will continue to play an even more important role in striving towards an accident-free air travel. At the 77th IATA Annual General Meeting in Boston, USA, on October 4, 2021, a resolution was passed by IATA member airlines committing them to achieving net-zero carbon emissions from their operations by 2050. To succeed, it will require the coordinated efforts of the entire industry (airlines, airports, air navigation service providers, manufacturers) and significant government support. A similar commitment is in order to bring down the number of aircraft accidents and fatalities to zero.

Acknowledgements

The authors would like to place on record the valuable suggestions and feedback provided by Prof. Zain Anwar Ali, academic editor, in bringing out this book chapter.

Conflict of interest

The authors declare no conflict of interest.

Notes/thanks/other declarations

The authors are grateful to Vidya Kamalesh for the neat illustration, reflecting the work pressure from top management under which an aircraft technician is working. The authors are grateful to CWong for permitting to use the photograph of Boeing 737–800 series aircraft with registration number B-1791 available in https://www.jetphotos.com/photo/10528109.

Appendices and nomenclature

ATC	Air Traffic Control
CRM	Cockpit resource management / Crew resource management
FAA	Federal Aviation Administration
HFACS	Human Factors Analysis and Classification System
IATA	International Air Transport Association
ICAO	International Civil Aviation Organization
IVHM	Integrated Vehicle Health Monitoring
MEDA	Maintenance Error Decision Aid
MRO	Maintenance, Repair, and Overhaul
NTSB	National Transportation Safety Board
PEAR	People, Environment, Actions and Resources
PEAT	Procedural Event Analysis Tool
SHEL	Software, Hardware, Environment, and Liveware
SMS	Safety Management System

Author details

Kamaleshaiah Mathavara* and Guruprasad Ramachandran
CSIR-National Aerospace Laboratories, Bengaluru, India

*Address all correspondence to: kamaleshaiah.csirnal@gmail.com

References

[1] faa_order_8020.11d. Aircraft accident and incident notification, investigation, and reporting [Internet]. 2018. Available from: https://www.faa.gov/documentlibrary/media/order/faa_order_8020.11d.pdf

[2] ICAO Doc 9962 AN/482. Manual on Accident and Incident Investigation Policies and Procedures. ICAO Doc 9962 AN/482. International Civil Aviation Organization, Canada;2011

[3] Bellis M. History of Flight: The Wright Brothers Invention of the First Powered, Piloted Airplane. Thought Co; New York. [Internet] 2019. Available from: https://www.thoughtco.com/history-of-flight-the-wright-brothers-1992681

[4] Statista. Countries and Regions with the Highest Number of Fatal Civil Airliner Accidents from 1945 through February 28, 2022. Statista; Hamburg. [Internet] 2022. Available from: https://www.statista.com/statistics/262867/fatal-civil-airliner-accidents-since-1945-by-country-and-region/

[5] Bureau of aircraft accidents and archives. Geneva. [Internet] 2022. Available from: https://www.baaa-acro.com/crashes-statistics

[6] China Eastern plane crash likely intentional, US reports say [Internet]. 2022. Available from: https://www.bbc.com/news/business-61488976

[7] Aviation safety network. An exclusive service of flight safety foundation [Internet]. 2022. Available from: https://aviation-safety.net

[8] MEDA investigation process. Effect of reducing maintenance errors [Internet]. 2007. Available from: https://www.boeing.com/commercial/aeromagazine/articles/qtr_2_07/article_03_2.html

[9] Department of Transport and Regional Development; Bureau of Air Safety Investigation. Human factors in Fatal Aircraft Accidents [Internet]. 1996. Available from: https://www.atsb.gov.au/media/28363/sir199604_001.pdf

[10] A statistical analysis of commercial aviation accidents 1958-2021 [Internet]. 2022. Available from: https://accidentstats.airbus.com/sites/default/files/2022-02/Statistical-Analysis-of-Commercial-Aviation-Accidents-1958-2021.pdf

[11] Statistical summary of commercial jet airplane accidents. World operations 1959-2020 [Internet]. 2021. Available from: https://www.boeing.com/resources/boeingdotcom/company/about_bca/pdf/statsum.pdf

[12] Report on the accident to Boeing 707 321C, G-BEBP near Lusaka International Airport, Zambia, 14 May 1977. Report No: 9/1978 [Internet]. 2014. Available from: https://www.gov.uk/aaib-reports/9-1978-boeing-707-321c-g-bebp-14-may-1977

[13] Aircraft Accident Report 92-11 EL AL Flight 1862 [Internet]. 1994. Available from: https://reports.aviation-safety.net/1992/19921004-2_B742_4X-AXG.pdf

[14] In-flight uncontained engine failure Airbus A380-842, VH-OQA [Internet]. AO-2010-089_final.pdf. 2013. Available from: https://www.atsb.gov.au/publications/investigation_reports/2010/aair/ao-2010-089.aspx

[15] Aircraft Accident Investigation Report [Internet]. 1987. Available from: https://www.mlit.go.jp/jtsb/eng-air_report/JA8119.pdf

[16] Accident Investigation Final Report. All Engines-out Landing Due to Fuel Exhaustion [Internet]. 2001. Available from: https://www.fss.aero/accident-reports/dvdfiles/PT/2001-08-24-PT.pdf

[17] Report of court of inquiry on mid-air collision between Saudi Arabian Boeing 747 and Kazakhstan IL-76 [Internet]. 1996. Available from: https://www.baaa-acro.com/sites/default/files/2020-12/UN-76435.pdf

[18] Accident of the Boeing 747-200 aircraft [Internet]. 1996. Available from: https://skybrary.aero/bookshelf/books/1719.pdf

[19] Second-hand parts scam linked to 10 air crashes [Internet]. 2002. Available from: https://www.theguardian.com/business/2002/jan/29/theairlineindustry.internationalnews

[20] Black market in bogus parts poses peril to airline passengers [Internet]. 1996. Available from: https://www.latimes.com/archives/la-xpm-1996-12-15-mn-9234-story.html

[21] The design, development and certification of the Boeing 737 Max [Internet]. 2020. Available from: https://transportation.house.gov/download/20200915-final-737-max-report-for-public-release

[22] The role of human factors in the FAA [Internet]. 2022. Available from: https://www.hf.faa.gov/role.aspx

[23] Fundamental human factor concepts. CAP719. Safety Regulation Group, Civil Aviation Authority [Internet]. 2002. Available from: https://publicapps.caa.co.uk/docs/33/cap719.pdf

[24] William Johnson & Michael Maddox. A PEAR Shaped Model for Better Human Factors. CAT Magazine, United States: Department of Transportation, Federal Aviation Administration, Washington DC. 2007;**2**:20-21. [Internet] 2007. Available from: https://www.faa.gov/about/initiatives/maintenance_hf/library/documents/media/reports_publications/pear_civil_aviation_training_magazine_4-07.pdf

[25] Investigation of human factors in accidents and incidents. ICAO Circular 240-AN/144. 1993

[26] US Department of Transportation. Chapter 14. In: Aviation Maintenance Technician Handbook – General, FAA-H-8083-30A. US Department of Transportation; Federal Aviation Administration. OK USA. [Internet] 2018. Available from: https://www.faa.gov/sites/faa.gov/files/regulations_policies/handbooks_manuals/aviation/amt_general_handbook.pdf

[27] Ghohua L, Baker SP, Grabowski JG, Rebok GW. Factors associated with pilot error in aviation crashes. Aviation, Space, and Environmental Medicine. 2001;**72**(1):52-58

[28] Human factors in aviation [Internet]. 2022. Available from: https://www.baumhedlundlaw.com/aviation-accident/why-planes-crash/human-factors-in-aviation/

[29] Reason J. Human Error. New York: Cambridge University Press; 2009

[30] Reason J, Education and debate. Human error: models and management. BMJ. 2000;**320**:768-770

[31] Human factors process for reducing maintenance errors [Internet]. 2022. Available from: https://www.boeing.com/commercial/aeromagazine/aero_03/textonly/m01txt.html

[32] Shappell SA, Weigmann DA. The Human Factors Analysis and

Classification System – HFACS. Report No. DOT/FAA/AM-00/7. Washington, DC: Office of Aviation Medicine; 2000

[33] Shappell SA, Wiegmann DA. HFACS Analysis of Military and Civilian Aviation Accidents: A North American comparison. In: Proceedings of the 35th Annual International Seminar held in Queensland, Australia. VA, USA: ISASI; 2004. pp. 135-140. [Internet]. Available from: https://www.isasi.org/Documents/library/Seminar-Proceedings/Proceedings-2004.pdf

[34] Douglas Wiegmann, Albert Boquet. Human error and general aviation accidents: a comprehensive, fine-grained analysis using HFACS. 2005. Report No. DOT/FAA/AM-05/24

[35] Scott A Shappell, Douglas A Wiegmann. Reshaping the way we look at general aviation accidents using the human factors analysis and classification system [Internet]. 2003. Available from: https://www.researchgate.net/publication/251800381_RESHAPING_THE_WAY_WE_LOOK_AT_GENERAL_AVIATION_ACCIDENTS_USING_THE_HUMAN_FACTORS_ANALYSIS_AND_CLASSIFICATION_SYSTEM

[36] Scott A Shappell, Albert Boquet. Human error and commercial aviation accidents: a comprehensive, fine-grained analysis using HFACS. 2006. Report No. DOT/FAA/AM-06/18

[37] Scott A Shappell, Douglas A Wiegmann. A human error analysis of general aviation controlled flight into terrain accidents occurring between 1990-1998. 2003. Report No. DOT/FAA/AM-03/04

[38] Shappell S, Detwiler C, Holcomb K, Hackworth C. Human error and commercial aviation accidents: An analysis using the human factors analysis and classification system. Human Factors. 2007;**49**(2):227-242

[39] Douglas A Weigmann, Scott A Shappell. A human error analysis of commercial aviation accidents using the human factors analysis and classification system (HFACS). 2001. Report No. DOT/FAA/AM-01/3.

[40] Hulme A, Stanton NA, Walker GH, Salmon PM. Accident analysis in practice: A review of human factors analysis and classification system (HFACS) applications in the peer reviewed academic literature. In: Proceedings of the Human Factors and Ergonomics Society 2019 Annual Meeting. Human Factors and Ergonomics Society; Santa Monica, CA, USA. pp. 1849-1853. [Internet]. Available from: https://journals.sagepub.com/doi/pdf/10.1177/1071181319631086

[41] Gui F, Xie X, Qingsong J, Zonghan L, Ping C, Ying G. The development history of accident causation models in the past 100 years: 24Model, a more modern accident causation model. Process Safety and Environmental Protection. 2019;**134**:47-82

[42] Safety Report, ICAO [Internet]. 2021. Available from: https://www.icao.int/safety/Documents/ICAO%20Safety%20Report%202021%20Edition.pdf

[43] Miyamoto T, Whitehead N, Santos E. Investigating airplane crash data with Watson analytics and Cognos analytics. In: 3rd International Conference on Computing and Big Data. Taichung, Taiwan: ACM Digital Library. 2020. [Internet]. Available from: https://dl.acm.org/doi/10.1145/3418688.3418689

[44] Miller M, Mrusek B. The REPAIRER reporting system for integrating human factors into SMS in aviation maintenance. In: International Conference on Applied

Human Factors and Ergonomics. Cham: Springer; 2018. pp. 447-456

[45] Mrusek B, Douglas S. From classroom to industry: Human factors in aviation maintenance decision-making. Collegiate Aviation Review International; University Aviation Association. 2020;**38**(2):1-13. [Internet]. Available from: https://ojs.library.okstate.edu/osu/index.php/CARI/article/view/8066/7433

[46] Claire Blackett. Human-centered design in an automated world. Proceedings of the 4th International Conference on Intelligent Human Systems Integration (IHSI 2021), Italy. Advances in Intelligent Systems and Computing 1322. Cham, Switzerland: Springer Nature Switzerland AG; 2021

Chapter 10

The Impact of the Pandemic Effect on the Aviation in the Environmental Quality of the Air Transport and Travelers

Clélia Mendonça de Moraes

Abstract

The spread of the COVID-19 pandemic, caused by the SARS-CoV-2 virus occurs by the dissemination of viral infections, forcing the need for actions to control the virus. COVID-19 caused a pandemic that impacts the health system in biomedical and epidemiological order on a global. One of the measures taken by governors to contain the dissemination of the virus was the closure of airports, ports, and land borders, keeping only essential repatriation flights. The concern about agglomeration of people in public spaces causes the need for ventilation control in order to reduce the contagion and maintain hygiene in airports and planes. The sum of these factors brought, as a consequence, a resumption of decisions about how to adopt postures to control the contagion. Based on this analysis it turns out that ventilation is the fundamental factor to control the spread of the COVID-19 pandemic. In the civil aviation sector for passengers transport on planes and airports, the following related aspects are presented: (1) determining the air conditioning system coefficients in commercial airplanes for passenger transport using CFD (Computational Fluid Dynamics) simulations to check airflow; (2) present new hygiene technologies for planes and airports.

Keywords: COVID-19, airplane cabin and environmental quality

1. Introduction

In the civil aviation scenario, the pandemic affected the economic circumstances (...) showing the need to reevaluate the demand projections of passengers, aircraft, and load [1]. The efforts of the civil aviation sector are to seek safety guidelines, to intensify the sanitation of surfaces, the use of masks and alcohol gel, frequent hand cleaning with soap/water, the practice respiratory etiquette, and proper ventilation, to keep the environment decontaminated and the ventilation controlled in order to reduce the contagion in airports and planes. Since environmental quality in civil aviation is facing COVID-19 it is necessary to seek comfortable resources in the ventilation itself in an attempt to solve or soften the discomfort during the cruise. The

incipient individualization of passengers' thermal comfort is one of the biggest problems faced by companies in the aviation sector. Exposed, multiple times, to considerable variation of thermal sources and different temperatures of asymmetric airspeed fields, passengers suffer the consequences of neglect with solutions that seek the individual space optimization without compromising the comfort provided in aircraft's cabins. To evaluate the thermal comfort, one must know the environmental comfort criteria to the relevant thermal environment parameters, along with the methods to its prediction (project phase) or measurement (commissioning and operation phase). From this basic premise, we need to: (a) define which are the main internal climatic parameters of temperature and asymmetric airspeed due to the cabin geometry projected with pitch,[1] and what is the restricted average width between the armchairs reducing the space between the passengers; (b) quantify its influence on the passengers, and (c) discern the plane and HVAC system in these parameters.

A large number of researches about thermal comfort was written and published. This extensive research literature was written in international standards [2–8], with the intent to guide the aeronautical project professionals to project and maintain the internal thermal environment comfortable, being internationally known as indoor climate or indoor air.

In this chapter, we research the thermal comfort and the adaptive comfort standard (ACS) based on variable climatic expectations that shift the locus of thermal regulatory responsibility to the environment of commercial and passengers transport aircraft, and back again to the airplane cabin occupants. The occupants are obligated to become way more active or interactive with the airplane internal cabin to implement the adaptation opportunities offered by the plane to create an acceptable indoor climate for passengers. After elaborating the methodological differences between these two perspectives about the person-environment relationship, the chapter examines the implications of standards and practices of thermal comfort using the computational simulation tool CFD, which allows describing the project guidelines to decision-making during the air distribution planning, considering the aircraft cabin's geometry. Confident that the obstacles to thermal comfort in the concerned aircraft can be solved with what is observed in simulations made in computational fluid dynamics – capable not only of making predictions about the thermal field and its speed but also of indicating the particle concentration of ventilated environments. The chapter finishes with a discussion about the increase of passengers' thermal comfort, adapting to variations and adjustments in the thermal environment. Such variations allow the creation and distribution of personalized ventilation that is formed around the passengers, and the best way to control this environment is through insufflation, temperature, and flow rate. Personalized ventilation, through air diffusers, highlights the Indoor Air Quality (IAQ), and the thermal comfort research gives a better understanding of the relationship between the human body and surrounding environments. In this regard, passengers play a central role in the aircraft cabins' internal environments. It is noted that, although experimental researches using mannequins provided valuable information about airflow, speed, temperature, and pollutants concentration, some other detailed information such as the airflow field around a person and the relation between the amount of heat transfer by radiation and the transfer of convective heat between the human body and its surroundings cannot be obtained in experiments. The innovation happened in the past years with the introduction of CFD

[1] Pitch is the distance between the plane's armchairs.

technology, which developed and made it possible to analyze the microclimate around a human being. It can simulate the passengers' transient inhalation and exhalation in the processes, having the geometrical representation of the Computational Thermal Manikin (CTMs) which represents the human body, being a significant factor for the ventilation personal study, representing the turbulence, grid generation, and boundary conditions model selection. The researchers conducted in Denmark (Aalborg University and the Technical University of Denmark), Japan (The University of Tokyo), and Germany (Hamburg University of Technology) use computational thermal manikins (CTMs) with the intention of determining indexes that are either unable or at least very hard to be acquired through experiments.

Because the topic is clearly within the jurisdiction, to present some of the results obtained in our investigation, we first bring a brief literature review about the subject. At this point we highlight the work in which we based the present chapter and, which yet not recognized by scientists due to lack of information about the subject, we also present observations taken sometimes from the visits we made to the airlines and theirs web portals from 2014 to 2020, sometimes from the interviews granted by old employees, whose reports mainly focused on the aircraft's internal environment development in Brazil. In short, being useful to thermal comfort practitioners.

This will allow the identification of the airport, plane, and passengers with contagion control purposes by airborne contamination, we hope that the professionals who work directly in airplanes and airports' organization and maintenance consider more actively the elements that involve environmental quality and human thermal comfort.

2. Pandemic effects on aviation

2.1 Pandemic, airport, and planes

The first identification of SARS-CoV-2 in human beings happened in Wuhan, China (2019). In that period there was paralyzation of air traffic in China. Right after the COVID-19 virus had spread to South Korea, caused the cancellation of flights, then to Iran and Italy. In that period, there were already cases of COVID-19 around the world. In March 2020, the United Nations (UN) declared a pandemic caused by the new SARS-CoV-2 virus, impacting the health system in biomedical and epidemiological order on a global scale. This fact imposed social isolation, among other measures, to protect health. At that time airports, ports, and land borders were closed except essential flights (**Figure 1**).

In earlier times the aviation sector had already suffered before, in 1976 there was the Ebola virus contamination, affecting human beings and other mammals. There was a union of forces between the civil aviation secretary and the World Health Organization (WHO) to avoid the transmission of the Ebola virus, especially improving the internal environment quality of passenger airplanes.

In 2009, emerged the Flu A H1N1 pandemic and later on with a new sub-type of influenza A (H1N1). In response to the outbreak, on April 25 the World Health Organization declared a Public Health Emergency of International Concern. Then, on April 27, the WHO announced phase 4 (human-to-human transmission) and phase 5 (sustained transmission) pandemic [9], and phase 6 (global spread) on June 11th, 2009. On this date, there were already 30 thousand cases reported in 74 countries.

Figure 1.
The impact of the COVID-19 pandemic in international airports.

The World Health Organization (WHO) declared the pandemic in March 2020, which was a decisive moment to air traffic that came with a change of attitude for the aerospace industry. However, aviation impacts also occurred in 2001, 2008, and 2010.

On September 11th, 2001 many flights were canceled, both in the United States and in other countries, due to terrorist attacks. In this period the discussions about airport security had begun, nowadays every airport security forms are the result of the standards established at that time.

In 2008 because of the US economic recession tourist and business travel decreased. Generally speaking, the business class customers are loyal company customers. In this same period, there was an increase in oil prices, which was reflected in aviation till 2011.

In 2010, the volcanic eruption in Iceland Eyjafjllajökull disrupted European air transport, especially passengers flights between the US and Europe.

According to Faury, Guillaume (CEO of Airbus), 2020 "We are now in the midst of the gravest crisis the aerospace industry has ever known". The planes used to conduct many cruises were forced to stand still, which requires maintenance before returning to operation. The airplane's maintenance, in general, follows the "Parking Mode" (1) easy to get back to service; (2) maintenance (more frequent: engine and main systems); and the "short term" (a) preserve engines; (b) remove fluids; (c) cover all entries (sensors, cracks, engines, mechanical ventilation, etc.); (d) disconnect batteries, and (e) lower the shutters of the windows. The airplanes with outdated technology (with old models and large airplanes) or for sale are stored in deserts such as Victorville, California, and Pinal County, Arizona in the United States (**Figure 2**).

It is noted that the coronavirus side effect is the use of better technologies, especially when it comes to air quality. The cargo companies besides cargo-specific planes also have passenger planes that transport a portion of cargo. The Belly Cargo (Long haul Flights) is a cargo plane with passengers that carries out 23% of all the world's cargo. An important aspect of freight transport is hospital equipment products, this happens because, due to the pandemic, it was necessary to protect the whole hospital teams with suitable materials to assists patients with COVID (such as masks, aprons, hospital equipment products, etc.) which no country had in stock. Most of these products are manufactured in Asia, especially in China. In this regard, air transport is being requested to save lives (**Figure 3**).

Figure 2.
American aircraft boneyard. Commercial aircrafts in Southern California Logistics Airport (former United States Air Force base), Victorville, California, USA. Source: https://www.jocelynkelley.com/fatos-interessantes/10-cemiterios-de-aeronaves-incomuns/.

Figure 3.
Dissemination of COVID-19.

2.2 Operations in the civil aviation sector during the pandemic period

The Brazilian National Civil Aviation Agency (ANAC) acted to soften the pandemic impacts, reducing the contamination risks to the users and employees through the gradual resumption of operations of the internal and external market, with ANAC Ordinance No. 1126 of 23/4/2020 to combat an infectious agent in the standards for fighting COVID-19 published according to the International Health Regulations, in the Collegiate Board Resolutions, (Resolution—RDC No 02, 2003, Resolution—RDC No 21, 2008 and Resolution—RDC No 56, 2008 and in the guidelines of the Ministry of Health. It follows the international protocol to fight COVID and establishes (1) the central systems in operation as long as the air renewal is open at its maximum capacity, and (2) compliance with the Maintenance, Operation, and Control Plan—PMOC of the installed air conditioning systems, especially the filter, in the airport. In airplanes cleaning occurs in the supervision of the cleaning teams with cleaning and disinfection procedure in each scale, before the boarding of new passengers. With the closing of the doors, whenever possible, the airplanes air conditioning system turned on and the mode without air recirculation selected.

2.3 Aircraft's cabin air conditioning and pressurization system

The air conditioning and pressurization systems are responsible for ensuring good health and comfort conditions for aircraft's occupants since they are the components of environment control.

While in buildings we have homogeneous environments, aircraft are considered non-homogeneous once they present different temperature and velocity gradients [10]. The difference between aircraft and building air conditioning system design is due to the aircraft's weight and the pressure difference between the outside and inside of the aircraft in high altitudes. When it comes to aircraft air conditioning special equipment capable of handling temperature asymmetries or radiant temperature is necessary.

In a good air conditioning system, the airflow must occur at a high speed at the top part of the airplane. In the bottom part, the recirculation is characterized by the mixed air present in the cabin (MV, mixing ventilation). Afterward, the engine must direct the outside air to the inner parts of the cabin, where, under very high temperature and pressure, it will be breathed in. Therefore, besides promoting air conditioning, the pressurization system avoids any discomfort or damage, because of the altitude changes that the cabin undergoes, for the occupants (the fast air change in the cabin eliminates odor and removes any traces of stale air).

Usually, the command cabin controls the pressurization systems that are incorporated in a sealed unit with the luggage compartment. The pressurization system is capable of containing air under higher pressure than the outside atmospheric pressure. Although in high altitudes the aircraft's external environment does not present viable conditions to the survival of human beings. The air is dry with extremely low temperatures and pressure: according to Lombardo [11, 12], the atmosphere consists of 21% oxygen, 78% nitrogen, and 1% other gases in its volume; however, the increase in altitude implies air rarefaction and a decrease of pressure lowering the amount of oxygen necessary for human functions. That is why aircrafts that do not have air conditioning and pressurization system are usually limited to low altitudes.

The pressurization is directly related to the quality of the partial pressure of oxygen available in the breathing air inside the fuselage compartments of the airplane, occupied by the flight crew. Its purpose is to maintain the indoor pressure equal to or greater than the value of the atmospheric pressure at 8000 feet altitude. Because when the airplane flies at higher altitudes, there will be a reduction in fuel consumption.[2]

The ventilation, one of the functions for which the air conditioning system is designed, consists of a dynamic intake of pressurized air. This function is done with the aid of an airflow fan, a heating operation on the ground, or a compressor when the aircraft has pressurized air ducts installed in the front, the top, or the bottom. The air goes into the main air entrance of the heater and is heated when passing over the radiator surfaces from where it is then distributed.

The refrigeration system, which is located next to the ventilation methods, are installed to ensure comfortable atmospheric conditions to the aircraft regardless of the altitude where the plane is situated. It also works to maintain the appropriate volume of air circulating at the correct temperature and humidity inside the aircraft. The capacity of the refrigeration system depends on the fuselage cavity proportions so that the circulation of air and vapors occurs. In both cases, the treated air is pumped only in the overhead bins region at a high speed and the outlet is made by side air vents in the bottom. Meanwhile, the cabin air conditioning is made by the central air conditioning and heating system, which provides outflows of up to 700 m^3/h (412 cfm) and controls the indoor air temperature from 14 to 35°C.

---

[2] For example, the indoor air of Boeing aircraft is made up of 50% outside air and the other 50% air filtered or recycled by the engine, while the air outside the plane in high altitudes is clean, pure, and cold (under −37°C) and has a low partial pressure of oxygen.

Before being recycled, the recirculated air is filtered by high-performance filters such as HEPA (High-Efficiency Particulate air filter), which is capable of retaining 99.97% of the cabin's airborne particles.

The cabin air circulation and ventilation inside an airplane are carefully designed to disperse and redirect contaminants, changing the entire cabin air volume from 20 to 30 times per hour in airplanes with the E-Jet model [13]. Higher is the frequency of air change, lower is the risk of viral dissemination, however, this air change occurs only when the plane is free-flying. The Airbus Chief Engineer Jean-Brice Dumont highlights the importance of air quality design being extremely clean with air renewal every two or three minutes, about 20 to 30 times per hour.

2.4 Air transport, travelers, and viruses

The distance between countries as well as the time to travel these distances, have decreased with the development of the aeronautic engineering industry applied to air transport. Due to factors such as international scientific conferences, work, sport or artistic events, celebrations, etc. culture and habits dissemination happens more frequently.

In that sense, air quality becomes a priority to avoid infectious pathologies and maintain public health by preserving health safety in airplanes and airports.

According to WHO director-general, Tedros Adhanom Ghebreyesus, in a press conference on Wednesday (11/03) "If the countries work to detect and track the disease, isolate the cases and mobilize human resources to respond to COVID-19, it is possible to prevent those places with few cases from becoming centers of virus dissemination and consequently from sustained community transmission." The director-general also pointed out the WHO guidelines to the countries which follow them: activate and expand the emergency response mechanisms, communicate with the population about the risks and how to protect themselves, find, isolate, test, and treat every case of COVID-19 apart from tracking all the infected.

In this context, keeping strict control on air transport before, during, and after the trip, it is possible to prevent the virus dissemination and its corresponding strains. The precautions before the flight, such as proper face mask usage, packing the luggage with plastic at the airport and/or using alcohol gel before the luggage is placed in the baggage compartment of the plane. As the International Air Transport Association states simple measures, such as the usage of masks by passengers and crewmates, as well as the guidance to use elbows to intercept coughs and sneezes, minimize the risks almost completely.

As the COVID virus could transmit among passengers on touching the infected surfaces and carelessness in using disinfecting substances, the main air companies of the world adopted new cleaning procedures to ensure that the aircraft is scrubbed after each flight, as well as ensuring passengers follow the required health and safety measures.

The air circulation in the cabin of the aircraft is done by a tube that captures external air and heats it during the flight by the engines, or by the auxiliary power unit when the airplane is on the ground. By a process of environmental control, the air is pressurized and cooled down to appropriate temperature for passengers and then it joins the recirculated air.

The air in the airplane's cabin comes from the ceiling, flows to the ground, and drains below the luggage compartment. As the air flows from top to bottom, the risk of dissemination of infectious agents diminishes regarding the front-to-back direction, the longitudinal orientation of the cabin.

2.5 Air conditioning and pressurization system

The air conditioning and pressurization systems are responsible for ensuring good health and comfort conditions to the aircraft's occupants since they are the components of environment control.

While in buildings we have homogeneous environments, the aircraft is considered non-homogeneous once they present different temperature and velocity gradients. The difference between aircraft and building air conditioning system projects is due to the aircraft weight and the pressure difference between the outside and inside of aircraft in high altitudes. When it comes to aircraft air conditioning, special equipment, capable of handling temperature asymmetries or radiant temperatures, is necessary.

In a good conditioning system, the airflow must occurs at a high speed at the top part of the airplane. In the bottom part, the recirculation is characterized by the mixed air present in the cabin (MV, mixing ventilation). Afterward, the engine must direct the outside air to the inner parts of the cabin, where, under very high temperature and pressure it will be breathed in. Therefore, besides promoting air conditioning, the pressurization system avoids any discomfort or damage for the occupants because of the fast air change in the cabin due to the altitude changes that the cabin undergoes, which eliminates odors and removes any traces of stale air.

The pressurization is directly related to the quality of partial pressure of oxygen available in the breathing air inside the fuselage compartments of the airplane, occupied by the flight crew. Its purpose is to maintain the indoor pressure equal to or greater than the value of the atmospheric pressure at 8000 feet altitude. Because, if the airplane flies at higher altitudes, there will be a reduction in fuel consumption.

One of the functions for which the air conditioning system is designed, the ventilation, is performed by a blower to help air circulation and by a heater operation on the ground. From a dynamic compressed air valve or a compressor in aircraft which has ducts of pressurized air installed in its front, bottom, or top surfaces. The air goes into the main entrance of the heater and is heated when passing over the radiator surfaces of the heater from which it is then distributed.

The refrigeration system, which is located next to the ventilation methods, is installed to ensure comfortable atmospheric conditions for the aircraft regardless of the altitude the plane is located. They also work to maintain the appropriate volume of air circulating in the correct temperature and humidity inside the aircraft. The capacity of the refrigeration system depends on the fuselage cavity proportions in which the air cycle[3] and the vapor cycle[4] occur. In both cases, the treated air is pumped only in the overhead bins at a high speed and the outlet is made by inferior exit ducts. In the meanwhile, the cabin air conditioning is given through the air conditioning and heating central system, which provides outflows of up to 700 m^3/h (412 cfm) and controls the indoor air temperature from 14°C to 35°C.

According to Conceição [14], the cabin must also have a humidifying system, responsible for maintaining the relative air humidity between 20 and 70% inside the cabin. It also must control the temperature of the walls once again from 14°C to 35°C, by an additional climatization and temperature control system, as shown in **Figure 4**.

---

[3] The air cycle refrigeration type consists of an expansion turbine (refrigeration turbine), an air-to-air heat exchanger and valves that control the airflow through the system.

[4] The refrigeration system for vapor cycle is used in multiple large sized transport aircrafts.

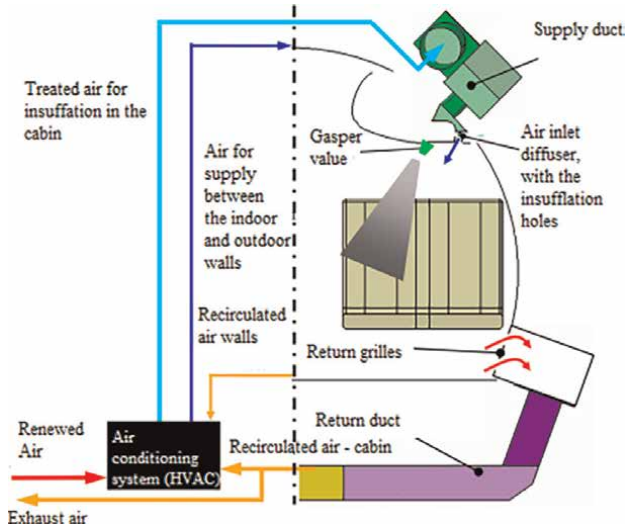

Figure 4.
Cross-section of thermal mock-up. Source: Conceição [14].

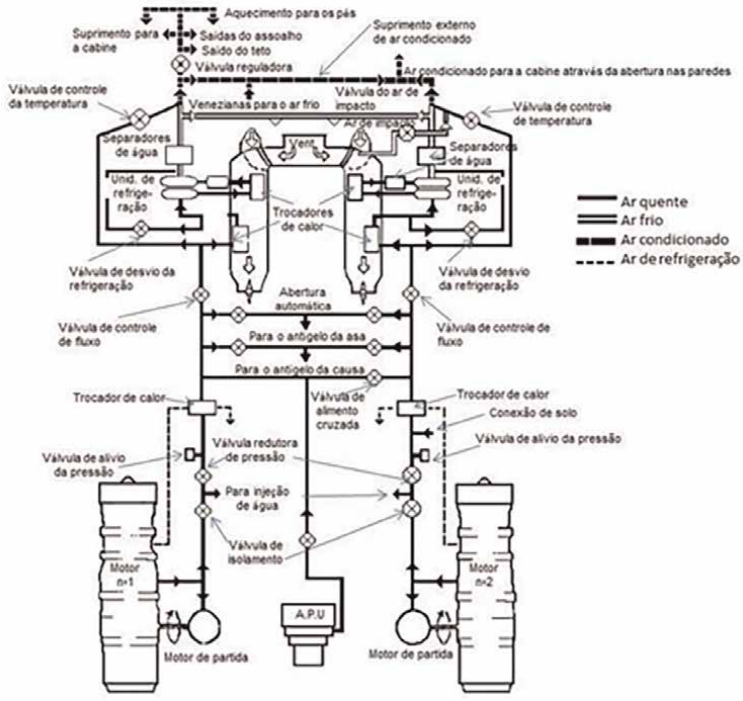

Figure 5.
Typical air conditioning and pressurization system. Source: ANAC [1].

Control valves, sensors, and electrical cables regulate the indoor air temperature when activated by air conditioning system valves, located in the cockpit panel (**Figure 5**). If there is an automatic control malfunction, there must be manual controls available.

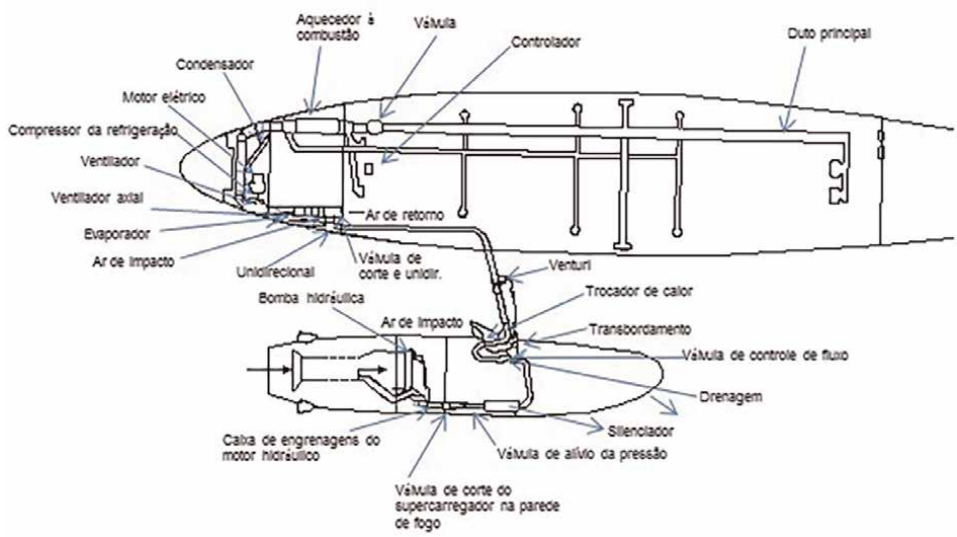

Figure 6.
Typical air distribution system. Source: ANAC [1].

It can be seen that the cabin's air distributor includes air ducts (with rectangular or circular sections when used in air distribution systems (**Figure 6**), or with other shapes when allocated in the passengers' individuals air exits and the window defroster), filters and heater exchangers, silencers, unidirectional valves, humidifiers, sensors of mass flux control and meters. The cabin's pressure sources cover positive displacement compressors (superchargers), centrifugal compressors, and supercharger controls. Supercharger tools working as airflow meters, pressurization valves, pressurization controls, cabin pressure regulator, and also air pressure safety valve.

According to Lombardo [11], the refrigeration machines which operate with air cycle are the predominant systems in aeronautical applications, especially when it comes to passenger transport aircrafts. The option is justified because of the availability of the working fluid (compressed air from the plane's propulsion system) and also by the fact that the air cycle (air cycle machine or ACM) do not demand the transport of new working fluid, which would require weight and occupied space restrictions. So, the air is partially treated in high-quality filters, similar to those used in hospitals surgery rooms, and thereafter is mixed with the same proportion of external air. The renovation of conditioned air is necessary for long distance flights and with a large number of crew members in the airplane cabin in a closed environment. The airflow must therefore meet thermal comfort requirements through an air conditioning operating system and be compliant with external environmental atmospheric conditions.

Researches related to air conditioner maintenance of airlines such as TAM and Embraer (2014) show that the air distribution is operated by a container that works at 35% of its capacity, meanwhile, the other 65% of the air volume stands still on the floor, without returning to circulate through the cabin. In other words, the clean air is not used in the internal environment of the aircraft and likewise, the same air used before circulates yet again causing many airborne viral pathologies to be transmitted. Besides, in these situations, health problems caused by engine oil particles that were found in the air filters have become common.

Given the possible damages to passengers' health, there were established flow standards for air conditioning systems. Maintaining the internal air quality demands that the renewal tax of the external air be high. In the same way, it is fundamental that the supply of external and recirculated air occurs in the appropriate temperature and relative humidity conditions. The temperature control of the cabin's interior avoids areas with stagnated air, as well as enables the dissipation of contaminants and odors.

Efforts to maintain the good air quality inside the cabins turn out to be especially important as Quinyan Chen and her partners' researches in the Purdue University College of Engineering (USA) pointed out that ventilation causes the dispersion of contaminants from expiratory activities (for example sneezing, coughing, talking or breathing). Presenting their studies about the main characteristics of particles dissemination in airplane cabins, researchers demonstrated how they can be involved in contamination events. Nevertheless, they suggested the relevance of paying attention to the subject, since there is little research about personalized ventilation systems that can be used along with a mixed ventilation system. It is known that before being supplied to the cabin, the recirculated air is filtered through equipment with high-efficiency particles. Those air filters also known as HEPA filters must be capable of reducing the risks of a cross and longitudinal infection of the airflow supply [15]. Next, Computational Fluid Dynamics (CFD) analysis of the airflow will be used to determine air conditioning coefficients in commercial passenger airplanes.

2.6 Methodological procedure

The aircraft cabin e-170 uses the normal ventilation system with a longitudinal direction. In this chapter, it will be applied and validated, in a testing phase, in mock-ups, with digital thermal manikins controlled by the Autodesk software with a Computational Fluids Dynamic (CFD) tool in order to determinate the temperature and speed coefficients and their corresponding thermal loads.

The tests include three steps: construction of the aircraft prototype; model construction of the empty cabin, with passengers standing and with the digital manikins seated; analyzing the actual air conditioning system to define the cabins' thermal environment characteristics inside a commercial aircraft for passengers transport.

3. Research development

3.1 The construction of the aircraft prototype with the manikins seated and standing

Prototype construction of the aircraft e-170 with the internal layout of armchair, luggage rack. A digital mock-up will be used for the tests to reproduce the cabin section of a commercial airplane with the dimensions of $3 \times 3 \times 2.5$ m in height **Figure 7**.

The construction of the passengers digital model is made from the use of the digital thermal manikin, built using the software "Solid Works", it helps in the anthropometric analysis of the armchair to evaluate the equivalent temperatures. The thermal manikin has 1.70 m in height, which allows a more representative temperature modeling of the surface of the body, to verify the passengers' comfort and discomfort.

Figure 7.
Prototype construction of the aircraft e-170.

The thermal manikin, for now described to the passenger as a digital-physical model controlled by three control modes: constant temperature (air temperature and speed), constant power, and Fanger's comfort equation.

Fanger's method will be used to verify the thermal exchanges and the thermal balance of the human body, in other words, the "CLO-FANGER-MET" method with the influence of atmospheric pressure. The air temperature and speed are measured in the cabins' thermal environment **Figure 8**.

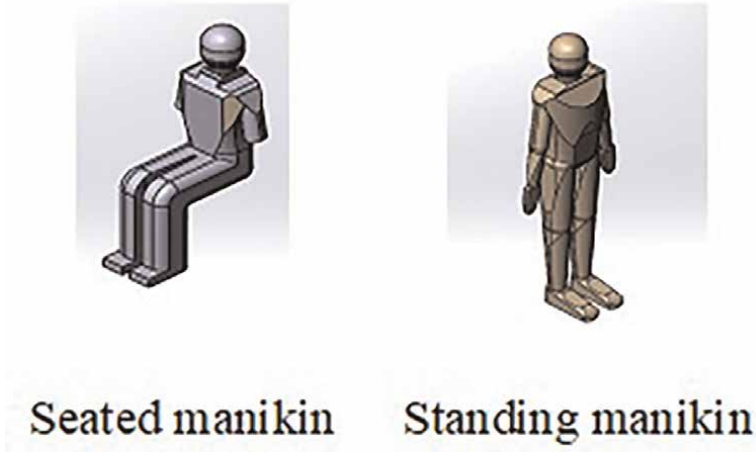

Figure 8.
Digital model construction of the passenger.

4. Results and discussion

4.1 Simulation steps in CFD

The air quality and its impact on humans during the cruise are determined by the aeronautical comfort design and have strong influences on the thermal conditions of the passenger. The air recirculation used before the airborne pathologies by various types of viruses. For example, according to researches presented during the Roomvent Congress, 2014, ventilation is related to the circulation of contaminants in airplanes cabins which from expiratory activities, cause cross-contamination events. Belonging to the list of studies about environmental comfort this research therefore, evaluates the actual thermal behavior of the airplane commercial user. In the face of the need to investigate air diffusers, responsible for the crew discomfort and for the transmission of diseases such as the so-called SARS (Severe Acute Respiratory Syndrome), and the challenges that are imposed on the intentions to design a healthy and comfortable environment in the cabins, we analyze the air distribution in the interior project of such cabins. The research focuses around the armchair and duct shapes with the use of the Computational Fluid Dynamic (CFD) tool.

The results of this chapter present a model based on computation that can predict the temperature and airflow as well as the parameters of environmental air distribution in commercial airplanes cabins, in empty cabins, and with passengers seated or standing. The model is known as CFD (Computational Fluid-Dynamic Model). The purpose of this item is to present to the reader some of the main fundamentals that are necessary for the applications of CFD related to internal environmental technology in commercial aircrafts.

This item presents the information used in the data entry for the CFD commercial airplane e-170 cabin simulation: **Figure 9**.

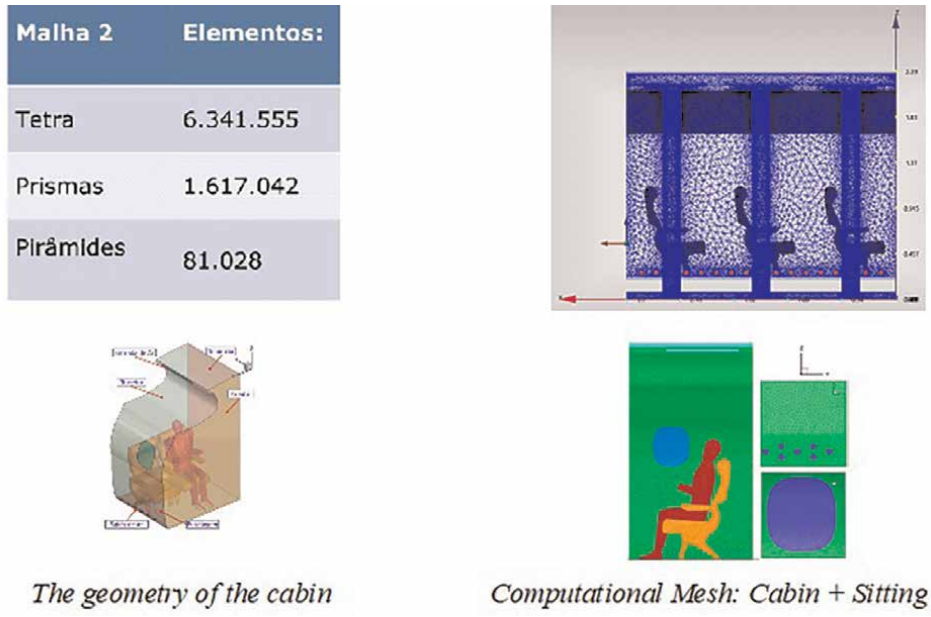

Figure 9.
Mesh refinement.

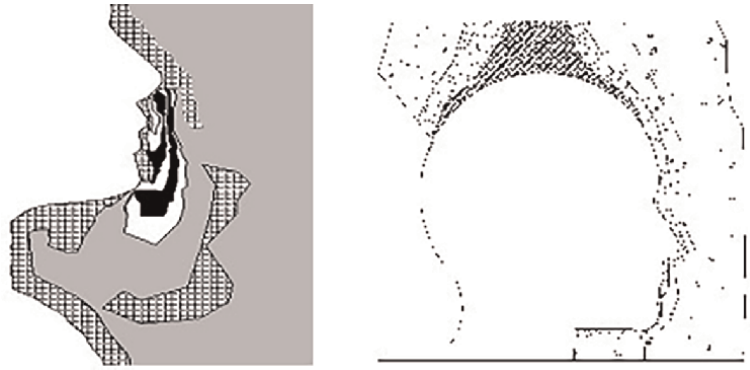

Figure 10.
Shows the air breathed by passengers.

4.2 Results

The results of this chapter present a model based on computation parameters that the air distribution and environment temperature in the commercial aircraft cabin are the passengers breathing, empty cabin, and with the passenger seated or standing. The

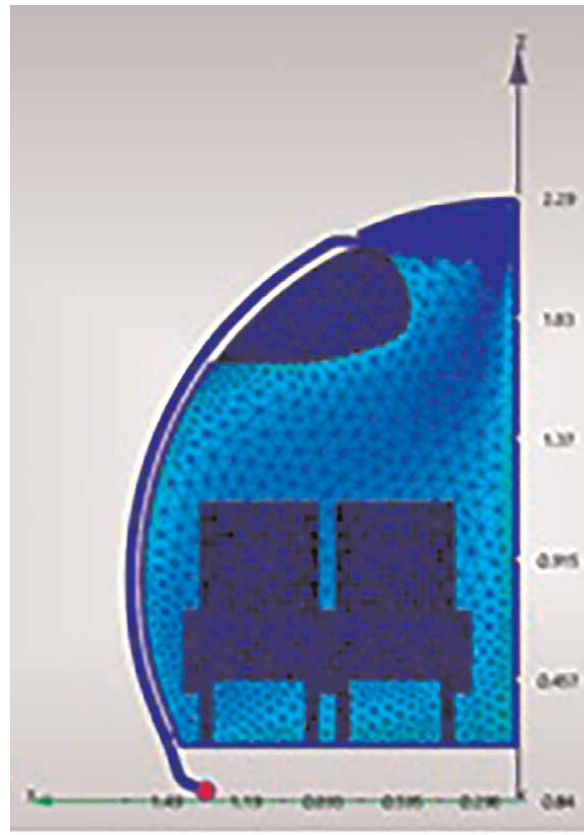

Figure 11.
Air supply diffuser representation using a computational mesh to demonstrate a Fluid Domain mesh.

purpose of this item is to present to the reader some of the main fundamentals that are necessary for the applications of CFD related to the internal environmental technology for commercial aircrafts.

4.3 Passengers breathing

The passangers breathing inside the plane's cabin is presented in **Figure 10**.

4.4 Empty cabin

The representation of the empty cabin with the representation of the air supply diffuser going from the top part to the bottom one with the cabin height of 0–1.70 m and 0–1.50 m length is presented in **Figure 11**. **Figure 12** identifies the magnitude velocity from 0 to 0.9 m/min noticing that the maximum airspeed is concentrated close to the gasper outlet, decreasing its speed throughout the path to the air outlet at the bottom of the cabin. The air temperature in degree Celsius is presented in **Figure 13**, ranging from 22°C to 28°C, notice that this temperature is used for tropical climate inhabitants, different from the countries located in Scandinavia, where temperature above 18°C is the upper limit in summer. The air supply diffuser using a computational mesh through the cabin is shown in **Figure 14**. **Figures 15** and **16** demonstrate, as an example, the points of a constant air temperature value and speed for an empty cabin.

4.5 Front view of the cabin with the standing manikin

The airspeed with the passenger standing is represented in **Figure 17** with a variation of magnitude velocity from 0 to 0.11 m/s. **Figure 18** presents the air surface

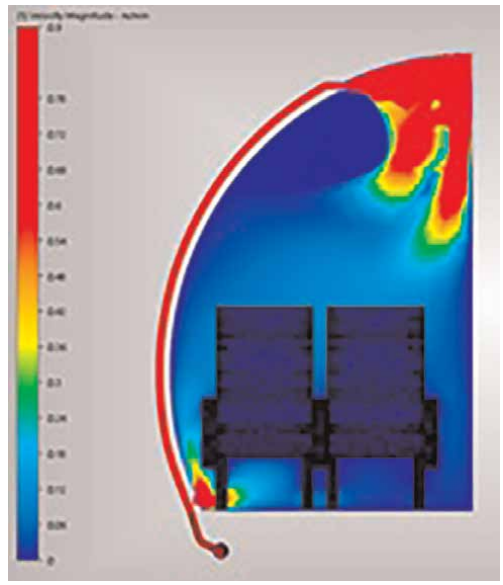

Figure 12.
Airspeed in the empty cabin.

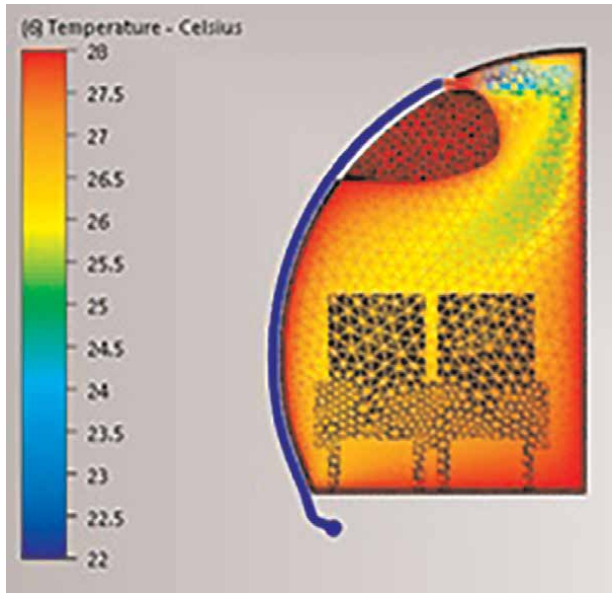

Figure 13.
Air temperature in the empty cabin.

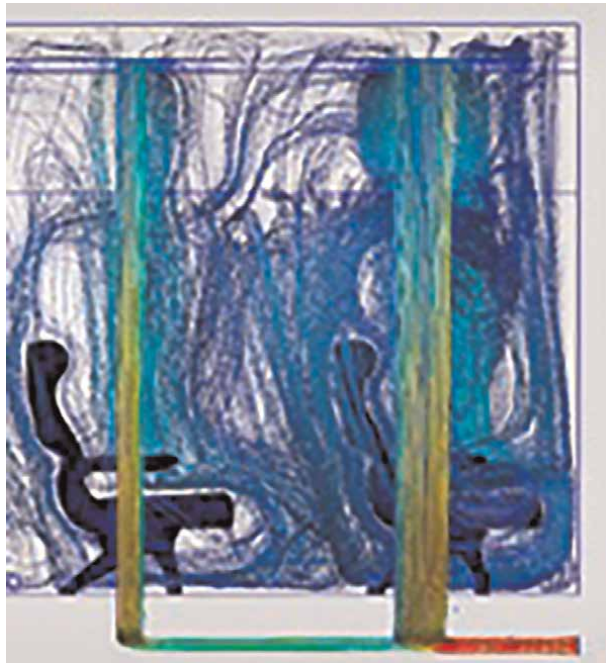

Figure 14.
Air supply diffuser representation using a computational mesh.

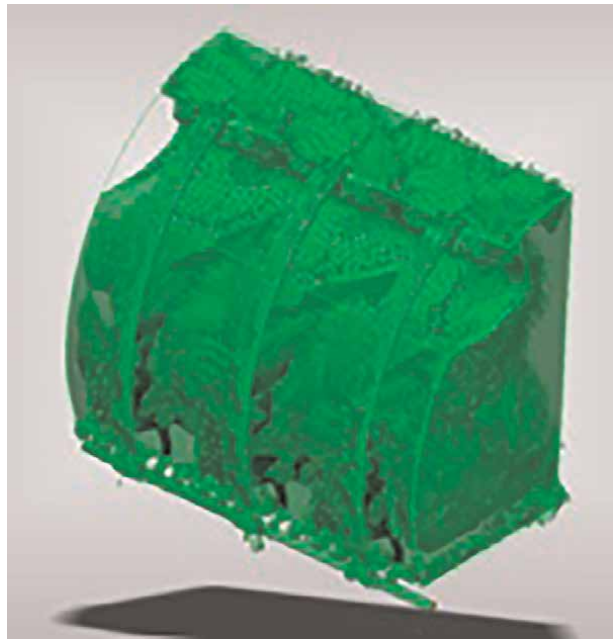

Figure 15.
Iso surface are surfaces that represent points of a constant number. For example, temperature and airspeed.

Figure 16.
Iso surface are surfaces that represent points of a constant number. For example, temperature and airspeed.

and **Figure 19** identifies the air temperature between 24.88 and 27.04°C. Demonstrated in **Figure 20** is the image from the perspective of the cabin. The cabin refining mesh is presented in **Figure 21**.

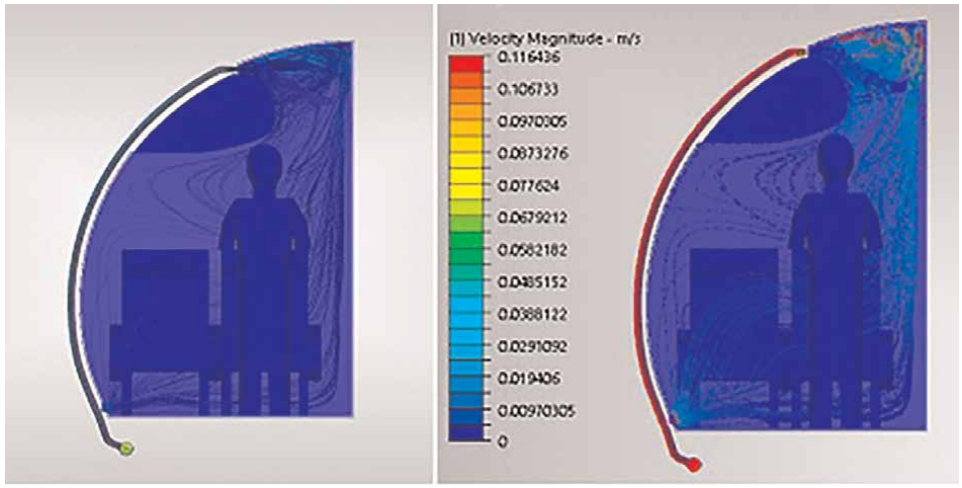

Figure 17.
Airspeed with passenger standing.

Figure 18.
Iso surface of the cabin with passenger standing.

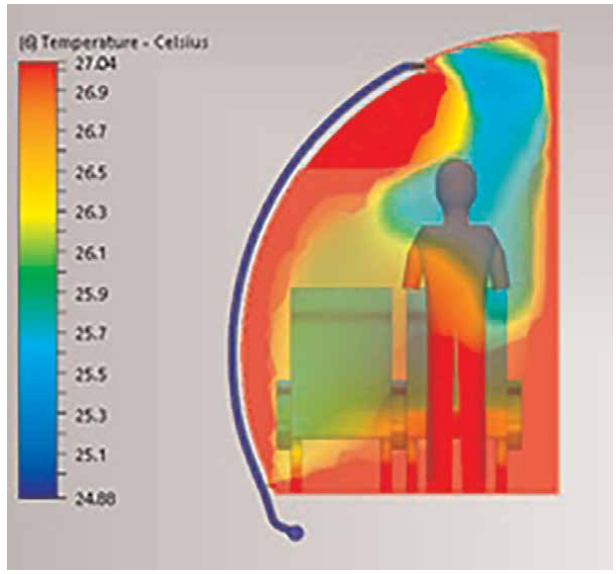

Figure 19.
Cabins temperature exhibition with passenger standing.

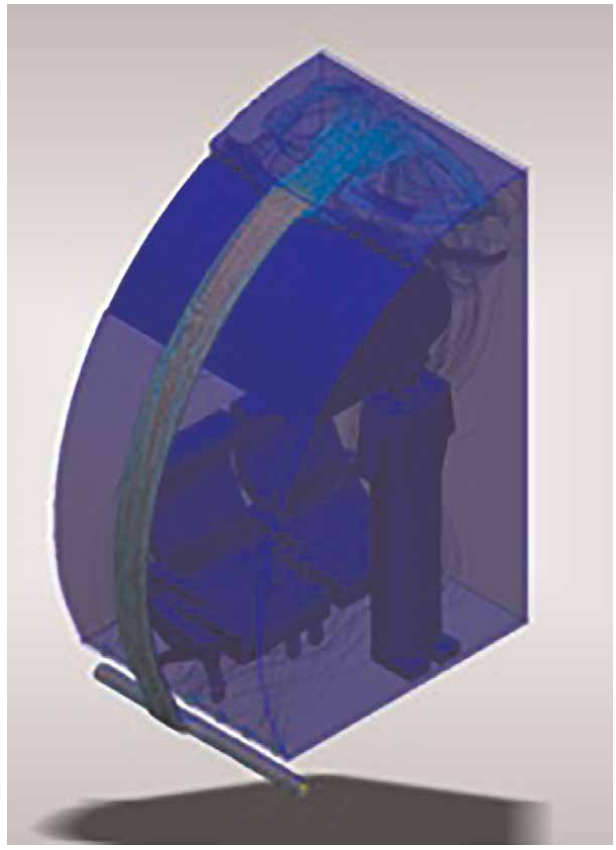

Figure 20.
Iso surface of the airflow line with passenger standing.

Figure 21.
Cabins mesh refinement with passenger standing.

4.6 Seated passenger

A seated passenger in the cabin has an isometric view with Magnitude Velocity from 0 to 0.007 m/s in **Figure 22**. In **Figure 23** the airspeed with the passenger seated (0.35–0.49 m/s) with the airflow going from the top part to the bottom part of the cabin. The air temperature with front view is shown in **Figure 24** with a variation of 23.4–27.4°C and the airspeed with a variation of 0–0.37 m/s in **Figure 25** and with airspeed ranging from 0 to 0.89 m/s in **Figure 26**. Seated passenger mesh refinement is presented in **Figure 27**.

4.7 Temperature and ventilation: computational fluid dynamics

The air quality and its impact on humans during the cruise are determined by the aeronautical comfort design and have strong influences on the thermal conditions of the passengers. The air recirculation used before the cause of airborne pathologies by various types of viruses. For example, according to researches presented during the Roomvent Congress, 2014, ventilation is related to the circulation of contaminants in airplanes cabins that from expiratory activities, cause cross-contamination events. Belonging to the list of studies about environmental

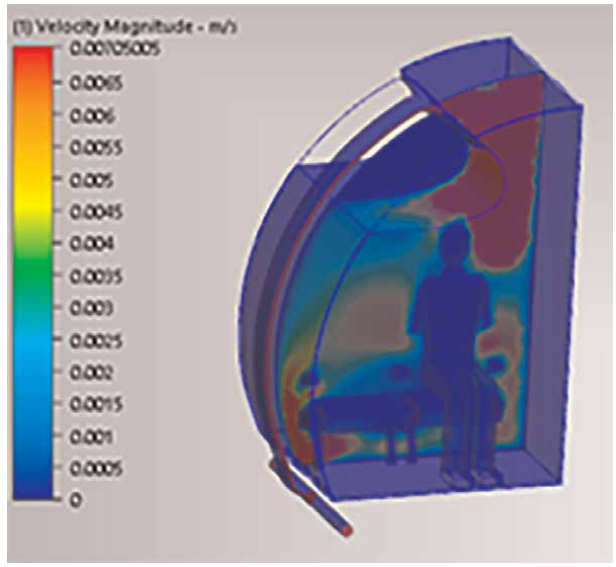

Figure 22.
Isometric view of passenger seated airspeed.

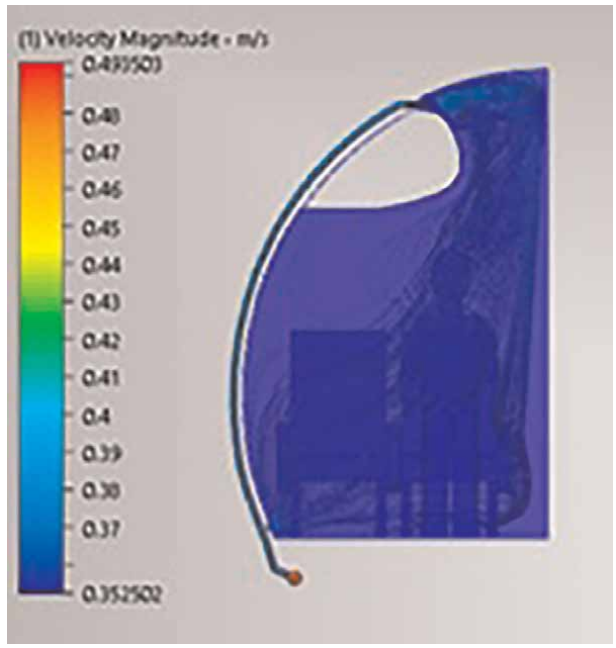

Figure 23.
Airspeed with a seated passenger (0.35–0.49 m/s).

comfort this research therefore, evaluates the actual thermal behavior of the airplane commercial user. In the face of the need to investigate air diffusers, responsible for the crew discomfort and for the transmission of diseases such as the so-called SARS (Severe Acute Respiratory Syndrome), and the challenges that are imposed on the intentions to design a healthy and comfortable environment in the cabins, we analyze

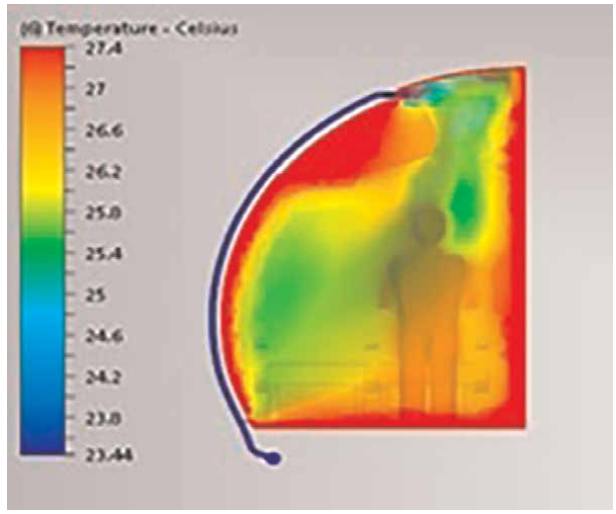

Figure 24.
Air temperature with a seated passenger (23.4–27.4°C).

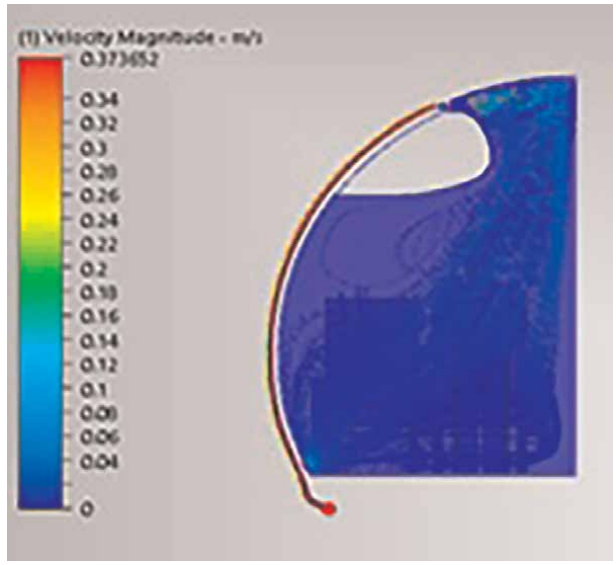

Figure 25.
seated passenger airspeed (0–0.37 m/s).

the air distribution in the interior project of such cabins. The research focuses on the armchair and duct shapes with the use of the Computational Fluid Dynamic (CFD) tool. The CFD simulation used the software Autodesk Geometry/Mesh/Solver/Post processing.

Through CFD simulations it was found that the air exits run from the top part to the bottom part of the plane.

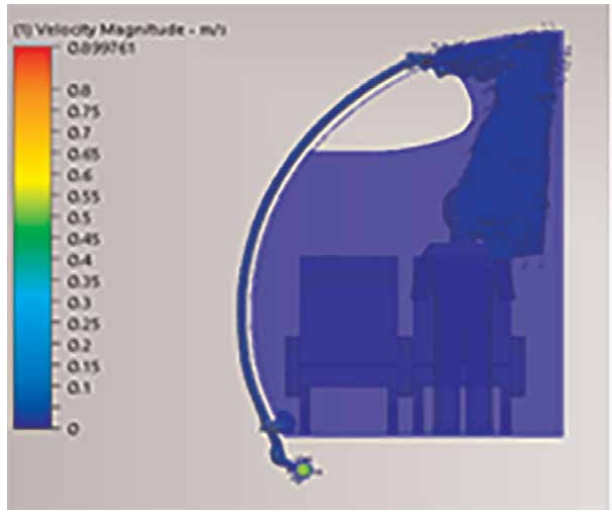

Figure 26.
Seated passenger airspeed (0–0.89 m/s).

Figure 27.
Seated passenger refinement mesh.

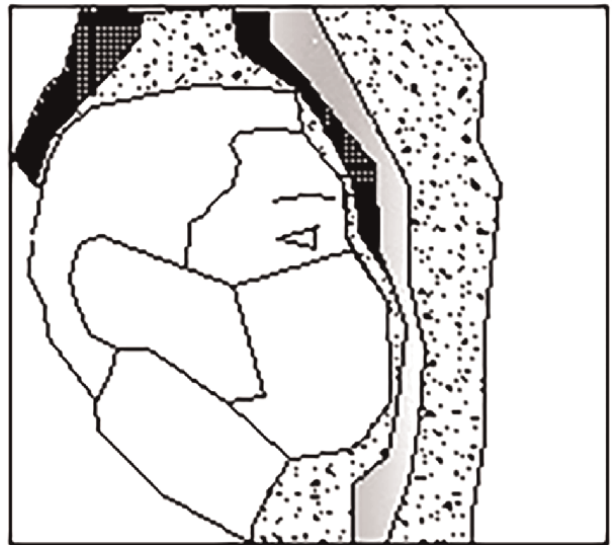

Figure 28.
Mask usage during flight.

Figure 28 shows the effect of the air current circulation and dispersion of particles throughout the aircraft cabin. This demonstrates that it is important to use personalized ventilation during the covid-19 pandemic period. According to Anvisa [16], the airflow of the gasper must be directed straight between passengers to avoid that they inhale the air from one another, avoiding disease dissemination.

5. Conclusion

The aeronautical project quality is essential for providing passengers with acceptable environmental conditions in order to achieve their thermal comfort. The research demonstrates the utmost importance of the aeronautical community (industries, research labs, and universities) in the fluids modeling field and the practical applications in the industry's daily job.

This research results present models based on Computational Fluid Dynamics (CFD) with parameters analysis of temperature and airspeed distributed in a real environment with a cabin sometimes empty, sometimes with passengers standing and/or seated.

It was verified that the temperature and airspeed are influenced by passengers' behavior, whether they are seated or standing in the plane's cabin. Breathing influences the airflow, being able to cause contamination in its environment. So, ventilation from the roof of the cabin promotes more particle dispersion throughout its area.

Another significant aspect to highlight is the importance of achieving the plane's thermal comfort in a cruise. Having an adequate air conditioning system that contributes to the well-being, health, and the aircraft's users' health, as well as the other aspects that influence the passengers' environmental comfort, when based on the cabins' geometry, the armchairs positioning and ergonomics will also contribute

positively in the aircraft's mechanic system. We suggest the use of the air insufflation systems to avoid contamination through the air in the interior of the cabin.

As this research's results demonstrate, simulations in CFD showed that there are three variables, and they must be considered to better evaluate the thermal comfort and indoor air quality in an aircraft cabin, which are- the profile of different temperatures, the airspeed, and human breathing. Therefore, the airflow circulation from the upper (ceiling) to the lower air supply duct (floor) promotes a wider dispersion of particles throughout the cabin that is associated with the characteristics of the mixing of this ventilation through passengers and the airplane's seats. However, it is also important to investigate the airspeed and temperature associated with air humidity.

The use of personalized ventilation is important during the pandemic period of COVID-19, for instance, when the gasper is opened, the airflow must pass between passengers, the air circulation must be oriented directed to the floor's lower duct. Another precaution that helps to protect the passengers is the use of masks and facial protectors during the flights, which must have non-ventilation and be approved by government agencies. Another security measure adopted to protect the people is to remain at a distance from others and always use alcohol gel.

The concern with passenger air transport relates to public health and safety aspects which must be analyzed in order to have a faster response for such risks. This is fundamental so that measures, such as prevention and vaccine development, in addition to efforts to mitigate COVID-19 transmission and dissemination, can be effective. Technical and scientific researches, as well as public policies to aid and enforce these measures must be constant and applied to the aeronautics industry everywhere in the world, with decisions made according to international health regulations. An additional investigation must be carried on about contamination of material carried in the aircraft.

Acknowledgements

English version by: Samantha A.L. Takatui, Mayor Edson da Silva and Eng. Nilson Carneiro, Prefeitura Municipal de Araraquara, São Paulo, Universidade Federal de São Carlos, PPGEU, Instituto de Pesquisa Tecnológica do Estado de São Paulo, IPT e Universidade de São Paulo, São Carlos.

Funding

This research did not receive any specific grant from funding agencies in the public, commercial, or not-for-profit sectors.

Author details

Clélia Mendonça de Moraes[1,2]

1 PMA Prefeitura Municipal de Araraquara, SP, Brazil

2 UFSCar, Federal University of São Carlos, Brazil

*Address all correspondence to: arqclelia@hotmail.com

IntechOpen

References

[1] https://www.gov.br/anac/pt-br/assuntos/coronavirus [Accessed at 03/06]

[2] ASHRAE. American Society of Heating, Refrigerating and Air Conditioning Engineers "Refrigeration Handbook (SI)". USA: ASHRAE; 2002

[3] ASHRAE. American Society of Heating, Refrigerating and Air Conditioning Engineers, "Applications Handbook (SI)". USA: ASHRAE; 1999

[4] International Organization for Standardization. ISO 9920: Ergonomics of the Thermal Environment: Estimation of the Thermal Insulation and Evaporative Resistance of a Clothing Ensemble. Geneva: 1995

[5] International Organization for Standardization. ISO/EN 7730: Moderate Thermal Environment: Determination of the PMV and PPD Indices and Specification of the Conditions for Thermal Comfort. Geneva: 1994

[6] Nielsen PV et al. The influence of draught on a seat with integrated personalized ventilation. In: Anais do Congresso Indoor Air. K Copenhagem, Denmark: 2008

[7] World Health Organization. International Travel and Health: Situation on January. Genebra: WHO; 2009

[8] Iemini PM. Medidas adotadas pela ANAC e ANVISA para o controle da disseminação do vírus influenza no transporte aéreo civil de passageiros durante as pandemias de influenza entre 2009 e 2017. Palhoça: Bacharel em Ciências Aeronáuticas, curso de Ciências Aeronáuticas, da Universidade do Sul de Santa Catarina; 2017. p. 35

[9] World Health Organization. New Influenza A (H1N1) virus infections: Global surveillance summary. Weekly Epidemiological Record. 2009;**84**(20):173

[10] de Moraes C, Vitorino F, Catalano FM. Air insufflation system development in airplanes cabins aiming the automated simulation process to improve thermal comfort in the personal microenvironment in aircraft cabins. In: Post-Doctoral Thesis Presented in the Novos Talentos Program of the Institute for Technological Research, with the collaboration of the Aeronautical Engineering of São Carlos School of Engineering. São Paulo: 2018

[11] Lombardo D. Aircraft Systems. 2nd ed. New York: McGraw-Hill; 1998

[12] Lombardo D. Advanced Aircraft Systems. New York: McGraw-Hill; 1993

[13] Embraer. 2020. Available from: https://journalofwonder.embraer.com/br/pt/232-ar-puro-e-cabine-limpa-para-um-voo-seguro [Accessed: June 30, 2021]

[14] Conceição ST. Contaminação aérea em cabines climatizadas: Processo de avaliação e análise da influência de sistema de ventilação personalizada. 2012. 218f. São Paulo: Tese (Doutorado em Engenharia Mecânica) – Escola Politécnica da Universidade de São Paulo; 2012

[15] Eurovent 4/11 – 2014. Energy Efficiency classification of air filters for general ventilation purposes - Second Edition. Available from: https://eurovent.eu/?q=content/eurovent-411-2014-energy-efficiency-classification-air-filters-general-ventilation-purposes [Accessed at 06/03]

[16] Agência Nacional de Vigilância Sanitária – ANVISA ... crescimento exponencial dos casos da COVID-19 e sobrecarga dos serviços de saúde, ... [14 April 2020]

Edited by Zain Anwar Ali and Dragan Cvetković

This book provides a comprehensive overview of aeronautics. It discusses both small and large aircraft and their control strategies, path planning, formation, guidance, and navigation. It also examines applications of drones and other modern aircraft for inspection, exploration, and optimal pathfinding in uncharted territory. The book includes six sections on agriculture surveillance and obstacle avoidance systems using unmanned aerial vehicles (UAVs), motion planning of UAV swarms, assemblage and control of drones, aircraft flight control for military purposes, the modeling and simulation of aircraft, and the environmental application of UAVs and the prevention of accidents.

Published in London, UK

IntechOpen

ISBN 978-1-80355-302-3
9 781803 553023